Author/s:
Ghimire, Smriti

Title:
The influence of mechano-regulation on bone fracture healing

Date:
2020

Persistent Link:
https://hdl.handle.net/11343/238450

The University of Melbourne

Doctoral Thesis

Influence of mechano-regulation on bone fracture healing

Author:

Smriti Ghimire
ORCID: 0000-0001-9978-7437

Supervisors:

A/Prof. Lihai Zhang
Dr. Saeed Miramini
A/Prof Martin Richardson

A

thesis

submitted in total fulfilment of the requirements

of the degree of Doctor of Philosophy

in the

Department of Infrastructure Engineering

February 2020

Abstract

Bone fracture healing is a unique biological process characterised by differentiation of mesenchymal stem cells (MSCs) in fracture callus into bone forming cells while the process is regulated by biochemical and mechanical factors. The mechanical microenvironment can be influenced by several factors, including mechanical loading, fixation stiffness and flexibility; and fracture geometry (i.e. gap and angle of fracture). However, the fundamental relationship between the various loading regimes and different healing outcomes has not been fully understood.

In this research, a computational model is developed to investigate advective transport of cells and growth factors under various strain and frequency of dynamic loading during early stage of diaphyseal bone healing. The model takes into account cell and growth factor transport under dynamic loading, and mechanical stimuli mediated MSC differentiation and tissue production. While literatures have suggested that dynamic loading induced deformation and fluid flow contributes to the biomechanical environment, the combined effects of biochemical and biomechanical stimuli on bone healing have not been fully investigated so far. To our knowledge, this is the first study to incorporate direct contribution of dynamic loading induced mechanical stimuli as well as the indirect contribution through advective transport of cells and growth factors into a computational model within the fracture callus which is the novelty of this work. The results demonstrate that, there is an optimal dynamic loading that enhances MSCs and growth factors transport in a spatially dependent manner (Ghimire et al., 2018).

This research further investigates the effects of fixation on the MSCs migration and differentiation as well as growth factor transport using finite element method (FEM) simulation. There is limited research on the effects of dynamic loading on growth factor and cell transport during early stage of fracture healing under different Locking Compression Plate (LCP) configurations and optimal LCP configurations for directed cell migration are yet to be established for various fracture geometries. Therefore, this represents the first step towards fundamental understanding of the mechanical loading mediated MSCs transport and differentiation under LCP fixation with various flexibilities,

and results demonstrate that MSCs and growth factor transport are highly dependent on flexibility of the fixation (Ghimire et al., 2019).

The model was further developed to simulate oblique bone fracture healing stabilized by different fixation configurations to study the influence of fracture geometry on the angiogenesis during bone fracture healing. Using the simulation results, the allowable level of partial weight bearing loading at early stages of healing for promoting angiogenesis and bone healing are suggested. The results of this study would assist in the design of patient specific weight-bearing exercises during bone fracture healing following a surgical intervention with internal fixations.

Osteoporotic fractures are generally different to normal bone fractures, due to the changes in the diffusion and perfusion of non-mineralised bone marrow with the loss of mineralised bone component. A better understanding of the impact of osteoporosis in fracture healing can lead to a better fracture treatment and optimum healing outcome in osteoporotic fractures. To achieve this aim, this research compares interfragmentary movement (IFM) between normal and osteoporotic bone fracture using ex-vivo mechanical experiments on ovine model of bone fractures under different bone plate distance (BPD) configurations of LCP. The experimental results suggest that osteoporotic bones experience more asymmetric healing across near and far cortex compared to healthy bones.

The bone formation rate between the two mechanisms of bone fracture healing (intramembranous and endochondral ossification) was compared in this research by developing a novel time dependent simulation of bone fracture healing using experimentally determined bone density data in sheep tibia stabilized by the Locking Compression Plate (LCP) fixation system. The model results show that, there are two different thresholds for intramembranous and endochondral ossification that activates significant bone formation. Upon reaching the threshold, the rate of bone formation in endochondral ossification is generally higher than that in intramembranous ossification.

In summary, through developing a computational model with consideration of biochemical as well as mechanical aspects of the fracture healing, this research is a significant step towards the crucial understanding of the mechanical loading mediated MSCs transport and differentiation under LCP with various flexibilities. The outcomes of

this research could potentially be implemented to assist orthopaedic surgeons in identifying optimal configuration of LCP and loading regimes for patient specific conditions (e.g. fracture geometry, body weight).

Declaration

This is to certify that

i. the thesis comprises only my original work toward the Doctor of Philosophy,
ii. due acknowledgement has been made in the text to all other materials used, and
iii. the thesis is fewer than 10,000 words, exclusive of tables, figures, and references.

Smriti Ghimire

February 2020

Acknowledgement

First and foremost, I would like to express my deepest gratitude to my supervisor A/Prof. Lihai Zhang for his unwavering support and guidance throughout this research. No words would be enough to thank him for taking his time out whenever I needed (everyday, at times) to discuss research ideas and supervise my work.

I am indebted to Dr. Saeed Miramini, for playing a significant contribution to the successful completion of this thesis. He has always been kind enough to support me in every aspects of research from writing to supervision to designing and execution of the experiments. I gratefully acknowledge the feedbacks I received from A/Prof. Martin Richardson and my advisory committee chairs Prof. Priyan Mendis and Dr. Felix Hui during my candidature.

I would like to thank Ganesharajah Ganadhiepan for exploring research ideas at length, including efficient computational modelling in COMSOL. I extend my sincere appreciation to him and Xuanchi Liu for helping me during experiments, to Oktay Balkis from Workshop laboratory, Steve Adams from Mammalian Lab, Laura Jukes from ceramics lab for helping me throughout the experiments. The academic and professional staffs at the department, Eileen, Pauline and Ana were very resourceful and willing to help whenever asked. The annual conference from the department was a great platform to share my ongoing research and get critical feedback.

I would like to sincerely acknowledge research, library and all forms of support from The University of Melbourne throughout my candidature. My time at the university was enjoyable, thanks to many programs and workshops I attended (and some organised) through Graduate Infrastructure Engineering Society (GIES), graduate group of Melbourne University Nepalese student's Society (MUNSS), Graduate Students Association (GSA) staffs and councillors during my tenure as a Councillor and Family Officer from 2016- 2018 and, Graduate Group of Student Parents. Special thanks to Dr. Mukta Sapkota, Seema Karki, Suwash Acharya, Shreemat Shrestha, Lubna Meempatta and other colleagues in my office for the ideas and knowledge we shared together during lunch time.

This thesis wouldn't have been possible without my husband, Dr. Tilak Pokharel who lighted the path ahead of me. I cannot express in words how much I value his endless love, constant encouragement and patience even on the darkest days. Thank you for being my pillar of support.

To my mom, for her devotion who had deepest passion for education but couldn't continue hers due to my poor health during childhood. She always hoped to see her dream in me, and I feel fortunate to be able to live her dream. To my dad, for his unconditional love and for raising me capable to embark on this journey. I'm eternally grateful to both of our parents who have tirelessly and patiently looked after Aayam while I undertook this research. Last but not the least, to Aayam who grew up alongside this research and has been very understanding that mummy needs to go to "office".

Preface

All the work done towards this thesis is original research and have been carried out during the enrolment in the PhD degree. The publication status of the chapters are as follows.

1. Ghimire, S., Miramini, S., Richardson, M., Mendis, P., & Zhang, L. (2018). Role of Dynamic Loading on Early Stage of Bone Fracture Healing. *Annals of biomedical engineering*, *46*(11), 1768-1784 (5-year Impact Factor: 3.605).
2. Ghimire, S., Miramini, S., Richardson, M., Mendis, P., & Zhang, L. (2019). Effects of dynamic loading on fracture healing under different locking compression plate configurations: A finite element study. *Journal of the mechanical behavior of biomedical materials*, *94*, 74-85 (5-year Impact Factor: 3.643).

Publications 1 and 2 are the bases of Chapters 3 and 4 respectively, and only text, format and referencing style have been modified to be consistent with the rest of the thesis. Publications 3, 4 and 5 are currently under internal review, and each form the bases of Chapters 5, 6 and 7 respectively.

In case of published articles that forms part of this thesis, I am the primary author and have contributed to more than 50% of the content in the publication. I was responsible for primarily planning, execution and preparation of the work for publication. I wrote initial draft of the work and subsequent editing in response to the comments and feedback from my co-authors and journal reviewers. For each published article, the co-author authorisation forms have been provided.

Finally, I would like to acknowledge the source of funding as Australian Government Research Training Program Scholarship, including fee offset scholarship.

Contents

List of Figures

List of Tables

Chapter 1.

Introduction

1.1. **Motivation**

The frequency and prevalence of bone fracture is alarming. In Australia alone, 1 fracture occurred every 3.6 minutes in 2013 and this is set to rise by 1 fracture in every 2.9 minutes by 2022 (Watts et al., 2013). Bone fractures are generally treated with non-surgical (for e.g. casts, splints) or surgical methods (for e.g. nails and screws, plates and screws, external rings) however, not all fractures heal successfully. It is estimated that around 5-10% of bone healing undergo impaired healing which can be in the form of delayed healing that takes longer time to heal or non-union that fails to heal without additional intervention within 6-9 months. This is an added burden on the patient due to painful and prolonged recovery. On a national level, fractures generate substantial cost to the health care system. Arthritis and musculoskeletal conditions accounted for 8.7% of total allocated health expenditure in 2008-09. At $5.69 billion, it was the fourth highest rate of expenditure, behind cardiovascular disease, oral health and mental disorders.

Bone fracture can occur even without a trauma, in medical conditions like osteoporosis. Osteoporosis is a condition predominantly associated with old age, where bone becomes

fragile leading to higher risk of fracture. 3 million Australians are estimated to have osteoporosis by 2021. Over 60 years of age, 2 in every 3 women and 1 in every 3 men are likely to suffer an osteoporotic fracture and the possibility of a second fracture is over 50%. With the increase in aging population in Australia, the total cost of osteoporosis and related fractures (direct and indirect cost including hospital visits, outpatient and rehabilitation services) alone is estimated to rise to $3.84 billion by 2022 (Watts et al., 2013). This shows how massive the costs associated with bone fracture is. Therefore, if we can find ways to enhance bone healing, there will be lesser incidence of impaired healing which will be a great contribution, not only to the patients' quality of life but also to the national health care system and economy.

1.2. **Background of research**

Bone fracture healing is a complicated phenomenon where the fractured bone heals by itself without a trace of scar. The regeneration of bone through tissue formation and spatial distribution in fracture callus depends on the biomechanical and biochemical microenvironment of the fracture site. It has been widely known that the mechano-regulation plays an important role in cellular activities and tissue formation during bone fracture healing (Carter et al., 1998a, Claes et al., 1997). The mechanical microenvironment of fracture is influenced by fractured bone loading (magnitude and frequency of loading), fracture geometry (fracture angle or gap size) and fixation stiffness.

After a fracture, the fracture gap is initially filled with hematoma which is gradually replaced by callus made of granulation tissue(Marsell and Einhorn, 2011). Following the fracture, MSCs and growth factors (e.g. chondrogenic and osteogenic growth factors) migrate into the fracture callus from surrounding soft tissues, bone marrow or broken periosteum(Gerstenfeld et al., 2003), as biochemical stimuli to exert their biological actions and influence bone fracture healing(Gerstenfeld et al., 2003). MSCs are the pluripotent cells that can differentiate into various bone forming cells like osteoblasts, chondrocytes and fibroblasts(Roubelakis et al., 2007). The MSCs differentiation is regulated by the presence of biochemical stimuli like osteogenic and chondrogenic growth factors(Yamaguchi, 1995). The localised expression of growth factors leads to

concentration gradient in the callus which plays a crucial role in bone and cartilage formation by regulating MSC migration and cell differentiation.

During early stages, the biological actions of MSCs is highly influenced by the mechanical microenvironment of callus (Klein et al., 2003, Lienau et al., 2005, Miclau et al., 2002). Previous studies have also suggested that deformation and interstitial fluid flow generated by dynamic loading could produce a biomechanical environment that can influence healing outcomes (Witt et al., 2014). However, the role of dynamic loading on cells and growth factors transport in fracture callus during early stage of healing has not been fully understood and the studies in this area are limited. Therefore, the fundamental understanding of the influence of both biochemical and biomechanical factors that govern bone healing process is critical to obtain an optimal healing outcome.

While adequate motion enhances callus growth and bone healing, excessive motion is inimical to successful bone healing(Carter et al., 1998a). The movement in the fracture site can be controlled through external dynamic loading or configurations of bone fracture fixation. The bone fracture fixations stabilize bone fractures and enhance healing through mechanical interventions. Early weight bearing has been shown to enhance bone fracture healing(Bailón-Plaza and van der Meulen, 2003), and flexible fixations like locking compression plate (LCP) allows early movement after surgical procedure. Both excessive movement from a highly flexible fixation and no movement at all from highly rigid fixation are detrimental to bone healing(Claes, 2011). Therefore, optimum configuration of fixation is critical for a successful healing outcome. Numerous studies have also examined the most suitable loading regime for best healing outcomes however, there is lack of clear understanding on how the fracture stability can influence molecular and cellular activities during bone healing. Although it is known that configurations of locking plate affect bone healing outcomes, there is limited research on optimal fixation configurations for different fracture geometries that result in optimum MSCs transport and differentiation at cellular levels.

Further the bone fracture healing is highly influenced by fracture geometry. When diaphyseal or long bone fracture occurs under impact like accident, the bone fracture doesn't necessarily result in transverse fracture. The fracture, particularly comminuted fracture, takes place in several different angles of obliquity. Shear movements

accompanies axial interfragmentary movements in oblique fracture and changes with different angle of obliquity. Although it is known that large shear interfragmentary movement could result in damage to the newly formed blood vessels in the fracture site, there is little understanding on how much loading can be applied on fracture bone without affecting angiogenesis. In particular, the influence of dynamic loading on the angiogenesis development under different fracture angle and fixation configuration during early stage has not been clearly understood.

While mechano-regulation influences the migration and differentiation of MSCs and growth factors, the ability of these cells and growth factors may change under medical conditions like osteoporosis. Osteoporosis is a degenerative bone disease that degrades bone mechanical strength making it porous and brittle. Due to the change in structure and reduced strength in osteoporotic bone, the local stress and strain induced due to loading could change as well. As a result, its influence on cells and growth factors and their resultant response within fracture callus would be different. However, under fractures stabilized by fixation like LCP, it is still not clear how the mechanical microenvironment of fracture is different between normal and osteoporotic fracture. Due to osteoporosis, there is change in diffusion and perfusion of bone marrow as well, which is home to the multipotent MSCs and can affect the concentration of these cells migrating to fracture site. However, how osteoporosis impacts fracture healing is still poorly understood and therefore, a better understanding of the impact of osteoporosis in fracture healing would lead to a better fracture treatment and optimum healing outcome in osteoporotic fractures.

1.3. **Problem statement**

Literatures have suggested that bone healing requires a favourable biochemical and biomechanical microenvironment together with adequate blood supply (Gómez-Benito et al., 2011). The transport of cells and biochemical stimuli (i.e. growth factors) are known to be influenced by fracture interfragmentary movement through advective transport mechanism. The interfragmentary movement is also directly affect the MSCs differentiation and tissue formation. However, the combined synergistic effects of biochemical and biomechanical stimuli on bone healing, especially the advective cell and growth factor transport on fracture callus induced by dynamic loading, have not been

investigated so far. In addition to external loading, the configurations of fracture fixation during bone healing also affects mechanical micro-environment of MSCs at fracture site. This regulates the cell migration and differentiation at cellular level, as well as formation of tissues during the healing process. However, the effects of dynamic loading on cells and growth factors transport during early stage of bone healing is yet to be established under different LCP configurations. In addition, the fracture geometry (for e.g. gap size or fracture angle of obliquity) also plays a crucial role in mechano-regulation. The resultant deformation and fluid flow vary for both different gap sizes (which changes interfragmentary strain) and different angle of obliquity (which changes callus shape, direction of interfragmentary motion and its shear properties). Therefore, optimal fixation configuration for oblique fractures may differ from that for transverse fractures. Further, the impact of medical conditions like osteoporosis on bone fracture healing is poorly understood. Furthermore, bone formation during fracture healing takes place through endochondral ossification or intramembranous ossification pathways. Although bone fracture healing has been qualitatively studied and demonstrated that these two ossification processes occur within fracture callus, the fundamental mechano-regulation principles governing different bone formation rates under the healing processes of intramembranous and endochondral ossification are not presently understood.

1.4. **Research objectives**

The central aim of this thesis is to investigate how the fracture post-operative loading can influence bone fracture healing under different locking plate fixation configurations and patient specific conditions (i.e. fracture geometry, osteoporosis condition). To achieve this aim, several objectives are outlined as follows:

1. Developing a computational model that consider the combined influence of biochemical & mechanical stimuli on bone fracture healing while taking into account the influence of advective transport of cells and growth factors induced by dynamic loading
2. Applying the model to investigate the effects of dynamic loading on cells and growth factors transport under various configurations of locking compression plate for better healing outcomes

3. Evaluating the effects of dynamic loading on various fracture geometries during bone healing stabilized under different LCP configurations
4. Investigating the effect of dynamic loading on biomechanical microenvironment of osteoporotic bone fracture
5. Investigating bone formation process under endochondral and intramembranous ossification during bone fracture healing

1.5. Thesis overview

This thesis comprises of 8 chapters in total and addresses the research objectives mentioned in the last section. Each result is presented as a standalone chapter (with its own introduction, methods and results). Two of the result chapters have already been published while some are in the process of review.

Chapter 1 provides a brief background on the research topic, motivation and aim of this research.

Chapter 2 discusses the background on the research topic with comprehensive literature review and the relevance of this research with the current literatures. A review of the factors affecting bone fracture healing and the role of dynamic loading on bone fracture healing will be discussed under various fracture geometry and fixation configuration with a focus on solute transport and angiogenesis threshold.

Chapter 3 presents an integrated computational model based on the porous media theory to evaluate the influence of dynamic loading on bone fracture during early stage of healing. The model incorporates cellular processes such as the MSCs differentiation and the advective transport of various cells and growth factors, and mechanical stimuli arising from dynamic loading. The developed model was validated with the available experimental data initially, and then implemented to predict the loading regimes that can produce optimal healing outcomes.

Chapter 4 further develops the model to incorporate locking compression plate fixation at early stages of healing. The purpose of this study is to computationally investigate the effects of physiologically relevant dynamic loading on early stage of fracture healing under different configurations of the Locking Compression Plate (LCP) fixation. The

relationship between dynamic loading enhanced transport of bone cells and growth factors in fracture callus and flexibility of the LCP fixation is evaluated.

Chapter 5 applies the fundamental model derived in previous chapter to different fracture geometries (fracture obliquity) and optimal dynamic loading for different LCP configurations and fracture obliquity angle at early stages of healing is investigated with a focus on developing angiogenesis. Further, this research investigated the influence of different fracture angle and fixation configuration and recommendations were made on allowable load bearing at early stage of healing.

Chapter 6 experimentally measures the interfragmentary movement in different regions of fracture gap of osteoporotic ovine bones stabilized with different LCP configurations and compared with that of healthy bone fractures. The objective of this experiment is to determine whether osteoporotic bones would experience a different fracture mechanical microenvironment compared to non-osteoporotic fractures; and how the configuration of locking plates could affect osteoporotic fracture mechanical microenvironment.

Chapter 7 investigates the rate of bone formation during bone fracture healing under intramembranous and endochondral ossification by developing theoretical model in conjunction with a series of animal experiments. Intramembranous and endochondral ossification are two bone differentiation pathways during bone healing process, and this research compared bone formation rate between these two pathways using experimentally determined mean bone densities in sheep tibia stabilized by the Locking Compression Plate (LCP) fixation system. The models consider the spatial and time dependent changes in material properties of fractured bone as a result of the change of new bone content as healing progresses. In addition, the model has the capability of quantifying the healing outcomes under different fixation configurations and loading conditions.

Chapter 8 concludes with a summary to the research outputs of each individual chapters and provides insights and recommendations for further works.

Chapter 2.

Literature Review

2.1. Bone

Bone is an integral part of our human body which forms a crucial part of musculoskeletal system and provides support to the entire body. It is a rigid tissue that starts to form during foetus development and being a live tissue, it forms and remodels continuously throughout the human life. It has a remarkable ability to repair itself upon injury without leaving any scar. After the healing process, a well healed bone would have same structural integrity as the surrounding unbroken bone.

2.2. Bone fracture

Very often, bones undergo fracture which would break the bone structure due to the impact (for e.g. traffic incidents, accidental falls) or due to underlying medical condition like osteoporosis. A fractured bone could be categorised into several types – simple, comminuted, open and close.

When bone cannot heal by itself, external intervention is required in the form of treatment. The primary objective of such interventions is to restore the biological and mechanical integrity of bone fragments to its pre fracture state (Chidgey et al., 1986, Tepic et al., 1997). Traditionally, simple fractures are treated with non-surgical methods like plaster and splint to support the bone. However, complete immobilization is required in such cases for few weeks. For more complex or comminuted fractures, operative treatment is unavoidable. Fixations like nails and screws, plates and screws or external rings are put in place by orthopaedic surgeons to hold the fractured bone together. They also have an added advantage as they allow early movement and full functioning of fractured bone.

Treatment of bone fractures by conventional methods may not always be adequate as delayed healing and non-union are reported in about 5 - 10% of the fractures (Calori et al., 2011, Tzioupis and Giannoudis, 2007, Zura et al., 2016), which continues to present a challenge for trauma and orthopaedic surgeons. Furthermore, the treatment of these bone is a high economic cost to the healthcare system and thus, huge socio-economic burden to the country in addition to the patient's discomfort, pain and limited mobility.

2.3. **Non-union or delayed healing**

Not all broken bones heal properly or without delay. When there is no visible progression in healing in subsequent radiographs for 3 months and fails to heal without additional intervention after 9 months of fracture then it is termed as non-union, while delayed healing is when the healing progression is still taking place but is taking longer than the average healing time (Fayaz et al., 2011). These are common complications that occur in about 5 – 10 % of all fractures (Tzioupis and Giannoudis, 2007, Zura et al., 2016), and are generally treated with autologous cancellous bone grafting, combined with internal fixation (Rosset et al., 2014). Peters et al. (2010) demonstrated histologically that delayed healing undergoes similar healing process to normal healing bone, except on a different healing timescale with prolonged inflammation and soft callus stage.

2.4. Different stages of healing

Bone starts to heal right after fracture occurs. Fracture healing enables broken bone to return to its original structure and functional ability. Bone fracture healing is a complex, multi-step procedure that can occur either by direct ossification or indirectly through the formation of callus. Accordingly, bone healing can be broadly classified into two types as follows.

2.4.1. Direct healing / primary healing

During primary healing, bone ends are in contact and direct ossification occurs throughout the contact surface. This type of healing requires absolute stability under rigid fixation system like compression plating and may take years to complete (Miramini et al., 2016b).

2.4.2. Indirect healing / secondary healing

In general, bone ends aren't in direct contact and when there is a large interfragmentary motion at fracture gap, there is formation of fracture callus and this process of healing is called secondary healing. The formation of callus at external surrounding of fracture gap increases the cross section at fracture gap which improves stability at fracture site, limits initial movement and increases callus stiffness (Isaksson, 2012). Secondary bone healing generally occurs through four overlapping stages of healing in endochondral ossification process (Doblaré et al., 2004), which are outlined as follows (Refer to **Error! Reference source not found.**):

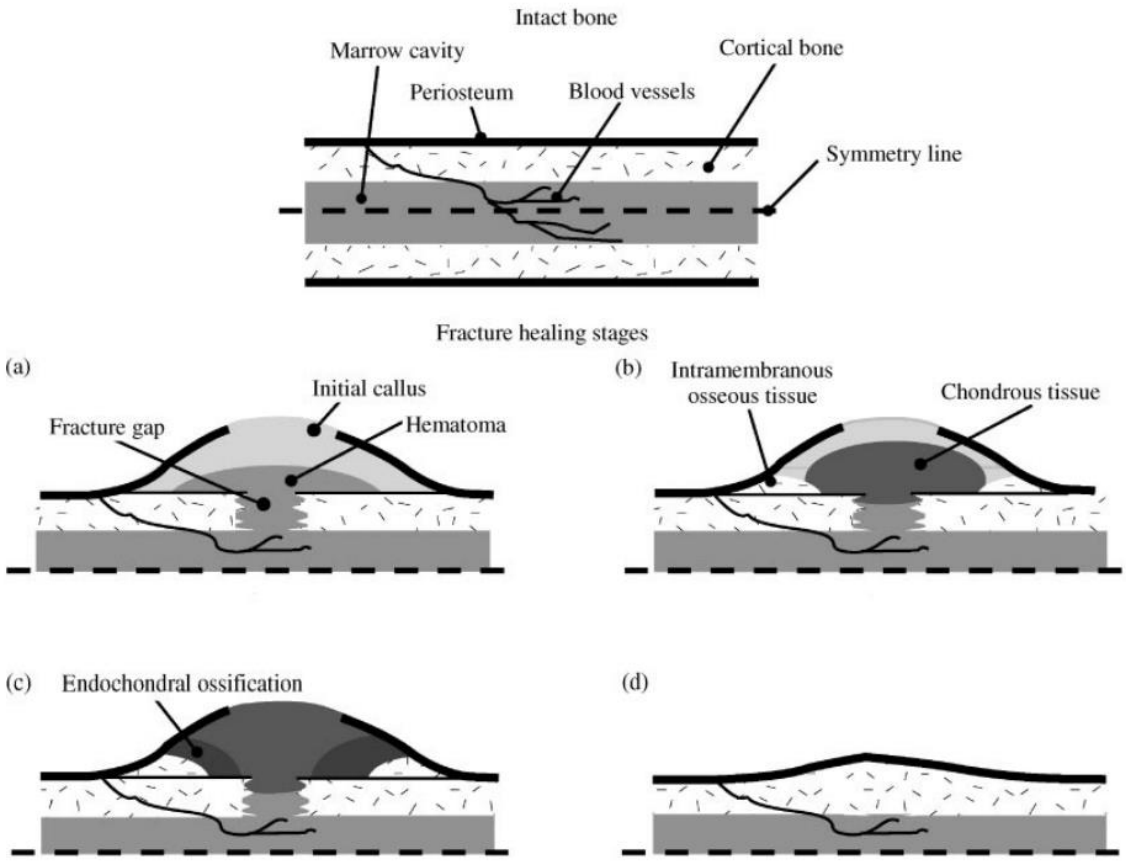

Figure 2.1 Schematic diagram of intact bone and four stages of secondary healing; (a) inflammatory stage; (b) soft callus stage; (c) hard callus stage; and (d) remodelling stage (Figure presented from Bailon-Plaza and van der Meulen (2001) with permission)Inflammation stage

After bone ends break due to trauma, blood vessels are ruptured, and inflammation occurs at the fracture site. The interruption in blood supply leads to lack of oxygen and consequently, cells start to die and necrosis occurs. All these debris and blood clot lead to the formation of hematoma. The pro-inflammatory cytokines are released upon injury while chemotactic effect results in the attraction and migration of inflammatory cells, and macrophages into fracture site (Rosset et al., 2014). The macrophages clear up debris and dead cells in fracture gap. Within a few days of bone fracture, macrophages clear the fracture site of debris and the fracture gap / hematoma is replaced with granulation tissue. Granulation tissue is composed of loosely formed fibrous tissue and has mechanical strength of about 2MPa. This stage generally lasts for a week and is deemed as early stage of healing (Gerstenfeld et al., 2003).

The growth factors are released by macrophages leading to concentration gradient which drives mesenchymal stem cells (MSCs) migration into fracture callus. The migration of stem cell can be both free migration (I.e. simple diffusion) or guided / directed migration. The guided migration due to chemical stimuli / growth factors is known as chemotaxis while the guided migration due to the fluid flow (resulting from mechanical loading condition) is known as advection / convection.

Soft callus stage

In soft callus stage, fibroblasts and chondrocytes differentiated from MSCs synthesize fibrocartilaginous callus tissue which gradually starts to replace the fibrous granulation tissue at the fracture gap (Einhorn, 1998). Since this tissue is not stiff enough, the fracture site still requires support which is usually provided by fixation. At this stage blood vessels also start to grow under angiogenesis process, and generally starts within 2 weeks post-operation (Einhorn, 1998).

Hard callus stage

Soft callus is replaced by hard callus as the soft fibrocartilaginous tissue is calcified and gets replaced by woven bone formed by osteoblasts. This is the stage where bone union starts to occur, and blood capillaries join and blood supply is established bringing in oxygen and nutrients.

Remodelling stage

This is the final stage of bone fracture healing where the woven bone gets replaced by lamellar bone under the action of osteoclasts and osteoblasts. As osteoclasts disintegrate the previously formed trabecular bone, it paves the path for osteoblasts to lay new lamellar bone in its place. Once the formed bone has similar integrity to the unbroken bone, the bone healing is complete (Schindeler et al., 2008).

2.4.3. Early stage of healing

During early stage of healing, mechanical loading has been shown to influence the differentiation of MSCs into fibroblasts, chondrocytes and osteoblasts (Le et al., 2001, Miclau et al., 2002). The mesenchymal stem cells are multipotent cells that are capable of differentiating into various cell lineages, such as fibroblasts, chondrocytes and osteoblasts during bone healing (Pittenger et al., 1999, Riminucci et al., 2015). MSCs

differentiation into these cells at early stage determine the pathway of bone healing which signifies the importance of this stage. For example, it has been show that applying controlled motion from day 5 till 3 weeks post-operation in sheep results in a higher callus strength and bone volume compared to unstimulated group (Tufekci et al., 2018). This shows the importance of mechanical stimulation during early proliferative phase of healing. Early stage of healing starts with the migration of MSC into fracture callus in inflammation stage up to the onset of soft callus formation stage when differentiated osteoblasts and chondrocytes start synthesizing bone and cartilage respectively.

2.4.4. Intramembranous and endochondral ossification

The degree of interfragmentary motion at the fracture site guides bone healing through intramembranous ossification or endochondral ossification process which constantly changes with level of callus stiffness (Wilson et al., 2015). At callus regions with considerably low interfragmentary motion, direct ossification of bone occurs through the process called intramembranous ossification. Intramembranous ossification doesn't involve cartilage formation and heals directly through bone union at external fracture callus. In the callus regions of moderate interfragmentary motion, MSC differentiates into fibroblasts and chondrocytes first, leading to the formation of fibrocartilaginous callus then the healing process is known as endochondral ossification (refer to Figure 2.2) (Claes et al., 2012). Under endochondral ossification, the cartilaginous callus is gradually replaced by bone and occurs closer to fracture gap (Malizos and Papatheodorou, 2005).

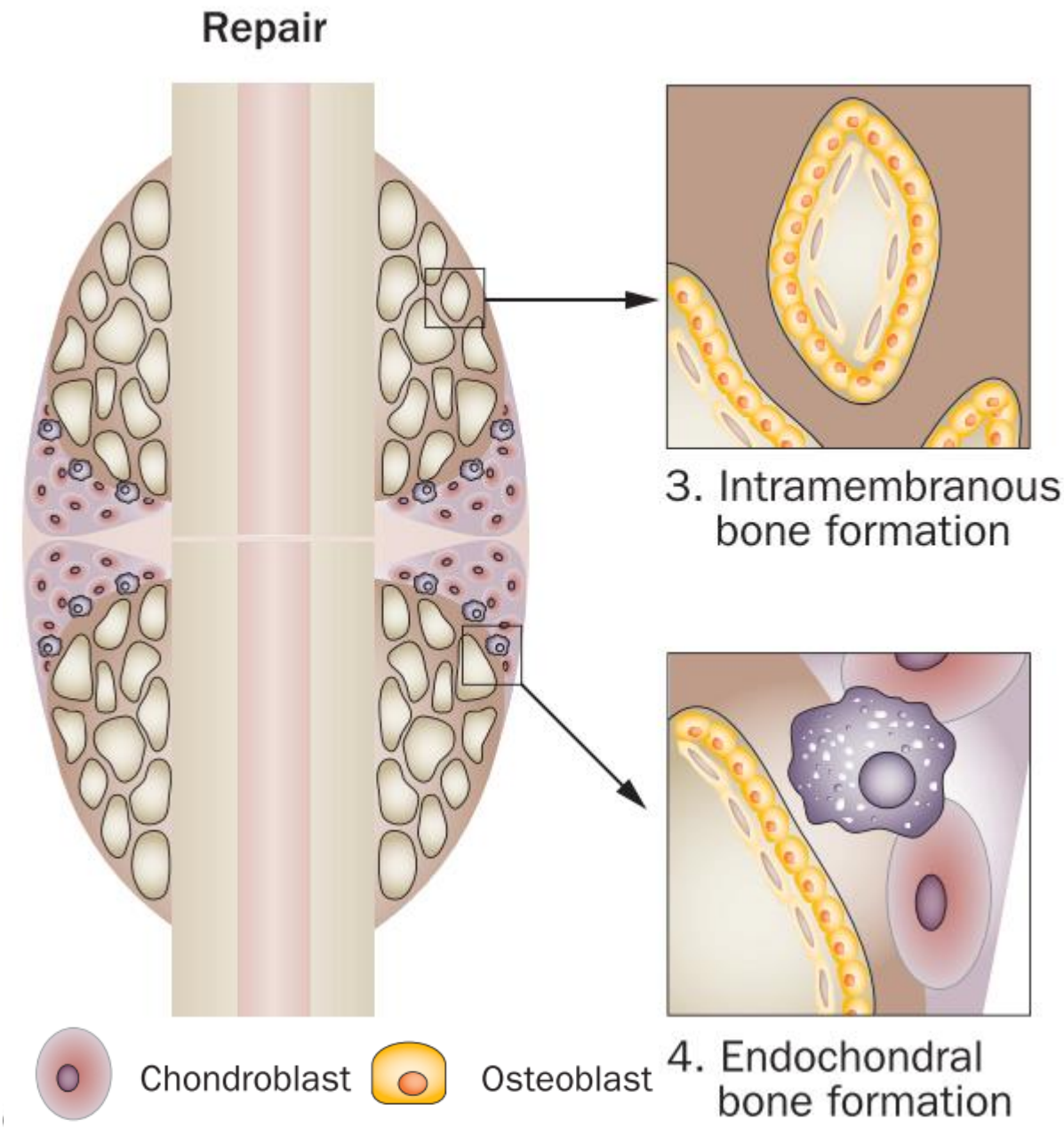

Figure 2.2 Schematic representation of fracture repair showing intramembranous ossification away from fracture gap, and endochondral ossification closer to fracture gap (Figure presented from Claes et al. (2012) with permission)

After trauma, fractured bone starts healing through intramembranous and endochondral ossification, which are two commonly known mechanisms of indirect healing. Bone formation seems to have different rate of production depending on the different pathway of healing. While there has been qualitative comparison between these differentiation pathways, the quantitative measurement of bone formation rate between these ossification processes hasn't been well defined. As a result, the fundamental

mechano-regulation principles governing different bone formation rates under the healing pathways of intramembranous and endochondral ossification are not clearly understood.

2.5. Factors affecting fracture healing

Several factors influence bone healing process directly or indirectly, such as genetic factors, age of the patient, type of fracture, blood supply, mechanical stability (Gomez Benito et al., 2005). Therefore, a clear understanding of the influence of the factors that govern the healing process is critical for achieving an optimum healing outcome. Some of the factors that are relevant to this research are discussed as follows.

2.5.1. Mechanical stimuli

It has been well documented that mechanical stimuli induced by mechano-regulation plays an important role in regulating the healing process through cellular actions and tissue regeneration during a diaphyseal bone healing (Carter et al., 1998a, Claes et al., 1997). Bailón-Plaza and van der Meulen (2003) observed delayed healing when mechanical stimuli was delayed until 6 weeks of fracture, which signifies the importance of mechanical stimuli at early stages of healing.

A favourable mechanical microenvironment can promote bone healing, while inimical microenvironment can lead to non-union or delayed healing (Claes et al., 1998, Goodship and Kenwright, 1985). Several mechanobiological studies (Carter et al., 1998a, Garcia-Aznar et al., 2007, Andreykiv et al., 2008, Prendergast et al., 1997, Lacroix et al., 2002b, Claes and Heigele, 1999, Gomez Benito et al., 2005, Isaksson et al., 2008a, Geris et al., 2004) have also considered the influence of mechano-regulation on cell processes like cell proliferation and differentiation and tissue regeneration. In fracture callus, the mechanical microenvironment is largely influenced by the interfragmentary movement at fracture site which is induced by musculoskeletal loading, stability of fracture fixation and various fracture geometries (Augat et al., 2005). The interfragmentary movement impacts local strain distribution and generates fluid flow and deformation within the fracture callus. This provides mechano-biological signals that affects cells and growth factors transport and mediates MSCs differentiation into different bone forming cell lineages (Augat et al., 2005).

Some of the factors that contribute to mechanical stimuli are discussed as follows.

Fracture geometry

Fracture geometry can be defined by fracture gap size and angle of fracture. Since the healing capacity of a fractured bone greatly reduces with increasing gap size, large displacement of bone fragments such as in comminuted fractures, may lead to delayed healing (Augat et al., 2005). Experimentally, it has been shown that larger fracture gaps lead to delayed healing due to the reduction in callus size and reduced bone formation (Claes et al., 1997). In fact, failure to bridge the gap has high possibility under fracture gaps greater than 6mm (Augat et al., 1998). Large displacement in smaller fracture gaps lead to large periosteal callus formation however, larger size of periosteal callus at fracture site may not always co-relate to superior healing process as Augat et al. (1997) demonstrated that large callus could indicate inadequate mechanical stability or premature weightbearing (Augat et al., 1996). Therefore, the size of the fracture gap play an important role in the quality of fracture healing outcome.

Depending on the angle of fracture, the fractured bone can be classified as transverse (horizontal line of osteotomy) or oblique fracture. Oblique fracture is generally caused by sharp bending forces with superimposed axial compression resulting in bone breaks diagonally (Pierce et al., 2004). They are more common in long bones such as tibia or femur. In oblique fractures, the angle of obliquity changes interstitial fluid pressure and deviatoric shear strain, which alters callus shape, interfragmentary motion direction and shear properties. This results in different mechano-regulation condition in callus, leading to change in healing pattern in oblique fractures. Under stable fixation, transverse fractures are considered to heal faster than oblique fractures (Aro et al., 1991). Excessive shear movement is believed to disrupt vascularisation and delay bone healing (Augat et al., 2003). Further, histological data showed lesser cartilage development due to large shear IFM compared to axial compression during early stages of healing (Peters et al., 2010). This could be explained through the detrimental effect of the translational shear force in a diaphyseal fracture model (Augat et al., 2003). Another study by Steiner et al. (2014) also predicted that translational shear movement is more detrimental to bone healing compared to torsional shear movement under loading. On contrary, Bishop et al. (2006) found enhanced healing outcome under torsional shear movement. Furthermore, shear force accompanied with axial loading contributes to fracture instability and this

force changes with different angle of obliquity (Lowenberg et al., 2008). Hence, fracture angle is an important factor to consider during bone fracture healing (Nassiri et al., 2013, Tan and Balogh, 2009).

Several computational studies have modelled transverse fractures (Bailón-Plaza and van der Meulen, 2003, Garcia-Aznar et al., 2007, Geris et al., 2006, Isaksson et al., 2007, Lacroix and Prendergast, 2002) and oblique fractures (Alierta et al., 2016, Aro et al., 1991, Comiskey et al., 2013, Loboa et al., 2001, Miramini et al., 2016a, Samiezadeh et al., 2014), however effect of fracture geometry on transport of cells and growth factors is still not well understood.

Mechanical loading

The influence of mechanical loading on tissue regeneration and cellular response is widely accepted (Carter et al., 1998a). Previously presented concepts for understanding mechanisms of bone fracture healing extensively involves external stimulation of fracture gap. Numerous experiments have been performed to examine the most suitable loading regimes for best fracture healing outcomes (Claes and Heigele, 1999, Kenwright and Goodship, 1989, Wolf et al., 1998).

Computational models provide good alternative to costly experimental stet up to investigate complex mechanism underlying bone fracture healing, including optimal loading conditions or fixation configurations (Wang et al., 2017). A series of studies have compared the healing outcome using computational models for bone fracture healing. These computational studies have also indicated that bone healing is accelerated by mechanical stimulus (Garcia-Aznar et al., 2007, Gomez Benito et al., 2005).

Frequency

Torres et al. (2018) compared a range of frequencies from 1Hz to 100Hz and showed that higher frequency cyclic loading promotes MSC differentiation into chondrocytes. In addition, it was shown that interstitial fluid flow is the most affected parameter due to frequency variation (González-Torres et al., 2010a).

However, external mechanical stimulation may not always be beneficial to the fracture healing. Cyclic tensile strains failed to enhance mechanical property of the healing bone significantly during fracture healing process (Augat et al., 2001). While axial compression generally associated with enhanced healing, shear force is regarded to be detrimental to

fractured stability. Influence of external mechanical stimulation on cell differentiation during bone healing studied by Torres et al. (2018) showed that lower external stimulation and higher gait stimulation (ratio of 20% to 80%) during healing represents the most real loading phenomenon, which signifies the importance of partial weight bearing on bone healing. The combined stimulation was considered from day 7 – 21, where a combination of 17 minutes of external stimulation at 90 Hz (Goodship and Kenwright, 1985) and 8.5 hours of gait (Pokorná et al., 2013) at 1Hz was considered per day (Torres et al., 2018). The combination case with 80% of lower frequency (1Hz) for longer time (8.5hrs per day) had resulted in better healing outcome compared to cases with 50% and 20% of 1Hz frequency. This might indicate that physiological loading conditions (for e.g. walking) is the optimum loading conditions.

Fixation

Fixation aims to stabilize the fracture site and improve bone fracture healing through medical intervention (Augat et al., 2001). In clinical practice, they are specifically preferred when there is complicated fracture and additional support is required for bone ends to be aligned. Depending on the application or mechanical stiffness, fixation can be external or internal fixation; rigid fixation or flexible fixation. Previous studies have shown that early weight bearing enhances the fracture healing process (Bailón-Plaza and van der Meulen, 2003, Geris et al., 2003), and fixation allows early motion and partial loading of fractured bone following a surgical procedure. Several animal models have been used to study the influence of fixation stiffness on fracture healing process (Goodship and Kenwright, 1985, Claes et al., 1998), and Schell et al. (2008) demonstrated that significant reduction in fixation stiffness could result in delayed healing and non-union.

Rigid fixation

When a rigid fixation plate is applied to fractured bone in conjunction with interfragmentary compression, it resists motion of the bone fragments. Due to the extensive implant bone contact and interfragmentary compression to maintain absolute stability, the compression plating induced a combination of primary bone healing and gap healing in the fractured bone (Claes et al., 2012, Perren, 2002c).

Flexible fixation:

Flexible fixation allows some interfragmentary motion across fracture while providing adequate stability to the fracture site, which has led to its popularity in clinical practice (Schmal et al., 2011). An increase in callus formation has been observed in fracture site stabilized by flexible fixation (Epari et al., 2010, Isaksson, 2012). This can result in better healing outcomes through endochondral ossification and angiogenesis development (Augat et al., 1998, Bottlang et al., 2017, Claes and Heigele, 1999, Claes et al., 1998).

Internal fixation using plates is generally applied on a single side to reduce the invasion to surrounding tissues. New implants like locking compression plates further reduce plate bone contact through pre-contoured plate and locking head screws (Refer to xx). This requires the implant to have optimum configurations to maintain adequate stability and preserve biological competence of surrounding tissues (Gautier and Sommer, 2003). The number of screws in the fixation need to be optimised, i.e. minimum number to reduce screw density and screw loading, at the same time enough to avoid screw breakage due to overload. At the same time, the potential risk of bone resorption and screw pull-out / loosening should be considered to ensure the construct stability. Due to locking head screws, the length of the screws does not contribute much to the fracture healing, therefore screws can be monocortical in dimension. While bicortical screws provide better stability due to increased bone screw interface, they do not perform better in terms of screw fatigue failure. Thus, monocortical screws are preferred where bone extremities are good quality(Gautier and Sommer, 2003), which may not be the case in osteoporotic bones (discussed in subsequent sections).

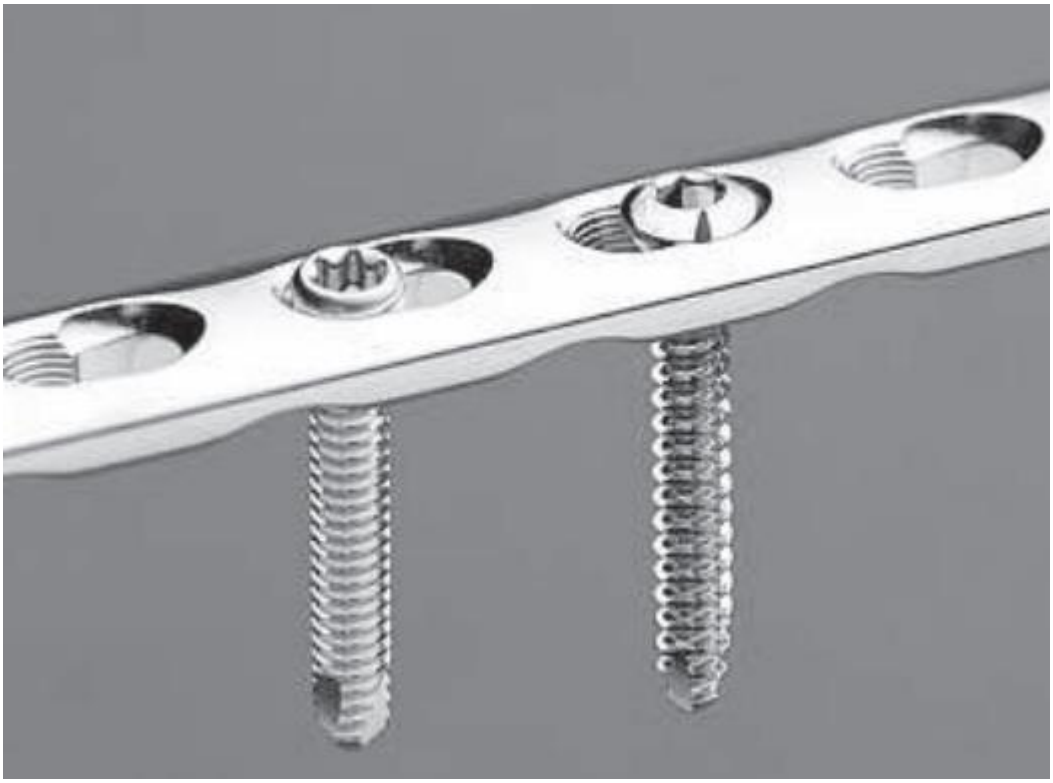

Figure 2.3 Photograph showing Locking Compression Plate (LCP) with locking screws (left) and conventional screws (right) (Figure presented from Aguila et al. (2005) with permission)

Orthopaedic surgeon can adjust the locking compression plate (LCP) mechanical stiffness and flexibility by configuring distance between bone and plate, i.e. BPD, or the distance between innermost screws across the fracture gap, i.e. Working length (WL). It is widely known that the configuration of bone fracture fixation affects mechanical micro-environment of the fracture site, however optimal fixation configurations are yet to be established for different fracture geometries (Epari et al., 2007). LCP constructs outperformed dynamic compression plates and limited contact dynamic compression plate (LC-DCP) in equine models in terms of yield strength and therefore, can withstand higher loads (Florin et al., 2005). Another study on distal metaphyseal gap in humerous of canine model compared LCP with DC-LCP in axial compression and torsion and observed that LCP constructs are stiffer in static axial compression, but less stiff in cyclic compression and torsion (Filipowicz et al., 2009).

Choosing optimum fixation configuration can also result in high plate span ratio and low plate screw density. A high span ratio is desirable as it decreases load onto the plate. Similarly, low plate screw density can reduce fatigue failure during cyclic loading

(Gautier and Sommer, 2003). They can be achieved by higher WL, as fewer screws need to be inserted (Gautier and Sommer, 2003). However, caution needs to be adopted while increasing working length, as it also increases the risk of screw pull-out or undermine the overall stability of the fixation.

Miramini et al. (2016b) compared IFS and MSC differentiation during early stage of healing for different LCP configurations under compressive quasi-static load, by adopting a widely accepted (Isaksson et al., 2006) mechano-regulation theory of Prendergast et al. (1997) and suggested that IFS of a relatively large gap size is very sensitive to the change of bone plate distance (BPD) and working length (WL) of a LCP. Stoffel et al. (2003a) demonstrated that risk of plate failures doubles for a gap size of 6mm compared to a smaller gap size of 1mm with an increase in WL under dynamic loading. Oblique fractures are believed to have reduced stability in comparison to transverse fracture and therefore the optimal configuration of LCP for oblique fractures may vary from transverse fractures. Therefore, more insight is necessary on how fixation stability can influence molecular and cellular activities during bone healing.

Various configuration of fixation can have varied impact on healing process. For example, too flexible fixation can have adverse impact on the stability of the fracture due to excessive IFM resulting in fibrous tissue formation, while too rigid fixation can impair the healing process due to lack of movement (Ahmad et al., 2007, Miramini et al., 2014a, Miramini et al., 2016b). Thus, optimum configuration of fixation is of utmost importance for fixation stability and optimum healing outcome. Further, there is limited research on the effects of dynamic loading on growth factor and cell transport during early stage of fracture healing under different LCP configurations.

Mechano-regulation principles

Several mechano-regulation principles have been proposed to explain bone fracture healing under mechanical stimuli. Pauwels (1960) initially identified invariants of strain and stress tensor as the stimuli that affects bone healing. Later on, Perren (1979) suggested interfragmentary strain (IFS) as the factor that regulates differentiation pathway during bone fracture healing. In a theory similar to Pauwels, a combination of octahedral shear and hydrostatic stress was proposed by Carter et al. (1988) to predict the tissue regeneration. It was proposed that deviatoric strains were beneficial to

osteogenic differentiation, while dilatational strains were detrimental to bone healing. Further, (Claes et al., 1998) quantified deviatoric strain as the influencing factors, while Prendergast et al. (1997) introduced a tissue differentiation model based on a biphasic poroelastic finite element model of tissues and proposed two biophysical stimuli as the mechanical factors affecting healing: octahedral shear strain of the solid phase and fluid flow velocity in the interstitial fluid phase (Isaksson, 2012). According to this theory, high deviatoric displacement and fluid velocity magnitudes result in fibrous tissue differentiation, whereas if both stimuli are low, bone formation may occur. Further, (Lacroix et al., 2002b) classified the types of differentiation according to the levels of biophysical stimulation. According to their theory, high stimulus levels favours differentiation into fibroblasts, intermediate levels favours chondrocytes and low levels favours osteoblasts. Isaksson et al. (2006) compared all these theories and concluded that mechano-regulation theory of Prendergast et al. (1997) can predict bone healing most accurately. These theories have been implemented in computational models to numerically predict tissue regeneration of fracture callus (Andreykiv et al., 2008, Carter et al., 1988, Claes and Heigele, 1999, Garcia-Aznar et al., 2007, Geris et al., 2004, Gómez-Benito et al., 2011, Isaksson et al., 2008a). Assuming MSC migration, proliferation and differentiation and tissue formation are governed by mechanical stimuli within the callus, these models have predicted the sequence and pattern of healing. It is known hat bone fracture healing is also influenced by the biological factors such as growth factors, but these were not considered in these theories.

2.5.2. Biochemical stimuli

The tissue formation and distribution throughout the healing process depend on both the biochemical and biomechanical microenvironment of the fracture site (e.g. concentration of growth factors and interfragmentary moment arising from fracture geometry, loading conditions and fixation stiffness) (Ghimire et al., 2018). Change in localised growth factors concentration can influence the type of tissue formed in callus (Joyce et al., 1990b).

Interstitial fluid flow

It has been well established that bone fracture healing requires stability and vascularisation. Decreased vascularity is associated with delayed fractured healing

(Loboa et al., 2001). Blood flow and interstitial fluid flow is paramount for the adequate supply of nutrients, oxygen and bone forming mesenchymal stem cells into the fracture site as well as removal of waste and debris from fracture callus like hematoma and blood clot. Interstitial fluid flow and fluid shear stress is known to mediate mechanical stimuli in fracture callus (Prendergast et al., 1997). Fluid flow velocity is highly affected by the change in loading frequency due to the viscoelastic nature of fluid filled poroelastic callus. Interstitial fluid delays the strain variation under cyclic loading. Further, the interstitial fluid has to evacuate from the pores before callus is deformed, which results in increased deviatoric strain and increased octahedral strain in a poroelastic callus model (González-Torres et al., 2010a).

MSCs

MSCs are the multipotent stromal cells from nonhematopoietic origin, that have ability to differentiate to multiple cell lineages including fibroblasts, chondrocytes and osteoblasts necessary for bone healing process (Fayaz et al., 2011). Due to their osteogenic and pro-angiogenic potential and proliferation ability (Decaris et al., 2012, Caplan and Dennis, 2006), they are able to stimulate the growth of bone, cartilage, adipose tissue, tendon and muscle and are widely used in a range of biomedical fields (Ivkovic et al., 2011, Miller et al., 2011, Pećina and Vukičević, 2007). During bone fracture, MSCs originate from in fracture are periosteum, bone marrow and surrounding soft tissues (Rosset et al., 2014). It has been shown that injecting of bone marrow with MSC alone resulted bone union in majority of patients who had reported delayed healing or non-union in these clinical studies (Goel et al., 2005, Siwach et al., 2001, Hernigou et al., 2005).

Mesenchymal stem cells differentiation pathway into fibroblasts, chondrocytes or osteoblasts under the influence of mechanical stimuli have been explained using the theory of Prendergast et al. (1997) as follows.

- $S < 1$ – MSC differentiation into osteoblasts
- $1 < S < 3$ – MSc differentiation into chondrocytes
- $S > 3$ – MSC differentiation into fibroblasts

Where, *S* is the mechanical stimulation index derived by Prendergast et al. (1997). Some studies have included mechanical stimuli mediated cell differentiation; however mechanical stimuli mediated cell migration hasn't been investigated yet.

Growth factors

MSC differentiation into osteoblast and chondrocytes are highly influenced by the cytokines and growth factors like TGF-beta family. Growth factors are the large molecules whose transport can be enhanced under dynamic loading in callus as a porous media (Mauck et al., 2003). The growth factors affecting bone healing can be categorized as osteogenic growth factors and chondrogenic growth factors, depending on their function. Osteogenic growth factors (e.g. BMP -2, -4, -6,) and chondrogenic growth factors (e.g. TGF β -2, -3) are two important types of growth factors, released from the periosteum of cortex (Barnes et al., 1999), that regulate the differentiation of MSCs into osteoblasts and chondrocytes, respectively (Cheng et al., 2004, Yamaguchi, 1995, Cho et al., 2002, Marsell and Einhorn, 2009, Solheim, 1998). The localised expression of growth factors leads to concentration gradient in the callus which plays crucial role in tissue regeneration by regulating MSCs migration and differentiation. In clinical practice, the bone fractures are often treated with growth factors from TGFβ superfamily, BMP-2 and BMP-7 to accelerate the bone healing process (Devescovi et al., 2008). The temporal distribution of different growth factors into fracture site has been documented in different animal models (Tsiridis et al., 2007). As they migrate into fracture site, their swift transport to all parts of callus can enhance bone healing. However, there's not enough literature to support that transport of growth factor can be enhanced by mechanical stimuli.

Bio-regulatory principles

An alternative approach has been developed for bone healing simulation, that recognises several bio-regulatory parameters affecting bone healing. In the very beginning, they are cytokines and macrophages that emit inflammatory signals to encourage migration of inflammatory cells. Later, they are the growth factors that regulate migration and differentiation of mesenchymal stem cells. Bailón-Plaza and van der Meulen (2003) first proposed a bio-regulatory model treating biochemical stimuli as the governing factor for fracture healing. They were the pioneers to incorporate these growth factors into fracture healing model. While their model could predict bone healing process through

several weeks in rats, their model did not account for the mechanical stimuli that can arise in bone during fracture healing. The PDE model was later further developed by other researchers (Amor et al., 2009, Geris et al., 2006, Ambard and Swider, 2006, Amor et al., 2011), and elaborated to simulate angiogenesis(Peiffer et al., 2011), oxygen (Carlier et al., 2015) and describe revascularisation, which is a critical healing process during later stages of fracture healing (Geris et al., 2008, Checa and Prendergast, 2009, Peiffer et al., 2011, Geris et al., 2010, Simon et al., 2011). However, the effects of dynamic loading on the transport of cells and growth factors were not explicitly investigated in these models (Refer to Figure 2.4).

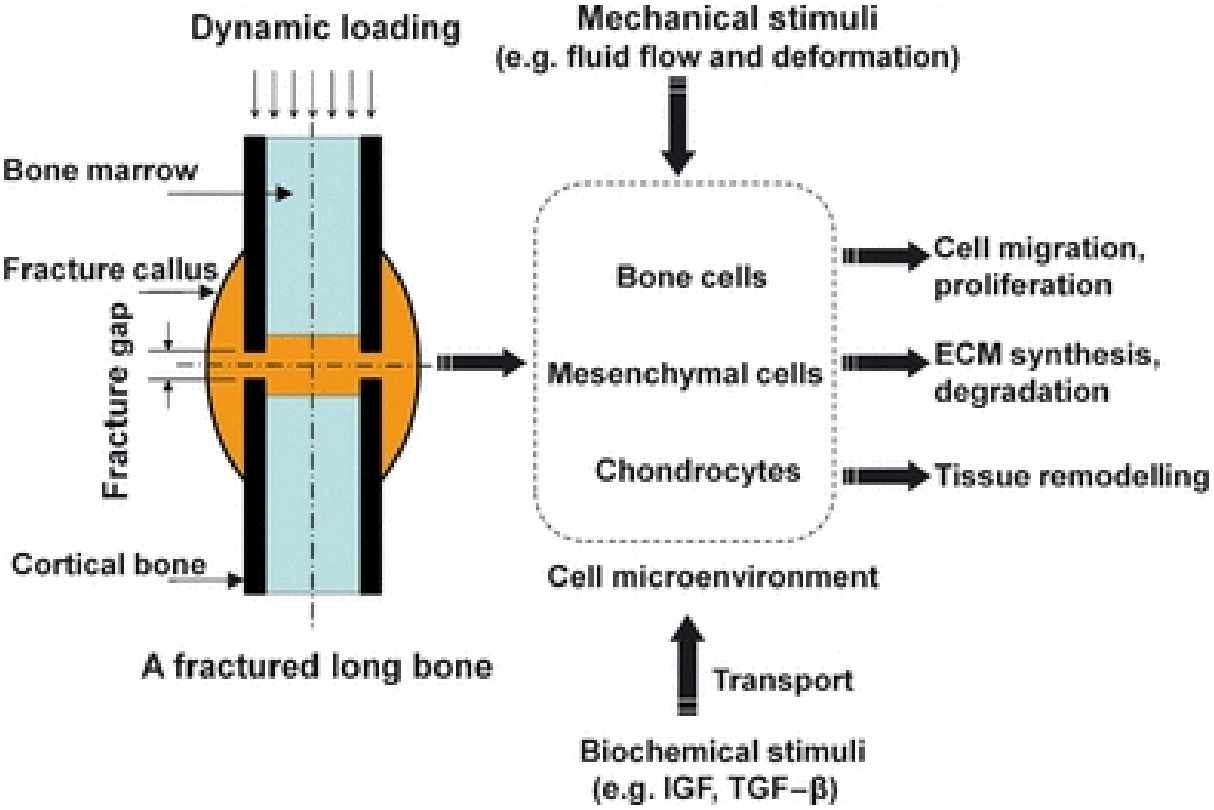

Figure 2.4 Schematic diagram showing mechanical and biochemical stimuli affecting cellular micro-environment of bone fracture healing (Figure presented from Zhang et al. (2012a) with permission)

2.5.3. Osteoporosis

Osteoporosis is the bone condition characterized by reduced bone density and porous bone, which is highly prone to fracture. As a result, osteoporotic bones are prone to delayed healing and amplify the risk of fixation failure. Generally, bone fracture occurs

when the load applied exceeds strength of the bone. In case of osteoporosis, bone fracture occurs with minimal trauma and is commonly termed as fragility fractures. The most common fractures of hip, humerous, wrist and vertebrae due to osteoporosis are usually associated with high risk of subsequent fragility fractures. Not only does this lead to loss of earnings, discomfort and reduced mobility to the individual, it also incurs a huge socio-economic burden to the country. In countries with higher elder population like Japan, the cost and incidence of osteoporotic fractures are equivalent to that of heart disease (Brandi and Piscitelli, 2013). With an increase number of active aging population, the osteoporotic fractures are already on the rise (Lewis et al., 2015). Accounting for the high prevalence of these osteoporotic fractures in projected world population with increased life expectancy, WHO has even regarded osteoporosis to be a critical health problem after cardiovascular diseases (Kanis et al., 2008). However, the impact of osteoporosis on fracture healing is still unknown and efficient management of osteoporotic bone fractures would require better understanding of the underling mechanisms (Zhang et al., 2017b).

Degenerative bone diseases like osteoporosis not only increase the risk of bone fractures, but also influence the speed of recovery during fracture repair and quality of healed bone (Anakwe et al., 2008). Further, the bone has higher fracture risk and its ability to heal back following a fracture is greatly reduced. Along with the loss of mineralised bone component, there is also changes in the diffusion and perfusion of non-mineralised bone marrow (Griffith, 2013). Since bone marrow is home to multipotent mesenchymal stem cells, the mesenchymal stem cells migrating to the fracture site from surrounding cells, periosteum and bone marrow is reduced as well, therefore the transport of these cells into all parts of callus is even more crucial. Moreover, there could be change in MSC differentiation away from osteoblasts (Nuttall et al., 1998) and the ability of these cells to respond to the mechanical stimuli may differ as well. As Biology and mechanics need to be in harmony for an optimum bone healing process, the altered biological processes may call for altered mechanical signals for healing to occur in osteoporotic bones.

LCP with bicortical screws are generally preferred in case of osteoporotic bone fractures (Gautier and Sommer, 2003). The thickness of cortical bone determines the screw working length while cortical bone have reduced thickness due to osteoporosis. As a result, monocortical thickness is insufficient for screw working length to withstand

rotational displacement and there are increased chances of threads wearing out in bone leading to implant failure (Alon, 2006).

2.6. Transport of cells and growth factors

Transport of cells and growth factors in fracture callus can occur through passive medium like diffusion, and through active transport like advection which requires energy to proceed. Experimental findings have supported enhanced solute transport (cells and growth factors) under loading (O'Hara et al., 1990).

Dynamic loading is one of the physiological processes that induce fluid flow in the callus. Interstitial fluid flow has been demonstrated to influence cell migration on tumour cells, fibroblasts and endothelial cells (Boardman and Swartz, 2003, Ng and Swartz, 2003, Polacheck et al., 2011, Shields et al., 2007). As adequate supply of nutrients and oxygen is vital for successful healing, quicker transport of such solutes into fracture callus is highly important during early stage of healing. Enhanced solute transport under dynamic loading has been supported by experimental studies on articular cartilage and callus tissue (Bonassar et al., 2001, Zhang, 2011, Witt et al., 2014). There was 20% increase in growth factor IGF-I in articular cartilage under a cyclic loading (Zhang et al., 2007). Their transport could be promoted by callus stimulation under the influence of external loading, particularly the frequency of loading. It has been observed that frequency of loading has direct impact on the fluid flow velocity of callus (González-Torres et al., 2010a). Enhanced transport of large solutes like growth factors were reported under dynamic loading with physiological range of frequency in a callus like porous media (Mauck et al., 2003).

This suggests that interstitial fluid flow guide cell migration, however the directed cell migration due to fluid flow under the influence of mechanical stimuli i.e. advection isn't well understood, and studies in this area are limited. The transport of cells and growth during early stage of healing under free diffusion, and chemical gradient has been incorporated in some computational models (Geris et al., 2008, Andreykiv et al., 2008, Isaksson et al., 2008a, Peiffer et al., 2011) however the transport of cells and growth factors through interstitial fluid under mechanical stimuli during bone healing haven't been studied so far.

Therefore, a model has been developed in this research that considers both direct contribution of mechanical stimuli induced by dynamic loading and indirect contribution through the advective transport of cells and growth factors within the fracture callus. Further, this research investigates the role of dynamic loading on cells and growth factor transport during early stage of bone fracture healing under different fracture geometries and fixation configuration of Locking Compression Plates (LCP). In addition, this research investigates the role of dynamic loading on biomechanical microenvironment in osteoporotic bones. Finally, the research also investigates bone fracture healing under intramembranous and endochondral ossification. Thus, this research has been undertaken to further extend the current understanding of impact of mechanical micro-environment on cell differentiation and tissue development during fracture healing processes.

Chapter 3.

Role of dynamic loading on early stage of bone fracture healing

3.1. Abstract

After fracture, mesenchymal stem cells (MSCs) and growth factors (e.g. chondrogenic growth factors and osteogenic growth factors) migrate into the fracture callus to exert their biological actions. Previous studies have indicated that dynamic loading induced tissue deformation and interstitial fluid flow could produce a biomechanical environment which significantly affects the healing outcomes. However, the fundamental relationship between the various loading regimes and different healing outcomes has not still been fully understood. In this study, we present an integrated computational model to investigate the effect of dynamic loading on early stage of bone fracture healing. The model takes into account cell and growth factor transport under dynamic loading, and mechanical stimuli mediated MSC differentiation and tissue production. The developed model was firstly validated by the available experimental data, and then implemented to identify the loading regimes that produce the optimal healing outcomes. Our results

demonstrated that dynamic loading enhances MSC transport in a spatially dependent manner. For example, in comparison to free diffusion, a dynamic loading could significantly increase MSC content in endosteal zone of callus but has little influence in periosteal and cortical zones. In addition, the dynamic loading is seen to significantly increase the uptake of chondrogenic growth factors in both cortical and periosteal zones of cartilage but has little effect on the osteogenic growth factor uptake in callus. Furthermore, there could be an optimal dynamic loading regime (e.g. 10% strain at 1Hz) which could potentially significant enhance endochondral ossification.

3.2. **Introduction**

Throughout the bone fracture healing process, tissue production and distribution depend on both the biochemical and biomechanical microenvironments of the fracture site (*e.g.* concentration of growth factors and interfragmentary movement) (Chao et al., 1998). The fundamental understanding of the influence of both chemical and mechanical factors that govern the healing processes is critical for achieving an optimum healing outcome.

Immediately after a fracture, the fracture gap is filled with hematoma formed as a result of the rupture of tissue and blood vessels. The tissue damage leads to the release of growth factors into the fracture site, which are responsible for a series of biological processes, such as chemotaxis of various cells (e.g. MSCs and fibroblasts) and modulation of tissue genesis (Schindeler et al., 2008). MSCs are multipotent cells that have the potential to differentiate into multiple cell lineages including fibroblasts, chondrocytes and osteoblasts (Baksh et al., 2004). Osteogenic growth factors (e.g. BMP -2, -4, -6,) and chondrogenic growth factors (e.g. TGF β -2, -3) are two important types of growth factors, released from the periosteum of cortex (Barnes et al., 1999), that regulate the differentiation of MSCs into osteoblasts and chondrocytes, respectively (Cheng et al., 2004, Yamaguchi, 1995, Cho et al., 2002, Marsell and Einhorn, 2009, Solheim, 1998). The localised expression of growth factors leads to concentration gradient in the callus which plays crucial role in formation of bone and cartilage tissue by regulating MSCs migration and differentiation.

During early stage of healing, cells and growth factors need to diffuse into the fracture site. Within the callus, it is suggested that interstitial fluid flow induced by physiologically-relevant loading regulates the transport of growth factors (Kelly and Jacobs, 2010). The cell migration with interstitial fluid flow has been shown experimentally in in-vitro studies on tumour cells (Polacheck et al., 2011, Shields et al., 2007), lymphatic cells (Boardman and Swartz, 2003) and fibroblasts (Ng and Swartz, 2003). The experimental study of Polacheck et al. (2011) demonstrated that cells seeded in porous scaffold migrates with interstitial fluid flow. Their experimental results showed that the strength of fluid flow as well as the gradient of cell density determines the direction of cell migration. Thus, it is reasonable to model cell migration within a fully saturated porous tissue by using diffusion-advection equation. By treating biological tissue as a three phase mixture (i.e. extracellular solid matrix, interstitial fluid and solute), previous studies have shown that cyclic loading enhances Insulin-like growth factor transport in cartilage and benefits cartilage tissue biosynthesis (Zhang et al., 2008c, Zhang et al., 2010b, Zhang et al., 2007). The enhanced solute transport when the tissue is subjected to cyclic loading has also been supported by experimental studies on articular cartilage (Bonassar et al., 2001, Evans and Quinn, 2006, O'Hara et al., 1990) and callus tissue (Witt et al., 2014). Further, there could be an optimal loading regime that significantly increases solute transport in cartilage compared to free diffusion (Zhang et al., 2007). However, the role of dynamic loading on solute transport in early fracture callus has not been fully understood and the studies in this area are limited.

The biological actions of MSCs are also mediated by their mechanical microenvironment (e.g. callus deformation and fluid flow) (Guilak et al., 2009). Experimental studies have also demonstrated that cellular response in the callus is very sensitive to the mechanical microenvironment (Klein et al., 2003, Miclau et al., 2002, Le et al., 2001). While adequate micromotion enhances the growth of callus at early stage of healing (Kenwright and Goodship, 1989, Goodship et al., 1998), excessive movements of fracture gap is detrimental to revascularization and tissue formation (Claes et al., 2002, Claes et al., 2003). Several mechano-regulation theories have been proposed to elucidate the influence of mechanical stimuli on tissue regeneration. Pauwels (1960) identified stress invariants as the stimuli to modulate tissue formation in fracture callus, and Perren (1979) suggested the interfragmentary strain (IFS) magnitude (IFS=gap movement over

gap size) plays an important role in tissue differentiation, with a low IFS magnitude (< 2%) leads to direct bone formation whereas higher strains (> 10%) results in fibrous tissue formation.

The mechano-regulation theories that modulate bone healing process have been implemented in computational models to numerically predict tissue regeneration in fracture callus (Carter et al., 1998a, Garcia-Aznar et al., 2007, Andreykiv et al., 2008, Prendergast et al., 1997, Lacroix et al., 2002b, Claes and Heigele, 1999, Gomez Benito et al., 2005, Isaksson et al., 2008a, Geris et al., 2004). Assuming that migration, proliferation and differentiation of MSCs, and tissue formation are governed by mechanical stimuli within the callus, these models predicted the sequence and pattern of healing (Lacroix and Prendergast, 2002, Gardner and Mishra, 2003, Isaksson et al., 2006). It was known that bone fracture healing is also influenced by biochemical stimuli like growth factors and cytokines, but their effects on healing were not taken into account in these models.

Bailon-Plaza and van der Meulen (2001) proposed a bioregulatory model treating biochemical stimuli as the governing factor for bone fracture healing, and the model was later on further extended to incorporate the effects of mechanical stimuli on cartilage and bone formation. Their results showed a significant reduction in bone formation when mechanical stimuli were delayed until 6 weeks after fracture, and demonstrate the importance of mechanical stimuli during early stage of healing (Bailón-Plaza and van der Meulen, 2003). The PDE model was later further developed by other researchers (Amor et al., 2009, Geris et al., 2006, Ambard and Swider, 2006, Amor et al., 2011), and elaborated to simulate angiogenesis and describe revascularisation, which is a critical healing process during later stages of fracture healing (Geris et al., 2008, Checa and Prendergast, 2009, Peiffer et al., 2011, Geris et al., 2010, Simon et al., 2011). However, the effects of dynamic loading on the transport of cells and growth factors were not explicitly investigated in these models.

The combined effects of biochemical and biomechanical stimuli on bone healing, particularly the dynamic loading induced advective cell and growth factor transport, have not been fully investigated so far. Therefore, the focus of this study is to investigate the effect of dynamic loading on solute transport and tissue differentiation within fracture callus, particularly at early stage of healing. As shown in Figure. 3.1, the

developed model takes into account the biomechanical stimuli mediated stem cell differentiation and tissue production, as well as advective transport of cells (i.e. MSCs, fibroblasts, chondrocytes and osteoblasts) and growth factors (i.e. osteogenic growth factors and chondrogenic growth factors) induced by interstitial fluid flow as a result of dynamic loading. The model is firstly validated by using available experimental data (Harrison et al., 2003), and then implemented to investigate the effect of different loading regimes on healing outcomes.

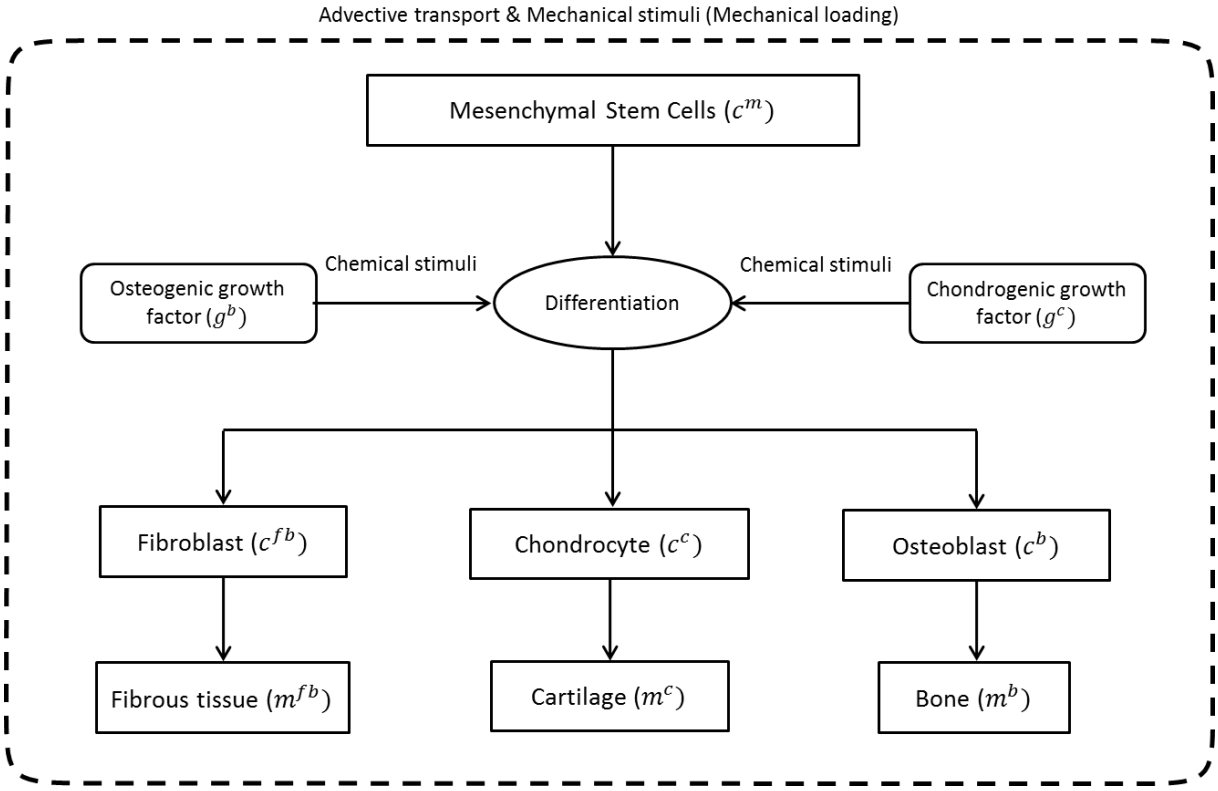

Figure. 3.1 A schematic overview of the model proposed in this study

3.3. **Methodology**

The theory of porous media has been applied in numerous studies to model biological soft tissues like fracture callus, blood vessels and articular cartilage (Hund and Antaki, 2009, Ambard and Swider, 2006, Miramini et al., 2016a, Zhang et al., 2012a). In present study, fracture callus was treated as a poroelastic material consisting of a solid phase representing various callus tissues (i.e. fibrous tissue, cartilage and bone), an interstitial fluid phase and a solute phase comprising of callus cells (i.e. MSCs, fibroblasts, chondrocytes and osteoblasts) and growth factors (i.e. chondrogenic and osteogenic

growth factors). Building on our previous developed computational models for fracture healing (Miramini et al., 2016b, Zhang et al., 2017a), the present study proposed an integrated model which takes into account cell and growth factor transport under dynamic loading, and mechanical stimuli mediated MSC differentiation and tissue production. The developed model could potentially be implemented to identify the loading regimes that produce the optimal healing outcomes.

The volume fraction of solid, fluid and solute phase of the porous callus domain can be represented by ϕ^s, ϕ^f and ϕ^w, respectively. As the volume of cells, growth factors and other nutrients are ignorable at tissue level compared to the volume of solid and fluid phase of the callus (Guérin et al., 2009), we obtain:

$$\phi^f + \phi^s \cong 1 \tag{3.1}$$

The relationship between the medium volume based solute concentration ($\bar{c}^{\,w}$) and solvent volume based solute concentration (c^w) can be expressed as:

$$\bar{c}^{\,w} = \phi^f c^w \tag{3.2}$$

Similarly, the medium volume based tissue concentration ($\bar{c}^{\,s}$) can be expressed as:

$$\bar{c}^{\,s} = (1 - \phi^f)c^s \tag{3.3}$$

where c^s is solvent volume based tissue concentration.

Transport of cells and growth factors

The transport equations for cells and growth factors can be obtained based on conservation of mass of the solute in fluid phase (Gardiner et al., 2007, Zhang et al., 2010a).

Mesenchymal stem cells (c^m)

$$\frac{\partial \bar{c}^{\,m}}{\partial t} = -\nabla \bullet \left(-D^m \nabla \bar{c}^{\,m} + \mathbf{v}^f \bar{c}^{\,m}\right) + S_p^m - S_d^m \tag{3.4}$$

where S_p^m and S_d^m are the production and degradation rate of MSCs, respectively. $\mathbf{v}^f$ is interstitial fluid velocity and D^m is the diffusion coefficient of MSCs with consideration of tortuosity factor for the callus matrix (Geris et al., 2008) as follows:

$$D^m = \frac{D^{hm} m}{(K^{hm})^2 + m^2} \tag{3.5}$$

where D^{hm} and K^{hm} are coefficients of cell migration depending on the total matrix density (m) of the callus.

As MSCs differentiate into fibroblast, chondrocyte and osteoblast in the callus domain, it leads to mass sink of MSCs (S_d^m) given by:

$$S_d^m = \left(k_d^{fb} + k_d^c + k_d^b \right) \bar{c}^{\,m} + \left(\lambda_d^{fb} + \lambda_d^c + \lambda_d^b \right) \bar{c}^{\,m} \tag{3.6}$$

where k_d^{fb}, k_d^c and k_d^b are the chemical stimuli mediated differentiation rates of MSCs into fibroblast, chondrocyte and osteoblast, respectively, which can be expressed by using Hill function (Bailon-Plaza and van der Meulen, 2001) as follows:

$$k_d^b = \frac{Y_1 g^b}{H_1 + g^b} \tag{3.7}$$

$$k_d^c = \frac{Y_2 g^c}{H_2 + g^c} \tag{3.8}$$

where g^c and g^b are concentration of chondrogenic growth factor and osteogenic growth factor, respectively. H_1, H_2, Y_1 and Y_2 are parameters representing growth factor mediated MSC differentiation. k_d^{fb} is assumed to be constant (Olsen et al., 1995).

Similarly, λ_d^{fb}, λ_d^c and λ_d^b are the mechanical stimuli mediated differentiation rates of MSCs into fibroblasts, chondrocytes and osteoblasts, respectively.

As shown in Figure. 3.1, mechanical loading directly influences MSC differentiation through changing the mechanical microenvironment of MSCs (i.e. simulation index, refer to Figure. 3b). On the other hand, mechanical loading induced interstitial fluid flow in callus enhances the transport of growth factors (i.e. osteogenic growth factor and chondrogenic growth factor) and therefore indirectly enhances chemical stimuli resulting in so called “synergistic effects” (Figure. 3.1), which has been experimentally

demonstrated in the previous experimental studies (Helm et al., 2005). In present study, these synergistic effects have been explicitly incorporated in our computational model.

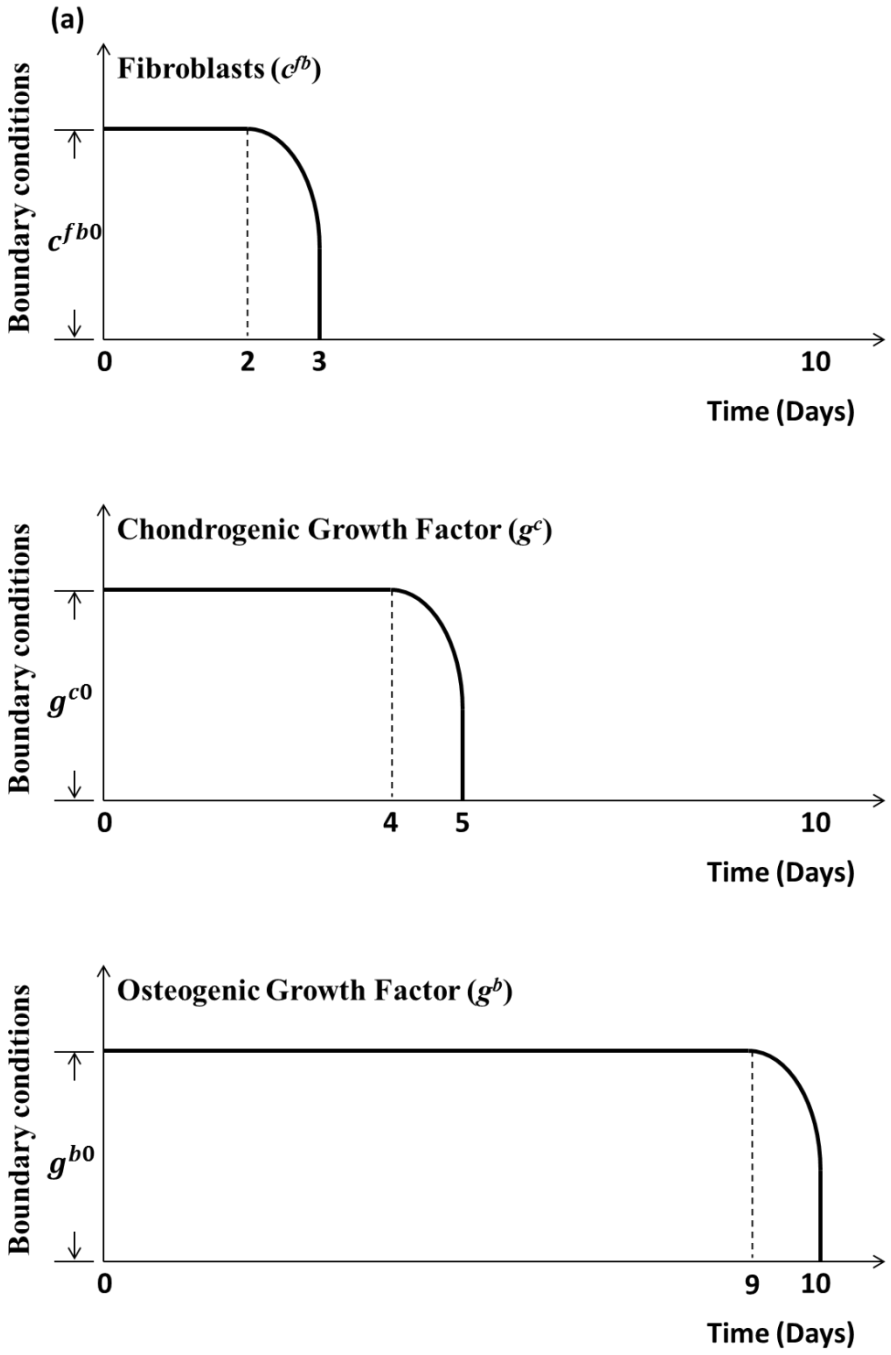

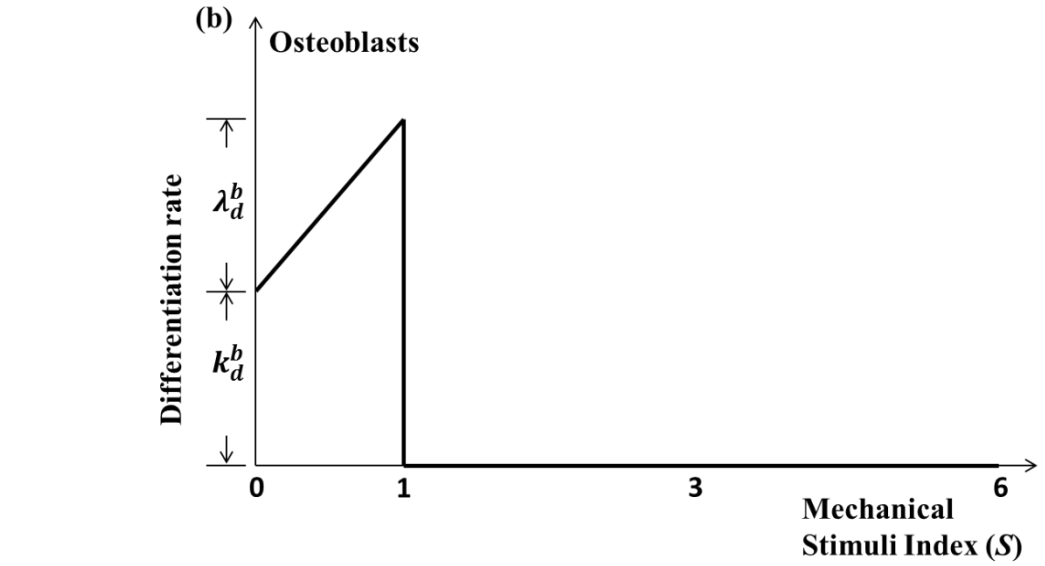
(b)
Osteoblasts
Differentiation rate
λ_d^b
k_d^b
0
1
3
6
Mechanical
Stimuli Index (S)

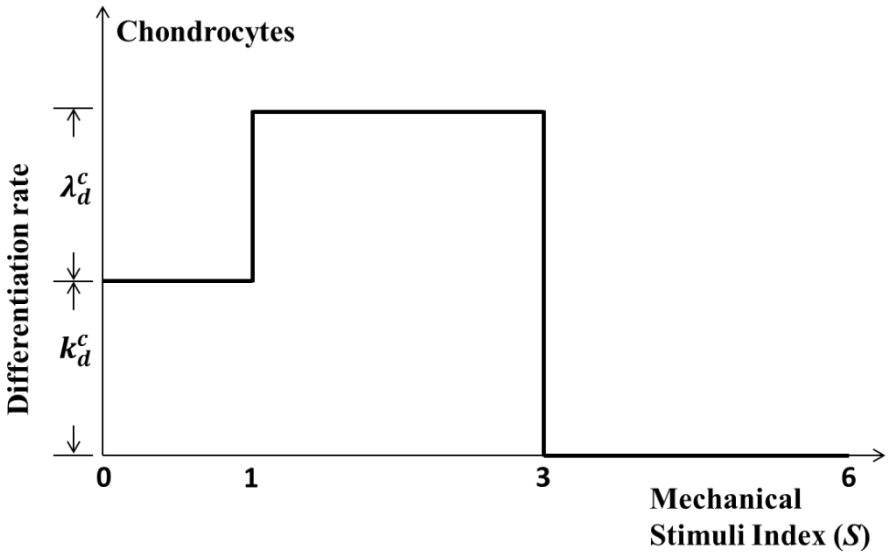
Chondrocytes
Differentiation rate
λ_d^c
k_d^c
0
1
3
6
Mechanical
Stimuli Index (S)

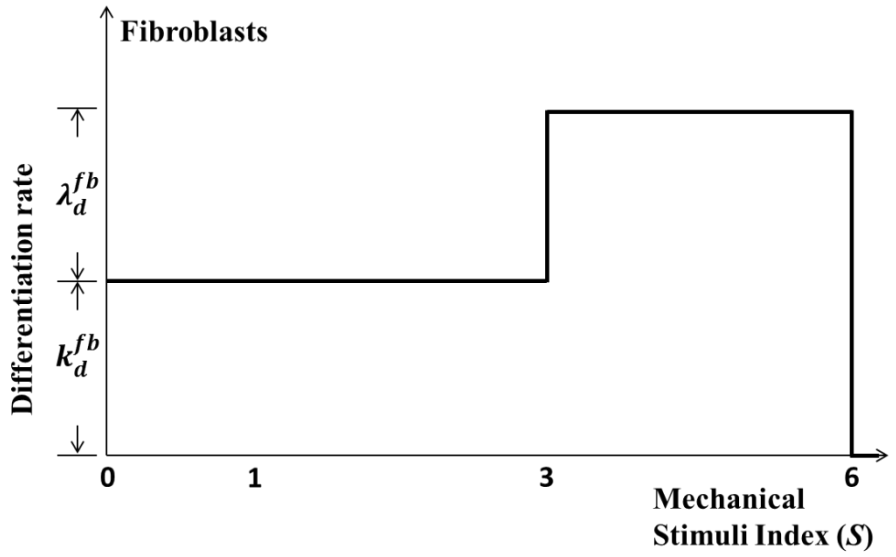
Fibroblasts
Differentiation rate
λ_d^{fb}
k_d^{fb}
0
1
3
6
Mechanical
Stimuli Index (S)

Figure. 3.2 (a) Boundary conditions of fibroblasts (c^{fb}); chondrogenic growth factor (g^{c}); and osteogenic growth factor (g^{b}) adopted in this study (Geris et al., 2008); and **(b)** Representative cell differentiation rate due to chemical stimuli and mechanical stimuli based on mechanical stimuli index (S) (Andreykiv et al., 2008, Miramini et al., 2016b). This is based on the concept that if the level of mechanical stimuli is unfavourable, the differentiation rate of MSCs into that cell type is completely inhibited (Bailón-Plaza and van der Meulen, 2003)

Fibroblasts (c^{fb}), Chondrocytes (c^{c}), Osteoblasts (c^{b})

The transport equations of Fibroblasts (c^{fb}), Chondrocytes (c^{c}), Osteoblasts (c^{b}) can be expressed as a combination of diffusion and advection (Flegg et al., 2015, Heck et al., 2015, Zhang et al., 2012a), i.e.

$$\frac{\partial \bar{c}^{\,\alpha}}{\partial t} = -\nabla \bullet \left(-D^{\alpha}\nabla \bar{c}^{\,\alpha} + \mathbf{v}^{f}\bar{c}^{\,\alpha}\right) + S_p^{\alpha} - S_d^{\alpha} \tag{3.9a}$$

$$S_p^{\alpha} = (k_d^{\alpha} + \lambda_d^{\alpha})c^{m} \tag{3.9b}$$

where, α = fb (fibroblasts), α = c (chondrocytes) and α = b (osteoblasts). S_p^{α} is the production rate of α cells which is assumed to be the sum of chemical stimuli mediated production rate (k_d^{α}) and mechanical stimuli mediated production rate (λ_d^{α}). S_d^{α} is the degradation rate of α cells and D^{α} is the diffusion coefficient of α cells in fracture callus.

The differentiation rates of MSCs into fibroblasts, chondrocytes and osteoblasts are assumed be regulated by mechanical stimuli depending on the magnitude of stimuli index (S), as follows:

$$S_{pm}^{w} = \begin{cases} S_{pm}^{b} = \lambda_d^{b}\,\bar{c}^{\,m}, & S_{pm}^{c} = S_{pm}^{fb} = 0\,, & for\ S < 1 & (osteoblasts) \\ S_{pm}^{c} = \lambda_d^{c}\,\bar{c}^{\,m}, & S_{pm}^{b} = S_{pm}^{fb} = 0\,, & for\ 1 < S < 3 & (chondrocytes) \\ S_{pm}^{fb} = \lambda_d^{fb}\,\bar{c}^{\,m}, & S_{pm}^{b} = S_{pm}^{c} = 0\,, & for\ S > 3 & (fibroblasts) \end{cases} \tag{3.10}$$

where S is obtained from interstitial fluid phase velocity ($\mathbf{v}^{f}$) and octahedral shear strain (τ) within the callus (Huiskes et al., 1997). It is assumed that, during early stage of healing, low magnitude of stimuli index (S < 1) results in differentiation of osteoblast, moderate magnitude of stimuli index (1 < S < 3) favours differentiation of chondrocytes while high magnitude of stimuli index (S < 1) leads to fibroblast differentiation (Miramini et al., 2016b) .

$$S = \frac{\tau}{0.0375} + \frac{\mathbf{v}^f}{3 \times 10^{-6}\,(m/s)} \tag{3.11}$$

Chondrogenic growth factors (g^c) and osteogenic growth factors (g^b)

The mass balance equation for chondrogenic (g^c) and osteogenic growth factor (g^b) is given by

$$\frac{\partial \bar{g}^{\,\beta}}{\partial t} = -\nabla \bullet \left(-D^{\beta} \nabla \bar{g}^{\,\beta} + \mathbf{v}^{\boldsymbol{f}}\, \bar{g}^{\,\beta}\right) + S_p^{\beta} - S_d^{\beta} \tag{3.12}$$

where $\beta = c$ (chondrogenic growth factors) and $\beta = b$ (osteogenic growth factors). S_p^{β} and S_d^{β} are the production rate and degradation rate of growth factors, respectively. D^{β} is the diffusion coefficient of the growth factors in fracture callus.

Fibrous tissue (m^{fs}), cartilage (m^{cs}) and bone (m^{bs}) production

The tissue production within the callus which depends on both chemical and mechanical stimuli (Peiffer et al., 2011, Isaksson et al., 2008a) can be expressed as follows:

$$\frac{\partial \overline{m}^{\,\gamma}}{\partial t} = S_p^{\gamma} - S_d^{\gamma} \tag{3.13a}$$

$$S_p^{\gamma} = \left(P_{pc}^{\gamma} + P_{pm}^{\gamma}\right) \bar{c}^{\,\alpha} \tag{3.13b}$$

$$S_d^{\gamma} = P_{pc}^{\gamma}\, k^{\gamma}\, \overline{m}^{\,\gamma}\, \bar{c}^{\,\alpha} \tag{3.13c}$$

where $\gamma = fs$ (fibrous tissue); $\gamma = cs$ (cartilage tissue); and $\gamma = bs$ (bone tissue). S_p^{γ} is the production rate of the relevant tissue which is assumed to be the sum of chemical stimuli mediated production rate (P_{pc}^{γ}) and mechanical stimuli mediated production rate (P_{pm}^{γ}). S_d^{γ} is the degradation rate of the tissue.

Similar to the cell differentiation pattern shown in Figure. 3.2b, the production rate of fibrous tissue, cartilage and bone due to mechanical stimuli also depends on dynamic loading as follows:

$$P_{pm}^{s} = \begin{cases} P_{pm}^{bs} = \lambda_p^{bs}\, \bar{c}^{\,b}, & P_{pm}^{cs} = P_{pm}^{fs} = 0\,, \quad for\ S < 1 \quad (bone\ formation) \\ P_{pm}^{cs} = \lambda_p^{cs}\, \bar{c}^{\,c}, & P_{pm}^{bs} = P_{pm}^{fs} = 0\,, \quad for\ 1 < S < 3 \quad (cartilage\ formation) \\ P_{pm}^{fs} = \lambda_p^{fs}\, \bar{c}^{\,fb}, & P_{pm}^{bs} = P_{pm}^{cs} = 0\,, \quad for\ S > 3 \quad (fibrous\ tissue\ formation) \end{cases} \tag{3.14}$$

Balance of linear momentum

Assuming callus as homogeneous, isotropic and linear elastic mixture having no body and inertial forces, for an infinitesimal strain, the balance of linear momentum can be expressed as (Zhang et al., 2009):

$$-\nabla p + (\lambda_s + 2\mu_s)\nabla(\nabla \bullet \mathbf{u}^{\boldsymbol{s}}) + \mu_s \nabla^2 \mathbf{u}^{\boldsymbol{s}} = 0 \quad (3.15)$$

where p is the interstitial fluid pressure; λ_s and μ_s are Lame's constants; and $\mathbf{u}^{\boldsymbol{s}}$ is the solid phase displacement vector.

Conservation of mass of solid and fluid phases

From the mass balance equation for solid and fluid phase and Darcy's law, the interstitial fluid motion within the callus (Zhang et al., 2007, Zhang et al., 2015b) can be expressed as

$$\nabla \bullet (\mathbf{v}^{\boldsymbol{s}} - \boldsymbol{k}\nabla p) = 0 \quad (3.16)$$

where $\mathbf{v}^{\boldsymbol{s}}$ is the solid phase velocity, $\boldsymbol{k}$ is the hydraulic permeability tensor and p is the interstitial fluid pressure.

3.3.1. Problem Description

The developed model was implemented to reproduce the experimental observations of Harrison et al. (2003) due to the availability of experimental details (i.e. time dependent healing progression through histological analysis). Figure. 3.3a shows a transverse fracture on a mid-section of diaphyseal rat femur. Our model predictions were firstly validated by the experimental data of Harrison et al. (2003). Then, a series of computational simulations were carried out to identify the optimal regime that enhances solute transport in fracture callus, stem cell differentiation and tissue formation at early stage of healing. The values of model parameters used this study are given in Table 1 based on the available information in previous studies (Bailon-Plaza and van der Meulen, 2001, Geris et al., 2008, Peiffer et al., 2011).

Table 3.1 Parameters used throughout this study. The typical values for time (1 day), length (3.5mm), cell density (10^6 cells/ml), tissue (0.1 g/ml) and growth factor concentration (100 ng/ml) used to non-dimensionalise above coefficients are adapted from Peiffer et al. (2011) (Peiffer et al., 2011). For computational purpose, molecular

weight of cartilage (0.4MDa) (Han et al., 2011) and growth factors (25 KDa) (Solheim, 1998, Joyce et al., 1990b, Mauck et al., 2003) resulted in the parameter values of Table 1. *Adjusted to account for the added boundary of MSCs at periosteum.

Parameters	**Expression**	**References**
Coefficient of stem cell diffusion (D^{hm})	0.1715 mm^2/day	(Peiffer et al., 2011)
Coefficient of stem cell diffusion (K^{hm})	0.025 g/ml	(Peiffer et al., 2011)
Diffusion coefficient of fibroblast (D^{fb})	0.245 mm^2/day	(Peiffer et al., 2011)
Diffusion coefficient of osteogenic growth factor (D^{gb})	0.06125 mm^2/day	(Peiffer et al., 2011)
Diffusion coefficient of chondrogenic growth gactor (D^{gc})	0.06125 mm^2/day	(Peiffer et al., 2011)
Differentiation of stem cells into fibroblasts due to chemical stimuli (k_d^{fb})	0.01/day	(Peiffer et al., 2011)
Differentiation of stem cells into fibroblasts due to mechanical stimuli (λ_d^{fb})	0.01/day	(Andreykiv et al., 2008)
Coefficient of chondrocyte differentiation due to chemical stimuli (Y_2)	40/day	(Bailon-Plaza and van der Meulen, 2001)
Coefficient of chondrocyte differentiation due to chemical stimuli (H_2)	10 ng/ml	(Peiffer et al., 2011)
Differentiation of stem cells into chondrocytes due to mechanical stimuli (λ_d^c)	0.3/day	(Andreykiv et al., 2008)

Coefficient of osteoblast differentiation due to chemical stimuli ($\boldsymbol{Y_1}$)	3/day	(Bailon-Plaza and van der Meulen, 2001)
Coefficient of osteoblast differentiation due to chemical stimuli ($\boldsymbol{H_1}$)	10 ng/ml	(Peiffer et al., 2011)
Differentiation of stem cells into osteoblasts due to mechanical stimuli ($\boldsymbol{\lambda_d^b}$)	(0.005 + 0.145xS)/day	(Andreykiv et al., 2008)
Synthesis of fibrous tissue due to chemical stimuli ($\boldsymbol{P_{pc}^{fs}}$)	0.2/day	(Peiffer et al., 2011)
Synthesis of fibrous tissue due to mechanical stimuli ($\boldsymbol{\lambda_p^{fs}}$)	0.06/day	(Andreykiv et al., 2008)
Synthesis of cartilage due to chemical stimuli ($\boldsymbol{P_{pc}^{cs}}$)	0.2/day	(Peiffer et al., 2011)
Synthesis of cartilage due to mechanical stimuli ($\boldsymbol{\lambda_p^{cs}}$)	0.2/day	(Andreykiv et al., 2008)
Synthesis of bone due to chemical stimuli ($\boldsymbol{P_{pc}^{bs}}$)	2/day	(Peiffer et al., 2011)
Synthesis of bone due to mechanical stimuli ($\boldsymbol{\lambda_p^{bs}}$)	0.05/day	(Andreykiv et al., 2008)
Degradation of fibrous tissue ($\boldsymbol{k^{fs}}$)	10 g/ml	(Peiffer et al., 2011)
Degradation of cartilage ($\boldsymbol{k^{cs}}$)	10 g/ml	(Peiffer et al., 2011)
Degradation of bone ($\boldsymbol{k^{bs}}$)	10 g/ml	(Peiffer et al., 2011)

Boundary condition of stem cells (c^{m0})	1.6×10^4cells/ml* (first 7 days after fracture)	(Peiffer et al., 2011)
Boundary condition of fibroblasts (c^{fb0})	2×10^4cells/ml (first 3 days after fracture)	(Peiffer et al., 2011)
Boundary condition of chondrogenic growth factor (g^{c0})	2μg/ml (first 5 days after fracture)	(Peiffer et al., 2011)
Boundary condition of osteogenic growth factor (g^{b0})	2μg/ml (first 10 days after fracture)	(Peiffer et al., 2011)

Geometry

As shown in Figure. 3.3a, the geometry and size of facture callus and femur adopted in this study were defined based on the experiments of Harrison et al. (2003). The 2D axisymmetric model used in simulation is shown in Figure. 3.3b. The simplified geometry used by Geris et al. (2006) was adopted to compare our finite element model results. As our model formulation has been implemented in a finite element framework, it can be solved over any complex geometry without limiting to a 2D geometry. Nevertheless, to avoid singularities due to the shape edges of the model geometry, the sharp edges of broken cortex and callus borders have been rounded with a fillet of 0.1mm radius."

Loading Protocol

As shown in Figure. 3.3c, it was assumed that the fractured femur was subjected to a dynamic loading representing foot loading patterns (*e.g.* loading rise time, loading time and recovery time) (Barker and Seedhom, 2001, Zhang et al., 2015b). The best healing outcome that encourages endochondral ossification through enhanced cartilage formation and suppressed fibrous tissue formation is chosen to be the optimal loading. To identify the optimal loading regime, the combination of various loading strains and frequencies was used in the simulation. The loading cases used in our simulation were selected based on previous experimental studies, i.e. 7%, 31% strain and 0.5, 10 Hz frequency (Goodship and Kenwright, 1985, Augat et al., 2001, Wolf et al., 1998, Moalli et al., 2000).

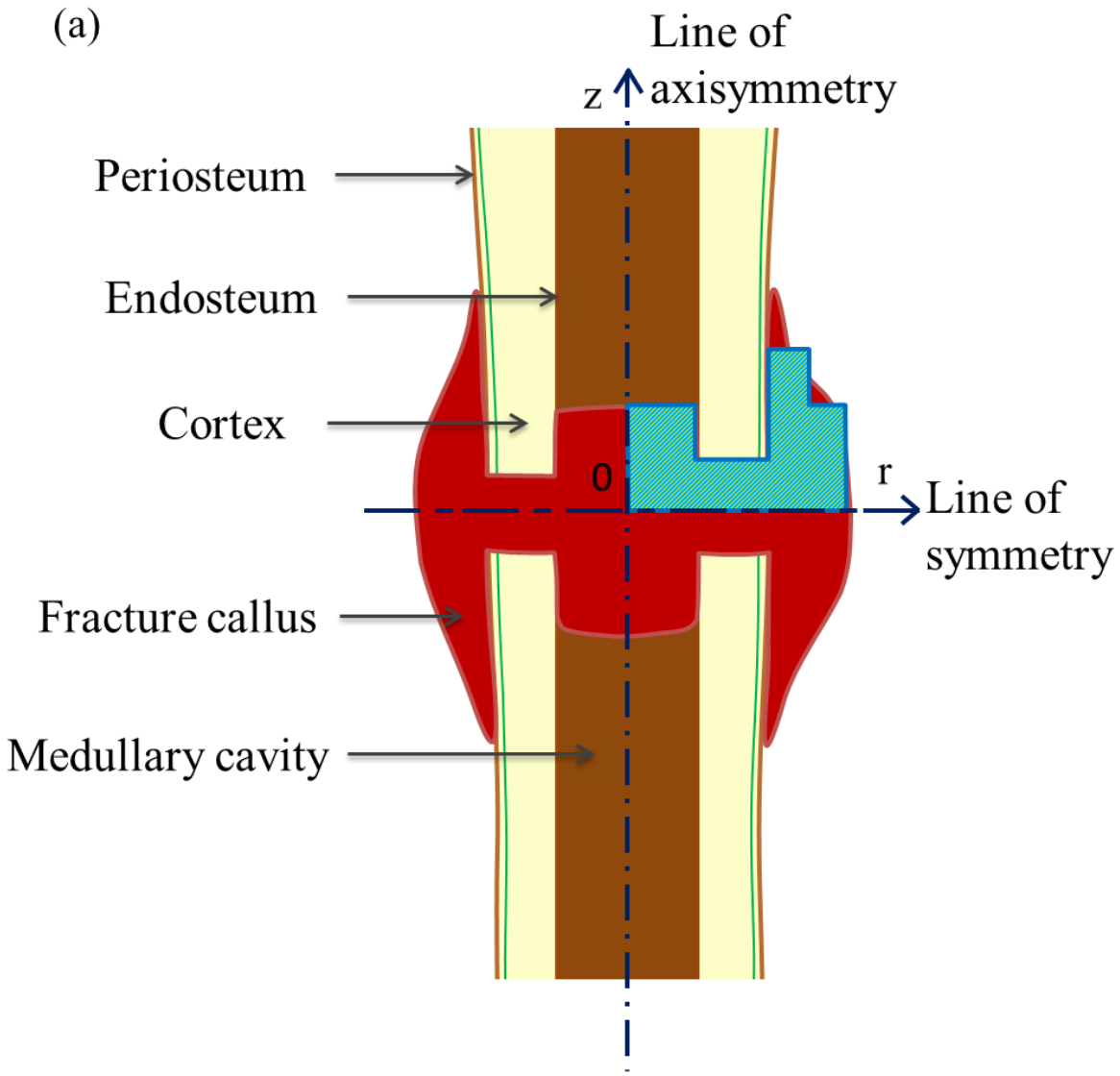
(a)
Line of
z
axisymmetry
Periosteum
Endosteum
Cortex
0
r
Line of
symmetry
Fracture callus
Medullary cavity

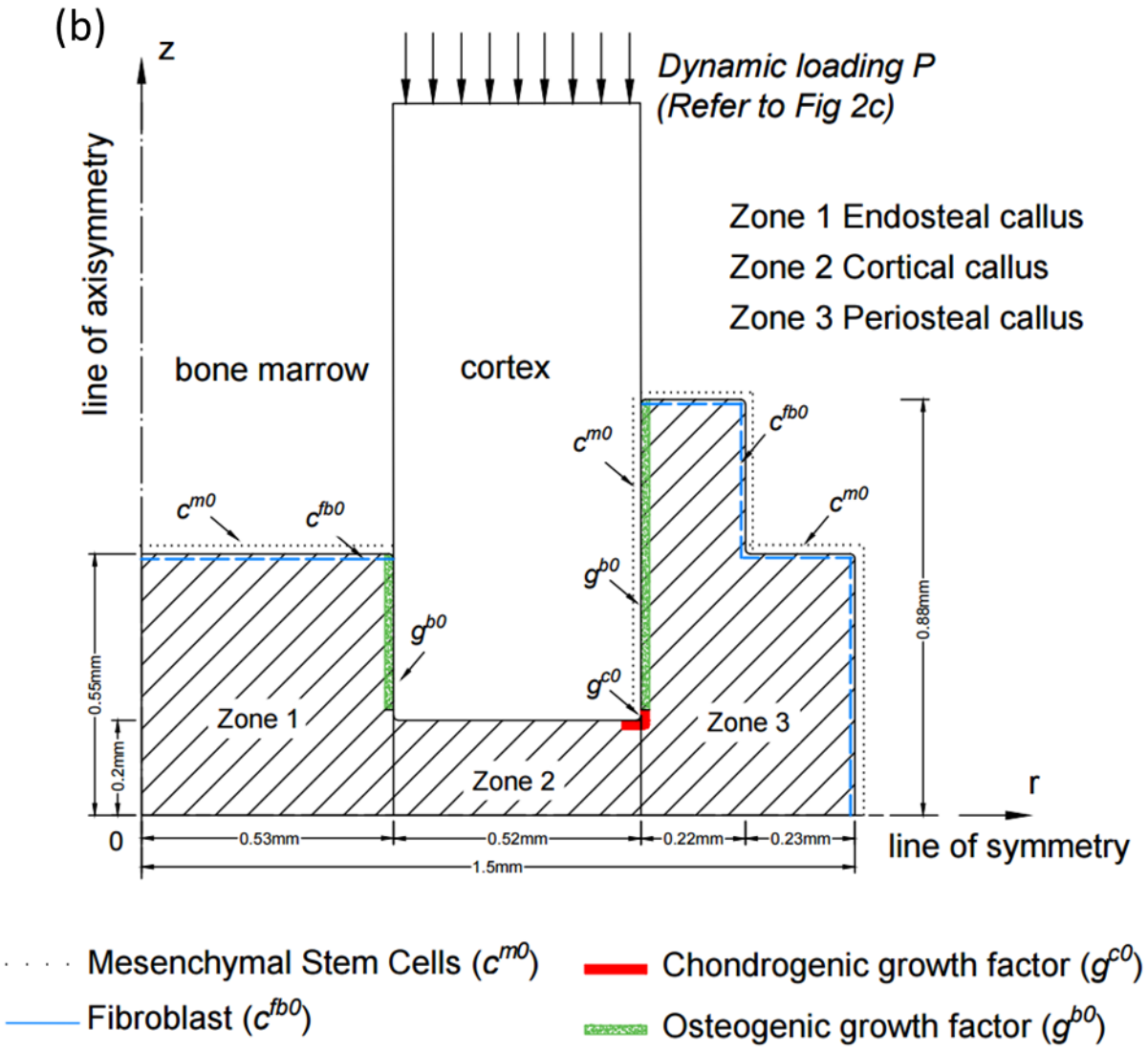
(b)
z
Dynamic loading P
(Refer to Fig 2c)
Zone 1 Endosteal callus
Zone 2 Cortical callus
Zone 3 Periosteal callus
line of axisymmetry
bone marrow
cortex
c^{m0}
c^{fb0}
g^{b0}
g^{c0}
Zone 1
Zone 2
Zone 3
0.55mm
0.2mm
0.88mm
0
0.53mm
0.52mm
0.22mm
0.23mm
1.5mm
r
line of symmetry
Mesenchymal Stem Cells (c^{m0})
Fibroblast (c^{fb0})
Chondrogenic growth factor (g^{c0})
Osteogenic growth factor (g^{b0})

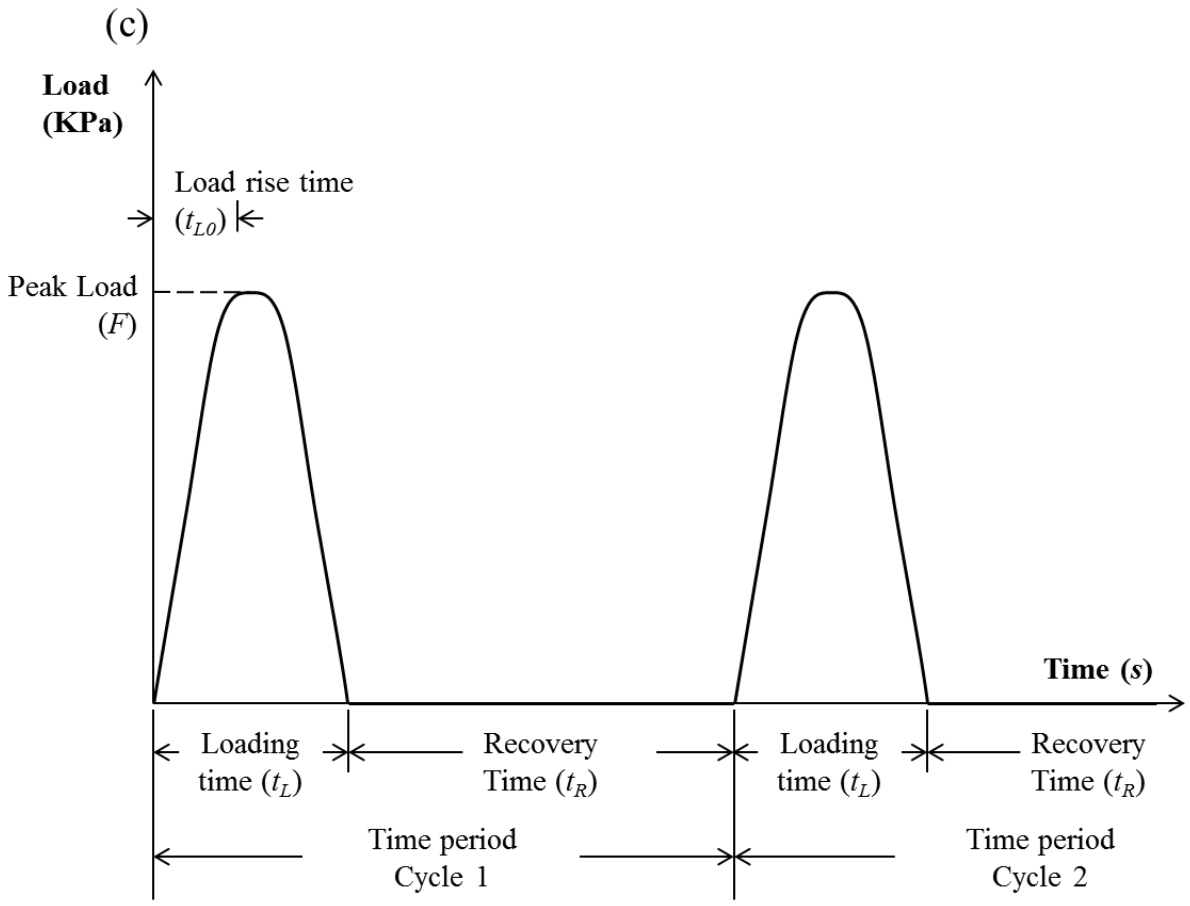

Figure. 3.3 (a) Schematic diagram of coronal section of a fractured femur; **(b)** Fracture callus domain of rodent femur, with dimensions adopted from Geris et al. (2008). c^{m0}, c^{fb0}, g^{c0} and g^{b0} are the boundary conditions of MSCs (c^m), fibroblasts (c^{fb}), chondrogenic growth factor (g^c), and osteogenic growth factor (g^b) respectively; and **(c)** Loading protocol used in this study (Barker and Seedhom, 2001, Zhang et al., 2015b). Each loading cycle consists of loading phase (t_L) and recovery phase (t_R) (i.e. time period T = $t_L + t_R$) and a peak load (F)

Assumptions

To simplify the complicated healing problem, the following assumptions were made in present study:

- The early stage of healing is mainly mediated by the biological actions of MSCs (Ito, 2011). At this stage, the majority of MSCs are originated from periosteum, bone marrow and external boundary of callus (Lacroix et al., 2002b, McKibbin, 1978a, Schindeler et al., 2008, Gerstenfeld et al., 2003) and there is little local proliferation of MSCs within the callus.
- The volume fraction of solid phase and fluid phase remains constant during early stage of healing (Gardiner et al., 2007, Markel et al., 1990).
- The degradation of cells and growth factors are ignored during early stage of healing.
- There is little change in callus size and geometry during early stage of healing.
- The total cell differentiation rate is the sum of chemical stimuli mediated differentiation rate and mechanical stimuli mediated differentiation rate.

Boundary Conditions

As shown in Figure. 3.3b, the following boundary conditions are assumed based on experimental evidences:

- The MSCs (c^{m0}) diffuse into fracture callus from periosteum, bone marrow and external boundary of callus (McKibbin, 1978a, Gerstenfeld et al., 2003, Brighton and Hunt, 1991, Henricson et al., 1987).
- The fibroblasts (c^{fb0}) diffuse into fracture callus from bone marrow and external boundary of callus (Postacchini et al., 1995) active during the inflammation phase for up to 3 days (Figure. 3a).
- The chondrogenic growth factors (g^{c0}) diffuse into fracture callus from the cambium region of periosteum at the fracture end of the cortex (Barnes et al., 1999), with a peak around 5 – 7 days after fracture (Cho et al., 2002).
- The osteogenic growth factors (g^{b0}) diffuse into fracture callus from both inner lining of cortex and periosteum (Barnes et al., 1999); and are active throughout the fracture healing, with a peak around 21 days (Cho et al., 2002).

- No flux boundary condition for osteoblasts and chondrocytes at all boundaries, since they are observed to originate from mesenchymal stem cells in the callus (Brighton and Hunt, 1991, Postacchini et al., 1995). All other cells and growth factors have no flux at the boundaries except mentioned above (Geris et al., 2008).

Initial conditions

The initial callus is filled with loose fibrous granulation tissue at early stage of healing (Schindeler et al., 2008, McKibbin, 1978a, Roberts and Rosenbaum, 2012). The initial conditions within callus can be assumed as

Cells:

$$\bar{c}^{\,m}\,(t=0)=0;\ \bar{c}^{\,fb}(t=0)=0;\ \bar{c}^{\,c}\,(t=0)=0;\ \bar{c}^{\,b}\,(t=0)=0 \tag{3.17}$$

Growth factors:

$$\bar{g}^{\,c}\,(t=0)=0;\ \bar{g}^{\,b}\,(t=0)=0 \tag{3.18}$$

Tissues:

$$m^{fs}\,(t=0)=10\ mg/ml \text{ (Peiffer et al., 2011)};m^{cs}\,(t=0)=0;\ m^{bs}\,(t=0)=0 \tag{3.19}$$

3.3.2. Numerical solutions

The governing equations (3.4), (3.9), (3.12) - (3.13), (3.15) - (3.16) were solved numerically using commercial finite element software package COMSOL Multiphysics® v5.2 (COMSOL). Early fracture callus domain shown in Figure. 3.3b was modelled using a structured free triangular meshing with 1933 elements. The transport of cells and growth factors into callus domain was modelled by using "transport of diluted species in porous media" module of COMSOL Multiphysics. In addition, the "poroelasticity" module of COMSOL was employed to simulate the interstitial fluid flow and mechanical behaviour of callus and bone cortex under dynamic loading. The convergence analysis was performed to determine the mesh size with error of 1%. The time dependent simulation was carried out using the generalised alpha solver with 20745 degree of freedoms for a relative tolerance of 10^{-3}.

3.4. **Results**

3.4.1. Model validation

The developed model was firstly validated against the experimental data of Harrison et al. (2003). Figure. 3.4 shows comparison of numerically predicted tissue distribution pattern of fibrous tissue, cartilage and bone at day 7 with experimental data in endosteal callus (Zone 1), cortical callus (Zone 2), and periosteal callus (Zone 3). It can be seen that the computational simulation results fit the experimental data reasonably well. The model findings are also consistent with the histomorphometric measurements of bone (around 16%) and cartilage (around 8.3%) percentage in callus area at day 8 post fracture in diaphyseal fracture of mice tibia (Geris et al., 2006). In addition, model predictions are in agreement with the histological study of Vetter et al. (2010) on diaphyseal healing of sheep tibia, which demonstrated a relatively high fibrous tissue content in the cortical and endosteal callus during early reparative phase compared to the periosteal callus which mainly consists of bony tissue. Further, our results are also consistent with other experimental findings which shows that cartilage tissue formation is mainly on the outer periosteal callus of rat tibia after days post fracture (Henricson et al., 1987), while bone tissue formation is seen in endosteal callus within 48 hours (Brighton and Hunt, 1991). The model predictions are also supported by the theoretical results of Geris et al. (2008), which suggested that callus is basically fibrous in nature at early stage of healing (one week post-operation). As healing progresses, the chondrocytes and osteoblasts derived from differentiating MSCs produce cartilage and bone. Moreover, consistent with previous findings (Marsell and Einhorn, 2011, Pivonka and Dunstan, 2012, Dimitriou et al., 2005), the simulation results in Figure. 3.4 shows that the cartilage tissue formation mainly happens in periosteal callus (Figure. 3.4c), new bone formation is mainly in periosteal and endosteal callus (Figure. 3.4a and c), while there is little cartilage and bone formation in cortical callus (Figure. 3.4b) as cells and growth factors need time to diffuse into this area.

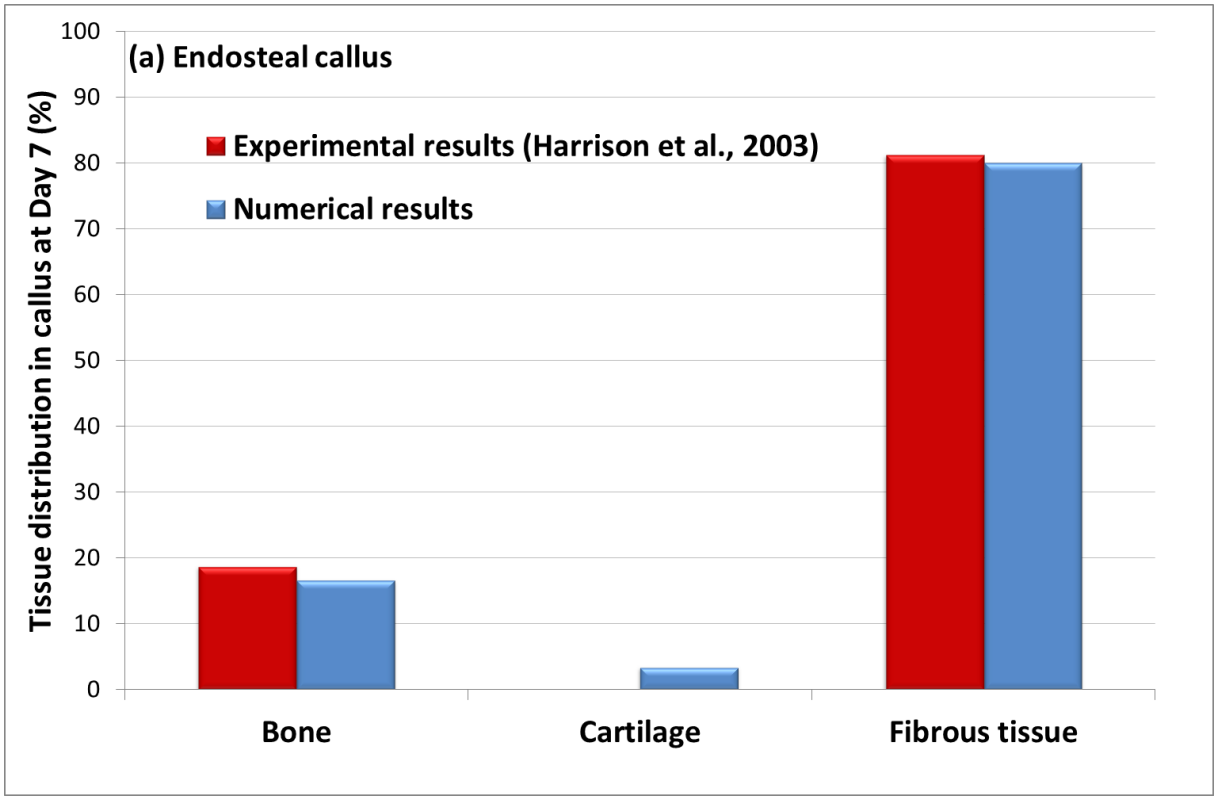
(a) Endosteal callus
Experimental results (Harrison et al., 2003)
Numerical results
Tissue distribution in callus at Day 7 (%)
100
90
80
70
60
50
40
30
20
10
0
Bone
Cartilage
Fibrous tissue

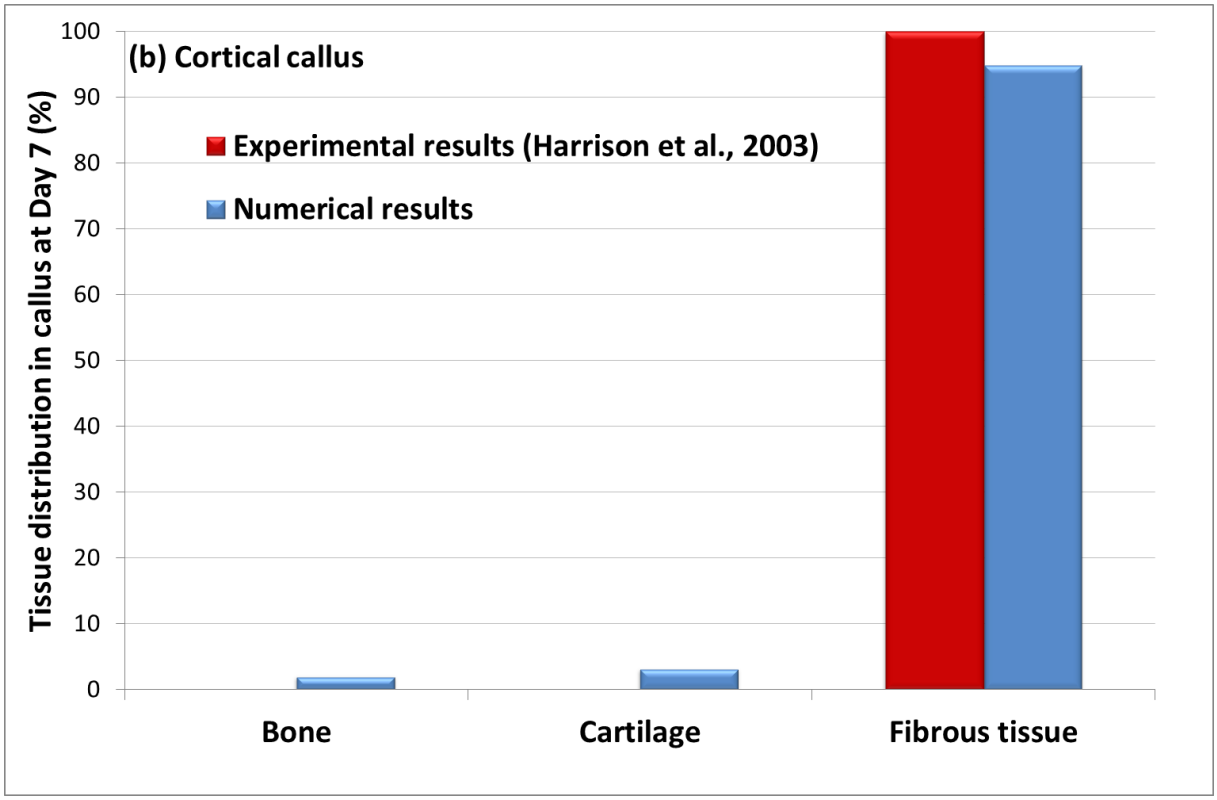
(b) Cortical callus
Experimental results (Harrison et al., 2003)
Numerical results
Tissue distribution in callus at Day 7 (%)
100
90
80
70
60
50
40
30
20
10
0
Bone
Cartilage
Fibrous tissue

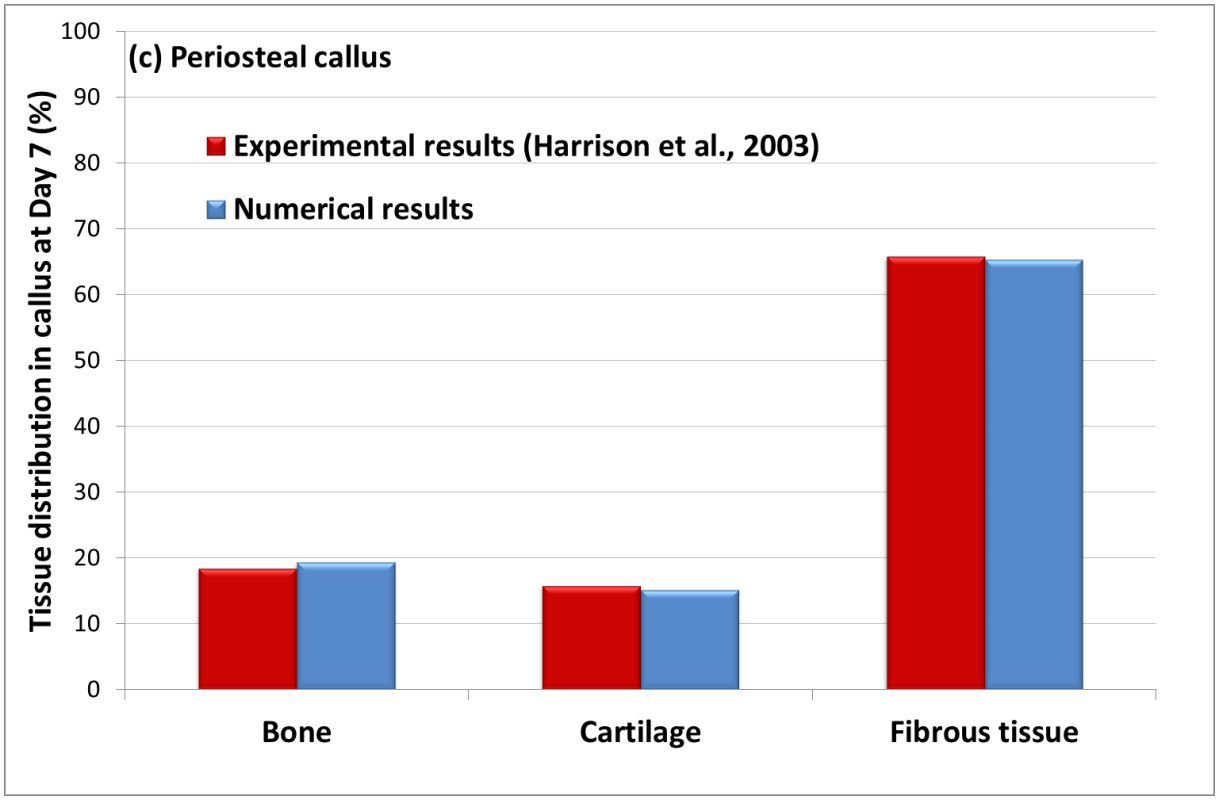

Figure. 3.4 Comparison of model prediction of callus tissue differentiation with experimental results of Harrison et al. (2003). **(a)** Endosteal callus; **(b)** Cortical callus; and **(c)** Periosteal callus

Sensitivity analyses have been carried out to evaluate initial boundary conditions of mesenchymal stem cells (c^{m0}), osteogenic growth factor (g^{b0}) and chondrogenic growth factor (g^{c0}) in tissue formation. The results show that the sensitivity of MSCs and growth factors in cartilage formation is spatially dependent, for example, MSCs and chondrogenic growth factor enhances cartilage formation in both endosteal and periosteal callus, whereas the formation of cartilage in cortical cartilage is insensitive to chondrogenic growth factor. On the other hand, MSCs and osteogenic growth factor general have a positive effect on bone generation across the callus while chondrogenic growth factor is shown to inhibit the bone formation (Refer to Figure. 3.5).

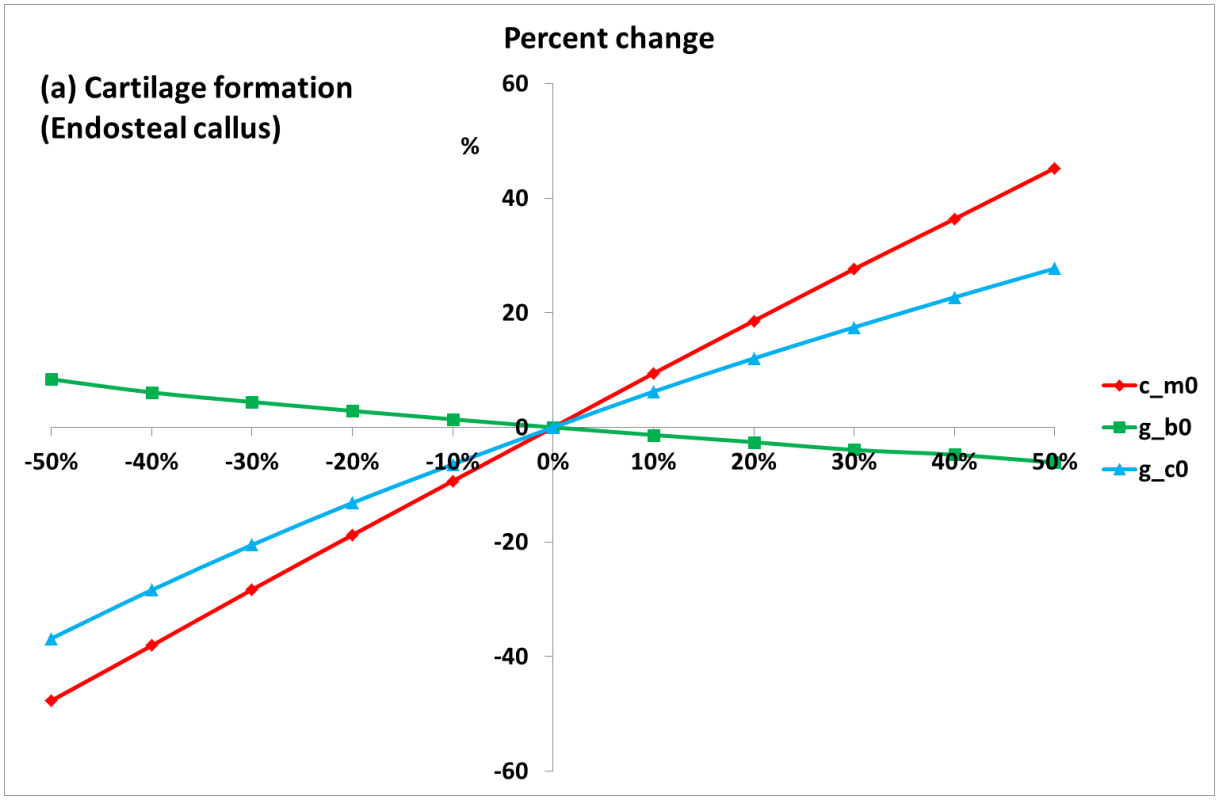
Percent change
(a) Cartilage formation
(Endosteal callus)
%
60
40
20
0
-20
-40
-60
-50%
-40%
-30%
-20%
-10%
0%
10%
20%
30%
40%
50%
c_m0
g_b0
g_c0

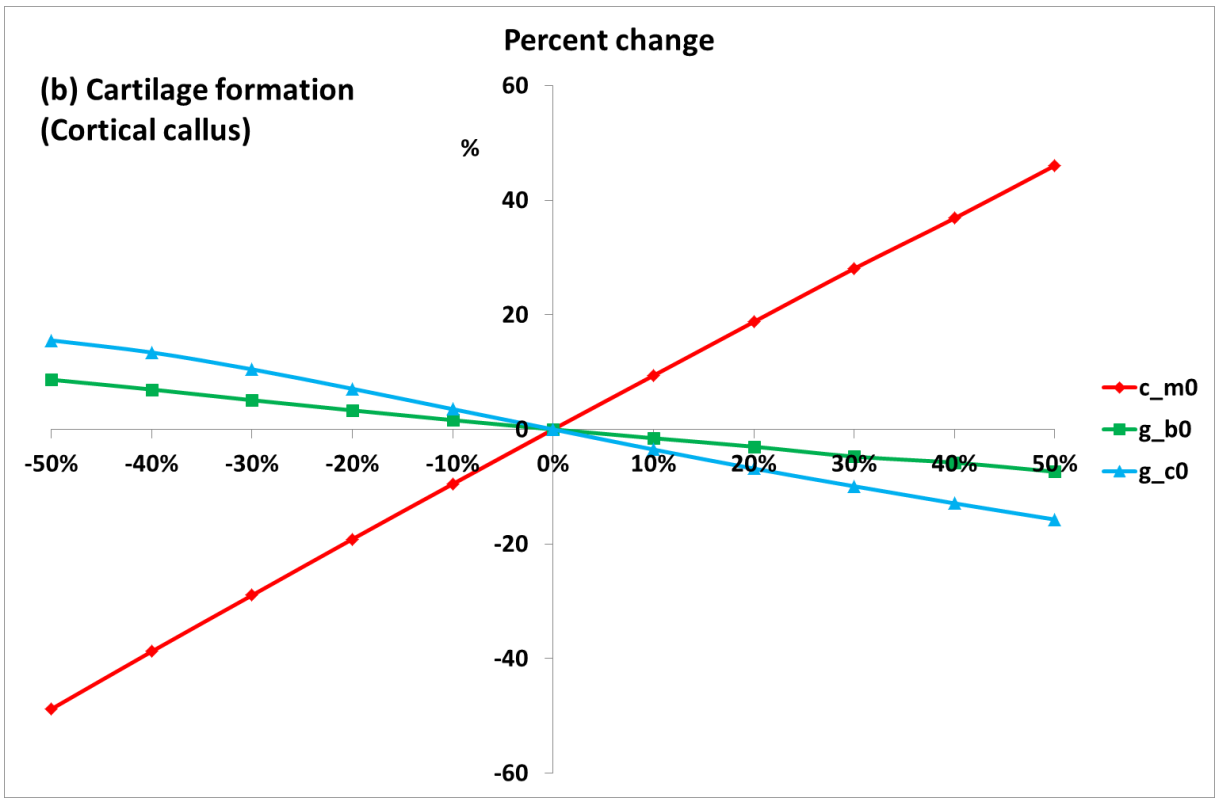
Percent change
(b) Cartilage formation
(Cortical callus)
%
60
40
20
0
-20
-40
-60
-50%
-40%
-30%
-20%
-10%
0%
10%
20%
30%
40%
50%
c_m0
g_b0
g_c0

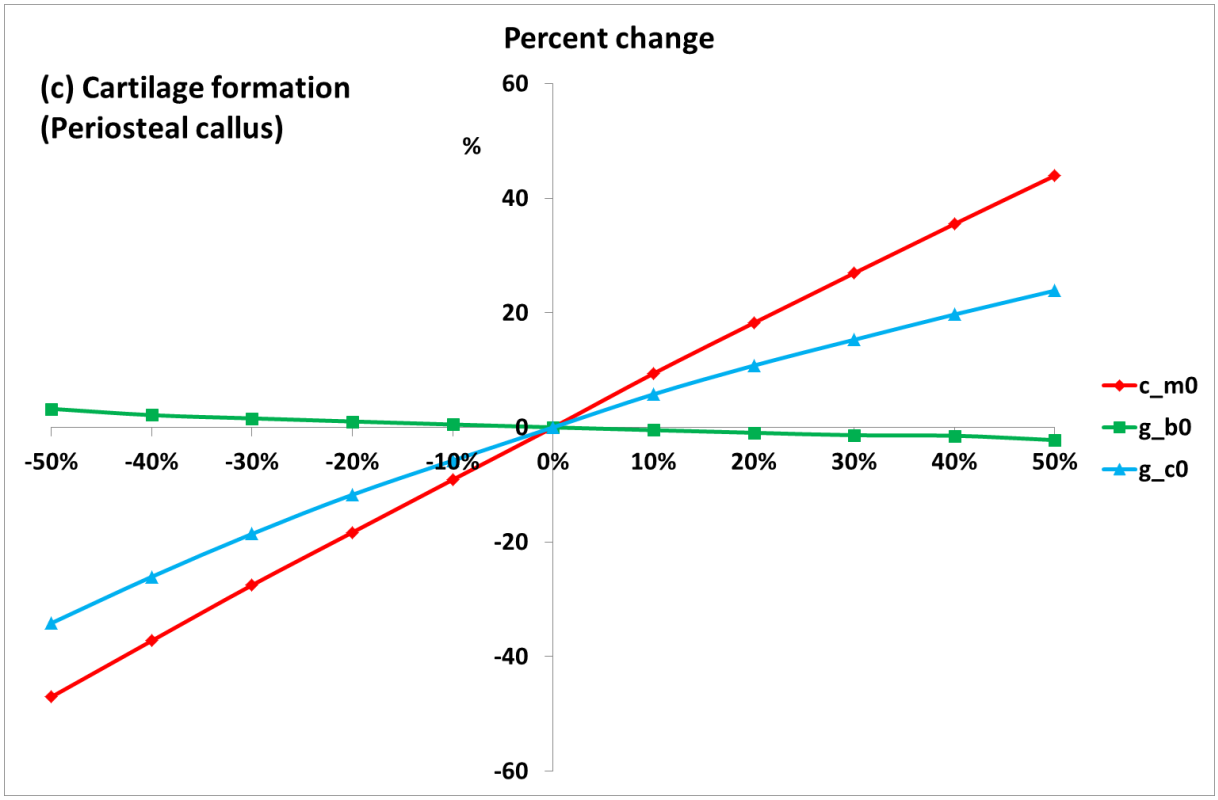
Percent change
(c) Cartilage formation
(Periosteal callus)
%
60
40
20
0
-20
-40
-60
-50%
-40%
-30%
-20%
-10%
0%
10%
20%
30%
40%
50%
c_m0
g_b0
g_c0

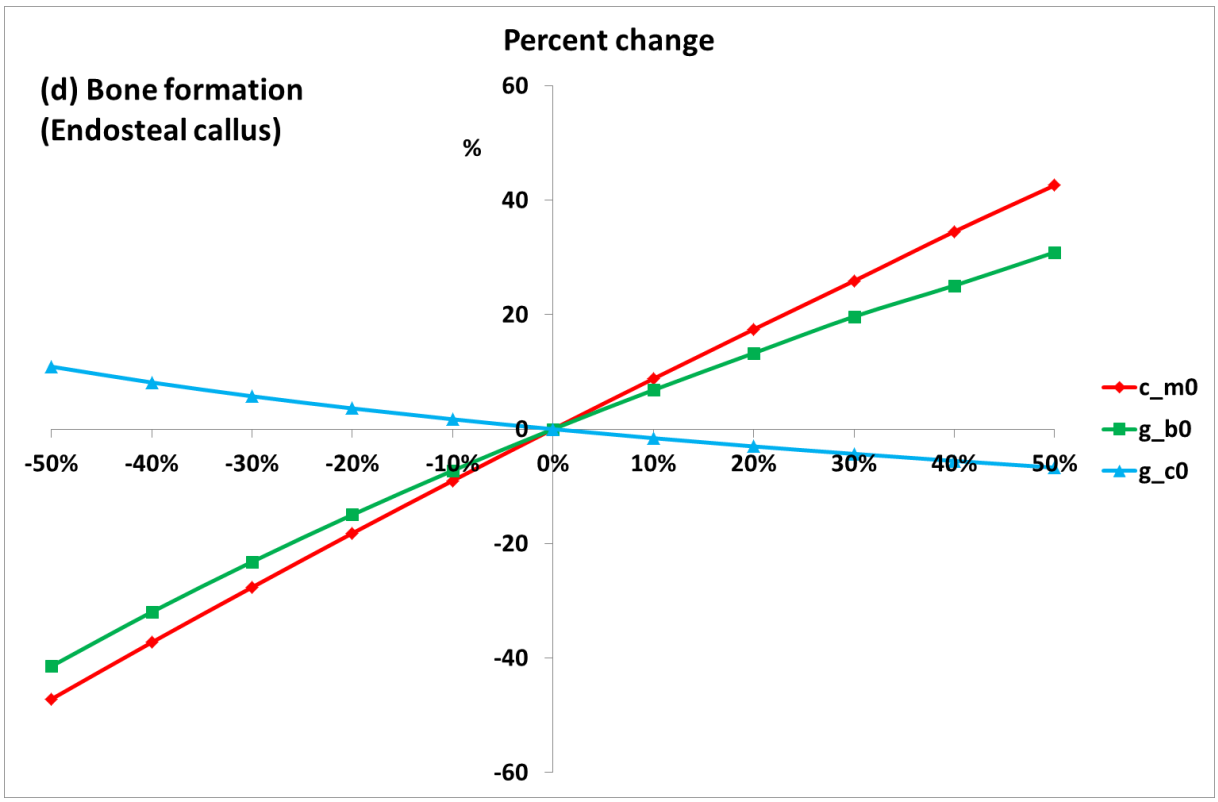
Percent change
(d) Bone formation
(Endosteal callus)
%
60
40
20
0
-20
-40
-60
-50%
-40%
-30%
-20%
-10%
0%
10%
20%
30%
40%
50%
c_m0
g_b0
g_c0

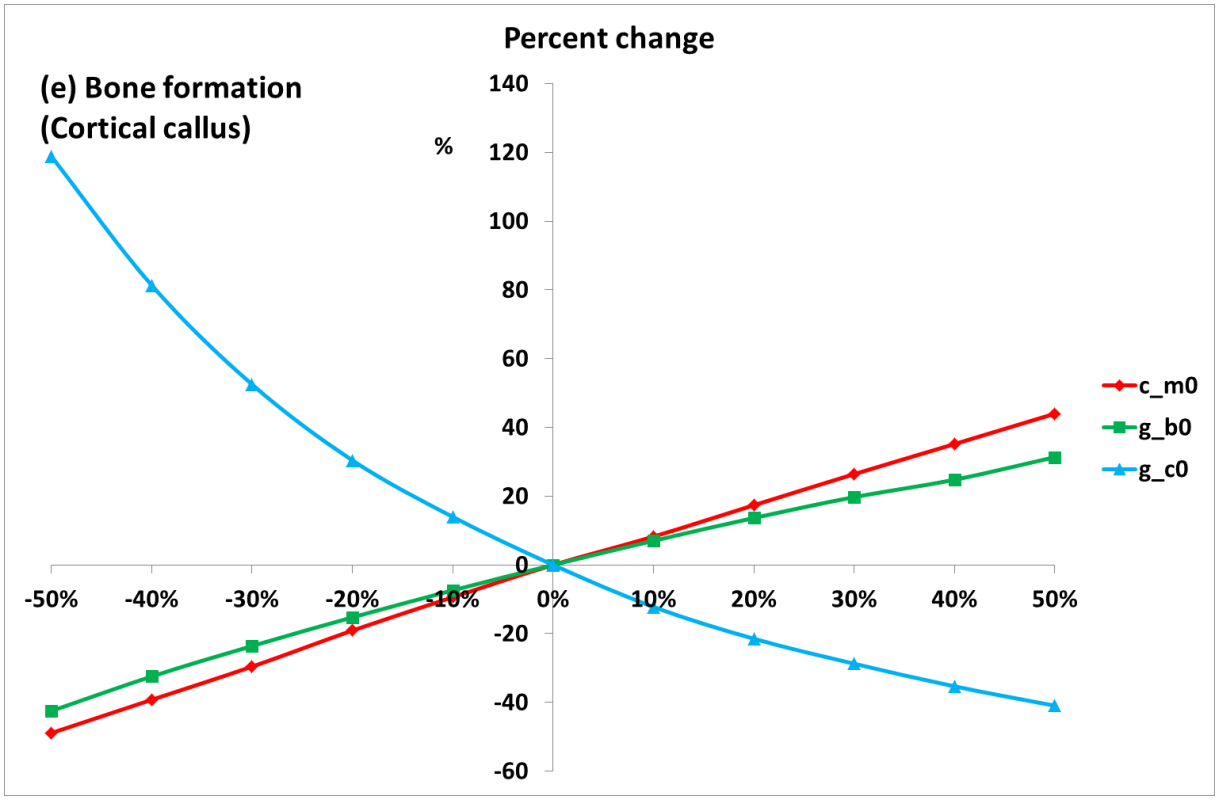

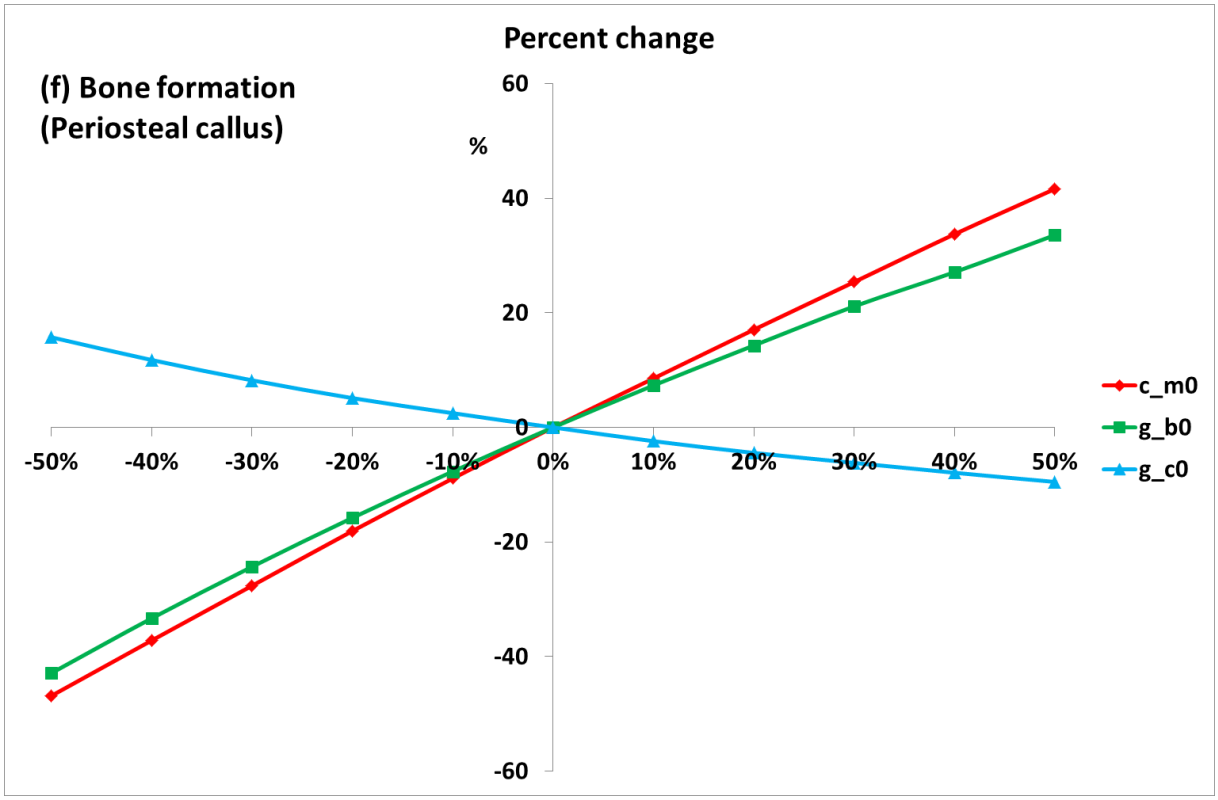

Figure. 3.5 Sensitivity analyses of the initial boundary conditions of mesenchymal stem cells (cm0), osteogenic growth factor (gb0) and chondrogenic growth factor (gc0) on tissue formation.

3.4.2. Free diffusion

After fracture, the MSCs migrate into fracture callus and differentiate into fibroblasts, osteoblasts and chondrocytes regulated by the growth factor concentration. The average normalised cell uptake ratio in each zone is computed as follows (Zhang et al., 2007, Mauck et al., 2003):

$$\bar{c}^{w}_{avg} = \frac{\int_0^{V_0} \bar{c}^{w} dV}{c_0^{w} V_0} \tag{3.20}$$

where $c^w = c^m, c^{fb}, c^c \; and \; c^b$ for MSCs, fibroblasts, chondrocytes and osteoblasts concentration, respectively. c_0^w is the saturated concentration of particular cell over callus volume V_0.

In order to compare the concentration of these cells within different zones of callus as a result of free diffusion and differentiation, their normalised uptake as a function of time in each zone is shown in Figure. 3.6. The concentration of MSCs (c^m) and fibroblasts (c^f) into callus are normalized to their respective boundary conditions ($c^{m0} \; and \; c^{f0}$); while the concentrations of chondrocytes and osteoblasts are normalised to the boundary conditions of MSCs (c^{m0}) as they are differentiated from MSCs. It can be seen from Figure. 3.6 that the uptake of all cells in callus is spatially dependent. As shown in Figure. 3.6a, the uptake of MSCs generally decreases with time due to differentiation of MSCs into fibroblast, chondrocyte and osteoblast within the callus. In addition, the model predicts a relatively high MSCs concentration in periosteal zone in comparison to that in other zones (e.g. two times and six times higher than that in endosteal and cortical zones, respectively, at day 7) since periosteal zone is surrounded by external soft tissue and periosteum which are the main sources of MSCs. On the other hand, it can be seen from Figure. 3.6b that the uptake of fibroblasts in perosteal callus initially goes up, reaches to its maximum and then gradually decreases to 0 by day 5 due to the fact that the supply of fibroblasts from bone marrow and external boundary of callus only lasts three days (Figure. 3.2a) (Geris et al., 2008).

Similarly, the normalised uptake of growth factors is plotted in Figure. 3.7 to understand its transport rate in each zone due to free diffusion and its average normalised uptake is computed as:

$$\bar{g}^{w}_{avg} = \frac{\int_0^{V_0} \bar{g}^{w} dV}{g^{w}_{0} V_0} \tag{3.21}$$

where $g^w = g^b$ and g^c for osteogenic growth factor concentration and chondrogenic growth factor concentration, respectively. The uptake of osteogenic and chondrogenic growth factors are normalised to their respective boundary conditions ($g^w_0 = g^{b0}$ and g^{c0}) . Figure. 3.7 shows that the uptake of growth factors is spatially dependent. Osteogenic growth factor uptake is relatively higher in endosteal and periosteal callus, while chondrogenic growth factor is higher in periosteal and cortical callus, due to the locations of their sources at early stage of healing (Figure. 3.3b). The concentration of chondrogenic growth factor goes down at day 6 in cortical callus and periosteal callus, as the supply of chondrogenic growth factor from its source only lasts for five days (Figure. 3.2a). The importance of these growth factors is demonstrated by the relatively high uptake of chondrocytes and osteoblast in periosteal callus compared to other zones (Figure. 3.6c and d), where there is relatively high concentration of chondrogenic and osteogenic growth factors and MSCs (see Figure. 3.7).

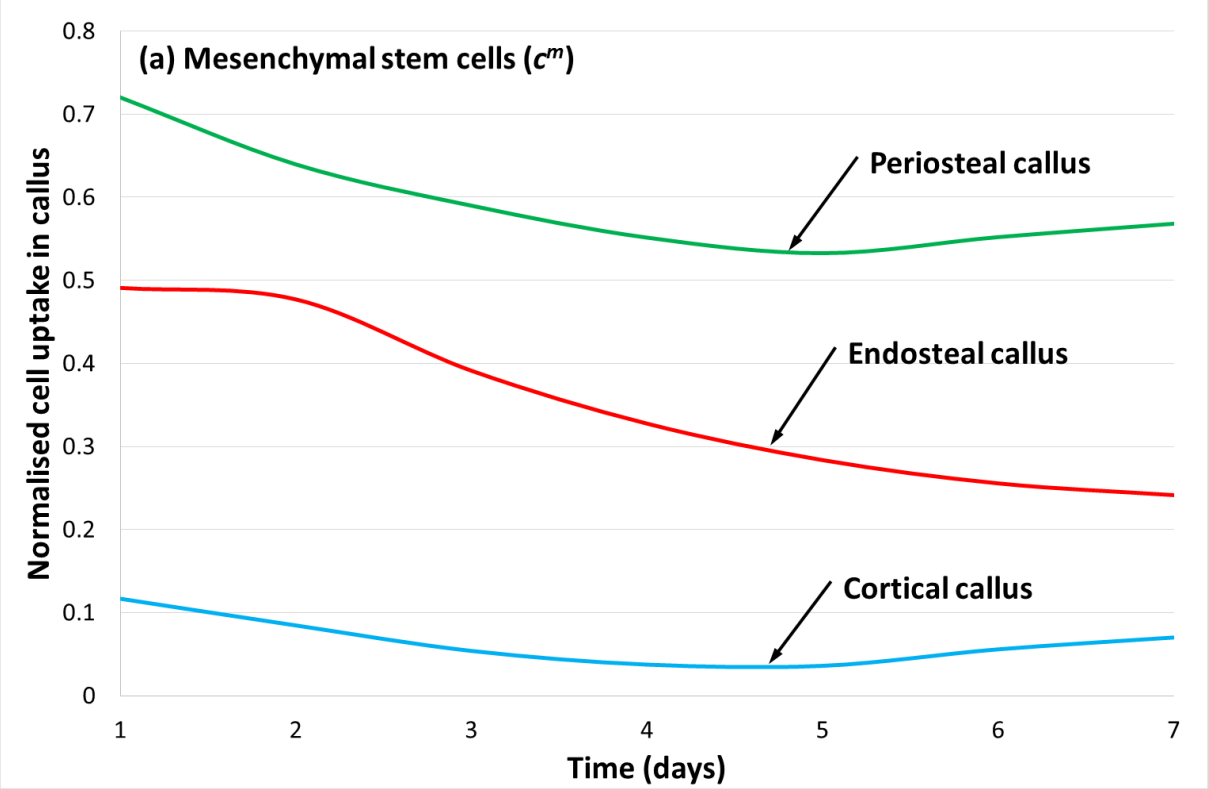

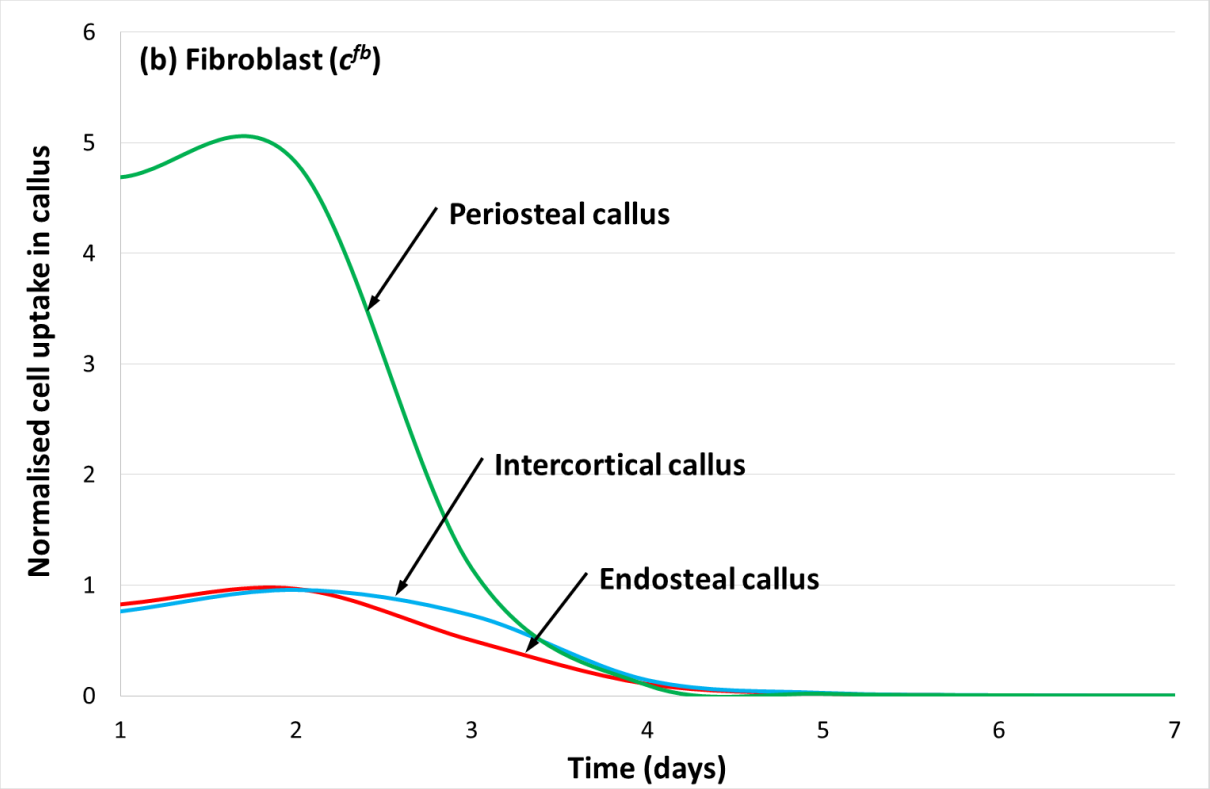
(b) Fibroblast (c^{fb})
Normalised cell uptake in callus
Periosteal callus
Intercortical callus
Endosteal callus
Time (days)
0
1
2
3
4
5
6
1
2
3
4
5
6
7

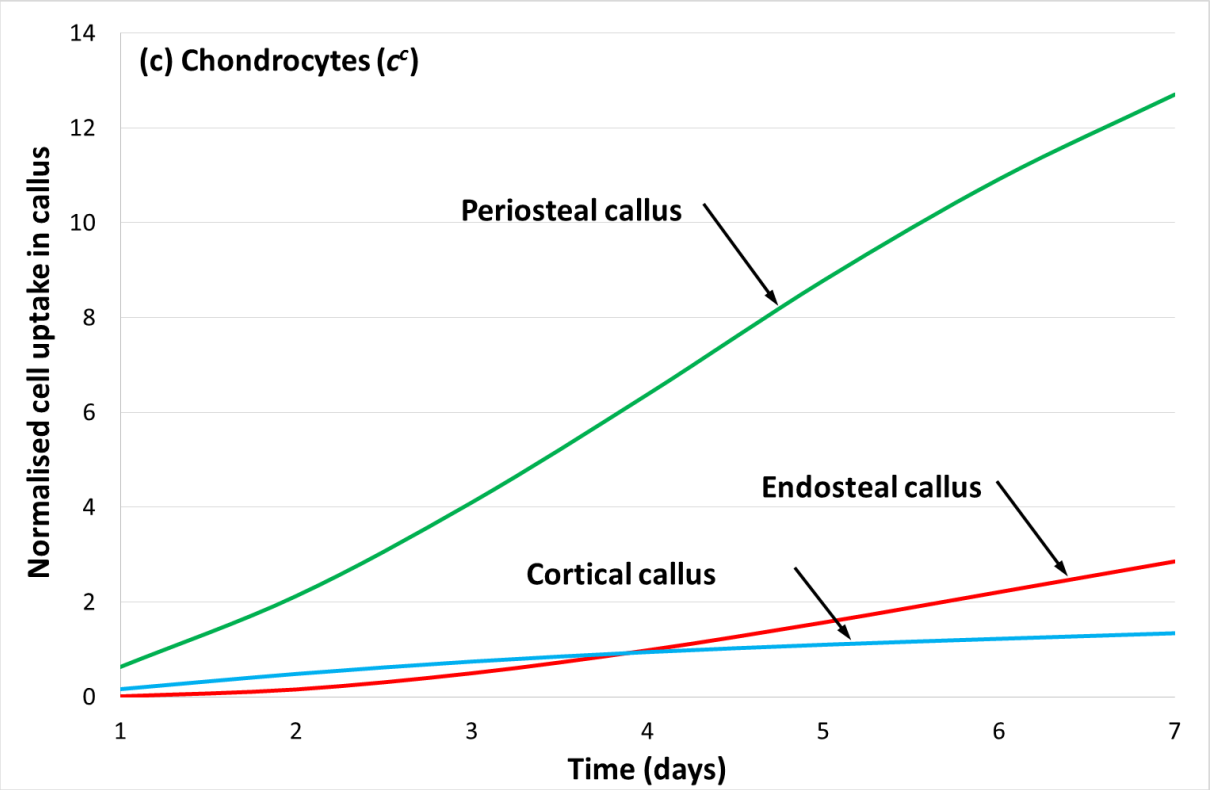
(c) Chondrocytes (c^{c})
Normalised cell uptake in callus
Periosteal callus
Endosteal callus
Cortical callus
Time (days)
0
2
4
6
8
10
12
14
1
2
3
4
5
6
7

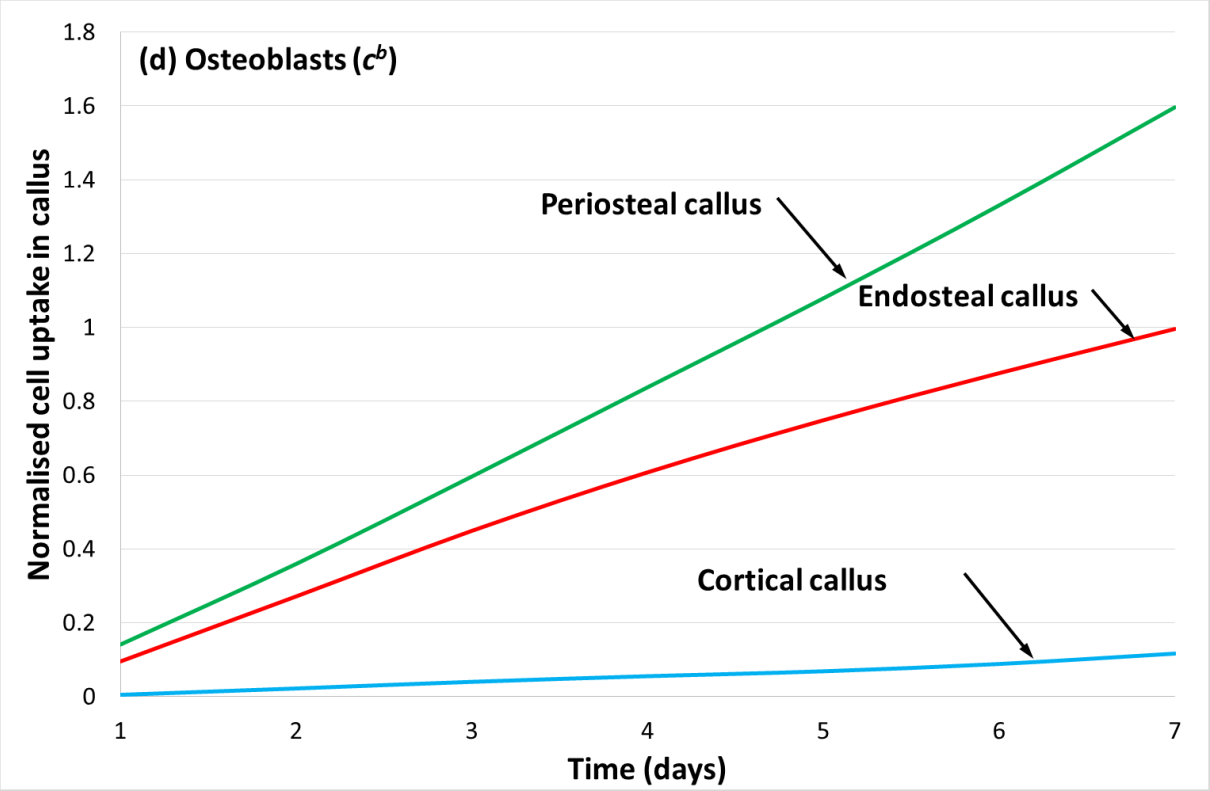

Figure. 3.6 Normalised time dependent cell uptake in fracture callus under free diffusion across different callus regions (a) MSCs (c^m); (b) Fibroblasts (c^{fb}); (c) Chondrocytes (c^c) and (d) Osteoblasts (c^b). MSCs and fibroblasts are normalised to their boundary values (i.e. c^{m0} and c^{fb0}) respectively, while chondrocytes and osteoblasts are normalised to the boundary conditions of stem cells (i.e. c^{m0})

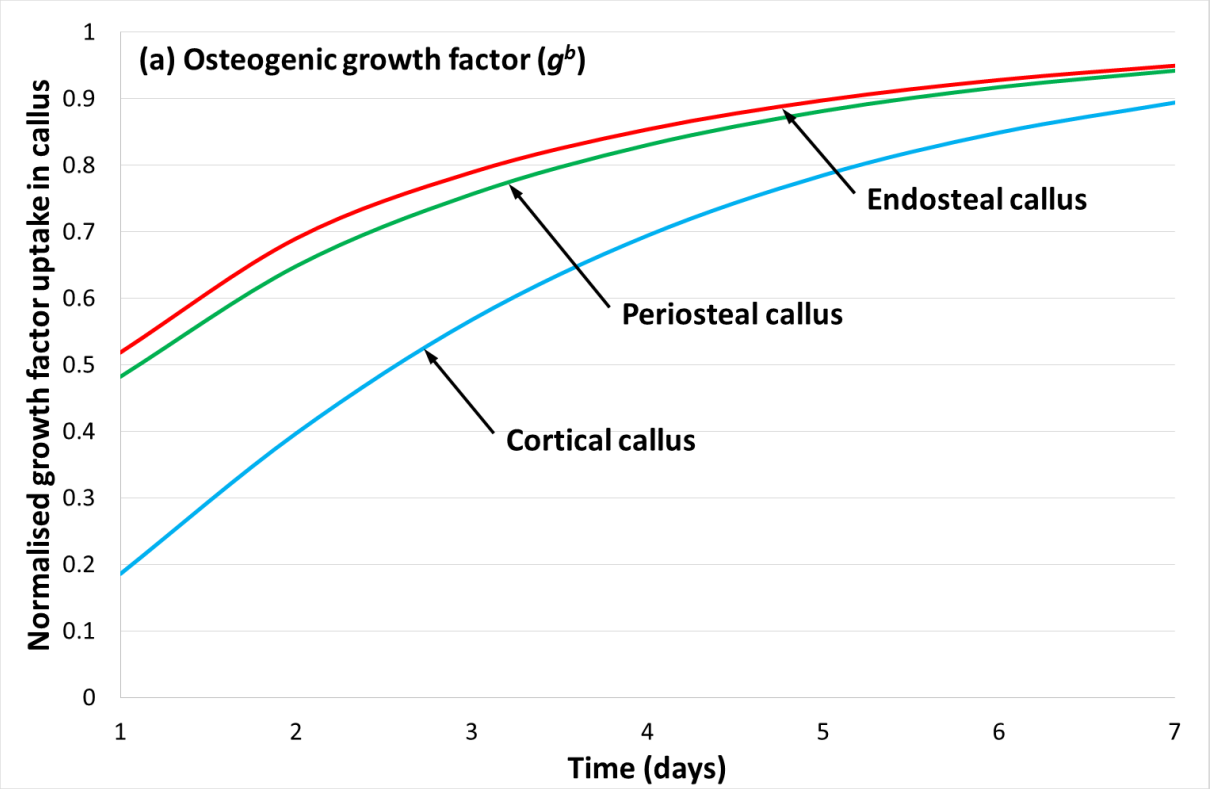

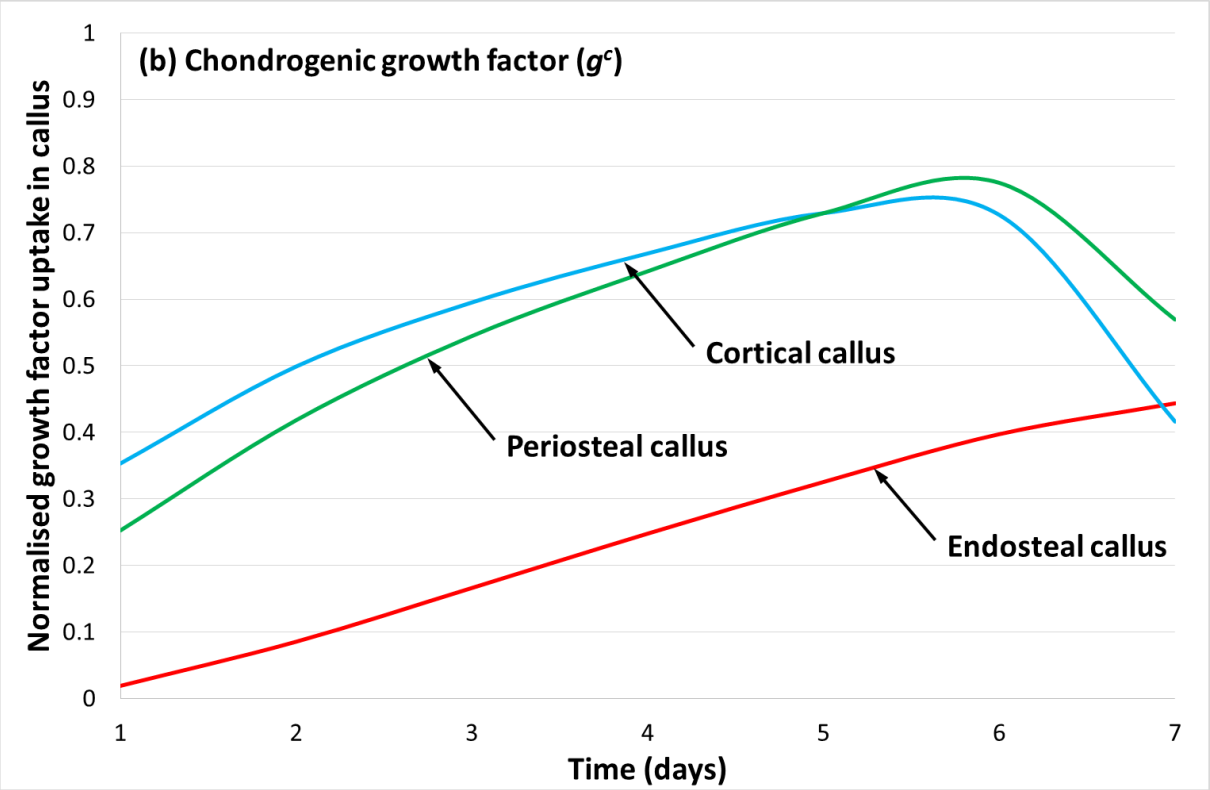

Figure. 3.7 Normalised time dependent growth factor uptake in fracture callus under free diffusion (a) Osteogenic growth factor across different callus regions (g^b) and **(b)**

Chondrogenic growth factor (g^c). Growth factors g^b and g^c are normalised to their boundary conditions (i.e. g^{b0} and g^{c0}), respectively

3.4.3. Advection

To investigate the influence of mechanical loading on cells and growth factors transport, the normalised concentration of MSCs and growth factors under dynamic loading (i.e. advection) is compared with that under free diffusion (Figure. 3.8 and Figure. 3.9). Previous studies of advective transport of Insulin-like growth factor in cartilage have identified a strain magnitude of 10% and loading frequency of 1 Hz as the most effective dynamic loading parameters to enhance solute transport among a range of loading conditions (Zhang et al., 2007, Zhang, 2011). Correspondingly, a cyclic loading corresponding to 10% strain at 1 Hz frequency for 6 hours was adopted in this study (Refer to Figure. 3.3d).

The temporal as well as spatial effect of dynamic loading on the transport of MSCs is illustrated in Figure. 3.8. It can be seen from Figure. 3.8a that, in comparison to free diffusion, dynamic loading leads to a significant increase of MSCs in endosteal zone of callus, and this increase is more obvious at early stage of loading (e.g. 20% increase during the first hour of loading) and gradually goes down with the increase of loading time (e.g. down to 10% increase after 5 hour of loading). The simulation results are consistent with previous studies on dynamic loading induced advective solute transport in biological tissues (e.g. cartilage) (Zhang et al., 2007, Zhang, 2011, Zhang et al., 2008a). In addition, the enhancement of MSC uptake as a result of dynamic loading could be four times higher in endosteal callus than that in periosteal callus, while dynamic loading has little effect on MSC uptake in cortical callus due to the fact that much less MSCs concentration would have reached this zone over 5 hours. Furthermore, the spatial increase of MSC uptake in Figure. 3.8b also suggests that the increase in MSC uptake is mainly in boundary zone of the endosteal callus, and the increment gradually moves further into the callus with the increase of loading time.

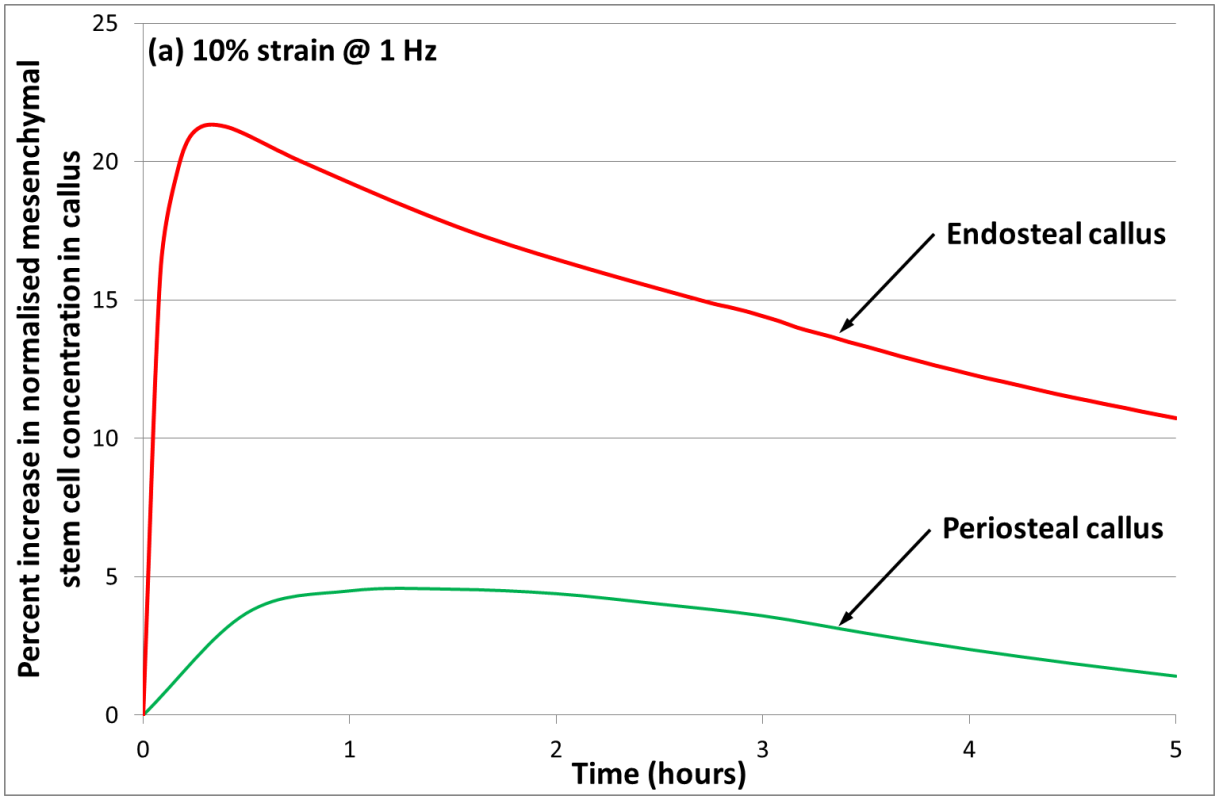

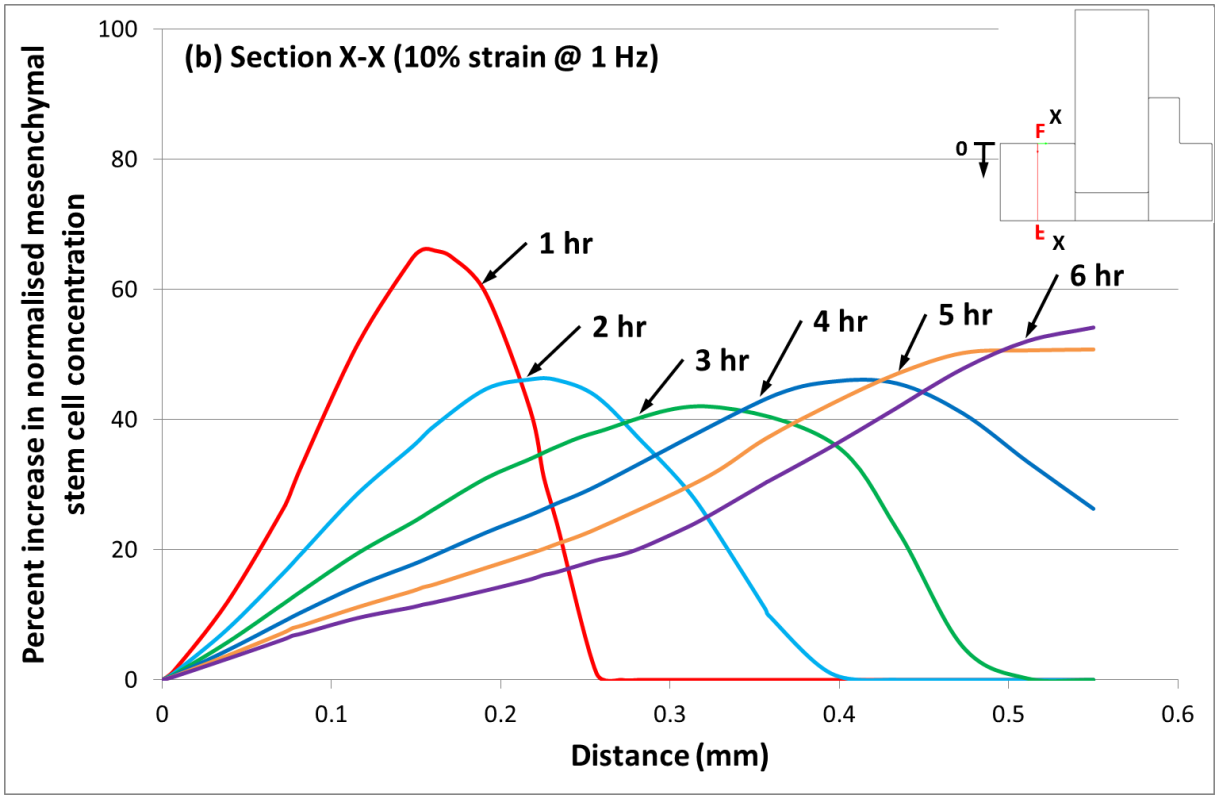

Figure. 3.8 Percent increase in normalised mesenchymal stem cell concentration under dynamic loading in comparison to free diffusion. (a) Time dependent stem cell concentration; and (b) spatial dependent stem cell concentration at Section X-X

The effects of dynamic loading on transport of growth factors in different zones of callus are shown in Figure. 3.9. In comparison to free diffusion, dynamic loading is seen to significantly enhance the uptake of chondrogenic growth factor by around 100% and 60% in cortical and periosteal callus, respectively, during the first 5 hour of loading. Among two growth factors, chondrogenic growth factor is predicted to experience a higher percent increase in its concentration compared to that of osteogenic growth factor, due to the fact that the source of chondrogenic growth factor being directly under the loading where there is a relatively higher fluid velocity at fracture gap specifically adjacent to the tip of the bone fragments (González-Torres et al., 2010a, Miramini et al., 2013a). On the other hand, the influence of dynamic loading in the uptake of osteogenic growth factor in both endosteal and periosteal callus is limited as the source of osteogenic growth factor is on the periosteal and endosteal layer of cortical bone where the fluid velocity is low.

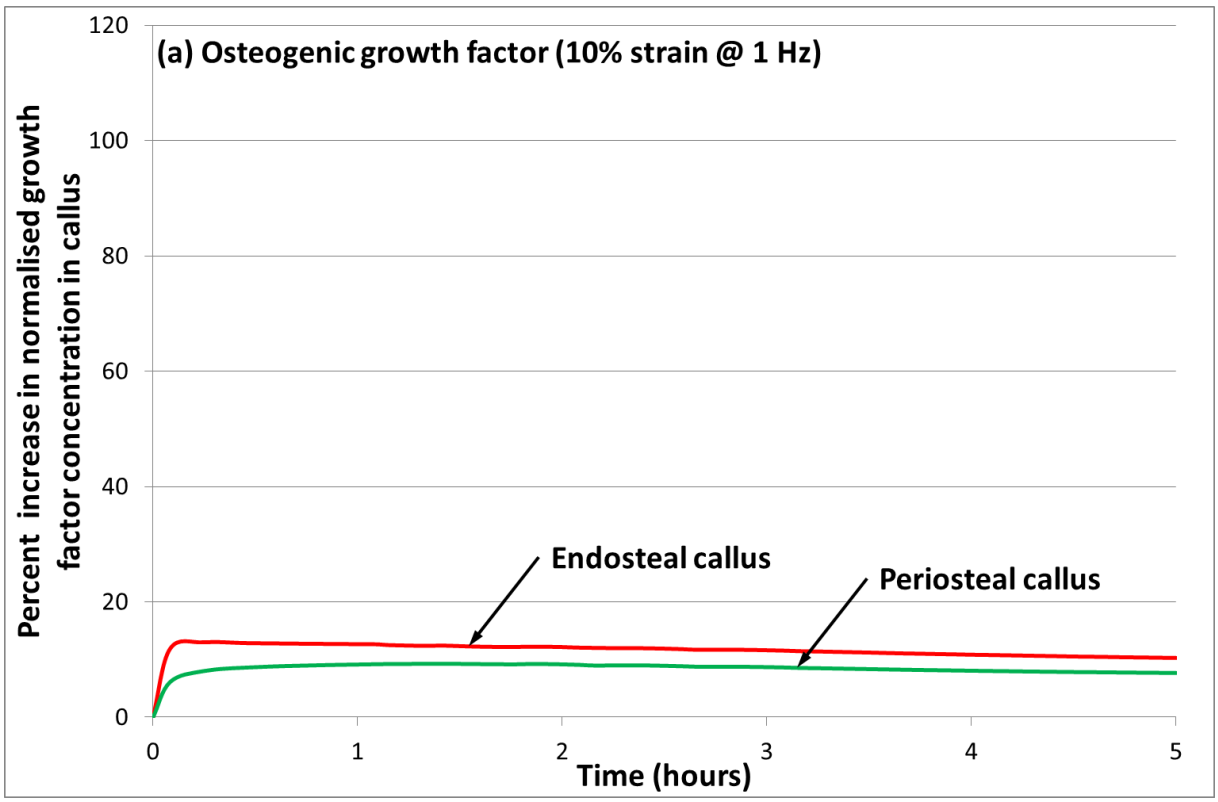

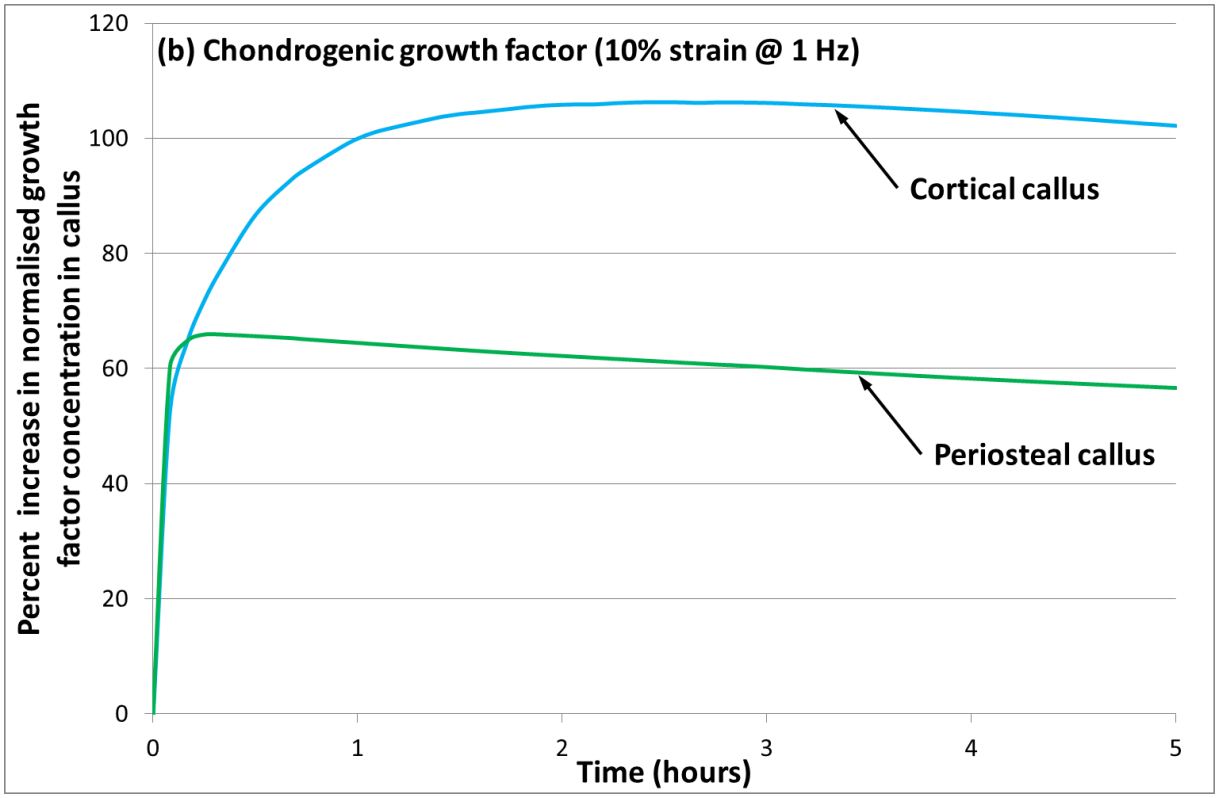

Figure. 3.9 Percent increase in normalised growth factor concentration under dynamic loading in comparison to free diffusion across different callus regions. (a) Osteogenic growth factor (g^b); and (b) Chondrogenic growth factor (g^c)

3.4.4. Mechanical stimuli mediated cell differentiation and tissue regeneration

While previous studies have suggested that cell differentiation (Geris et al., 2004) and tissue distribution pattern (Isaksson et al., 2007, Lacroix et al., 2002b, Prendergast et al., 1997) are directly regulated by fluid velocity within the callus, our computational results suggest that fluid velocity also plays an important role in cellular migration and growth factor transport during fracture healing, and thereby indirectly influences cell differentiation pattern and healing outcome. The percent increase in time-dependent fibrous, cartilage and bone tissue formation under different loading conditions is presented in Figure. 3.10. In consistent with previous studies (Doblaré et al., 2004, Geris et al., 2008), the results in insets of Figure. 3.10 show that bone tissue mainly forms in the boundary layer of periosteal callus. Also, the presence of cartilage in periosteal callus is higher towards the centre of fracture gap compared to periphery, as demonstrated by Geris et al. (2006) and Gerstenfeld et al. (2003). Further, the model results also show

qualitative compliance with findings of Dimitriou et al. (2005) and Einhorn (1998) which reported intramembranous ossification (new bone formation) away from fracture site, while endochondral ossification (cartilage formation) adjacent to the fracture periosteum.

The comparison of the results from Figure. 3.10(a-f) shows that a relatively high loading strain (i.e. 15%) results in fibrous tissue formation (Figure. 3.10a), while a relatively low loading strain (i.e. 5%) or frequency (i.e. 0.01Hz) suppresses the cartilage formation and thereby the endochondral ossification. The model predictions are consistent with the previous computational predictions which showed that low frequencies fail to promote endochondral ossification (González-Torres et al., 2010a). The model predictions suggest that there could be an optimal loading regime (e.g. 10%@1Hz) which encourages cartilage tissue formation while limits the fibrous tissue formation in the same time, and thereby enhances endochondral ossification. Previous experimental studies have also demonstrated that moderate levels of loading (e.g. 10% strain) improve cell differentiation and accelerate bone healing (Hou et al., 2009).

The sensitivity analysis regarding to different loading regimes with various strain and frequency combinations (Figure. 9) shows that the change of frequency has little influence on fibrous tissue formation and an increase in frequency by from 1Hz to 10Hz decreases cartilage formation by around 5%. In addition, the increase in strain by from 10% to 15% increased fibrous and cartilage tissue formation by around 5% and 15% relative to control, respectively.

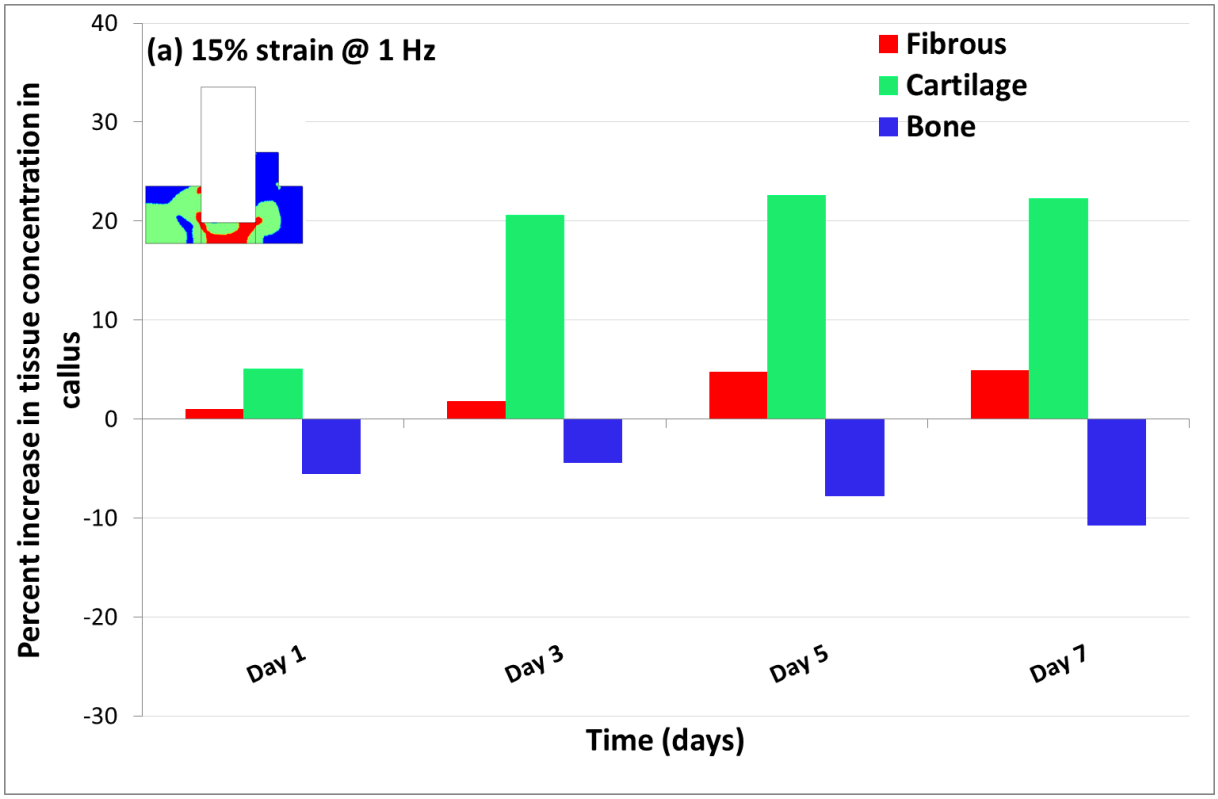
(a) 15% strain @ 1 Hz
Fibrous
Cartilage
Bone
Percent increase in tissue concentration in callus
40
30
20
10
0
-10
-20
-30
Day 1
Day 3
Day 5
Day 7
Time (days)

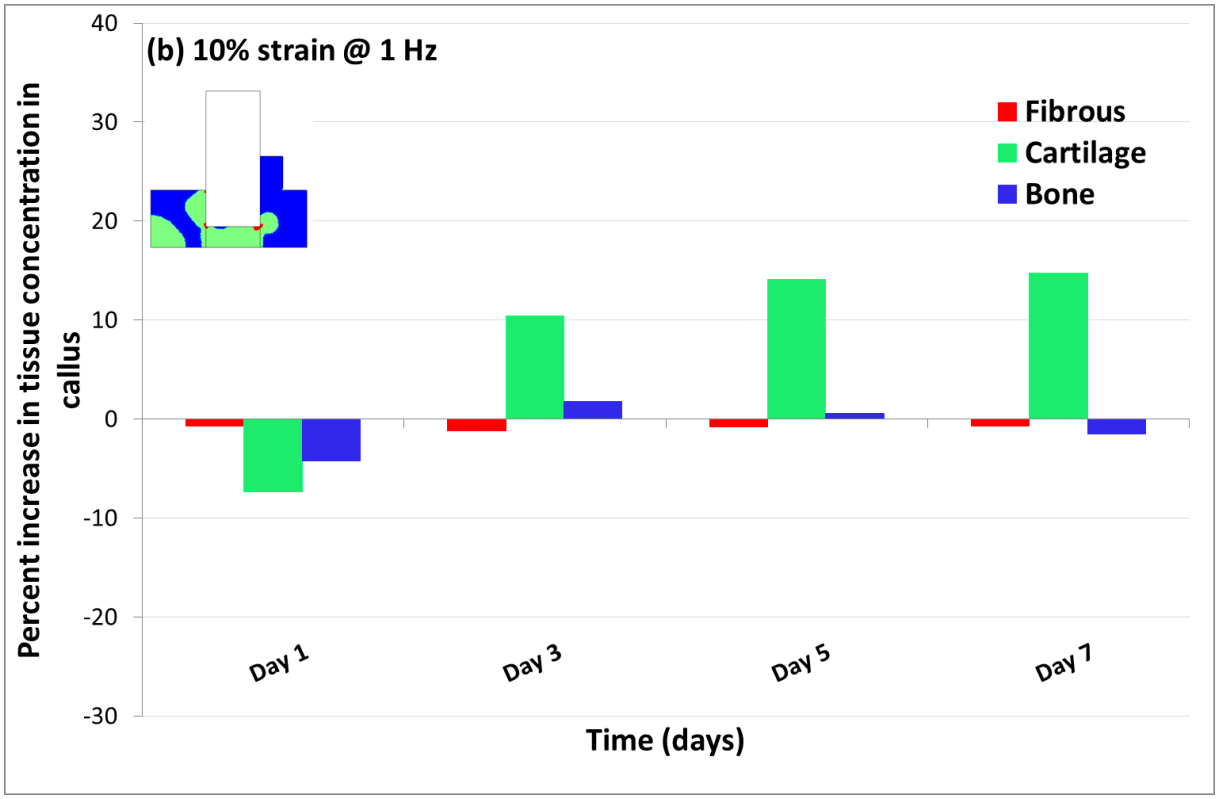
(b) 10% strain @ 1 Hz
Fibrous
Cartilage
Bone
Percent increase in tissue concentration in callus
40
30
20
10
0
-10
-20
-30
Day 1
Day 3
Day 5
Day 7
Time (days)

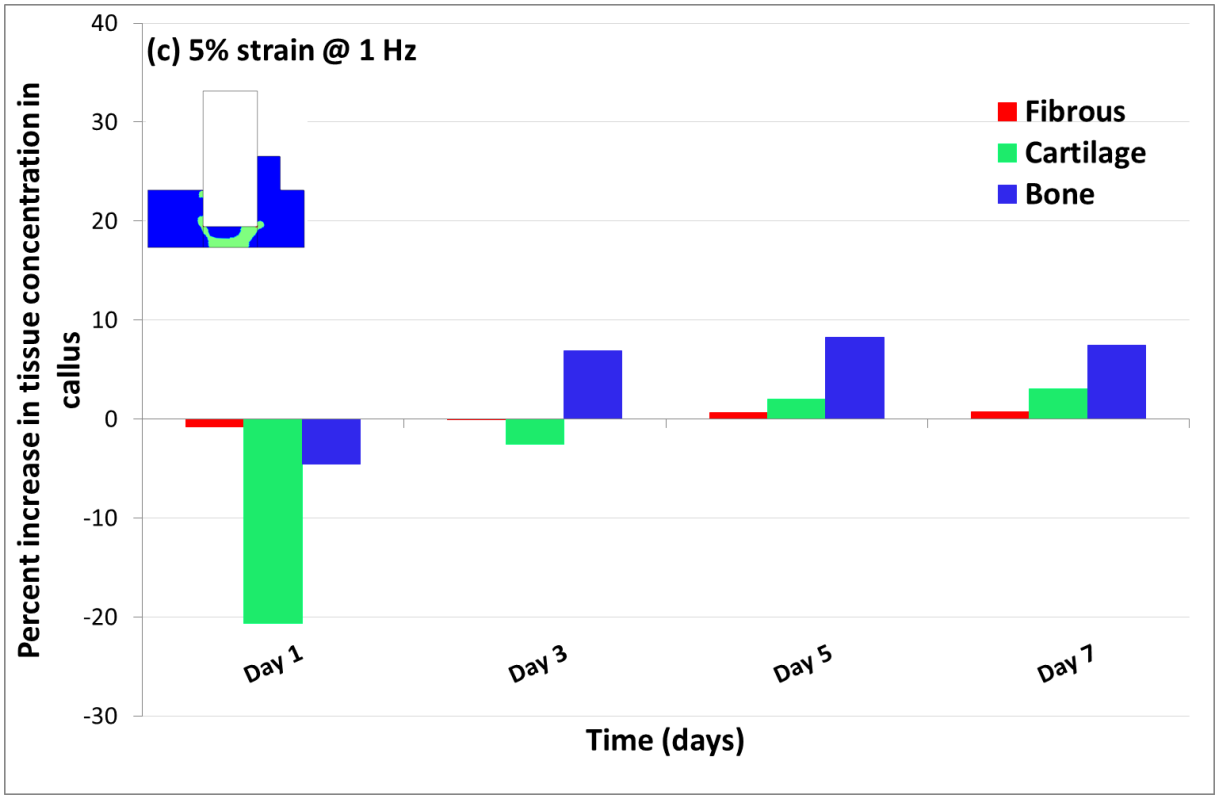
(c) 5% strain @ 1 Hz
Fibrous
Cartilage
Bone
Percent increase in tissue concentration in callus
40
30
20
10
0
-10
-20
-30
Day 1
Day 3
Day 5
Day 7
Time (days)

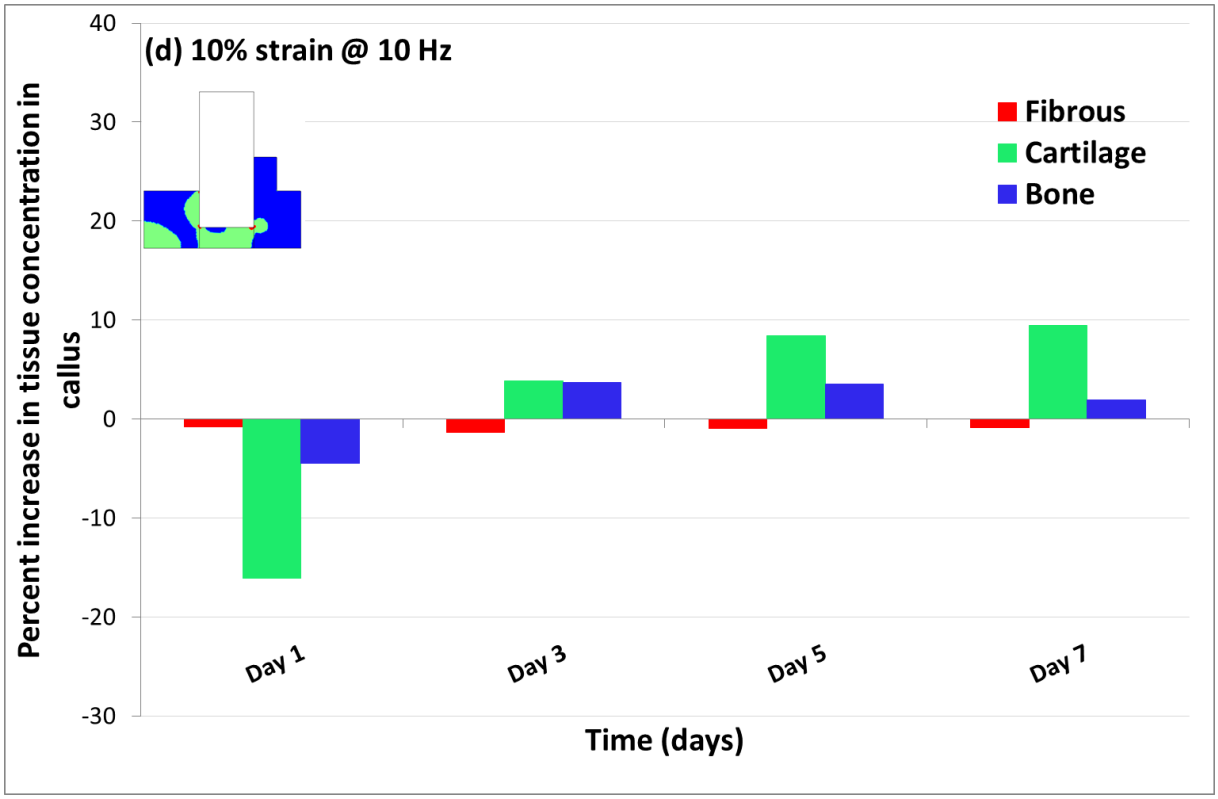
(d) 10% strain @ 10 Hz
Fibrous
Cartilage
Bone
Percent increase in tissue concentration in callus
40
30
20
10
0
-10
-20
-30
Day 1
Day 3
Day 5
Day 7
Time (days)

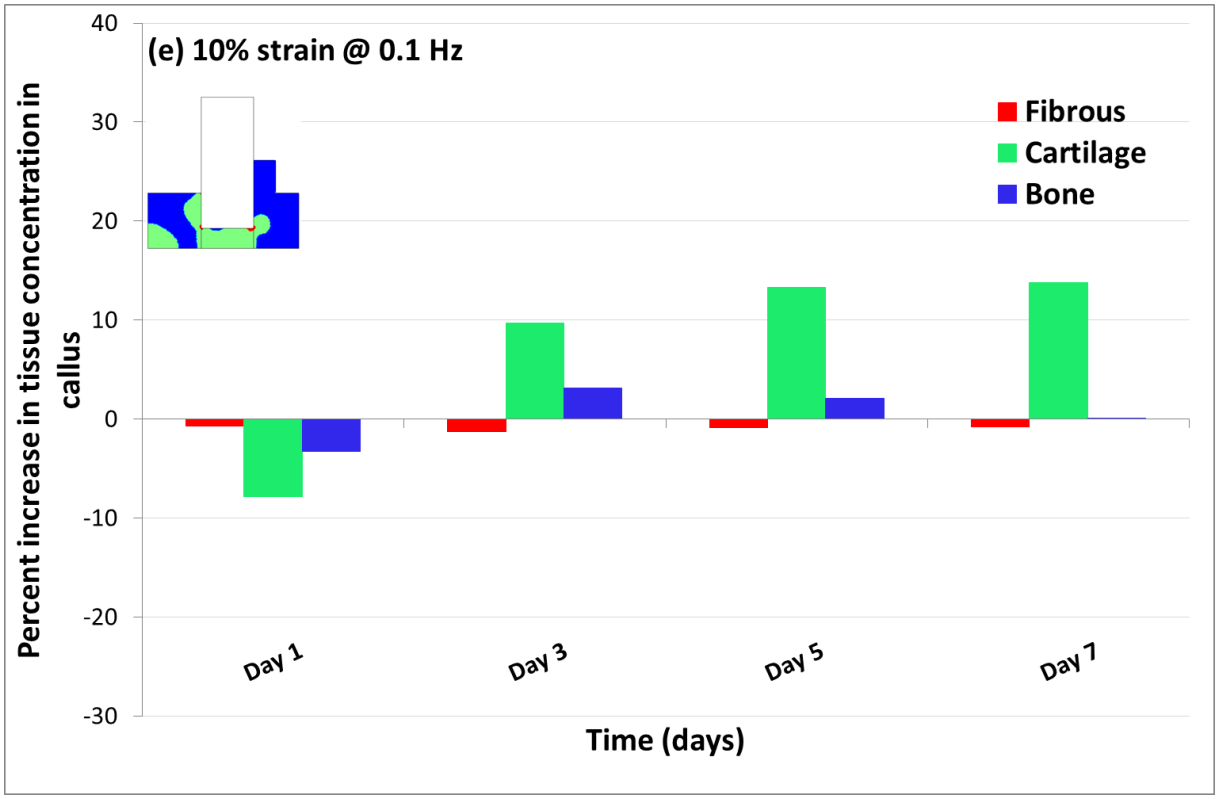

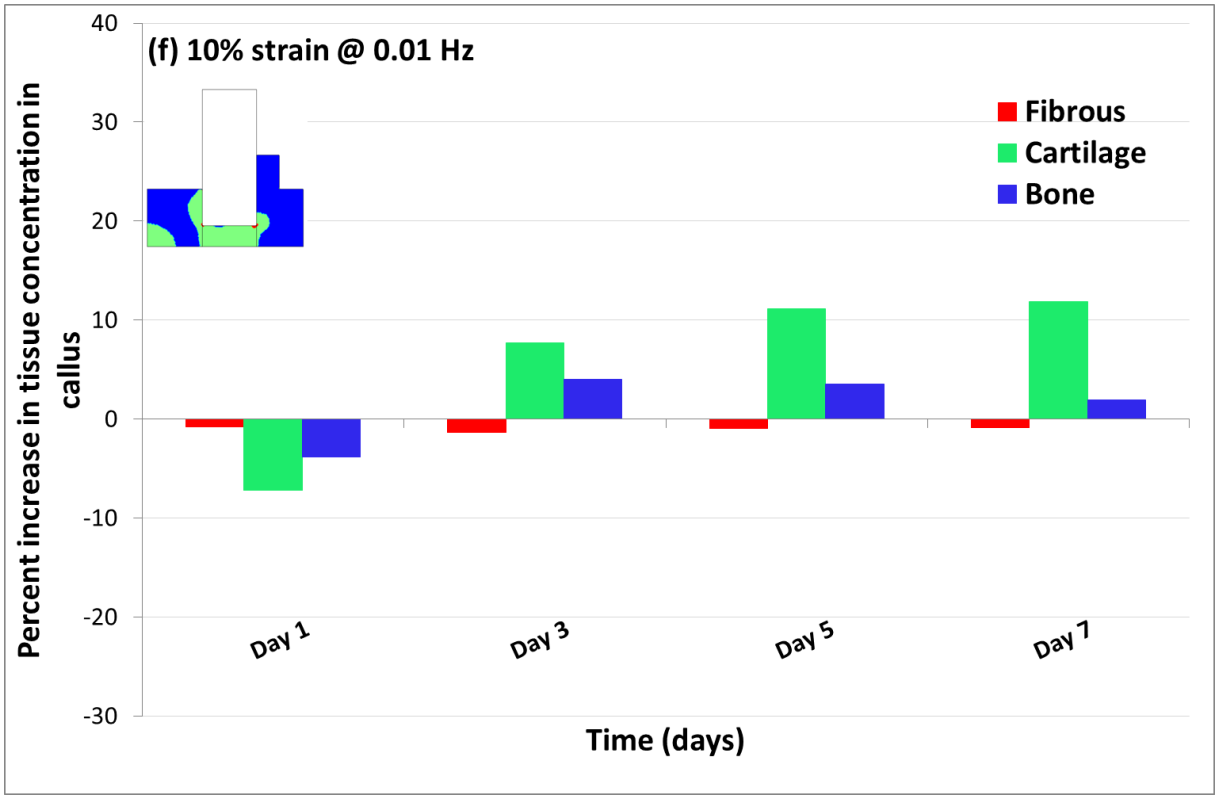

Figure. 3.10 Percent change in fibrous tissue, cartilage and bone concentration in callus under different loading conditions relative to control (i.e. free diffusion). Each inset

diagram shows spatial distribution of actual tissue concentration under corresponding loading conditions.

3.5. Discussion

This study investigates the cellular activities including proliferation, migration, differentiation and tissue formation mediated by both biochemical stimuli (i.e. growth factors) and mechanical stimuli (i.e. strain and fluid velocity) during bone healing. The developed model takes into account the direct contribution of dynamic loading induced mechanical stimuli as well as its indirect contribution through the advective transport of cells and growth factors within the fracture callus. To our best knowledge, this is the first study that incorporates all the above-mentioned healing mechanism into a computational model which could potentially be implemented in identifying optimal loading regimes for better healing outcomes.

Our computational simulation results suggest that tissue formation advances progressively from the callus regions where both MSCs and growth factors are abundant. The spatio-temporal distributions of MSCs and growth factors across all three regions: periosteal callus, cortical callus and endosteal callus is described from Figure. 5 to Fig 9. At day 7 post fracture, the model predicted a very low concentration of cartilage in the endosteal callus compared to that in periosteal callus due to the fact that there a lower concentration of both MSCs and chondrogenic growth factors in periosteal callus than that in periosteal zone (Figure. 3.6a and Figure. 3.7b). The model prediction is consistent with histological observation showing that little cartilage tissue is formed in the endosteal callus during early stage of healing (Harrison et al., 2003, Vetter et al., 2010). Our simulation results indicate that spatial tissue formation depends on both the concentration of both cells and stimulating growth factors, and thereby highlighting the importance of the transport of both cell migration and growth factors into the callus.

It is known that dynamic loading generally enhances the transport of solutes through interstitial fluid flow (Bonassar et al., 2001, Mauck et al., 2003, Zhang, 2011). Our simulation results show that the enhanced transport of MSCs and growth factors in the callus due to advection is more obvious during the first hour of loading. In addition, the increased cell and growth factor concentration under the influence of dynamic loading is

spatial dependent due to the spatially dependent interstitial fluid velocities. Figure. 3.9 shows that the percent increase of chondrogenic growth factors in the periosteal zone of callus due to dynamic loading is more than 3-fold than that of osteogenic growth factors because the interstitial fluid velocity in the region near the source of chondrogenic growth factors is much higher than that of osteogenic growth factors (González-Torres et al., 2010a) (Refer to Figure. 3.3b).

In addition, the model predicted a detrimental effect of dynamic loading immediately post fracture (i.e. inhibit the MSC differentiation into chondrocytes and osteoblasts). Our results show that, at Day 1 post-fracture, tissue formation under dynamic loading is less than that under free diffusion without loading. The model predictions are consistent with the experimental observation which showed that mechanical loading may impair cellular response at Day 1. (Moalli et al., 2000, Gardner et al., 2006). It should also be mentioned that the application of mechanical loading at fracture site immediately after fracture could result in further tissue damage, ultimately a delayed healing (Augat et al., 1996, Wolf et al., 1981). Our simulation results indicate the time of loading has to be carefully chosen to prevent possible negative effects on healing.

It is well known that adequate interfragmentary movement resulting from partial weight bearing exercise during healing encourages endochondral ossification (Augat et al., 1996, Wolf et al., 1981). Our model predicts a significant enhancement in cartilage tissue formation within the callus specifically in the cortical and endosteal regions following the application of dynamic loading (e.g. 10% strain @ 1 Hz as shown in Figure. 3.10b). As shown in Figure. 3.10a, although a large strain (e.g. IFS=15% and frequency of 1 Hz) could also increase cartilage tissue formation, it may lead to excessive fibrous tissue formation specifically in the cortical callus and thereby cause delay fracture gap bridging. The singularities in the inner corner of periosteal borders (Refer to Figure. 9a) is due to the shape adopted, however this doesn't influence the numerical results (Geris et al., 2010). There are numerous experimental evidences suggesting that formation of cartilage tissue in the fracture gap during the early stage of healing is favourable as it results in indirect fracture healing through endochondral ossification which is a much better healing process compared to direct bone formation in the fracture gap (i.e. direct healing) (Claes et al., 1995b, Perren, 2002b, Perren, 2008, Woo et al., 1983, McKibbin, 1978a). Further, the simulation results from Figure. 3.10 suggest there could be an

optimal loading regime (e.g. 10% strain @ 1 Hz as shown in Figure. 3.10b) which encourages cartilage tissue formation but inhibits fibrous tissue production.

3.5.1. Limitations

The present study mainly focused on the early stage of bone healing (i.e. first week after fracture) during which both the chemical and mechanical conditions are of critical importance for the entire healing process (Klein et al., 2003, Le et al., 2001). The boundary conditions shown in Figure. 3a are only valid in this stage. In addition, it is assumed that the mechanical properties of callus remain unchanged at this stage. However, as healing progresses (e.g. second week post-fracture), the mechanical properties of fracture callus should be updated in the model with increase of time. Furthermore, our future study should incorporate the angiogenesis which plays a key role in bone healing.

3.6. Conclusions

In this study, we have developed an experimentally validated computational model to investigate the effect of dynamic loading on the early stage of bone healing. The model is based on porous media theory and incorporates processes such as the advective transport of cells and growth factors, and mechanical stimuli resulting from tissue deformation and interstitial fluid flow induced by the dynamic loading. The followings are some major findings:

1. During the first week after the fracture, the major component of callus is fibrous tissue and the distribution of various tissues is spatial dependent. For example, the amount of fibrous tissue in cortical zone and periosteal zone is 95% and 65%, respectively. In addition, the content of cartilage tissue is highest in periosteal zone of callus, which is close to the source of MSCs and chondrogenic growth factors. As for the bone content, it is a similar in periosteal and endosteal zones of callus (i.e. 18%), whereas there is little bone and cartilage formation in cortical zone.
2. A physiologically relevant dynamic loading could enhance the transport of MSCs further into the endosteal callus (around 20% during the first hour of loading) but has limited influence in MSC uptake in periosteal and cortical callus. In addition,

the dynamic loading enhances the uptake of chondrogenic growth factor uptake by around 100% and 60% in cortical and periosteal callus, respectively, but has little effect on the transport of osteogenic growth factor.

3. An optimal dynamic loading regime (i.e. 10% strain @ 1Hz) produces the best healing outcomes through encouraging endochondral ossification by enhancing cartilage tissue formation and suppressing fibrous tissue content.

Chapter 4.

Effects of dynamic loading on fracture healing under different locking compression plate configurations: A finite element study

4.1. Abstract

The design of patient specific weight-bearing exercises after the surgical implementation of internal fixations is of critical importance for bone fracture healing. The purpose of this study is to theoretically investigate the effects of physiologically relevant dynamic loading on early stage of fracture healing under different locking compression plate (LCP) configurations. The finite element results show that dynamic loading enhanced transport of bone cells and growth factors in the fracture callus is much dependent on the flexibility of LCP. In comparison to free diffusion, a relatively flexible LCP together with dynamic loading could significantly enhance solute transport in callus. For example, a flexible LCP achieved by increasing WL (Working Length) and BPD (Bone Plate Distance) (*e.g.* WL=100mm and BPD=2mm) together with a 5-hour 150N@1Hz dynamic loading could increase the uptake of chondrocytes by around 280% compared to free diffusion, osteoblasts by around 180%, osteogenic growth factors by around 120% and chondrogenic growth factors by around 220%. In addition, dynamic loading enhanced transport of cells and growth factors under LCP is spatially dependent with a relatively higher enhancement in far cortex zone than that in near cortex zone. The outcomes from

present study could potentially assist orthopaedic surgeons to determine optimal loading regimes with consideration of patient specific LCP configurations.

4.2. **Introduction**

It has been widely known that the configuration of a bone fracture fixation and external dynamic loading affect mechanical micro-environment of the stem cells at the bone fracture site which influences cellular activities, and ultimately tissue formation during the healing process(Klein et al., 2003, Miclau et al., 2002). For example, it is well documented that the mechano-regulation plays an important role in cellular actions and tissue regeneration during diaphyseal bone healing (Carter et al., 1998a, Claes et al., 1997).

Bone fracture fixations, which aim to stabilize bone fracture and improve the healing outcome through mechanical intervention(Augat et al., 2001), can be classified into two types based on their mechanical stiffness, *i.e.* rigid fixation and flexible fixation. Recently, application of flexible fixation has become increasingly popular in clinical practice due to its capability of allowing a certain degree of interfragmentary movement (IFM) at the fracture site while still providing adequate stability for angiogenesis development(Schmal et al., 2011). As conventional compression plates are usually applied through extensive implant-bone contact and interfragmentary compression to maintain the absolute stability of a fracture site, they normally lead to primary healing (Claes et al., 2012, Perren, 2002c). On the other hand, a flexible fixation can result in accelerated healing outcomes through secondary bone healing and endochondral ossification due to its ability of enhancing mechanical stimuli mediated healing (Augat et al., 1998, Claes et al., 1998, Claes and Heigele, 1999). One of the most popular types is the locking compression plate (LCP) which can adjust its mechanical stiffness and flexibility through configuring distance between bone and plate [i.e. bone plate distance (BPD)], plate length or the distance between innermost screws across the fracture gap [i.e. working length (WL)]. While a flexible configuration of LCP can potentially improve callus formation and encourage secondary bone healing, a too flexible configuration may also result in too much fibrous tissue formation, ultimately delayed healing (Ahmad et al., 2007, Miramini et al., 2016a, Miramini et al., 2015). As evident from previous studies, both excessive IFM (due to flexible fixation with unrestrained loading) and no IFM (due

to rigid fixation with no loading) are detrimental for bone healing(Bailón-Plaza and van der Meulen, 2003). Therefore, fixation stability is a key element of uneventful and successful healing.

Physiologically relevant mechanical loading is a key factor which affects fracture fixation stability and IFM, ultimately fracture healing(Miramini et al., 2016b), in particular during the early stage of healing(Klein et al., 2003, Thompson et al., 2002). Previous studies have shown that early weight bearing enhances the fracture healing process(Geris et al., 2003, Bailón-Plaza and van der Meulen, 2003) and implants like LCP allow early movement of fractured bone after surgery. Further, the bone healing is also dependent on the fracture geometry (*e.g.* gap size and oblique angle)(Tan and Balogh, 2009, Nassiri et al., 2013). For example, previous studies suggested that the interfragmentary strain (=IFM/gap size) of a relatively large gap size (>3mm) is very sensitive to the change of BPD and WL of a LCP(Miramini et al., 2015). Similarly, Stoffel et al.(Stoffel et al., 2003a) demonstrated that risk of plate failure doubles for a gap size of 6mm compared to a smaller gap size of 1mm with an increase in WL under dynamic loading. However, more insight is necessary on how the fracture stability can influence molecular and cellular activities during bone healing, and the optimal LCP configurations are yet to be established for different fracture geometries(Epari et al., 2007).

Numerous experiments have been performed to examine the most suitable loading regimes for best fracture healing outcomes(Claes and Heigele, 1999, Kenwright and Goodship, 1989, Wolf et al., 1998). Gonzalez-Torres et al.(González-Torres et al., 2010a) applied range of frequencies from 1Hz to 100Hz and indicated that high frequency cyclic loading promotes chondrogenesis [i.e. mesenchymal stem cells (MSCs) differentiation to chondrocytes]. Previous studies have also indicated that MSCs commitment to osteoblast or chondrocyte differentiation during the initial stage of healing is influenced by their mechanical environment(Miclau et al., 2002, Le et al., 2001). Miramini et al. (Miramini et al., 2016b, Miramini et al., 2015) compared interfragmentary strain and MSCs differentiation during early stage of healing for different LCP configurations under compressive quasi-static load, by adopting a widely accepted(Isaksson et al., 2006) mechano-regulation theory of Prendergast et al(Prendergast et al., 1997). Interstitial fluid flow is well established to guide cell migration, but the directed cell migration due to fluid flow under dynamic loading has not been accounted for in these bio-mechanical

studies. As adequate supply of nutrients and oxygen is vital for successful healing, quicker transport of such solutes into fracture callus is desired during early stage of bone healing. Callus stimulation could promote their transport due to the influence of external stimulation, particularly frequency of loading, on the fluid flow velocity of callus(González-Torres et al., 2010a). Recent experiments on cartilage and callus constructs have also demonstrated that dynamic loading can enhance solute transport through advection(Zhang, 2011, Zhang et al., 2009, Bonassar et al., 2001, Witt et al., 2014). Insulin like growth factors (IGF-I) were enhanced by around 20% in articular cartilage under a cyclic loading with 10% strain magnitude(Zhang et al., 2007). Another study reported enhanced transport of large solutes under dynamic loading of physiological frequency ranges in any porous media, including biological tissue like callus(Mauck et al., 2003). Growth factors like osteogenic and chondrogenic growth factors are large solutes with a molecular weight of 25KDa(Joyce et al., 1990a). Further, the solute enhancement was prominent during the initial stage of loading, which is also supported by experimental findings(O'Hara et al., 1990). Furthermore, our previous study in fracture callus also predicted an increase in MSCs concentration by around 25% within first 5 hours under dynamic compressive load (10% strain @ 1Hz)(Ghimire et al., 2018). However, there is limited research on the effects of dynamic loading on growth factor and cell transport during early stage of fracture healing under different LCP configurations.

Therefore, this paper aims to investigate the effects of different LCP configurations (i.e. WL and BPD] on the MSCs migration and differentiation as well as growth factor transport using finite element method (FEM) simulation. The current study represents the first step towards fundamental understanding of the mechanical loading mediated MSCs transport and differentiation under LCP with various flexibilities.

4.3. **Materials and methods**

In present study, the early stage soft callus is modelled as a three-phase mixture consisting of solid phase (*i.e.* solid extracellular matrix, such as various tissues), fluid phase (*i.e.* interstitial fluid) and solute phase (cells like MSCs, fibroblasts; and growth factors like osteogenic growth factor and chondrogenic growth factor)(Zhang et al., 2008c, Zhang et al., 2007, Zhang et al., 2008a, Zhang, 2011, Zhang et al., 2009, Miramini

et al., 2018). As presented in Figure. 1, the developed model considers the change of biomechanical microenvironment of bone cells in fracture callus due to the change of LCP configurations, fracture geometry and loading conditions. The cells and growth factors transport due to advection resulting from the interstitial fluid flow in callus generated by the dynamic loading is taken into account. The FEM model also incorporates the synergistic effects of fracture biomechanical microenvironment on bone healing directly through mechanical stimuli, and indirectly through the advective transport of biochemical stimuli (i.e. growth factors) which is the novelty of this work (Refer to Figure. 4.1).

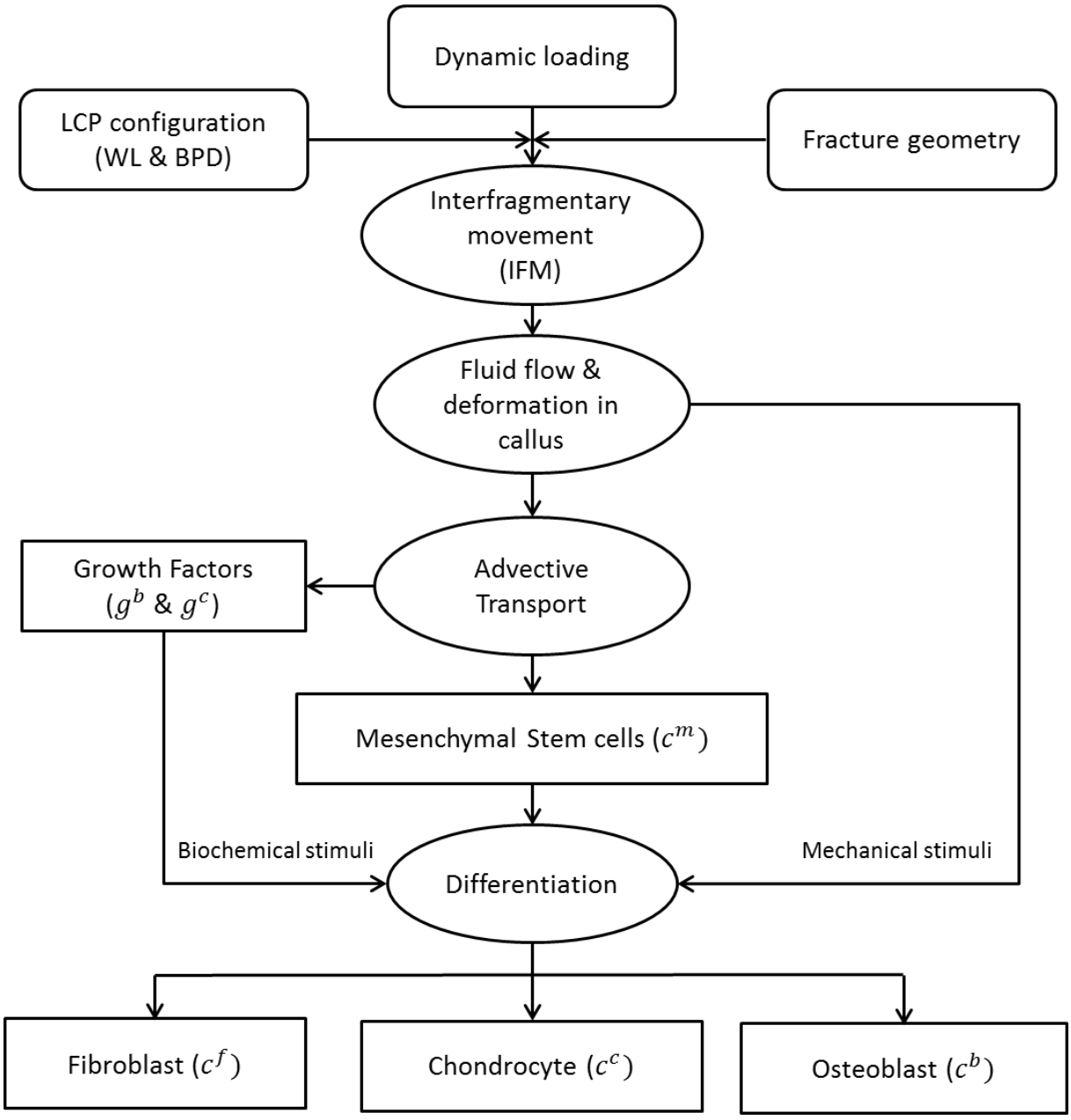

Figure. 4.1 A schematic diagram showing the methodology used in this study.

4.3.1. Governing Equations

Assuming the volume fraction of solute to be negligible ($\emptyset^w \sim 0$), the volume fraction of solid ($\emptyset^s$) and fluid phase ($\emptyset^f$) is given by

$$\emptyset^s + \emptyset^f \cong 1 \tag{4.1}$$

In addition, it can be reasonably assumed that the early soft callus experiences infinitesimal strain under LCP implant and partial weight bearing. Further, by treating callus as a homogeneous, linearly elastic and isotropic mixture, the conservation of linear momentum of callus leads to

$$-\nabla p + (\lambda_s + 2\mu_s)\nabla(\nabla \bullet \mathbf{u}^s) + \mu_s \nabla^2 \mathbf{u}^s = 0 \tag{4.2}$$

where,

p = incremental interstitial fluid pressure;

λ_s = Lame's constant;

μ_s = Lame's constant; and

$\mathbf{u}^s$ = solid phase displacement vector.

Similarly, by modelling the fluid motion within the callus using Darcy's law(Zhang, 2011, Zhang et al., 2009, Zhang et al., 2015b), the mass conservation for solid phase and fluid phase can be expressed as

$$\nabla \bullet (\mathbf{v}^s - \boldsymbol{k}\nabla p) = 0 \tag{4.3}$$

where,

$\mathbf{v}^s$ = solid-phase velocity; and

$\boldsymbol{k}$ = tissue hydraulic permeability tensor.

4.3.2. Mechano-regulation mediated cell differentiation

Several mechano-regulation theories have been proposed to predict fracture callus cell differentiation under different fracture callus mechanical microenvironment(Pauwels, 1960, Perren, 1979). Strain magnitude and fluid flow were identified as the mechanical stimuli that determine course of healing(Claes and Heigele, 1999). Prendergast et al(Prendergast et al., 1997) suggested that cell differentiation and tissue formation during bone healing are affected by the value of mechanical stimulation index (i.e. S-index) which depends on octahedral shear strain (τ) and the interstitial fluid phase velocity ($\mathbf{v}^f$), as follows:

$$S = \frac{\tau}{0.0375} + \frac{\mathbf{v}^f}{3 \times 10^{-6}\ (m/s)} \tag{4.4}$$

Other independent studies have shown that *S*-index is the best indicator to simulate the MSCs differentiation and tissue formation under different mechanical loading conditions(Isaksson et al., 2006). A low *S*-Index (<1) results in osteoblast differentiation, moderate Stimulation Index (1 < *S* < 3) leads to chondrocyte differentiation while a high *S* (>3) results in fibroblast differentiation, based on values obtained (Huiskes et al., 1997).

4.3.3. Transport equation for cells and growth factors

The reaction - diffusion equations were applied for cells and growth factors transport and can be expressed based on our previous work as follows(Ghimire et al., 2018, Zhang et al., 2010a):

$$\frac{\partial \bar{c}^{\,\alpha}}{\partial t} = -\nabla \bullet \left(-D^{\alpha}\nabla \bar{c}^{\,\alpha} + \mathbf{v}^{\boldsymbol{f}}\bar{c}^{\,\alpha}\right) + S_p^{\alpha} - S_d^{\alpha} \tag{4.5a}$$

where,

D^{α} = diffusion coefficient of α cells/growth factors in fracture callus;

S_p^{α} = rate of production rate of α cells/growth factors; and

S_d^{α} = rate of degradation rate of α cells/ growth factors.

$c^{\alpha} = c^{m}$, c^{f}, c^{c} *and* c^{b} represents cell concentration of MSCs (c^{m}), fibroblasts (c^{f}), chondrocytes (c^{c}), and osteoblasts (c^{b}); and $c^{\alpha} = g^{b}$ and g^{c} represents growth factor concentration of osteogenic growth factors (g^{b}), and chondrogenic growth factor (g^{c}), respectively. g^{b} (osteogenic growth factors such as BMP -2, -4, -6) and g^{c} (chondrogenic growth factors such as TGF β -2, -3) are known to regulate differentiation of MSCs into chondrocytes and osteoblasts respectively(Cho et al., 2002, Marsell and Einhorn, 2009, Solheim, 1998).

The degradation / differentiation rate of MSCs is influenced by both biochemical and mechanical stimuli. The mechanical stimuli mediated MSCs differentiation S_d^m is assumed to depend on the *S*-index (S) magnitude, as follows:

$$S_d^m = \begin{cases} S_{pm}^b = \lambda_d^b \, \bar{c}^{\,m}, & S_{pm}^c = S_{pm}^{fb} = 0\,, & for\ S < 1 & (osteoblasts) \\ S_{pm}^c = \lambda_d^c \, \bar{c}^{\,m}, & S_{pm}^b = S_{pm}^{fb} = 0\,, & for\ 1 < S < 3 & (chondrocytes) \\ S_{pm}^{fb} = \lambda_d^{fb} \, \bar{c}^{\,m}, & S_{pm}^b = S_{pm}^c = 0\,, & for\ S > 3 & (fibroblasts) \end{cases} \tag{4.5b}$$

MSCs differentiation rate into fibroblasts, chondrocytes and osteoblasts due to biochemical and mechanical stimuli is dependent on *S*-index, in such a way that the differentiation of MSCs into a particular cell type is inhibited altogether in the event of unfavourable mechanical stimuli for that cell type(Bailón-Plaza and van der Meulen, 2003).

The degradation of MSCs as it differentiates into other cells (fibroblasts, osteoblast and chondrocyte) leads to the production of those cells. Thus, the production rate of fibroblasts, chondrocytes and osteoblasts can be expressed as follows:

$$S_p^{\alpha} = (k_d^{\alpha} + \lambda_d^{\alpha}) c^m \tag{4.5c}$$

where,

k_d^{α} = production rate of α cells mediated by biochemical stimuli; and

λ_d^{α} = production rate of α cells mediated by mechanical stimuli;

The parameter values are given in Table 4.1.

Table 4.1 Parameters used throughout this study. The values used to non-dimensionalise above coefficients are adopted and rescaled from Peiffer et al(Peiffer et al., 2011).

Parameter	**Value**	**References**
MSCs diffusion coefficient ($\boldsymbol{D^m}$)	0.3456 mm^2/day	(Andreykiv et al., 2008)
Fibroblast diffusion coefficient ($\boldsymbol{D^f}$)	0.245 mm^2/day	(Peiffer et al., 2011)
Osteogenic growth factor diffusion coefficient ($\boldsymbol{D^{gb}}$)	0.06125 mm^2/day	(Peiffer et al., 2011)
Chondrogenic growth factor diffusion coefficient ($\boldsymbol{D^{gc}}$)	0.06125 mm^2/day	(Peiffer et al., 2011)
MSCs differentiation into fibroblasts under biochemical stimuli ($\boldsymbol{k_d^{fb}}$)	0.01/day	(Peiffer et al., 2011)
MSCs differentiation into fibroblasts under mechanical stimuli ($\boldsymbol{\lambda_d^{fb}}$)	0.01/day	(Andreykiv et al., 2008)
Differentiation coefficient of chondrocyte under biochemical stimuli ($\boldsymbol{Y_2}$)	40/day(Bailon-Plaza and van der Meulen, 2001)	(Bailon-Plaza and van der Meulen, 2001)
Differentiation coefficient of chondrocyte under biochemical stimuli ($\boldsymbol{H_2}$)	10 ng/ml	(Peiffer et al., 2011)
MSCs differentiation into chondrocytes under mechanical stimuli ($\boldsymbol{\lambda_d^c}$)	0.3/day	(Andreykiv et al., 2008)
Differentiation coefficient of osteoblast under biochemical stimuli ($\boldsymbol{Y_1}$)	3/day	(Bailon-Plaza and van der Meulen, 2001)

Differentiation coefficient of osteoblast under biochemical stimuli ($\boldsymbol{H_1}$)	10 ng/ml	(Peiffer et al., 2011)
MSCs differentiation into osteoblasts under mechanical stimuli ($\boldsymbol{\lambda_d^b}$)	(0.005 + 0.145xS)/day	(Andreykiv et al., 2008)
MSCs boundary condition ($\boldsymbol{c^{m0}}$)	2×10^4cells/ml	(Peiffer et al., 2011)
Fibroblasts boundary condition ($\boldsymbol{c^{f0}}$)	2×10^4cells/ml	(Peiffer et al., 2011)
Chondrogenic growth factors boundary condition ($\boldsymbol{g^{c0}}$)	2μg/ml	(Peiffer et al., 2011)
Osteogenic growth factors boundary condition ($\boldsymbol{g^{b0}}$)	2μg/ml	(Peiffer et al., 2011)
Callus Young's Modulus	0.05 MPa	(McCartney et al., 2005)
Cortex Young's Modulus	2×10^4MPa	(Lacroix and Prendergast, 2002)
Callus Poisson's ratio	0.1(Lacroix and Prendergast, 2002)	(Lacroix and Prendergast, 2002)
Cortex Poisson's ratio	0.3(Lacroix and Prendergast, 2002)	(Lacroix and Prendergast, 2002)
Callus Permeability	1×10^{-14}m^4/Ns	(Lacroix and Prendergast, 2002)
Cortex Permeability	1×10^{-17}m^4/Ns	(Lacroix and Prendergast, 2002)
Callus Fluid compression modulus	2.3×10^3MPa	(Lacroix and Prendergast, 2002)

Cortex Fluid compression modulus	2.3×10^3MPa	(Lacroix and Prendergast, 2002)
Callus Solid compression modulus	2.3×10^3 MPa	(Lacroix and Prendergast, 2002)
Cortex Solid compression modulus	13920 MPa	(Lacroix and Prendergast, 2002)

4.3.4. Cells and growth factors Uptake

The average normalised cells / growth factors uptake in callus is defined as the average cells / growth factors concentration in total volume of callus (Zhang, 2011) as follows:

$$\bar{c}^{\alpha}_{avg} = \frac{\int_0^{V_0} \bar{c}^{\alpha} dV}{c_0^{\alpha} V_0} \tag{4.6}$$

where

c_0^w = saturated cells / growth factors concentration in total volume of callus zone V_0

4.3.5. Problem Description

Geometry

Our previously developed 3D computational model of bone fracture stabilised under different LCP configurations (Miramini et al., 2015) was further developed in this study to investigate the influence of dynamic loading on cells and growth factors transport in fracture callus stabilized by LCP (Refer to Figure. 4.2 a, b and c). The 3D model geometry was reconstructed using the CT scan images of human tibia bone surrogates (387mm in length and 27mm in diameter) stabilized by LCP followed by an induced transverse osteotomy of 1mm or 3mm in the tibial diaphysis. As IFM is not uniform at fracture site under LCP implant, the cortex was divided into near cortex (NC) (i.e. fixation side cortex) and far cortex (FC) (i.e. opposite cortex) (Figure. 4.2b). Firstly, a cyclic loading similar to foot loading pattern during walking was applied on the proximal end of 3D tibia model to compute IFM at NC and FC under different LCP configurations (Figure. 4.2a). Then, the IFM values are applied as dynamic loading boundary conditions on proximal end of 2D

tibia model for computational efficiency (Figure. 4.2b and c). The transport of cells (i.e. MSCs, fibroblasts, osteoblasts and chondrocytes) and growth factors (i.e. osteogenic growth factor and chondrogenic growth factors) due to fluid flow and deformation in callus caused by IFM was incorporated in 2D model (refer to Figure. 4.1). Since different fracture gaps result in different interfragmentary strain, two gap sizes (i.e. 1mm and 3mm) were considered. The 2D model was then used to simulate the time dependent growth factors and cells transport due to mechanical microenvironment as well as MSC differentiation due to mechanical and biochemical stimuli for bone fractures stabilised by different configurations of LCP subjected to dynamic loading application.

Assumptions

In order to simplify the healing mechanism, following assumptions were made in present study:

- There is little change in callus size and geometry during early stage of healing.
- The total differentiation rate is the sum of rate of cell differentiation mediated by chemical and mechanical stimuli.
- No flux is assumed for all cells and growth factors within fracture callus.
- 2D model in longitudinal plane along the locking plate represents the spatial distribution of cells and growth factors throughout the callus of 3D model.

Boundary conditions

The boundary conditions for all cells (including osteoblasts and chondrocytes) and growth factors(Lacroix and Prendergast, 2002) were assumed impermeable (*i.e.* no flux) to fluid flow. In addition, it is assumed that:

- MSCs (c^{m0}) and fibroblasts (c^{f0}) diffuse from periosteum of cortex, internal bone marrow and external boundaries of callus(Henricson et al., 1987, Postacchini et al., 1995).
- Chondrogenic growth factors (g^{c0}) diffuse from the broken end of cortex; while osteogenic growth factors (g^{b0}) diffuse from the unbroken cortex lining(Barnes et al., 1999).

Initial conditions

All initial conditions are assumed to be zero for simplicity, i.e.

$$\bar{c}^{\alpha}(t=0)=0 \tag{4.7}$$

where $c^{\alpha}=c^{m},c^{f},c^{c}$ and c^{b} represents cell concentration of MSCs (c^{m}), fibroblasts (c^{f}), chondrocytes (c^{c}), and osteoblasts (c^{b}); and $c^{\alpha}=g^{b}$ and g^{c} represents growth factor concentration of osteogenic growth factors (g^{b}), and chondrogenic growth factor (g^{c}), respectively.

Loading Protocol

A partial weight bearing and physiologically relevant dynamic loading similar to human foot gait loading (i.e. ground reaction force) was applied on the proximal end of cortical bone (Barker and Seedhom, 2001, Zhang et al., 2015b) (Refer to Figure. 4.2a and c). Loading amplitudes of 150N (corresponding to 20% body weight of a person with average weight of 75kg) and 200N @ 1Hz were considered in the study(Miramini et al., 2016b, Zhang et al., 2007).

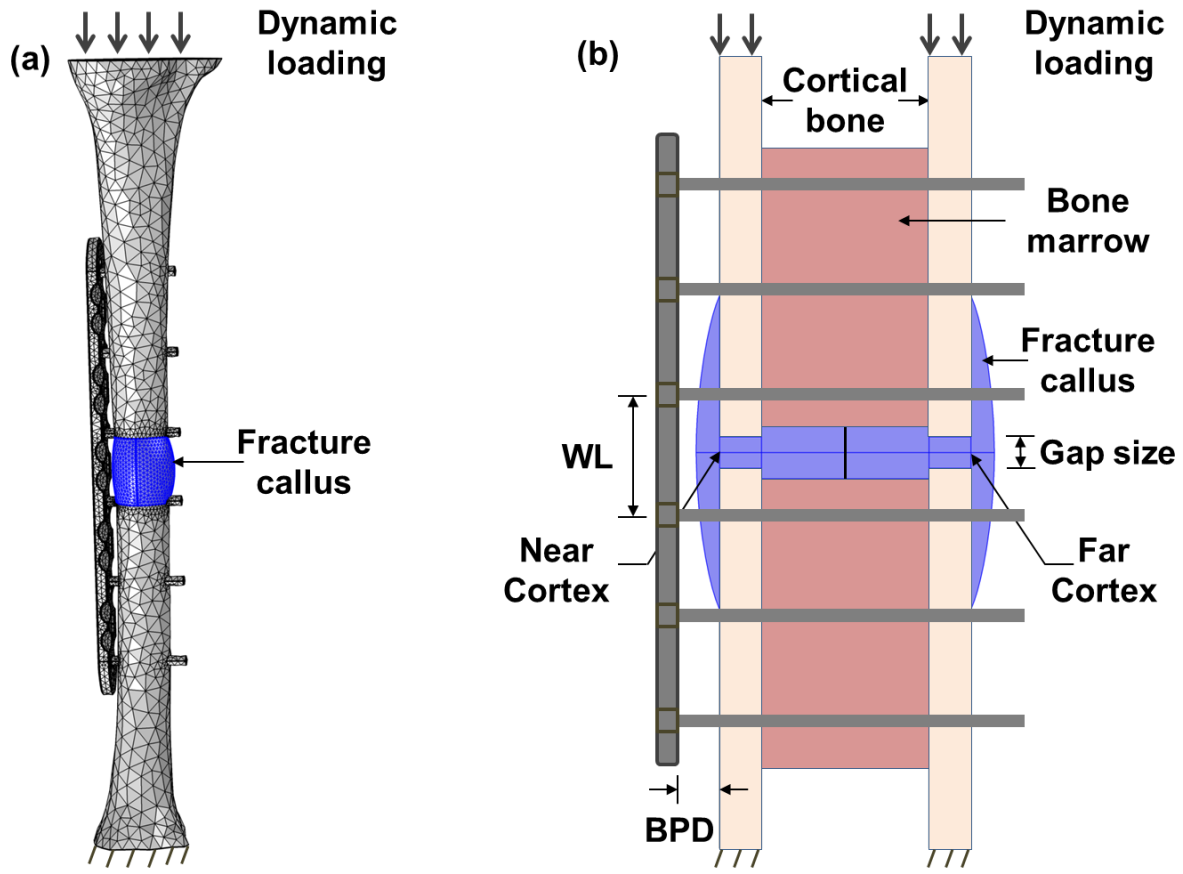

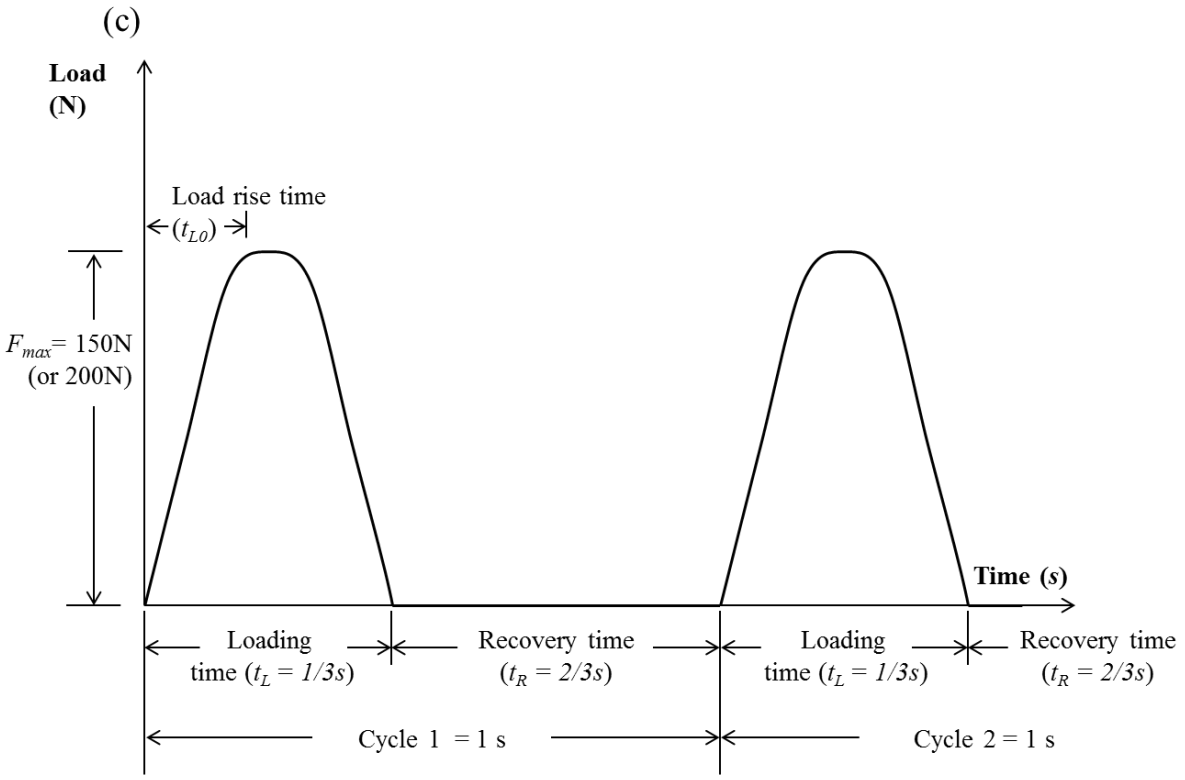

Figure. 4.2 A schematic diagram of fractured tibia (a) Finite element model; (b) details of LCP configuration; and (c) Loading protocol adopted in this study(Barker and Seedhom, 2001) (Peak load, F_{max} = 150N or 200N and a loading cycle of 1Hz consisting of loading phase, t_L = 1/3 s and recovery phase, t_R = 2/3 s).

Implant

The human tibia bone surrogates were stabilized by 4.5mm broad LCP. Stainless steel plates (11 locking holes in length 206mm, width 17.5mm and thickness 5.2mm) with locking screws (length 40mm and core diameter 4.5mm) manufactured by Johnson & Johnson DePuy Synthes (Oberdorf, Switzerland) were used on one side of cortex. Double plating is normally not preferred due to the significant invasion to surrounding tissues and blood vessels and no obvious improvement in healing outcomes (Teipner and Mast, 1980, Bai et al., 2018).

Fixation configuration

Previous studies have reported that BPD and WL of LCP are the most influential parameters in determining the IFM of fracture site(Stoffel et al., 2003a, Miramini et al., 2015). As the experimental study of Ahmad et al.(Ahmad et al., 2007) demonstrated that a bone plate distance of over 5mm leads to risk of implant failure, a combination of

different LCP configuration with BPD less than 5mm is adopted in this study. A control model is designed to be a relatively rigid fixation with BPD = 0mm with screws locked in first, third and fifth plate holes from fracture gap. Four LCP configurations (C_{BPD-WL}) with varying flexibility (i.e. different BPD and WL) were compared against control model (i.e. BPD = 0mm) (Refer to Table 4.2).

Table 4.2 LCP configuration cases used in this study(Miramini et al., 2016b)

Cases	BPD (mm)	WL (mm)
C_{0-30} (Control)	0	30
C_{2-30}	2	30
C_{4-30}	4	30
C_{2-100}	2	100
C_{4-100}	4	100

Numerical simulation

The governing equations (2), (3) and (6) were solved numerically using COMSOL Multiphysics package. The fracture callus domain was meshed with a structured free tetrahedral (for 3D model) and triangular (for 2D model) mesh with 11142 and 1124 elements respectively (Refer to Figure. 4.2a). The size of the mesh is determined by conducting convergence analysis with an error of 2%. In addition, a relative tolerance of 10^{-3} was adopted in this study.

4.4. **Results**

In this study, the transport of cells and growth factors four LCP configurations with varying BPD and WL (Refer to Table 4.2) were compared to a rigid fixation (C_{0-30} - Control model, 0mm BPD configuration). In addition, the effects of different gap sizes (i.e. 1mm and 3mm) and loading conditions (i.e. 150N@1Hz and 200N@1Hz) were investigated. The cortex and callus in the model were divided into NC and FC zone (refer to Figure. 4.2b) based on its proximity to the locking plate implant.

4.4.1. Model validation

As shown in Figure. 4.3, the FEM model predictions of IFM at NC and FC for different LCP configurations were compared with past experimental data(Miramini et al., 2016b). The predicted IFM ratio at FC to IFM at NC obtained from numerical simulations agree well with the experimental data (Miramini et al., 2016b) for all cases of LCP configurations under both 150N and 200N loading conditions.

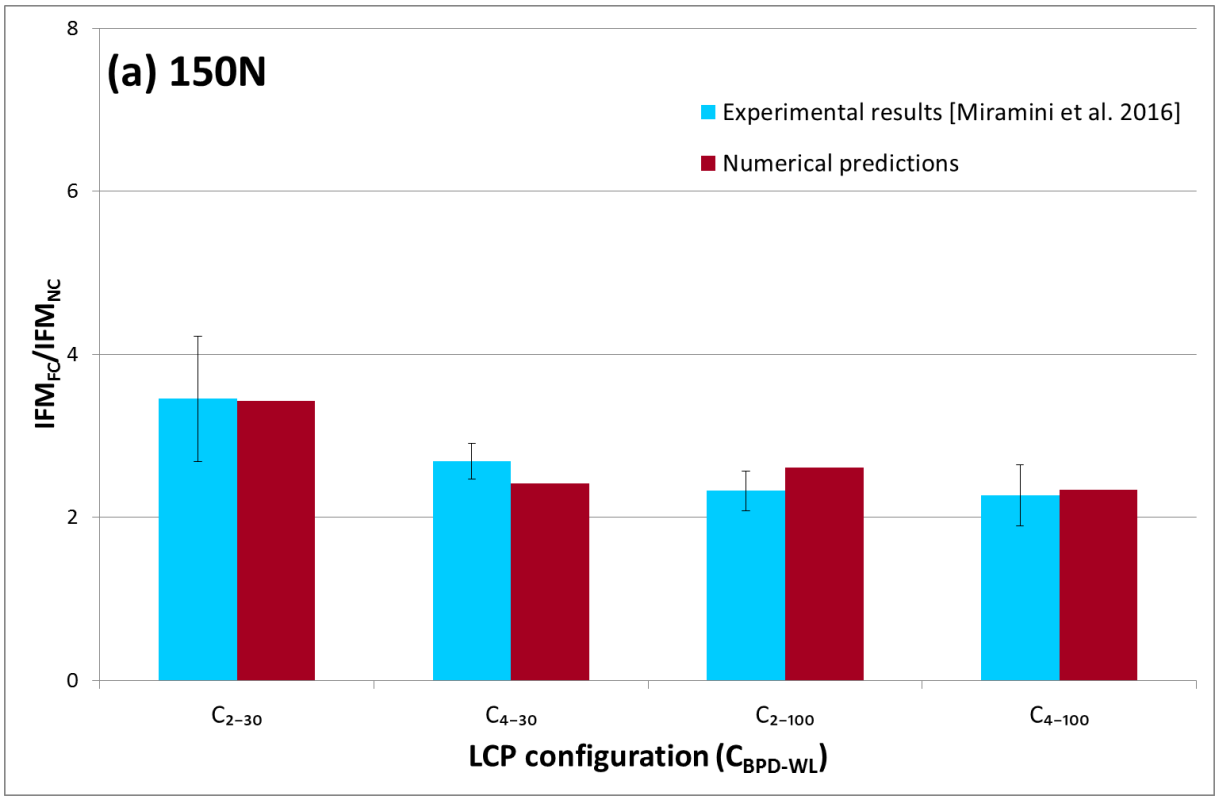

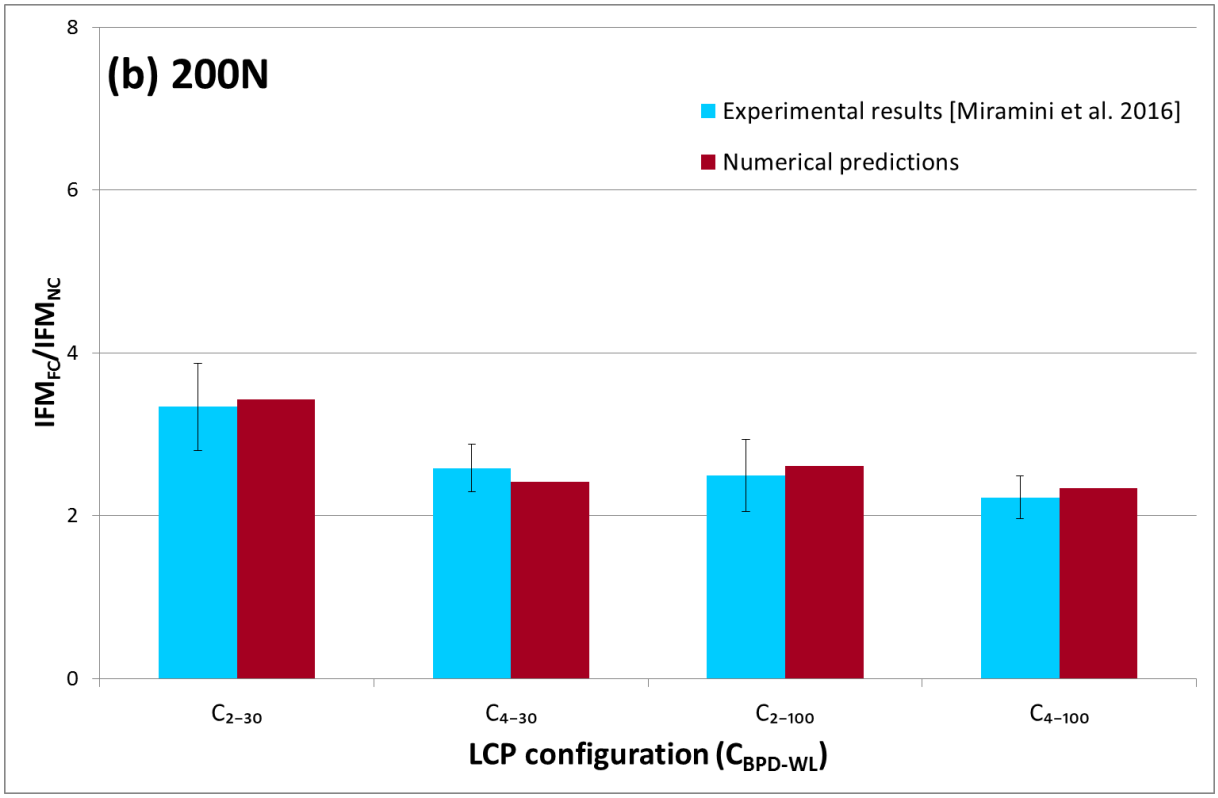

Figure. 4.3 Comparison of model predicted ratio of the interfragmentary movement (IFM) at far cortex (FC) to that at near cortex (NC) under different LCP configurations with previous experimental data(Miramini et al., 2016b).

4.4.2. Effects of LCP configuration on cells and growth factors under dynamic loading

Fig 4 shows the percent increase in the average uptake of cells and growth factors under dynamic loading (150N @1Hz) in comparison to free diffusion under different LCP configurations, respectively under 3mm gap size. The results show that dynamic loading generally enhances the uptake of cells and growth factors in fracture callus under relatively flexible fixation (e.g. $C_{4\text{-}100}$: BPD = 4mm and WL = 100mm) and this enhancement decrease with the increase of the mechanical stiffness of the fixation. Most importantly, it suggests that the enhancement induced by the 5-hour dynamic loading results is much more obvious for chondrocytes (around 280% compared to free diffusion), osteoblasts (around 180%), osteogenic growth factor (around 120%) and chondrogenic growth factors (around 220%), while moderate enhancement is seen for MSCs (around 22%) and fibroblasts (around 17%). These results are consistent with the clinical observations that patients subjected to axial micro-movement had a better

healing outcome compared to the rigid group(Kenwright et al., 1991). However, different fixation configuration with varying BPD and WL could also have significant influence on mechanical environment of callus, therefore the magnitude of S-index is calculated under NC and FC zones for different loading conditions and is presented in Table 4.3.

Table 4.3 Average S-index (S) magnitude in near cortex (NC) and far cortex (FC) zone of callus for a gap size = 3mm

	Load = 200N		Load = 150N (20% body weight)	
C_{BPD-WL}	NC	FC	NC	FC
C_{0-30}	1.3	1.5	1	1
C_{2-30}	1.01	1.8	0.76	1.3
C_{4-30}	1.5	2.2	1.1	1.6
C_{2-100}	2.5	4.1	1.8	3.1
C_{4-100}	3	5.6	2.2	4.2

$1 < S < 3$ (Chondrocyte differentiation)

$S > 3$ (Fibroblast differentiation)

From Table 4.3, we can see that the most flexible fixation (i.e. C4-100) leads MSC differentiation into fibroblasts in both NC and FC zones (i.e. S-index > 3) under 200N dynamic loading, which is also consistent with previous studies (Miramini et al., 2016b).

4.4.3. Effects of fracture geometry on cells and growth factors under dynamic loading

Figure. 4.6 shows the percent increase in normalised cells and growth factors uptake in NC and FC zones after 5-hour dynamic loading (150N @1Hz) in comparison to free diffusion for different gap sizes (GS = 1mm and 3mm), respectively. It shows that the enhancement of chondrocyte and chondrogenic growth factor uptake under a relatively small gap size (e.g. 1mm) is higher than that of 3mm gap size, and the enhancement of

chondrocyte uptake is very significant. In contrast, for MSCs, fibroblasts, chondrogenic growth factors, osteogenic growth factors, a relatively large gap size (e.g. 3mm) leads to a better outcome under dynamic loading. Significantly, it demonstrates that the dynamic loading induced enhancement is spatially dependent since NC and FC zones are subjected to different interfragmentary strain. The model predicted that spatially dependent cell and growth factor transport behaviour is consistent with the observations in previous animal studies(Lujan et al., 2010). In general, FC zone exhibited a higher enhancement in cells and growth factors uptake compared to that in NC zone under different types LCP configurations and gap sizes.

4.4.4. Effects of different loading regime on MSCs transport

Figure. 4.4 compares the uptake of MSCs (GS = 3mm and 1mm; $C_{2\text{-}100}$) under different loading conditions. The results show that a relatively high loading magnitude (200N) could result in around 10% increase in average MSCs uptake than a relatively low loading magnitude (150N) after 5-hour loading. In addition, under similar loading condition, the enhancement is higher for 3mm gap size than that for 1mm gap size, and the increase of MSCs uptake in FC zone is higher than that in NC zone.

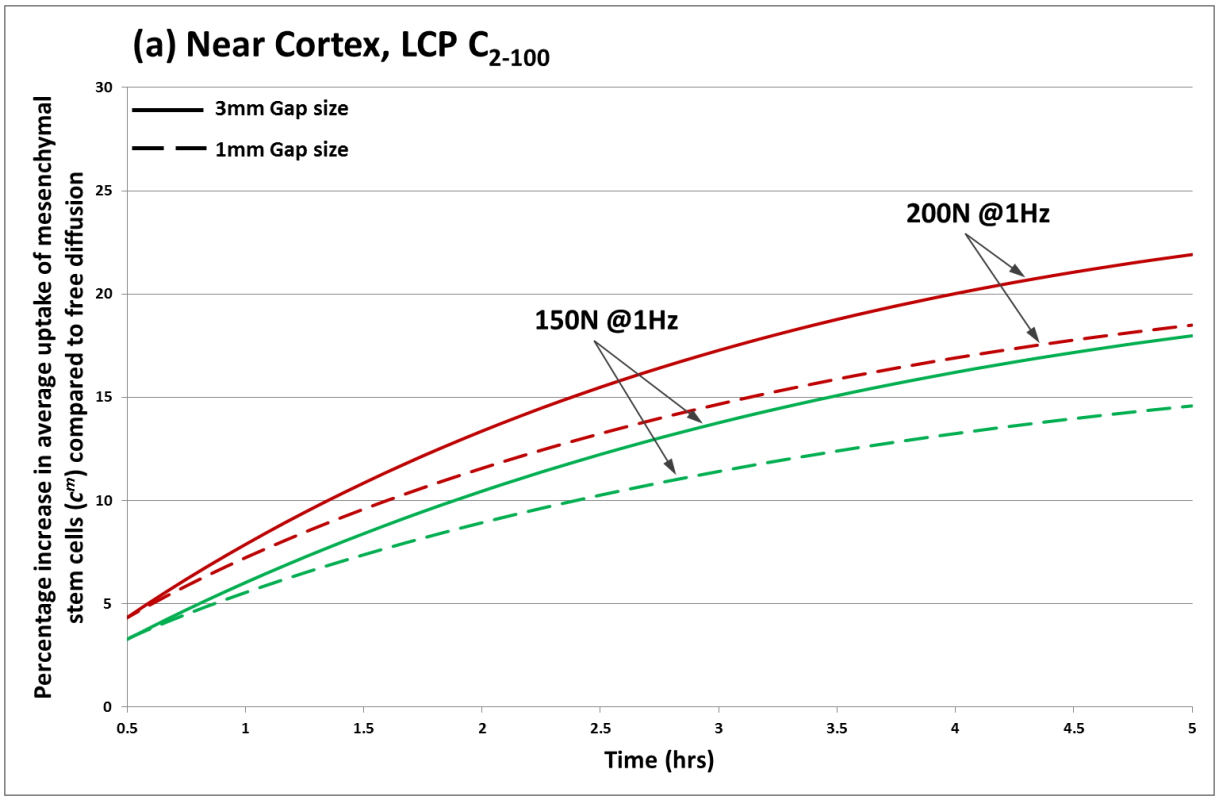

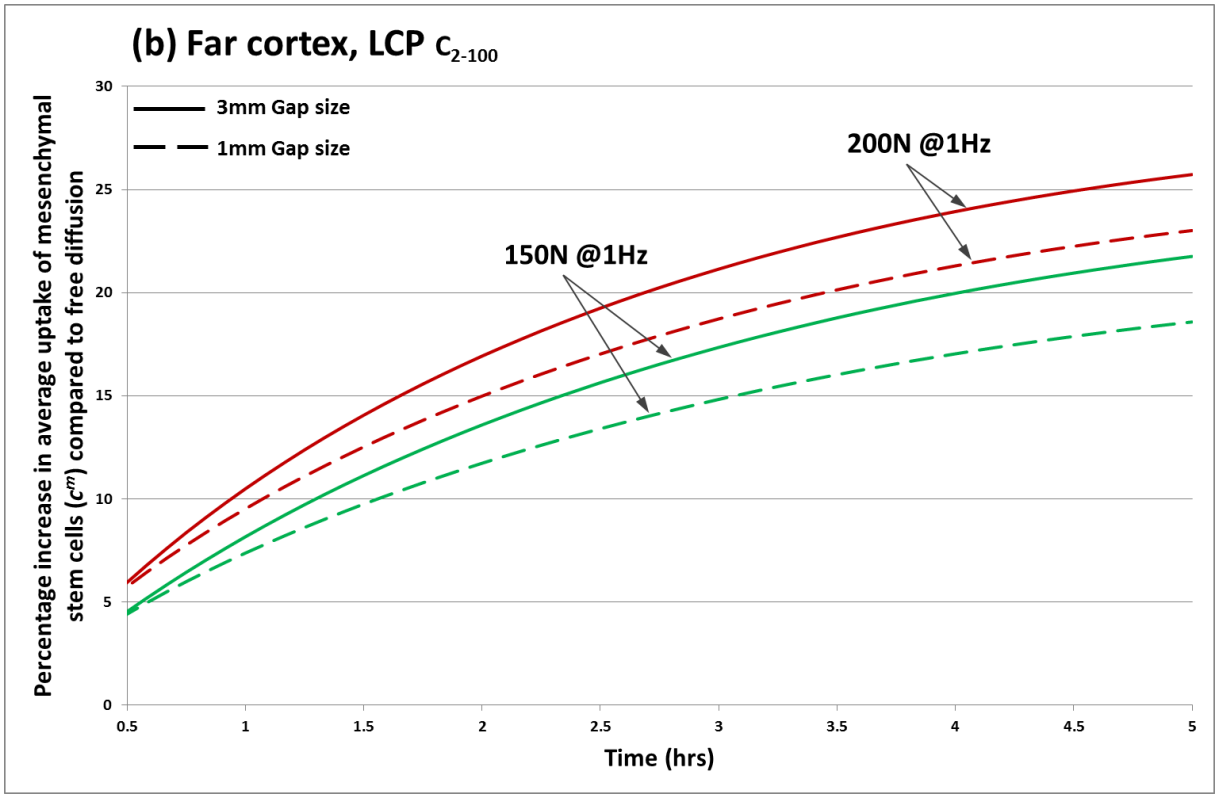

Figure. 4.4 Percent increase in the normalised uptake of mesenchymal stem cells (MSCs) under different loading conditions. (a) Near cortex callus zone; and (b) Far cortex callus zone for LCP configuration of $C_{2\text{-}100}$.

4.5. **Discussion**

As shown in Figure. 4.1, the mechanical microenvironment in fracture callus is influenced by dynamic loading, fracture geometry and fixation configuration; which causes fluid flow and deformation within the callus, affects the transport behaviour of cells and growth factors, ultimately the MSCs mediated cell differentiation(Zhang et al., 2012a, Zhang et al., 2017b). Previous in-vitro studies have indicated that physiological cyclic loading enhances solute transport during early stage of bone healing(Witt et al., 2014). Our results (Figure. 4.5-6) further demonstrate that, in comparison to diffusion, dynamic loading enhances cells (MSCs, fibroblasts, chondrocytes and osteoblasts) and growth factors (osteogenic and chondrogenic growth factor) transport under various plate configurations and gaps sizes.

It is known that the configuration of locking plate significantly affects bone healing outcomes. The developed computational model predicted that, compared to the control model with a rigid fixation configuration (i.e. BPD = 0mm and WL = 30mm), a relatively flexible fixation configuration enhances cells and growth factors uptake under dynamic loading. In addition, WL appears to be one of the critical parameters that significantly affect the transport of cells and growth factors within the callus under dynamic loading (Figure. 4.5 and Figure. 4.6). However, WL is limited by the position of screws in LCP plate, and a too large WL may lead to non-uniform tissue development in fractured bone(Miramini et al., 2016b). Increasing BPD or WL increases flexibility of the fixation, however there is a limitation beyond which the fixation is no longer stable and could lead to implant failure(Ahmad et al., 2007). BPD beyond 5mm is reported to significantly decrease axial stiffness(Ahmad et al., 2007). Similarly, increasing WL through removal of innermost screws on either side of fracture reduced axial stiffness by 64% and torsional rigidity by 36%; and 10% with every subsequent screw hole omission(Stoffel et al., 2003a, Nassiri et al., 2013). A higher WL can particularly reduce fixation stability for larger fracture gap sizes, which is unfavourable for fracture healing(Stoffel et al., 2003a, Nassiri et al., 2013). Besides reduced fixation stability, the configuration could also lead to unsuccessful healing outcomes, for e.g. non-unions or delayed unions. A successful healing can be achieved under favourable mechanical stimuli with MSC differentiation into osteoblasts (direct healing) and chondrocytes (secondary healing), whereas delayed healing or non-unions can occur when MSC differentiates into fibroblasts under unfavourable mechanical conditions, for e.g. excessive loading. A bony union can be predicted for a combination of BPD = 4mm and WL = 30 mm or BPD = 2mm and WL = 100 mm based on S-index values at near cortex and far cortex callus zones in Table 4.3. It should also be noted that upper limit of elasticity would be different if mechanical microenvironment would change, for e.g. different fracture geometry (i.e. gap sizes or angle of fracture) or loading conditions. In this case, a combination of BPD = 4mm and WL = 100 mm can lead to delayed healing or non-unions, particularly for a loading higher than 20% of the body weight during early stage of healing. Previous studies have shown that fixation configuration of $C_{4\text{-}100}$ is unfavourable for 1mm gap size as well, since smaller gap size sustain higher strain under same loading compared to larger fracture gaps(Miramini et al., 2016b). Therefore, the LCP configurations should be carefully chosen to promote MSCs mediated healing processes.

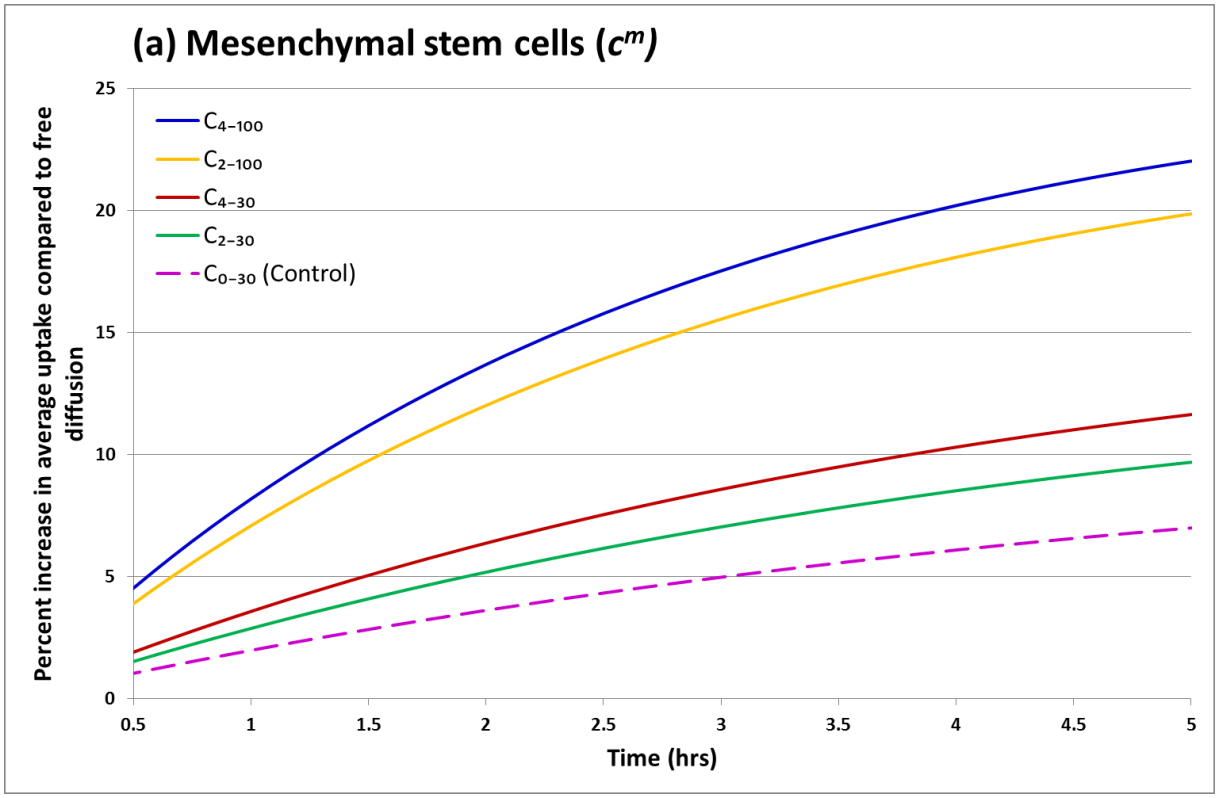
(a) Mesenchymal stem cells (c^m)
Percent increase in average uptake compared to free diffusion
Time (hrs)
C_{4-100}
C_{2-100}
C_{4-30}
C_{2-30}
C_{0-30} (Control)
0
5
10
15
20
25
0.5
1
1.5
2
2.5
3
3.5
4
4.5
5

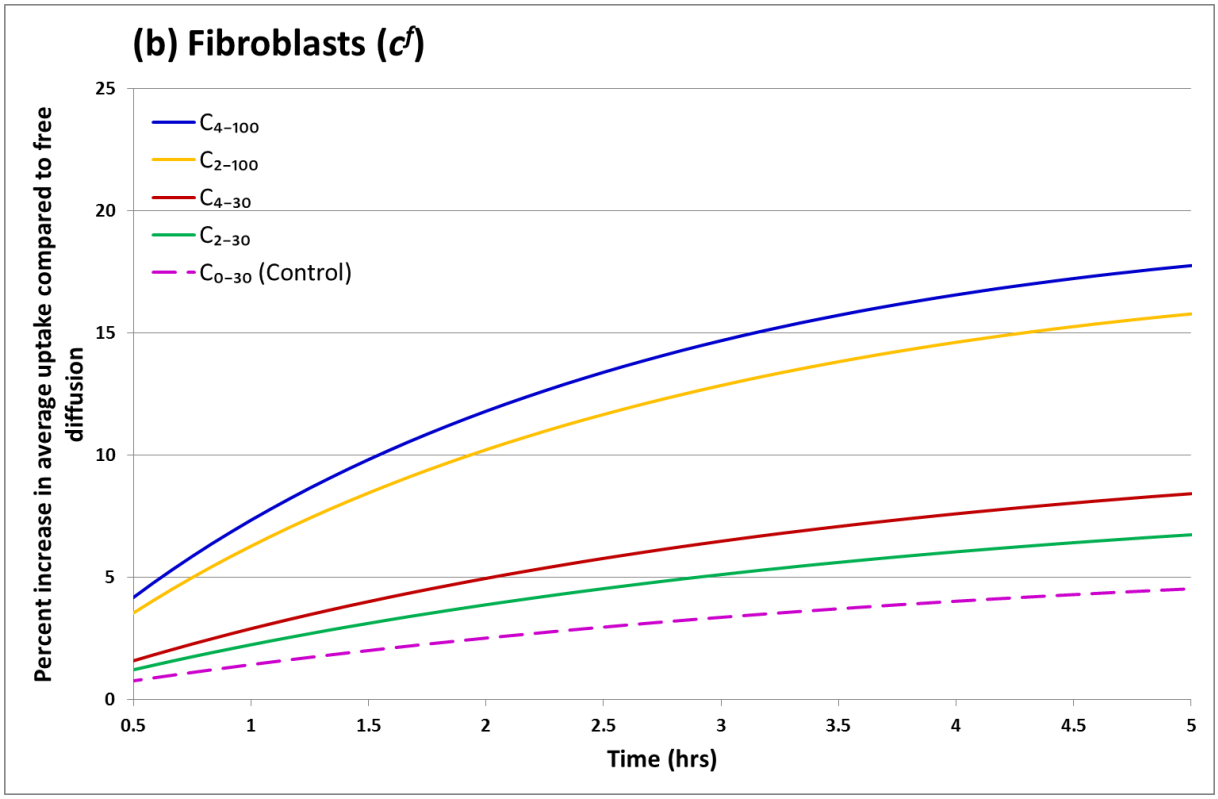
(b) Fibroblasts (c^f)
Percent increase in average uptake compared to free diffusion
Time (hrs)
C_{4-100}
C_{2-100}
C_{4-30}
C_{2-30}
C_{0-30} (Control)
0
5
10
15
20
25
0.5
1
1.5
2
2.5
3
3.5
4
4.5
5

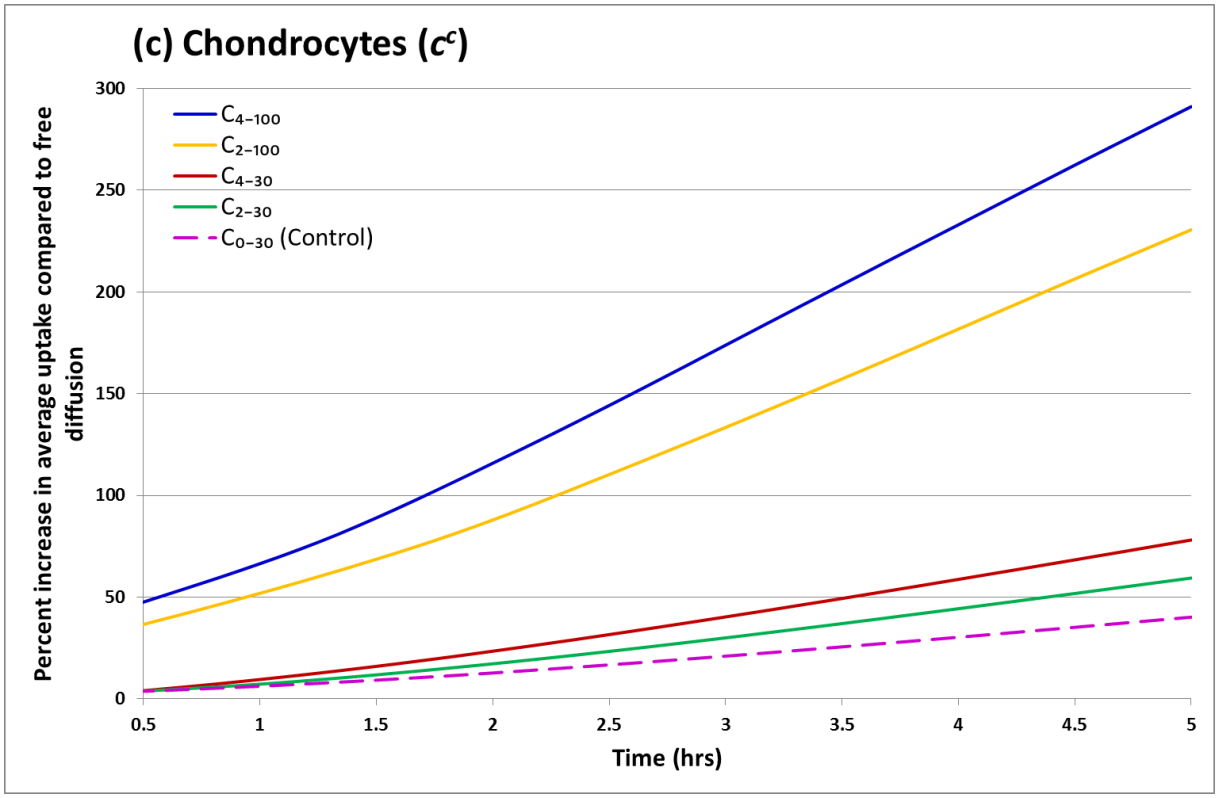
(c) Chondrocytes (c^c)
Percent increase in average uptake compared to free diffusion
Time (hrs)
C_{4-100}
C_{2-100}
C_{4-30}
C_{2-30}
C_{0-30} (Control)
0
50
100
150
200
250
300
0.5
1
1.5
2
2.5
3
3.5
4
4.5
5

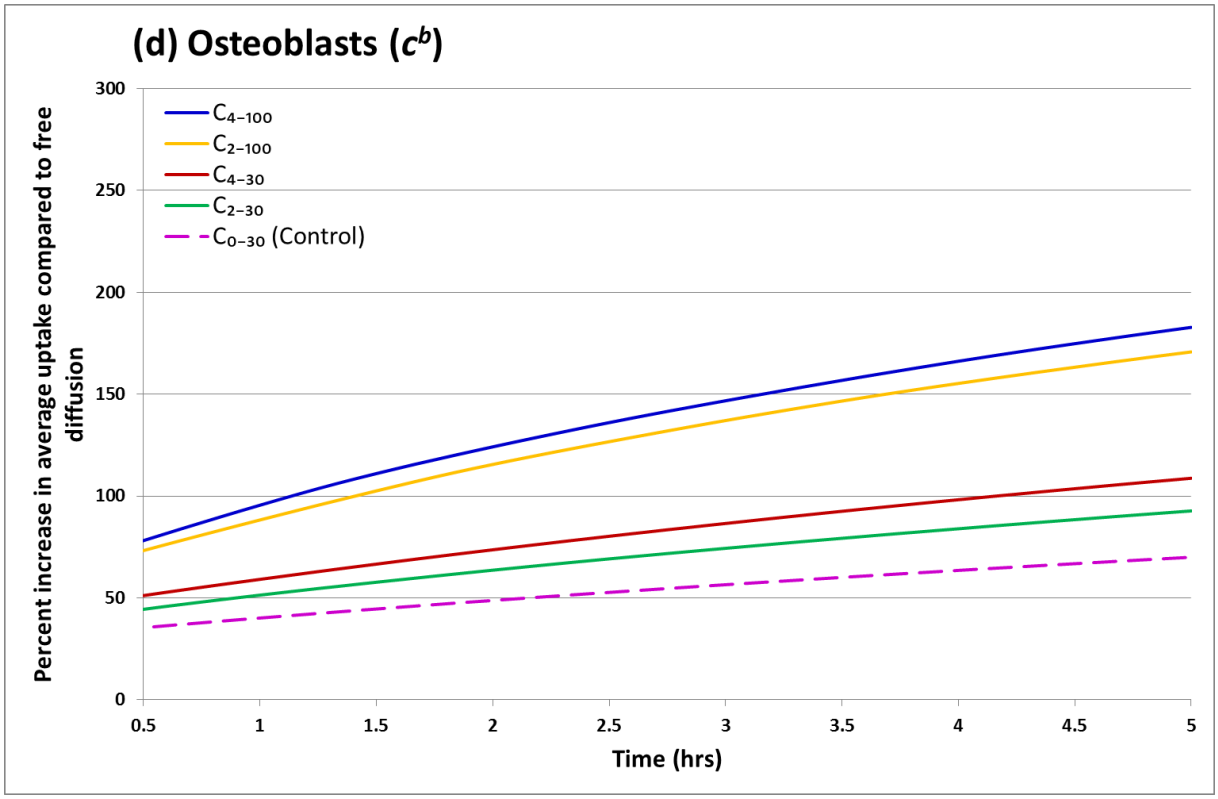
(d) Osteoblasts (c^b)
Percent increase in average uptake compared to free diffusion
Time (hrs)
C_{4-100}
C_{2-100}
C_{4-30}
C_{2-30}
C_{0-30} (Control)
0
50
100
150
200
250
300
0.5
1
1.5
2
2.5
3
3.5
4
4.5
5

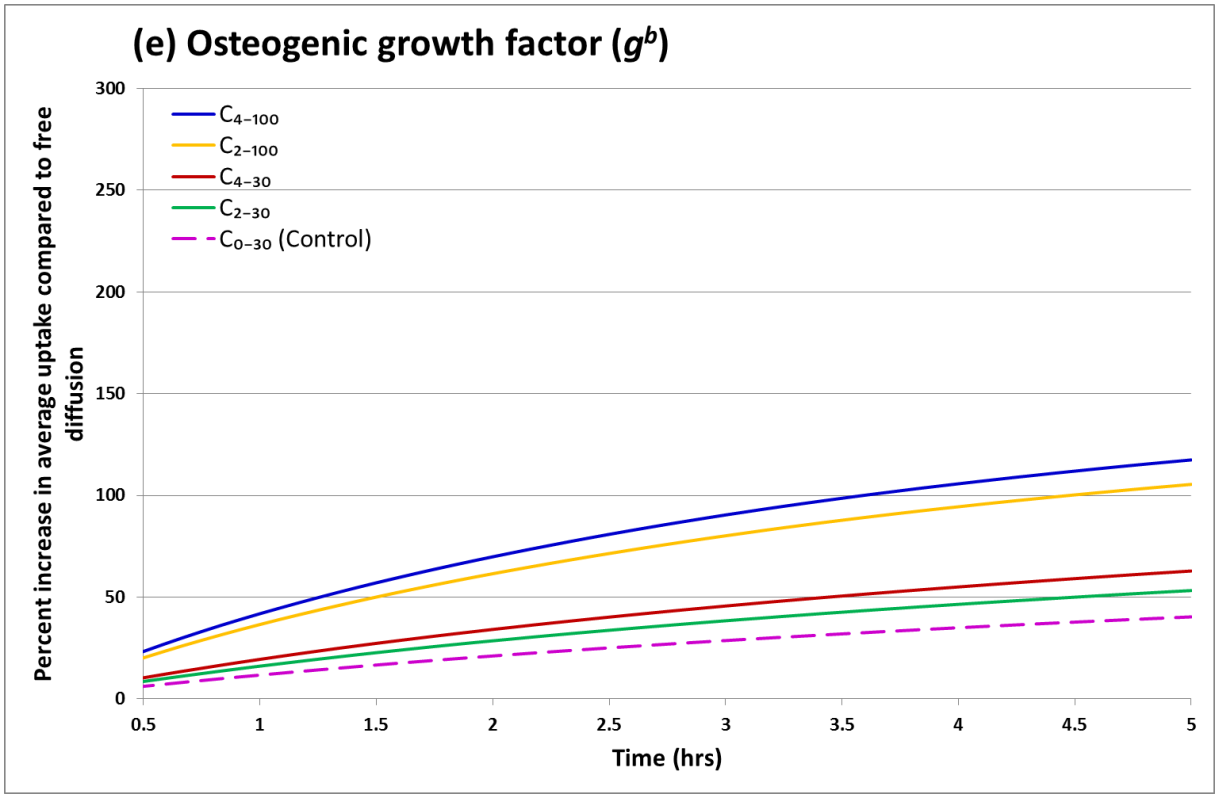

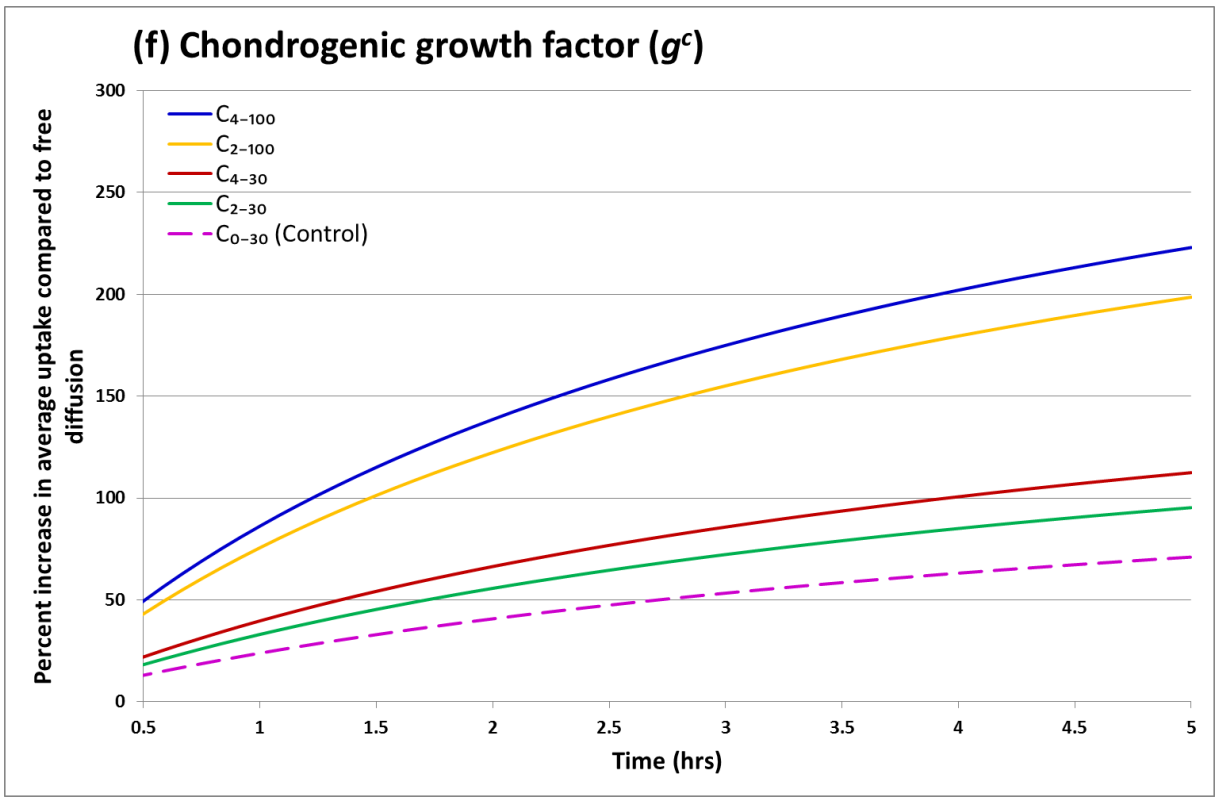

Figure. 4.5 Percent increase in normalised cells and growth factors uptake in callus under dynamic loading compared to free diffusion under different LCP configuration (gap size = 3mm, loading = 150N@1Hz). (a) Mesenchymal stem cells (c^m); (b)

Fibroblasts (c^f); (c) Chondrocytes (c^c); (d) Osteoblasts (c^b); (e) Chondrogenic growth factors (g^c); and (f) Osteogenic growth factors (g^b)

As LCP implant is normally applied at one side of a fractured bone, interfragmentary strain in NC and FC zone is generally different. This could result spatially dependent transport behaviour of cells and growth factors under dynamic loading, ultimately the asymmetrical tissue development across the fracture callus. Our numerical predictions indicate that dynamic loading induced enhancement of solute transport is more obvious in FC zone than that in NC due to the relatively flexibility of FC zone. In addition, this study shows that the variation in growth factor uptake in NC and FC zone is influenced by fracture gap with a more uniform growth factor uptake across the callus under a relatively small fracture gap (e.g. 1mm) under dynamic loading (Figure. 4.6e-f).

In addition, the fracture gap size can influence cellular activity and bone healing under LCP. For example, there is enhancement of cells for all plate configurations in 3mm gap size, except chondrocytes (Refer to Figure. 4.6c). The enhancement of chondrocytes in 1mm gap size results from the enhanced transport of chondrogenic growth factor (Refer to Figure. 4.6f), due to the increase of interstitial fluid velocity at the source of chondrogenic growth factors (i.e. under cortical bone) under dynamic loading.

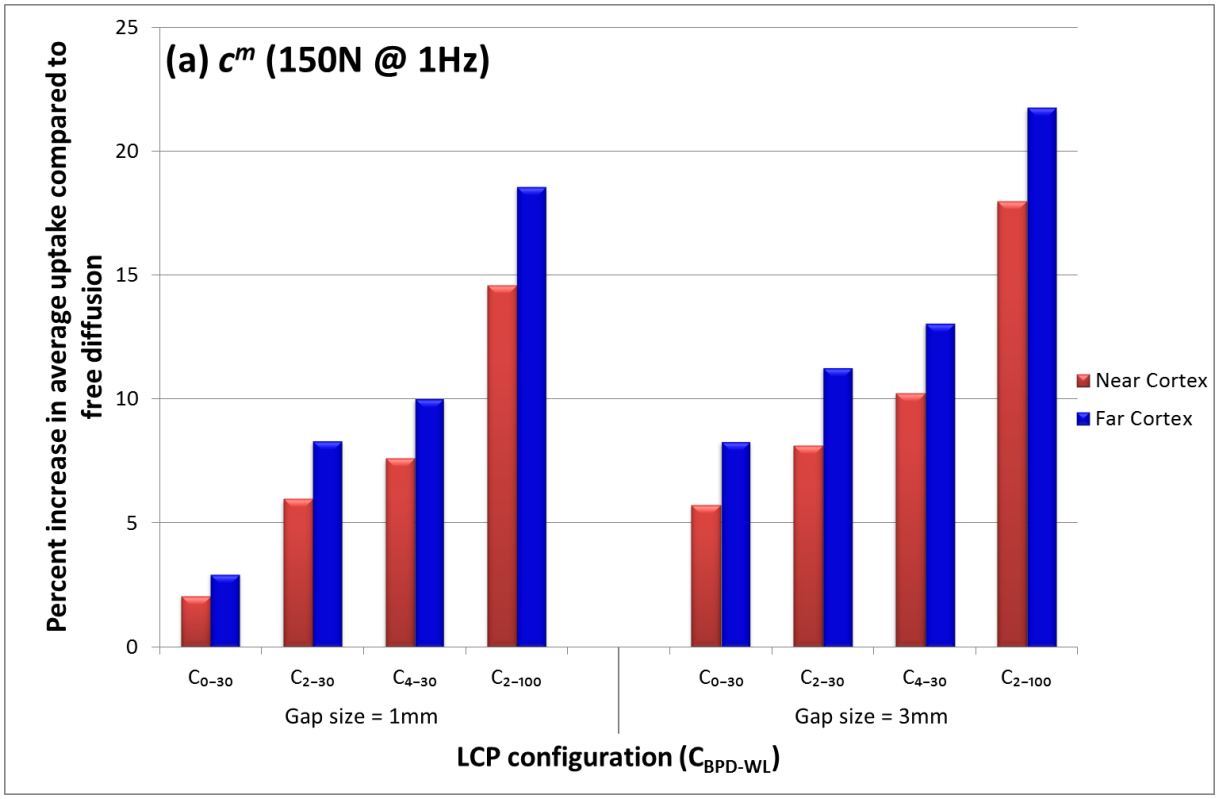

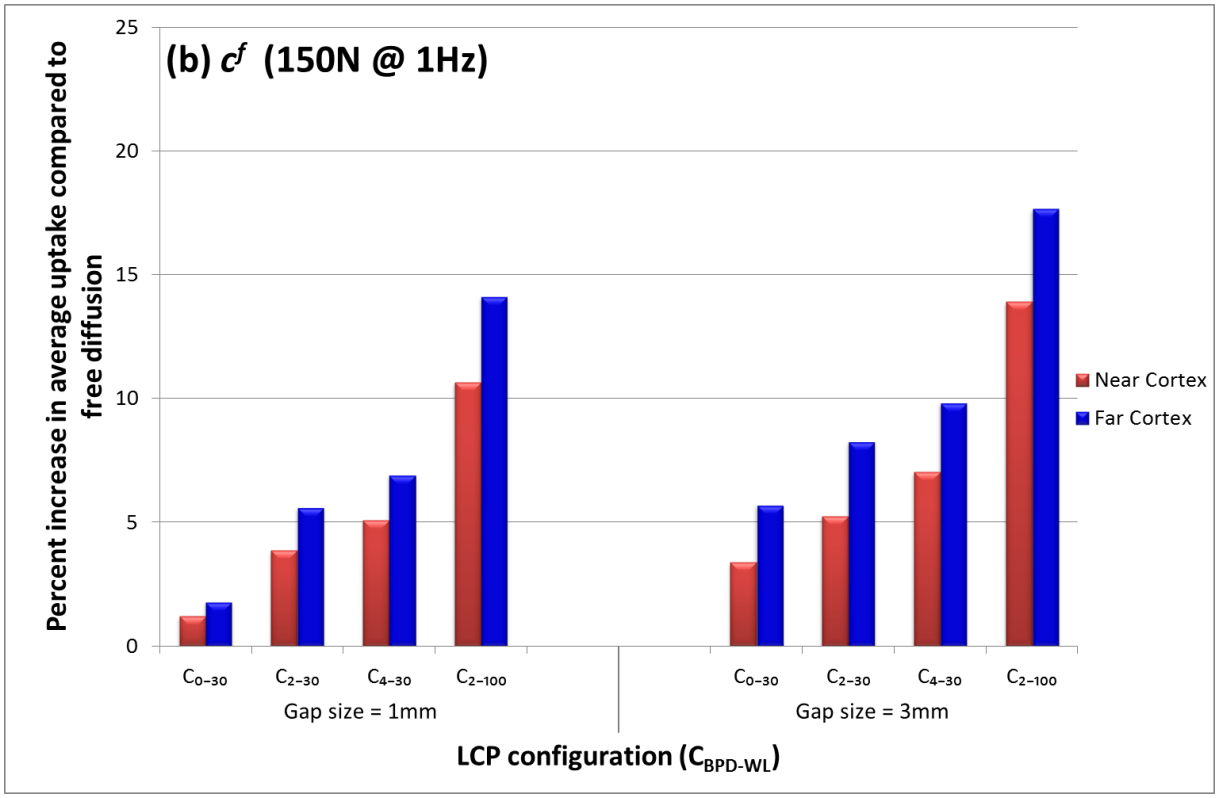
(b) c^f (150N @ 1Hz)
Percent increase in average uptake compared to free diffusion
25
20
15
10
5
0
Near Cortex
Far Cortex
C_{0-30}
C_{2-30}
C_{4-30}
C_{2-100}
Gap size = 1mm
Gap size = 3mm
LCP configuration (C_{BPD-WL})

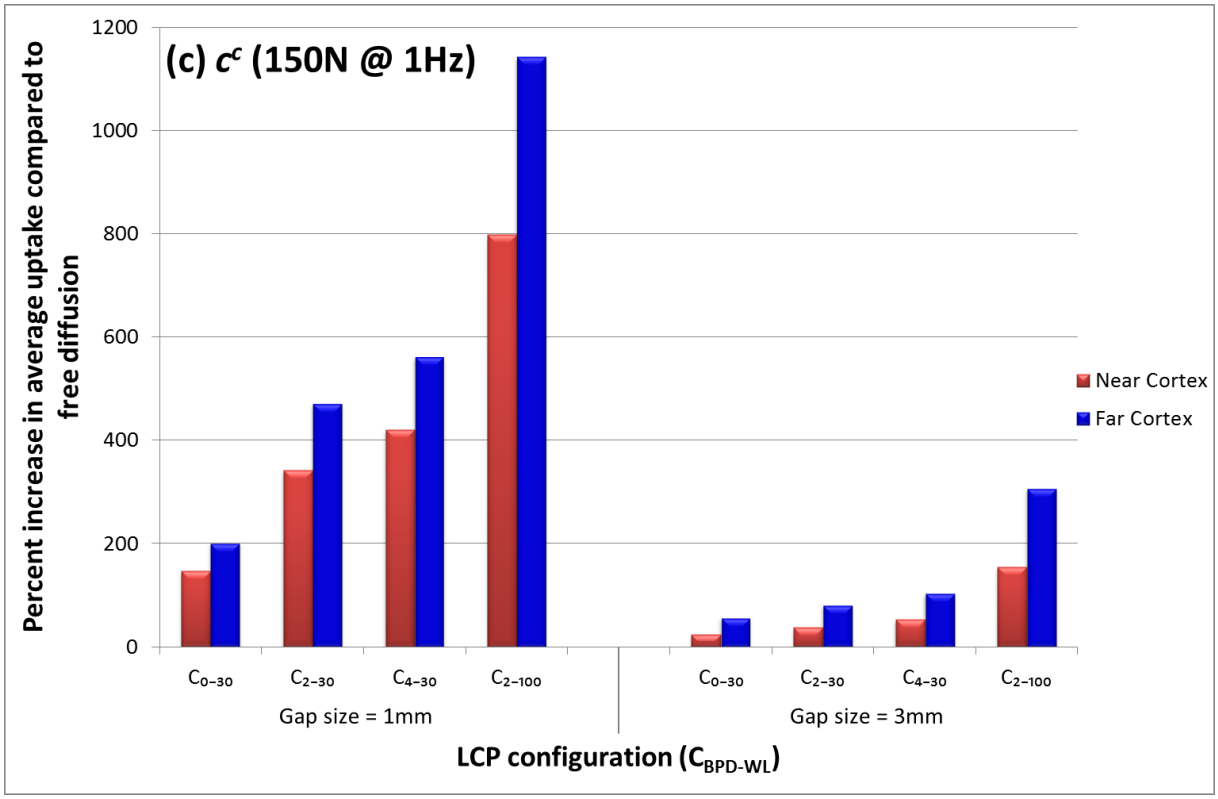
(c) c^c (150N @ 1Hz)
Percent increase in average uptake compared to free diffusion
1200
1000
800
600
400
200
0
Near Cortex
Far Cortex
C_{0-30}
C_{2-30}
C_{4-30}
C_{2-100}
Gap size = 1mm
Gap size = 3mm
LCP configuration (C_{BPD-WL})

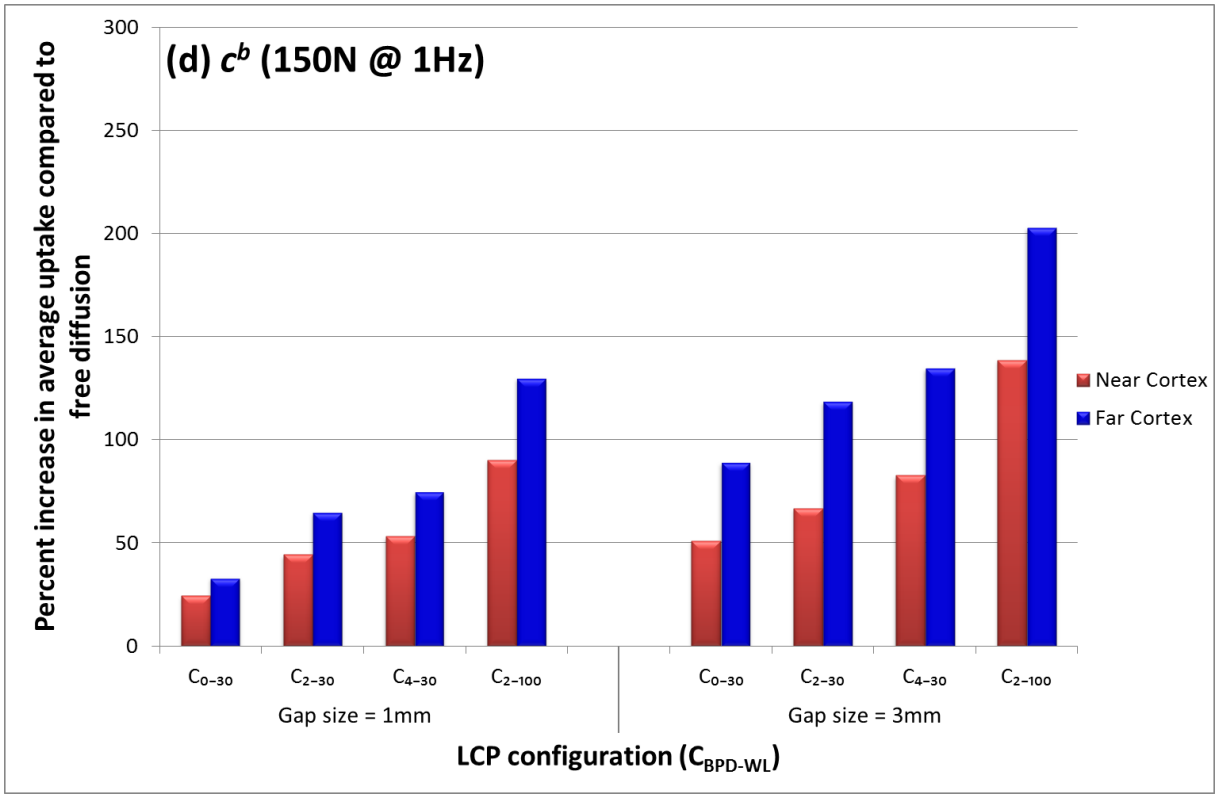
(d) c^b (150N @ 1Hz)
Percent increase in average uptake compared to free diffusion
300
250
200
150
100
50
0
Near Cortex
Far Cortex
C_{0-30}
C_{2-30}
C_{4-30}
C_{2-100}
C_{0-30}
C_{2-30}
C_{4-30}
C_{2-100}
Gap size = 1mm
Gap size = 3mm
LCP configuration (C_{BPD-WL})

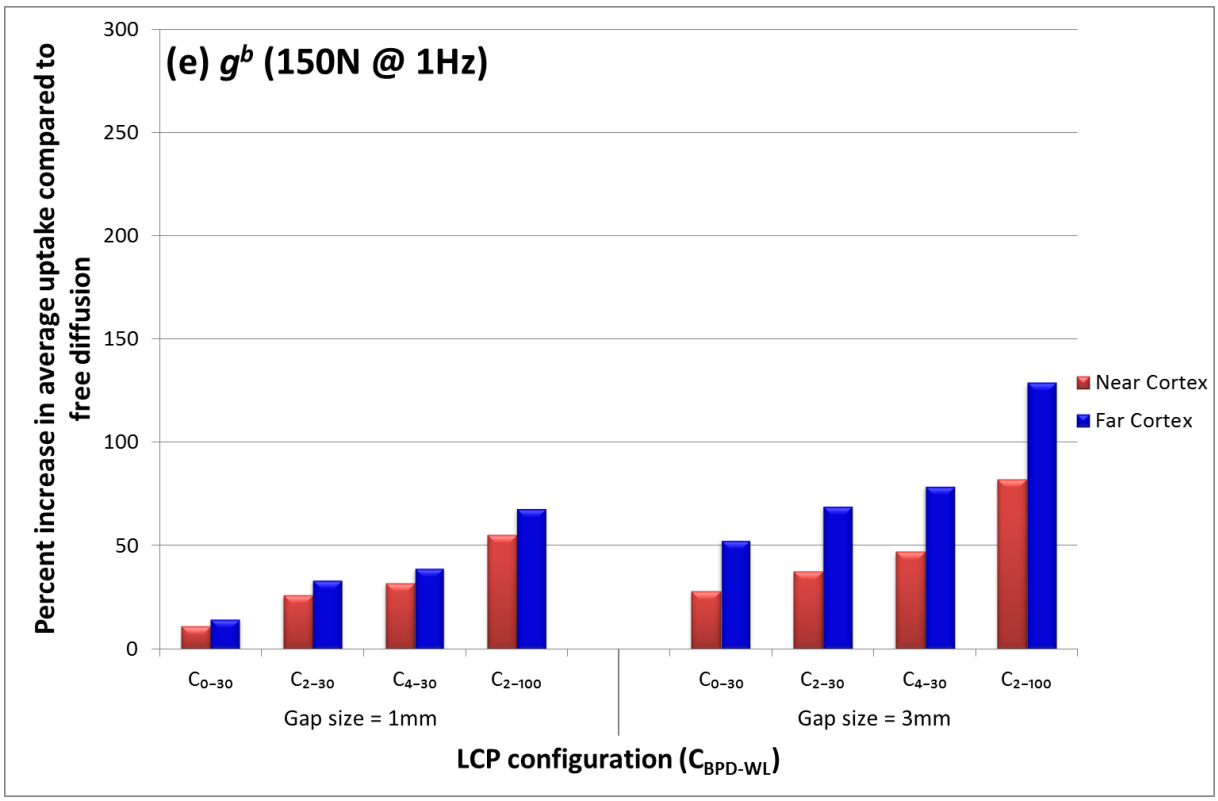
(e) g^b (150N @ 1Hz)
Percent increase in average uptake compared to free diffusion
300
250
200
150
100
50
0
Near Cortex
Far Cortex
C_{0-30}
C_{2-30}
C_{4-30}
C_{2-100}
C_{0-30}
C_{2-30}
C_{4-30}
C_{2-100}
Gap size = 1mm
Gap size = 3mm
LCP configuration (C_{BPD-WL})

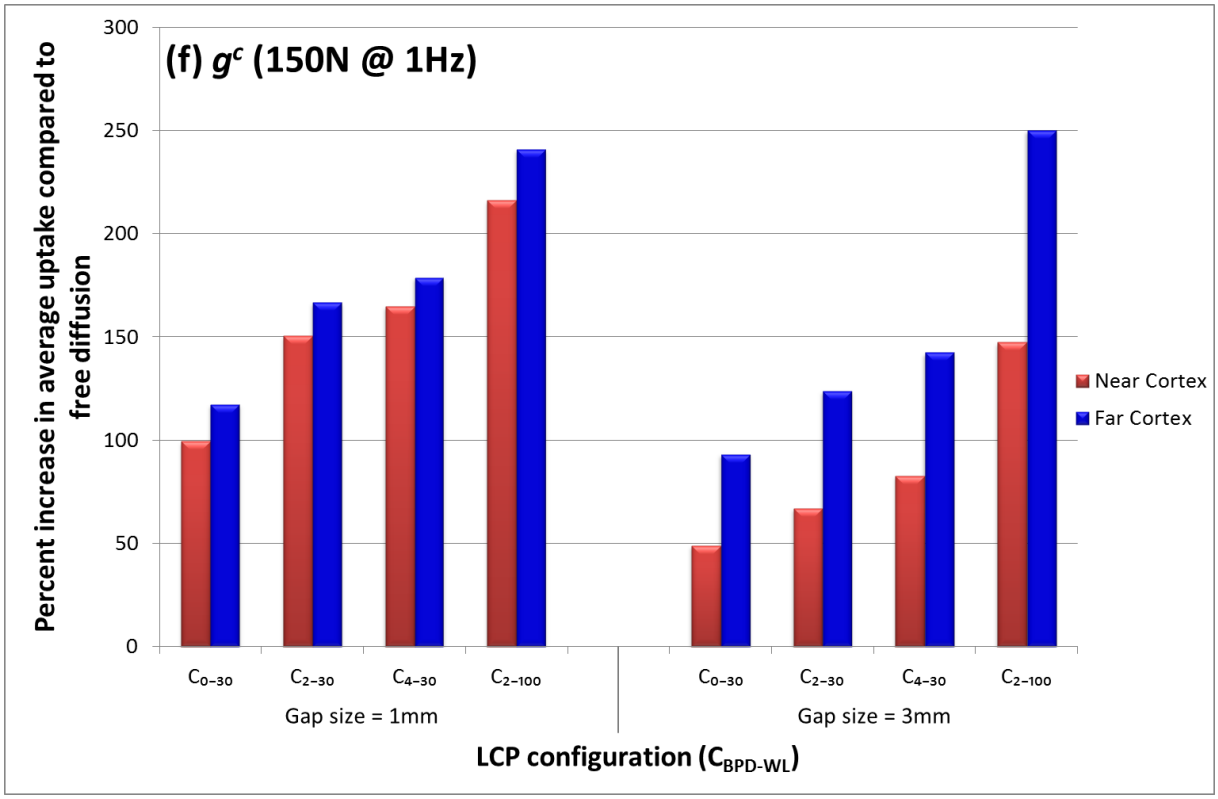

Figure. 4.6 Percent increase in normalised cells and growth factors uptake in near and far cortex zones after 5 hours dynamic loading (150N @ 1Hz) compared to free diffusion. (a) Mesenchymal stem cells (c^m); (b) Fibroblasts (c^f); (c) Chondrocytes (c^c); (d) Osteoblasts (c^b); (e) Chondrogenic growth factors (g^c); and (f) Osteogenic growth factors (g^b).

Consistent with previous studies(Zhang et al., 2008a), our model predicts that the rate of increase in normalised MSCs resulting from dynamic loading is relatively high during the initial stage of dynamic loading (i.e. first two hours), and rate of enhancement gradually decreases as the increase of MSCs concentration. The knowledge obtained from this study could help orthopaedic surgeons and physiotherapists to design effect physical therapy activity for improving bone fracture healing.

4.5.1. Limitation

It should be mentioned that this study has some limitations. Firstly, only axial cyclic loading is considered in this study. Throughout the life-span, bone is subjected to various types of physiologically relevant loads, such as axial compression, bending, shear and torsion from muscle, ligament or joint movement. Studies have shown that the diaphyseal part of a long bone is mainly axially loaded, with minimal torsional moments

during walking (Duda et al., 1997b, Duda et al., 1997a). After fracture operation, patients are encouraged to conduct partial load bearing exercise, for e.g. walking with aids during the early stage of healing and has been shown to enhance the healing process (Horn et al., 2011, Talkowski et al., 2009). Torsional forces would be significant when fracture occurs; however in fractures with fixation implants, the primary mode of loading is compression which translates into bending due to the bone geometry (Grant et al., 2015). Several experimental studies with fixation implants have also predominantly applied axial loads (Aro et al., 1990, Duda et al., 2002, Augat et al., 2001, Wehner et al., 2014, Claes et al., 1995a). Previous computational studies have indicated that torsional loads produce shear movements and overall strain magnitude is comparable under axial movement and combined axial and shear movement (Augat et al., 2008, Epari et al., 2006). Therefore, to simplify the complex problem, we have focused on the influence of axial cyclic loading on growth factor transport and cellular activities during early bone healing in this study. Furthermore, the present study mainly focuses on the early stage of healing and the FEM model predictions need to be further validated by the experimental data.

4.6. **Conclusions**

In this study, we theoretically investigate mechanical loading mediated MSC transport and differentiation under LCP with various flexibilities. The followings are the major conclusions:

- Dynamic loading enhances the transport of cells (MSCs, fibroblasts, chondrocytes and osteoblasts) and growth factors (osteogenic and chondrogenic growth factors) in callus compared to free diffusion and the enhancement depends on the flexibility of the fixation. Most importantly, it suggests that the enhancement induced by the 5-hour dynamic loading results is much more obvious for chondrocytes (around 280% compared to free diffusion), osteoblasts (around 180%), osteogenic growth factor (around 120%) and chondrogenic growth factors (around 220%), while moderate enhancement is seen for MSCs (around 22%) and fibroblasts (around 17%)

- In general, FC zone exhibited a higher enhancement in cells and growth factors uptake compared to that in NC zone under different types LCP configurations and gap sizes.
- The enhancement of chondrocyte and chondrogenic growth factor uptake under a relatively small gap size (e.g. 1mm) is higher than that of 3mm gap size, and the enhancement of chondrocyte uptake is very significant. In contrast, for MSCs, fibroblasts, chondrogenic growth factors, osteogenic growth factors, a relatively large gap size (e.g. 3mm) leads to a better outcome under dynamic loading.
- For MSCs, a relatively high loading magnitude produces a better result. In addition, under similar loading condition, the enhancement is higher for 3mm gap size than that for 1mm gap size.

Chapter 5.

Effects of dynamic loading on various fracture angle of obliquity during bone healing

5.1. Abstract

Bone fracture geometry (e.g. gap size or fracture angle of obliquity) plays an important role in the mechano-regulation. The deformation and fluid flow from mechanical stimulation vary for different angle of obliquity, which changes callus shape, direction of interfragmentary motion and its shear properties. While resulting octahedral shear strain has been shown to act as angiogenesis regulator, the influence of different fracture obliquity on regenerative blood vessels during early stage of bone healing is still poorly understood. In this study, the magnitude of mechanical loading conducive to angiogenesis was investigated by quantifying the maximum permissible load that can allow angiogenesis during early stage of fracture healing. Using the simulation results, the allowable level of partial weight bearing loading at early stages of healing for promoting angiogenesis and bone healing are suggested.

5.2. Introduction

Depending on the angle of fracture, simple fractures of long bone (i.e. tibia, femur or humorous) can be classified into transverse or oblique fractures (Garnavos et al., 2012). Transverse fracture occurs perpendicular to the longitudinal axis of the long bone,

usually resulting from bending forces while oblique fracture occurs diagonal to the longitudinal axis of long bone, usually under a combination of torsion and bending forces (Pierce et al., 2004). When diaphyseal or long bone fracture occurs under impact like accident, the bone fracture doesn't necessarily result in transverse fracture. The fracture, particularly comminuted fracture, takes place in several different angles of obliquity.

The regeneration of bone tissue after fracture is largely affected by mechano-regulation, which depends on fixation stability, fracture geometry and musculoskeletal loading. Internal fixation like Locking Compression Plate (LCP) is advantageous to conventional plate fixation due to its flexibility and increased stability under locking screws (Miramini et al., 2015). Several studies have previously considered oblique fracture models (Alierta et al., 2016, Aro et al., 1991, Comiskey et al., 2013, Samiezadeh et al., 2014, Loboa et al., 2001, Miramini et al., 2016a) that are stabilized by external fixators (Aro et al., 1991), internal locking plates (Miramini et al., 2016a) or intermedullary nails (Alierta et al., 2016, Samiezadeh et al., 2014). Since oblique fractures are suggested to have reduced stability compared to transverse fracture (Aro et al., 1991), the optimal fixation configuration for oblique fractures may differ from that for transverse fractures.

The fracture geometry (e.g. gap size or fracture angle of obliquity) also plays an important role in mechano-regulation. The resultant deformation and fluid flow vary for both different gap sizes (which changes interfragmentary strain) and different angle of obliquity, which changes callus shape, direction of interfragmentary motion and its shear properties. The shear movement in bone fracture is generally considered to have impeding effects to healing as it can rupture the newly formed vasculature (Augat et al., 2003, Yamagishi and Yoshimura, 1955). Steiner et al. (2014) predicted that translational shear movement under musculoskeletal loading is more detrimental compared to torsional shear movement. Further, callus stiffness in shear group were found to be lowest during initial stages of healing. Peters et al. (2010) also showed less cartilage development histologically under large shear IFM compared to axial compression during initial stages. Similarly, more cartilage was predicted under axial compression than shear loading conditions in another study (Steiner et al., 2013). Contrary to these findings, Bishop et al. (2006) suggested that torsional shear movements could enhance bone healing. A study by Park (1998) also showed enhanced healing with sliding shear in oblique fractures compared to compressive motion in transverse fractures, however

osteotomy in these oblique fractures generate compression as well, therefore enhanced healing in these oblique fractures cannot be attributed to shear movement only (Epari et al., 2010). Since, shear force accompanies axial loading in oblique fracture and changes with different angle of obliquity, the fracture angle is also an important factor that affects bone fracture healing (Lowenberg et al., 2008).

Literatures have also suggested that early weightbearing can accelerate secondary healing pathway of fractured bone (Bailón-Plaza and van der Meulen, 2003, Kubiak et al., 2013). Tufekci et al. (2018) applied fixator-controlled motion from day 5 till 3 weeks post-operation in sheep and found that early stimulated group had higher callus strength and bone volume compared to unstimulated group. This shows the importance of mechanical stimulation during early proliferative phase of healing. It has also been shown that interfragmentary movement (IFM) resulting from the mechanical stimuli influences migration and differentiation of mesenchymal stem cells (MSCs) at the early stage of healing (Ghimire et al., 2018, Kasper et al., 2007, Kelly and Jacobs, 2010, Klein et al., 2003). Depending on the mechanical microenvironment of bone fractures, biochemical stimuli (i.e. growth factors) and level of oxygen and nutrient supply, the stem cells in the fracture callus differentiate and form different tissues (i.e., bone, cartilage or fibrous tissue). Therefore, regeneration of damaged blood vessels and angiogenesis is another critical factor during early stages of bone healing (Einhorn, 1998, Schmidt-Bleek et al., 2012). Reduction in cartilage and bone formation leading to delayed healing or non-healing has been observed in healing of long bones due to disrupted blood supply (Brinker and Bailey, 1997, Lu et al., 2007).

It is evident that mechanical stimulation of bone fracture healing at early stages is critical for the successful healing of bone fracture (Epari et al., 2006). Several computational models have adopted a range between 100N to 200N for bone healing simulation during early stage of healing to represent allowable weight bearing after a surgical operation (Döbele et al., 2010, Miramini et al., 2014a, Miramini et al., 2016b). However, there is little understanding on how much loading during early stage is conducive to the regenerating blood vessels which are crucial to timely bone regeneration. Prendergast et al. (1997) have presented a widely accepted tissue differentiation criteria based on the mechanical environment, i.e. magnitudes of octahedral shear strain and interstitial fluid velocity and it has been further shown that octahedral shear strain also acts as a

regulator for angiogenesis inhibition (O'Reilly and Kelly, 2017). Therefore, the aim of this study is to quantify the relationship between different angle of obliquity and maximum permissible load that allow angiogenesis during early stages of healing under different LCP configurations. The knowledge of maximum permissible loading that can be applied at different stages of bone fracture healing has clinical relevance to orthopaedic surgeons to determine optimal LCP configuration depending on the severity or degree of fracture angles.

5.3. **Methods**

Following a fracture, the fracture gap is initially filled with hematoma which is gradually replaced by callus made of granulation tissue. As healing progresses, the callus gets stiffer with the production of fibro-cartilaginous soft tissue. In this study, the early stages of healing (granulation stage and early soft callus stage) are considered, as literatures have indicated that the mechanical microenvironment of early stages of healing influences the differentiation of MSCs into different cell types (Klein et al., 2003) that ultimately determines the tissue development in fracture gap. The material properties of initial granulation tissue, soft callus, bone marrow and cortical bone are taken from literatures and presented in Table 5.1. Similarly, the material properties of stainless-steel LCP are given in Table 5.2.

Table 5.1 Material properties of various callus stages and adjacent tissues used in this study

Parameters	**Stage I (Initial granulation tissue callus)**	**Stage II (Early soft callus)**	**Bone Marrow**	**Cortical Bone**
Young's Modulus of Elasticity (MPa)	0.05[a]	10[b]	2[b]	15750[c]
Poisson's ratio	0.167 [b]	0.167 [b]	0.167[b]	0.332[c]
Permeability (m4/Ns)	1E-14 [b]	5E-15[d]	1E-14[b]	1E-17[e, f]

Porosity	0.8[b]	0.8[b]	0.8[b]	0.04[g]
Fluid bulk modulus (MPa)	2300[d]	2300[d]	2300[d]	2300[c]
Solid bulk modulus (MPa)	2300[b]	3400[h]	2300[d]	15820[c]

a McCartney et al. (2005)

b Lacroix and Prendergast (2002)

c Smit et al. (2002)

d Armstrong and Mow (1982)

e Cowin (1999)

f Johnson et al. (1982)

g Schaffler and Burr (1988)

h Tepic et al. (1983)

Table 5.2 Material properties of Stainless Steel locking plates and screws of Locking Compression Plate (LCP) fixation used in the study (Fouad, 2010)

Parameters	**Stainless Steel LCP**
Young's Modulus of Elasticity (MPa)	220
Poisson's ratio	0.34

Early stage callus can be modelled as a multiphasic mixture of solid extracellular matrices phase, interstitial fluid phase and solute particles phase (for e.g. cells and growth factors) (Ganadhiepan et al., 2019a, Ganadhiepan et al., 2019b, Ghimire et al., 2018, Ghimire et al., 2019, Zhang et al., 2017a, Zhang et al., 2017b). Further, callus is assumed to be poroelastic, isotropic and homogenous which is a common assumption for similar computational models (Miramini et al., 2016b, Zhang et al., 2013). Using theory of porous media, the stress inside fracture callus can be determined by,

$$\boldsymbol{\sigma} = -p\boldsymbol{I} + \boldsymbol{\sigma}^{\boldsymbol{e}} \quad (5.1)$$

Where, p is interstitial fluid pressure incremental to load application, $\boldsymbol{I}$ is identity matrix and σ^e is the effective stress of solid matrix.

Assuming negligible body and inertial forces and infinitesimal strain under quasi static loads, the conservation of momentum leads to,

$$\nabla \bullet \boldsymbol{\sigma} = 0 \quad (5.2)$$

Where, $\nabla\bullet$ is the divergent operator.

For fluid saturated callus with incompressible solid phase and fluid phase, the continuity equation can be expressed as,

$$\nabla \bullet \left(\boldsymbol{v^d} + \boldsymbol{v^s}\right) = \mathbf{0} \quad (5.3)$$

Where, $\boldsymbol{v^d}(= \phi\left(\boldsymbol{v^f} - \boldsymbol{v^s}\right) = -\boldsymbol{k}\nabla p)$ is Darcy's velocity, ϕ is porosity of callus, $\boldsymbol{v^f}$ is fluid velocity, $\boldsymbol{v^s}$ is solid phase velocity and $\boldsymbol{k}$ is the hydraulic permeability tensor. These equations were solved using the finite element software, (COMSOL) Multiphysics v5.2.

5.3.1. Angiogenic threshold

Studies have proposed 6 - 9% octahedral shear strain as the threshold for inhibition of angiogenesis (O'Reilly and Kelly, 2017, Burke and Kelly, 2012). Since the onset of blood vessel restoration in fracture callus takes place after early stage of healing through cytokine stimulation (Cho et al., 2002, Dimitriou et al., 2005), it is reasonable to adopt this range at early stages of healing in this study.

Table 5.3 Study groups based on different fracture angle of obliquity

Study group	Angle of Obliquity
Group I	0°
Group II	15°
Group III	25°
Group IV	45°

5.3.2. Model geometry

The 3D model of bone fracture of human tibia surrogates stabilized by LCP reconstructed from its CT scan imaging developed by Miramini et al. (2016) was adopted in this study for cyclic loading. The tibia models for different angle of obliquity (α) adopted in this study are presented in Table 5.3. A fracture gap of 3mm is considered to investigate permissible loading allowed to sustain angiogenesis and new blood vessel formation (Refer to Figure 5.1).

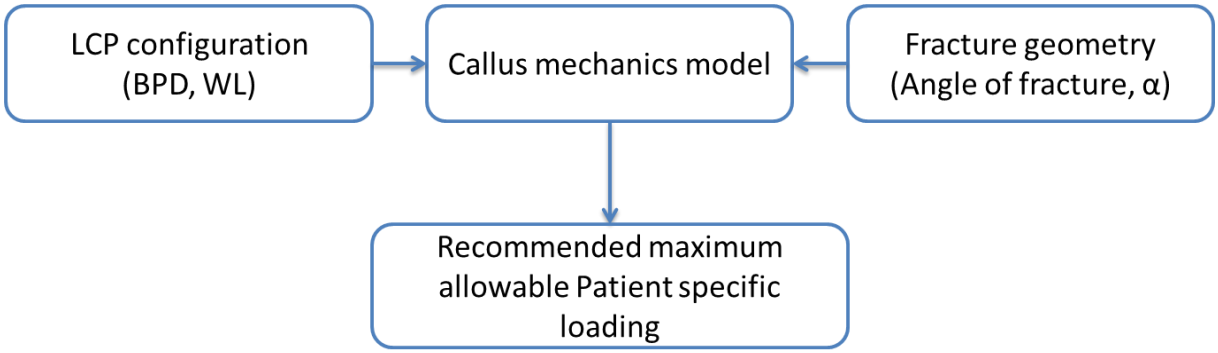

Figure 5.1 A schematic diagram showing the overview of the model

5.3.3. Fixation configuration

The fracture was stabilized by 12-holed 4.5mm broad locking plates (224mm in length, 17.5mm in width, 5.2mm in thickness) with standard locking screws. LCP are known to induce asymmetric healing in callus (Bottlang et al., 2010a, Richter et al., 2015), particularly due to high stiffness at Near Cortex (NC), which is the callus zone adjacent to locking plate. The callus zone on the opposite side of the plate is termed as Far Cortex (FC). Increasing flexibility of LCP fixation to promote a uniform callus formation, while at the same time ensuring fixation stability is one of the major challenges in bone fracture treatment. Literatures have shown that the flexibility of the Locking Compression Plate (LCP) constructs can be altered by changing Bone Plate Distance (BPD), which is the distance between the bone and the plate, and Working Length (WL), which is the distance

between two innermost screws (Ahmad et al., 2007, Stoffel et al., 2003a). In this study, we considered 4 LCP configuration cases with varying BPD and WL as shown in Table 5.4.

Table 5.4 Different cases of Locking Compression Plate (LCP) configuration adopted in this study based on the Bone Plate Distance (BPD) and Working Length (WL) of the fixation

LCP configuration	BPD (mm)	WL (mm)
$C_{2\text{-}30}$	2	30
$C_{4\text{-}30}$	4	30
$C_{2\text{-}100}$	2	100
$C_{4\text{-}100}$	4	100

5.3.4. Boundary conditions and Loading protocol

The external boundaries of callus were modelled impermeable to fluid flow.

A cyclic loading at 1Hz frequency was applied on the proximal end of the bone, while fixating the distal end. The maximum permissible load on the fractured bone was determined for each LCP configurations and angle of obliquity based on the angiogenic threshold of octahedral shear strain (Refer to Figure 5.2).

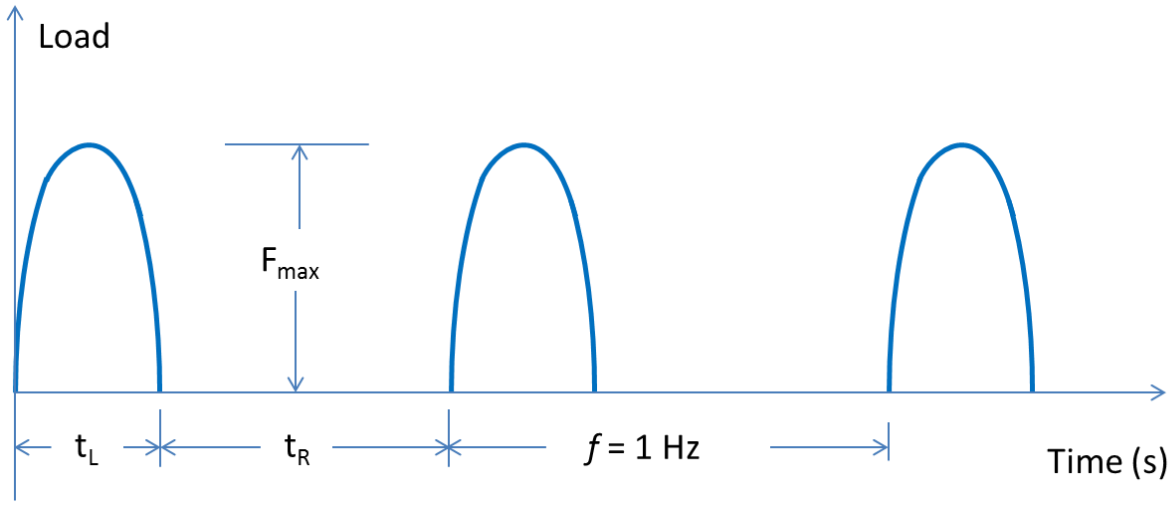

Figure 5.2 A schematic diagram showing patient specific loading protocol adopted in this study

5.3.5. Numerical simulation

In this study, a 3D FE model of bone fracture of human tibia surrogates stabilized by LCP developed by Miramini et al. (2016) has been further extended to investigate permissible loading allowed to sustain angiogenesis. The cortical bone, bone marrow and callus are modelled as poroelastic, while LCP fixation (i.e. locking plates and screws) is considered as linear elastic material. The 3D finite element model developed in this study and the corresponding longitudinal cross section of the model along the screws for clear depiction of fracture angles are presented in Figure 5.3 (a). The callus, cortex and fixation were meshed using 14643, 14436 and 18652 tetrahedral elements respectively. Time dependent solver of finite element software (COMSOL) Multiphysics v5.2 was used to solve the models.

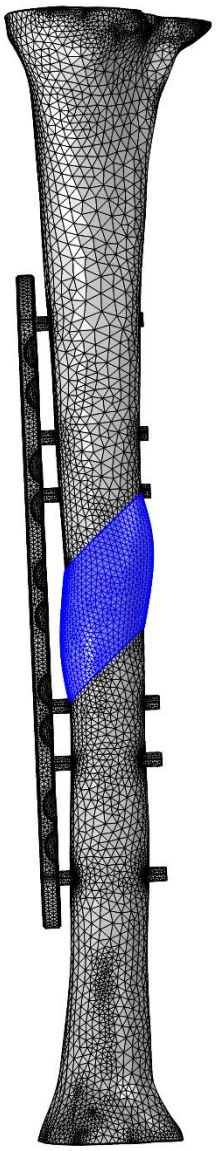

(a)

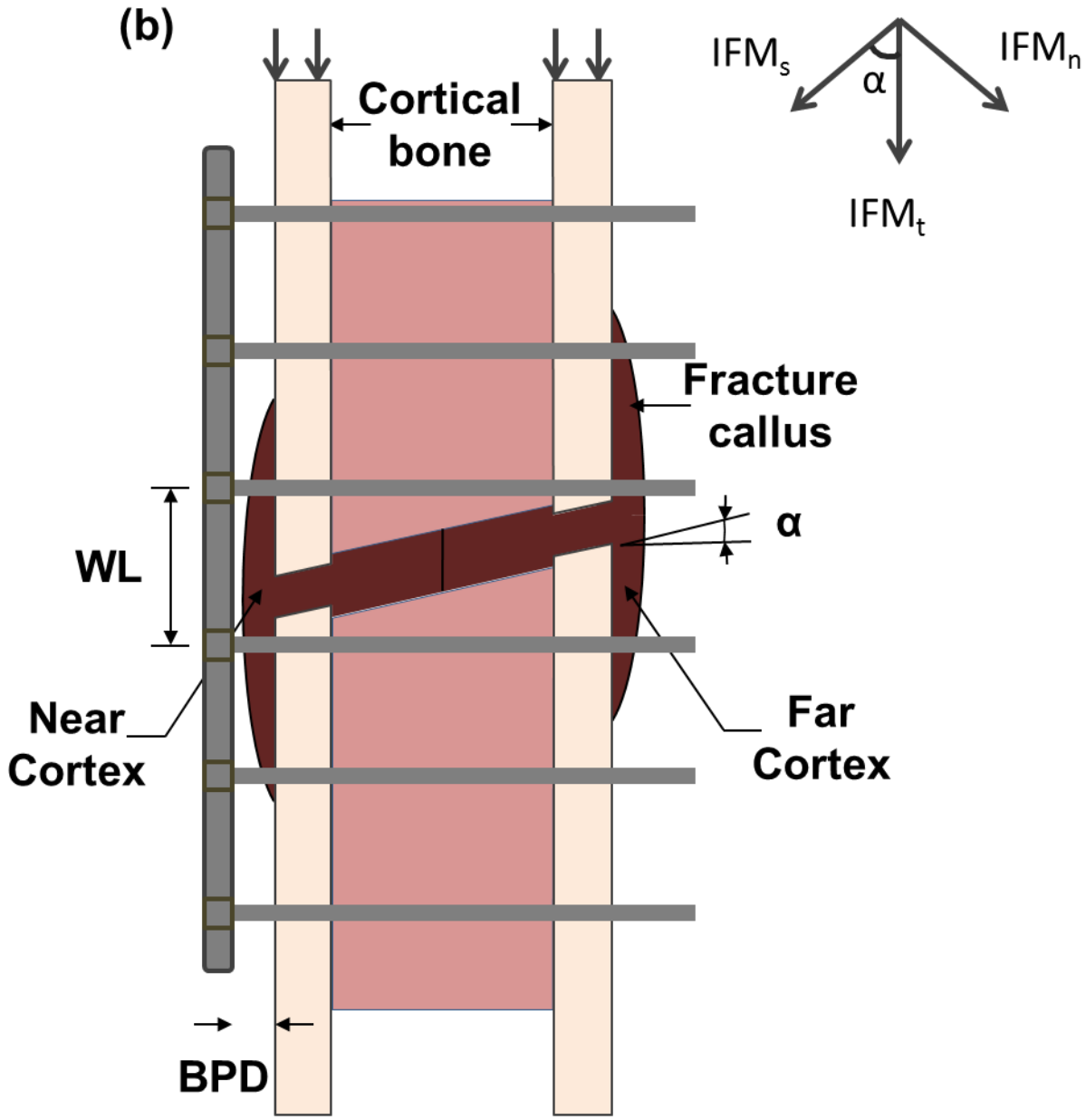

Figure 5.3 A schematic diagram of tibial fracture; (a) 3D finite element model; and (b) longitudinal section of the model showing details of LCP configuration parameters (BPD and WL) and fracture angle of obliquity

5.4. **Results and Discussion**

Since regeneration of damaged blood vessels (i.e. angiogenesis) ensures adequate supply of oxygen and nutrient in fracture callus, which is crucial to timely bone regeneration,

this phenomenon is another critical factor during early stages of bone healing. While octahedral shear strain in known to regulate angiogenesis, there is very little understanding on magnitude of loading during early stage conducive to the regenerating blood vessels which are crucial to timely bone regeneration. In this research, the influence of different fracture obliquity on regenerative blood vessels during early stage of bone healing and the magnitude of mechanical loading conducive to angiogenesis was investigated.

The maximum permissible load on the fractured bone was determined for each LCP configurations and angle of obliquity based on the angiogenic inhibitor threshold of octahedral shear strain i.e. 6% at early stages of healing (O'Reilly and Kelly, 2017) (Refer to Figure 1). Table 5.5 and Table 5.6 illustrates the maximum load magnitude in terms of percentage of body weight (BW) that can be applied in a cycle of 1 Hz frequency during the early granulation tissue (stage I) and early soft callus (stage II) respectively to improve indirect bone healing without inhibiting angiogenesis.

Table 5.5 Maximum allowable bodyweight (%) that can be applied to fracture callus at early granulation stage callus

Fracture angle	**$C_{2\text{-}30}$**	**$C_{4\text{-}30}$**	**$C_{2\text{-}100}$**	**$C_{4\text{-}100}$**
0°	8	5	3	3
15°	7	7	4	3
25°	8	7	5	4
45°	10	8	5	5

Table 5.6 Maximum allowable bodyweight (%) that can be applied to fracture callus at early soft callus stage (Week 1 – 2 post operation)

Fracture angle	**$C_{2\text{-}30}$**	**$C_{4\text{-}30}$**	**$C_{2\text{-}100}$**	**$C_{4\text{-}100}$**

0°	60	62	54	52
15°	59	57	49	55
25°	57	56	51	44
45°	57	55	41	39

From Table 5.5, we can see that the fracture callus can undertake extremely low weightbearing (hardly 3-10% BW) during initial granulation stage. This is consistent with studies which have shown non-union or delayed healing when full weightbearing was permitted during very early stage of healing (Augat et al., 1996). The sheep had applied around 80% preoperative BW to the operated leg by end of first week post-operation, and only 1 out of 5 sheep showed bony bridges after 9-week post operation. As granulation tissue is replaced by soft fibrocartilaginous cartilage during soft callus stage, the callus gets stiffer and can potentially withstand more loading. The model predicted, an allowable level of partial weightbearing of up to 60% BW which could be applied to the fracture callus during early (week 1 and week 2) soft callus stages without exerting any damage to the regenerating blood vessels as healing progresses (Refer to Table 5.6). Thus, allowable level of partial weight bearing loading at early stages of healing for promoting angiogenesis and bone healing are suggested using simulation results.

A lower load bearing capacity can be seen in fractured bone with an increase in fracture angle of obliquity as indicated in Table 5.5 and Table 5.6. This shows that oblique fractures have higher deviatoric strain / octahedral shear strain for same magnitude of load applied. This can be explained by increased shear interfragmentary movement for higher fracture angle of obliquity under same loading magnitude, which is inimical to healing. Thus, higher obliquity leads to lower stability in fracture callus. Identification of maximum permissible loading that can be applied at different stages of bone fracture healing has clinical relevance to orthopaedic surgeons to determine optimal LCP configuration depending on the severity or degree of fracture angles.

From left to right in both tables (Table 5.5 and Table 5.6), an increase in the flexibility of fixation (by increasing either BPD or WL or both) leads to lower load bearing capacity of the fractured bone. An increase of both BPD and WL ($C_{4\text{-}100}$) results in the lowest permissible load in all fractured angles. This is consistent with the previous studies (Ahmad et al., 2007, Miramini et al., 2016a) who have reported increased instability in fractures stabilized with large BPD and WL of LCP fixation. This result contrasts with the study by Alierta et al. (2016) which showed little variation in bone union in rigid and dynamic configuration during early stage of fracture healing in oblique fractures. On the other hand, previous studies by Claes et al. (1995a) and Bishop et al. (2006) showed that controlled movement in bone fracture enhances healing process compared to absolute stability models. Therefore, an optimum fixation configuration needs to be identified for patient specific condition to provide enough flexibility to promote uniform callus formation while maintaining adequate stability.

5.5. **Conclusions**

This study quantifies relationship between different angle of obliquity and maximum permissible load that allow angiogenesis during early stages of healing. This information can be particularly relevant to orthopaedic surgeons to understand maximum permissible loading that can be applied at different stages of bone fracture healing depending on the severity or degree of fracture angles. It should be acknowledged that, to simplify the complex problem in this study, only axial loading is considered in the simulation. Nonetheless, this study is able to propose different loading patterns for different angles of fracture obliquities. Furthermore, this study concluded that oblique fractures can withstand lower weight bearing compared to transverse fractures during the course of healing.

Chapter 6.

An ex-vivo experimental study to compare the fracture IFM between normal and osteoporotic bones

6.1. Abstract

With an increased life expectancy of Australians, the number of fractures associated with osteoporosis is also on the rise. Osteoporotic fractures are generally different to normal bone fractures which can affect the fracture healing process, due to the changes in the diffusion and perfusion of non-mineralised bone marrow with the loss of mineralised bone component. In this study, bone fracture healing in healthy bone is experimentally compared with osteoporotic bone at early stage of healing, under dynamic loading conditions stabilized with different fixation (LCP) configuration. Our study shows that osteoporotic bones resulted in more asymmetric healing across near and far cortex compared to healthy bones. Furthermore, increase in flexibility of fixation resulted in less uniform IFM in both healthy and osteoporotic bones.

6.2. Introduction

While most fractures heal successfully after treatment, there are still many cases of non-healing or delayed healing, which constitutes about 5 – 10% of all fractures (Zura et al., 2016, Tzioupis and Giannoudis, 2007, Calori et al., 2011). Several factors, including mechanical, biochemical, genetics or medical conditions like osteoporosis can influence fracture healing process, leading to the healing impairment (Geris et al., 2010). Among them, osteoporosis is a degenerative medical condition predominantly associated with an old age, where reduction of the bone density results in brittle and porous bone. Due to the degradation of micro-architectural structure and mechanical strength, osteoporotic bones are more susceptible to fracture and its ability to heal back following a fracture is also greatly reduced. Osteoporotic bones have often been linked with delayed healing and orthopaedic complications, like fixation failure (Barrios et al., 1993, Waters et al., 2000). Moreover, the healed bone in osteoporotic femur fractures was found to have reduced strength in ovariectomised rats (Meyer Jr et al., 2001). This shows that, how osteoporosis impacts fracture healing is still poorly understood.

With an increased life expectancy of Australians, the number of fractures associated with osteoporosis is also on the rise. Osteoporosis Australia estimates around 5% of the total population of Australia is affected by osteoporosis (i.e. around 4.74 million Australians over age 50) (Watts et al., 2013). Further, over 50% of population aged 80 years or above are diagnosed with osteoporosis in Australia and it is predicted that an osteoporotic fracture occurs every 3.7 minutes by 2021 (Economics, 2006, Sambrook et al., 2002). Accounting for the high prevalence of these osteoporotic fractures in projected world population with increased life expectancy, WHO has even regarded osteoporosis to be a critical health problem after cardiovascular diseases (Brandi and Piscitelli, 2013). This understandably has a huge financial burden on individuals, community, national economy as well our health care system. These fractures are estimated to cost $33.6 billion by 2022 (Watts et al., 2013), including direct and indirect costs in ambulance services, hospital services and aged care and community services, which makes it a high priority on national health. Therefore, a better understanding of the impact of osteoporosis in fracture healing would lead to a better fracture treatment and optimum healing outcome in osteoporotic fractures.

Osteoporotic fractures are generally different to normal bone fractures, in the sense that they are low energy fractures involving considerably low loads, for e.g. falls from standing height in elderly people. Along with the loss of mineralised bone component during osteoporosis which can increase the fracture risk, there is also changes in the diffusion and perfusion of non-mineralised bone marrow which can affect the fracture healing process (Griffith, 2013). Since bone marrow is home to multipotent mesenchymal stem cells, the mesenchymal stem cells migrating to the fracture site from surrounding cells, periosteum and bone marrow is reduced as well. In addition, there could be change in MSC differentiation away from osteoblasts (Nuttall et al., 1998). Following a fracture, inflammatory cells, macrophages and mesenchymal stem cells are the first cells to migrate to the fracture site in response to the expression of cytokines and growth factors. These cells and growth factors are also sensitive to the change of mechanical microenvironment of the fracture callus (Weiss et al., 2002, Ghimire et al., 2018), as previous studies have shown that mechano-regulation influences upregulation of growth factors and the migration and differentiation of MSCs. And the ability of these cells to respond to these mechanical and biochemical stimuli may change under medical conditions like osteoporosis. Literatures have also suggested that osteoporotic bones may respond differently to mechanical stimuli (Augat et al., 2005). Unlike normal bones, mechanical loading didn't increase proliferation of osteoblasts or release of osteogenic growth factors (Neidlinger-Wilke et al., 1995), which indicates different threshold of mechanical stimulation for osteoporotic bones.

Due to the change in structure and reduced strength in osteoporotic bone, the local stress and strain induced due to loading could change as well. As a result, its influence on cells and growth factors and their resultant response within fracture callus would be different. Thus, the optimum healing outcomes in such conditions may not be achieved using conventional methods of treatment, i.e. the treatment process for normal fractures may not lead to the best healing outcomes in case of osteoporotic bones. For example, the degree of fixation stability or weight bearing adopted for normal bone fractures may result in considerably different outcome in osteoporotic bone, due to the difference in their bone density, stiffness, structural rigidity and porosity. The stability achieved from conventional rigid constructs also reduces gradually with time, particularly in osteoporotic bones (Szypryt and Forward, 2009). Furthermore, there is high risk of

fixation failure due to reduced bone mass and the risk of subsequent fracture increases in osteoporosis after each fracture due to its fracture cascade effect. Therefore, the nature of the relationship between the degree of mechanical stability provided by a flexible fixation and the optimal healing outcomes in osteoporotic bone has not been fully understood and osteoporosis in fractured bone continue to pose a challenge to fracture stabilization by fixation (Augat et al., 2005).

Previous studies have reported successful healing using locking plates fixation in elderly patients with osteoporosis(Anakwe et al., 2008). Flexible fixation like locking compression plates (LCP) has been shown to encourage the formation of fracture callus, leading to better healing outcomes. The cells in fracture callus respond to change in their mechanical microenvironment due to different configurations of LCP, particularly in the early stage of healing. Increasing flexibility of the LCP by changing the bone–plate distance (BPD) or the plate working length (WL) could enhance inter-fragmentary strain (i.e. interfragmentary movement / gap size) in the presence of a relatively large gap size (3 mm). Furthermore, locking plates allow screw to be fixed to the plate by the use of locking heads, thereby reducing the risk of screw loosening and construct failure (Szypryt and Forward, 2009). Therefore, locking plates have added advantage to conventional compression plates in osteoporotic bone fractures by enhancing fixation stability (Anakwe et al., 2008). Furthermore, locking plates like locking compression plates (LCP) are designed to reduce bone-plate contact and therefore preserve periosteal blood supply and has been found to yield superior healing compared to the conventional compression plates, which are compressed against bone and destroy vascularity to the bone underneath (Tepic et al., 1997). However, it is still not clear how the mechanical microenvironment of fracture under LCP fixation is different between normal and osteoporotic fracture.

Furthermore, external loading (like exercise) has shown to prevent age related osteoporosis and enhance bone mineral content in osteoporotic bones (Tolomio et al., 2010, Cussler et al., 2005, Kemmler et al., 2004, Todd and Robinson, 2003), however there are limited research on how the external loading like weight bearing exercise affects bone healing process in such osteoporotic fractures. Therefore, the aim of this study was to compare bone fracture healing in normal and osteoporotic bone at early

stage of healing due to dynamic loading conditions under different fixation (LCP) configuration.

6.3. **Methodology**

The objective of this experiment is to determine (a) whether osteoporotic bones would experience a different fracture mechanical microenvironment compared to non-osteoporotic fractures; and (b) how the configuration of locking plates could affect osteoporotic fracture mechanical microenvironment. Interfragmentary movement (IFM) induced by load and fixation stiffness will strongly influence fracture mechanical microenvironment and consequently affect fracture healing (Augat et al., 2005). Therefore, in this study, the interfragmentary movement in different region of fracture gap was experimentally determined in osteoporotic bones stabilized with different LCP configurations and compared with that of healthy bone fractures.

In this pilot ex-vivo experimental study, sheep animal models were used to determine the interfragmentary movement (IFM) between normal and osteoporotic bone stabilized by LCP fixation in different regions of fracture gap. Due to their similarities with human weight and size of long bone, sheep are preferred experimental models for the evaluation of bone regeneration, particularly for osteoporotic models (Egermann et al., 2005). The key problem to be investigated is whether IFM in fracture gap would differ in osteoporotic bone and healthy bone stabilized by LCP fixation. And whether increasing flexibility of the fixation by increasing BPD 0mm to BPD 2mm would reduce asymmetrical healing process.

6.3.1. Design of experiment:

Ex-vivo experiments were carried out on the normal and osteoporotic sheep tibia, obtained from Veterinary Research Laboratory, Charles Sturt University (CSU). The study was approved by the Charles Sturt University Animal Care and Ethics Committee (Ethics Approval no 14/031 and 15/099).

6.3.2. Animal Study:

Eight adult healthy and skeletally mature female sheep of age between 4-5 years and average body weight of (**59** kg) were selected from sheep flock and identified with individual ear tags. These sheep went through clinical examination before admission to the study and their health condition was recorded in the standard CSU animal health report form. The sheep were provided twice daily with a 50:50 mixture of wheaten and Lucerne chaff, and ad libitum fresh water. The sheep were randomly assigned to two study groups of 4 animals (refer to Table 6.1), and the sheep in osteoporotic group had induced osteoporosis over the span of 9 months by providing food deficient in calcium and vitamin-D together with oestrogen deficiency.

Table 6.1: Total samples for different models were used in the experiment with Bone Plate Distance

Bone type	**BPD 0mm**	**BPD 2mm**
Healthy tibia	3 (Control group)	1
Osteoporotic tibia	3	1

6.3.3. Preparation of samples

Animals were sacrificed with an intravenous injection of pentabarbitone (200mg/kg) and the sheep tibia was extracted with standard procedures. Since the fracture tibia is obtained in the early stage of healing, there is no callus formation. A transverse fracture with a gap size of 3mm was generated in the mid diaphyseal sheep tibia similar to the standardised osteotomy model (Wilson et al., 1999) using an oscillating bone saw.

6.4. Fracture stabilization

The osteotomised tibia was stabilized with stainless steel Locking Compression Plate (LCP) by SYNTHES *(VP4041.10-3.5 mm LCP Plate 10-hole, 131 mm)* with 3.5mm locking screws, maintaining 3mm fracture gap. The screws were placed at holes 2, 4 and 5 on either side of the fracture gap. Previous studies have shown than flexibility of the LCP

fixation can be changed by increasing the bone plate distance (BPD) (Ahmad et al., 2007), which is the distance between the plate and bone. Therefore, two fixation configurations, i.e. BPD 0mm and a relatively flexible configuration of BPD 2mm were considered. Out of 4 normal bones, 3 bones were randomly selected to stabilize with BPD 0mm and served as control bones, and 1 bone was stabilized with BPD 2mm for comparison. Similarly, 3 osteoporotic bones were stabilized with BPD 0 mm, and 1 osteoporotic bone was fixated with BPD 2mm configuration.

Healthy tibia with 0mm BPD served as the control group.

6.4.1. Experimental set-up

To secure the bone for the experiments and ensure that load application was vertical, the distal bone end was potted in customized pots using epoxy (BIS-HY, ICCONS Australia)). With the distal end of tibia fixed at the bottom, dynamic loading of 100N and 200 N each were applied on the proximal end of the cortical bone using Universal testing machine Instron 5944 with 2KN force capacity (refer to Figure 6.1).

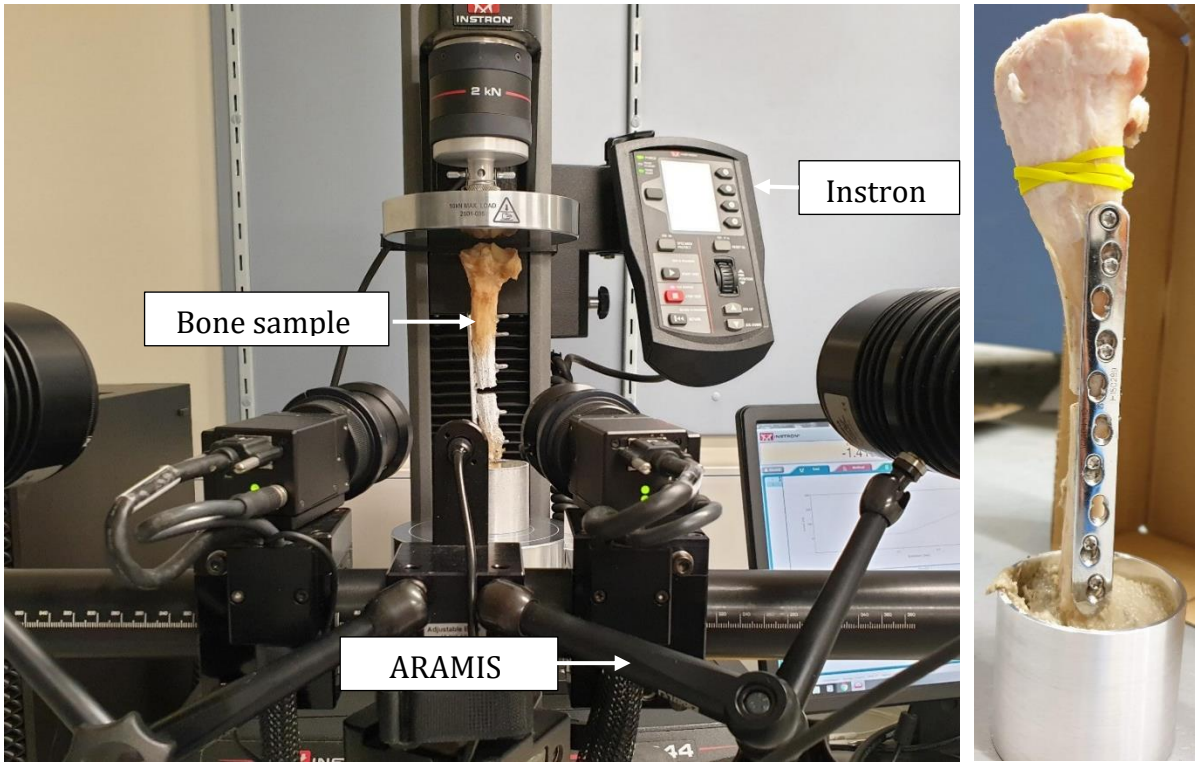

Figure 6.1 Photograph showing experimental set-up with bone sample, Instron testing system (to load the sample) and ARAMIS digital image correlation system (to measure deflection optically) (left), and bone specimen showing plate and screws placements potted in a metal cylinder using epoxy (right)

6.4.2. Outcome measurements:

The corresponding interfragmentary movement (IFM) was measured using optical measuring instrument ARAMIS (BOM, Germany) that provides non-contact measurements using digital image correlation principle. The equipment uses 3D digital photogrammetry through optical sensors to measure specimens under load and requires speckled pattern on the face of the test specimen. For this purpose, the bone surface facing the cameras was sprayed with white paint in the background, followed by black paint dots to create the speckles. By recording digital images before and after load application, the deformation is analysed by ARAMIS by measuring the relative movement of the speckles created (Refer to Figure 6.2). The data obtained were cross-validated with force deflection curve obtained from Instron machine.

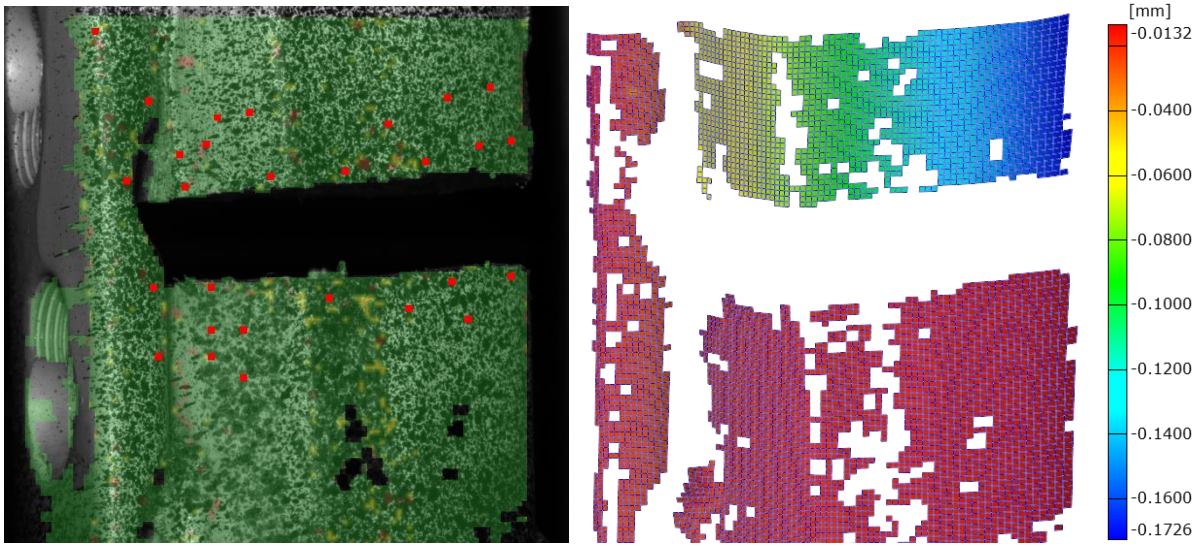

Figure 6.2 Image of bone specimen captured by ARAMIS during the experiment (left), and deflection of bone specimen due to load application following analysis of the captured images by ARAMIS (right)

6.4.3. Statistical analysis

A statistical analysis using unpaired t-test with 5% level of significance was carried out for each magnitude of applied load to compare IFM at near and far cortex of the two experimental groups, i.e. control and osteoporotic sheep tibia.

6.5. Results

The main aim of this study is to compare the bone fracture healing (in terms of interfragmentary movement) between normal and osteoporotic bone in near and far cortex. Further, the effect of different fixation (LCP) configuration (i.e. BPD 0 mm and BPD 2mm) at early stage of healing is assessed to determine if different configuration of locking plates could enhance fracture healing in osteoporotic bone.

The axial interfragmentary movement (IFM) of control and osteoporotic sheep tibia at NC and FC were measured and Figure 6.3 shows the IFM under externally applied loading of (a) 100N and, (b) 200N respectively. The increase in loading magnitude from 100 to 200N increased IFM in control bones by 100% (doubled) in both near and far cortex. Same loading increased IFM in osteoporotic bones by around 70%. Overall, the IFM of osteoporotic bones is notably different from control bones, particularly in far cortex. However, owing to small sample size and large variation in control bones IFM (refer to error bars in Figure 6.3), the difference wasn't found to be statistically significant.

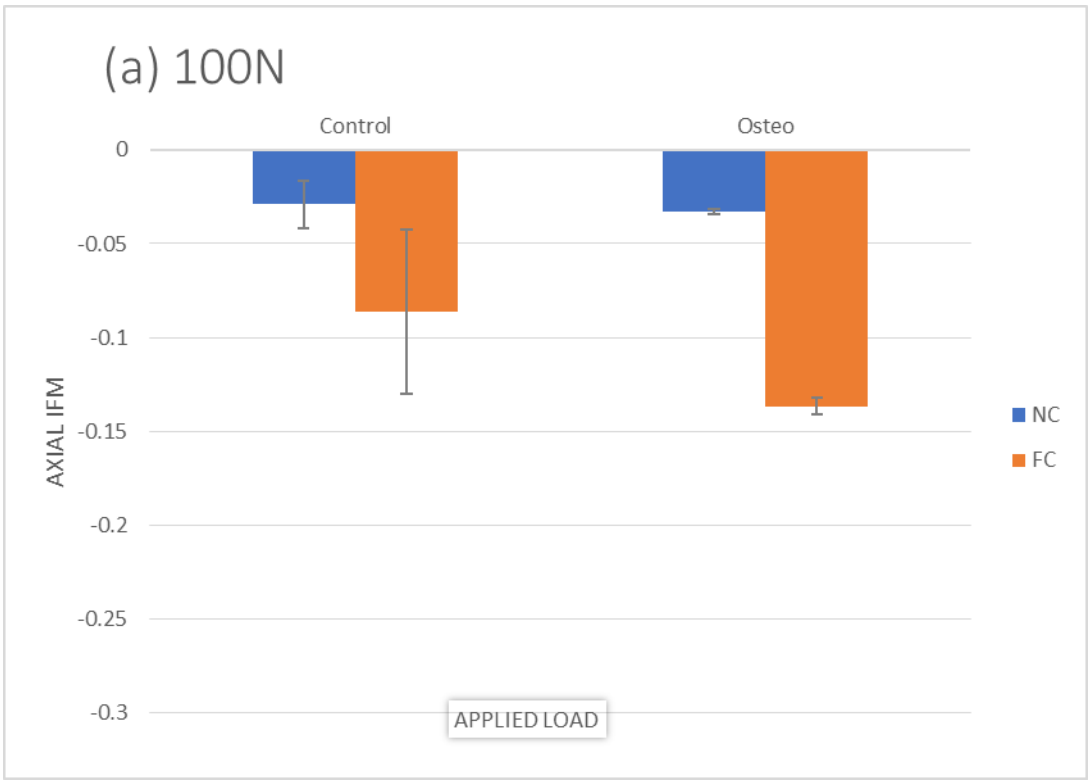

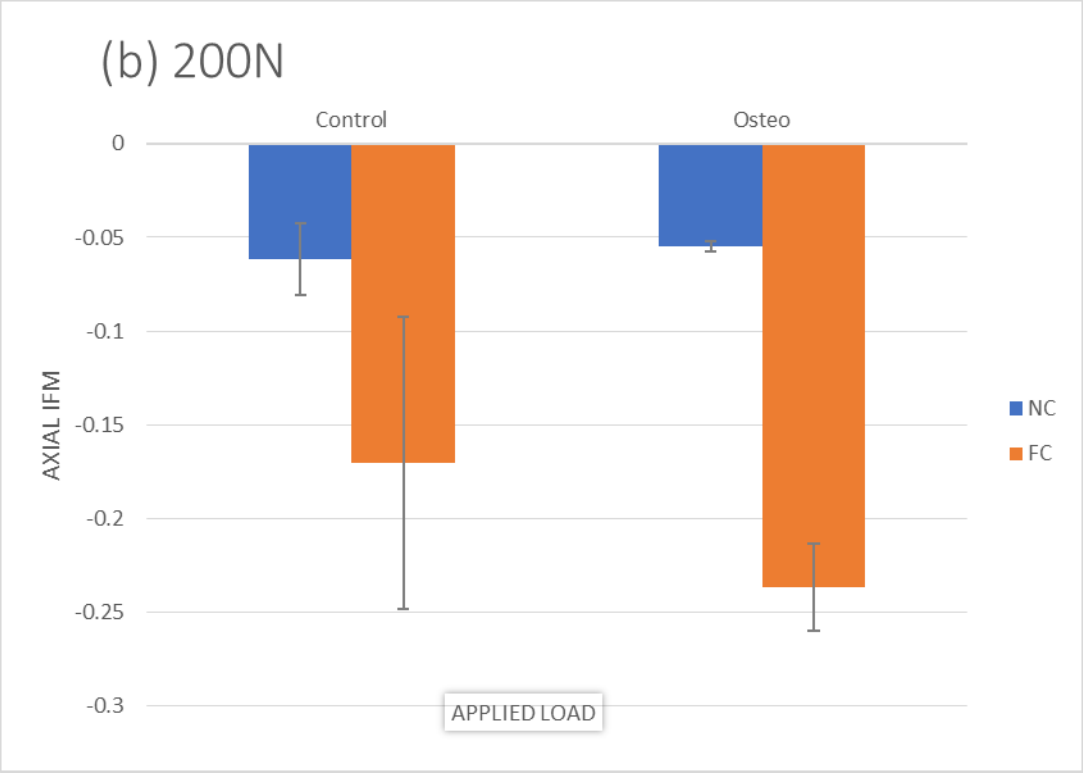

Figure 6.3 Experimentally measured axial Interfragmentary Movement (IFM) in control and osteoporotic bones in near and far cortex under (a) 100N, and (b) 200N loading conditions. The standard errors are shown at tip of each mean values.

Further it can be seen that, far cortex has significantly higher IFM compared to near cortex for both control and osteoporotic bone ($p<0.05$). This is consistent with previous studies that have shown non-uniform IFM in near and far cortex of the bone when stabilized by plate fixation (Bottlang et al., 2010a, Lujan et al., 2010). To compare the non-uniformity in IFM between normal and osteoporotic bones due to Locking Compression Plate (LCP), the ratio of IFM at FC to NC was calculated and presented in Figure 6.4. The value closer to 1 represents more uniform IFM across NC and FC. The IFM ratio of FC/NC at 200N obtained for normal bone is consistent with the IFM ratio of FC/NC measured in tibial surrogates by Miramini et al (2016) (Miramini et al., 2016b). Figure 6.4 shows that the IFM is comparatively less uniform in osteoporotic bones compared to normal bones ($p<0.05$), which indicates that osteoporotic bones result in larger asymmetric healing. The non-uniformity is observed to be higher for osteoporotic bone in the more flexible fixation of BPD = 2mm.

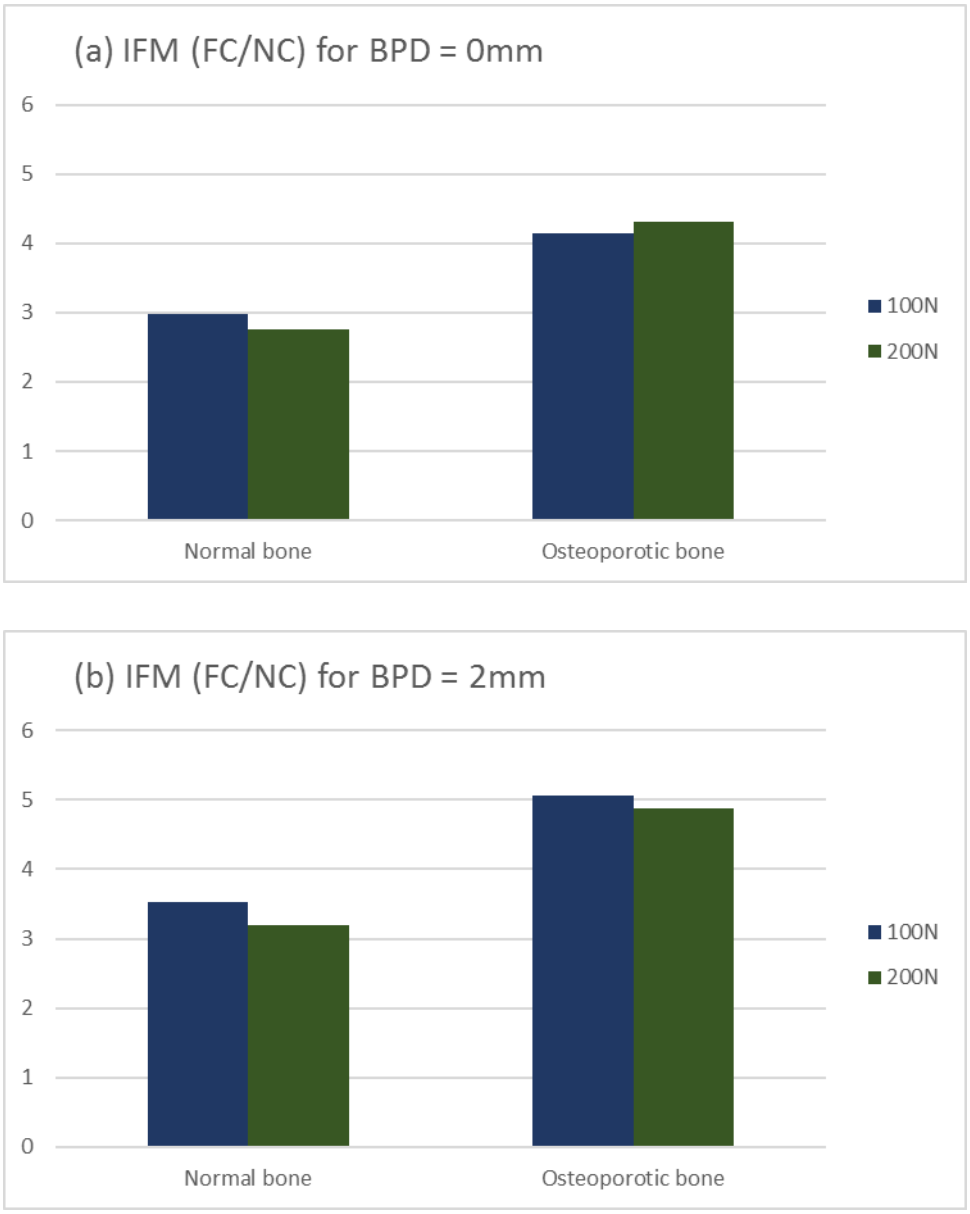

Figure 6.4 Ratio of axial Interfragmentary Movement (IFM) in Far Cortex to Near Cortex (FC / NC) for normal and osteoporotic bones under 100N and 200N of applied load for the fixation configuration of (a) Bone Plate Distance (BPD) = 0mm, and (b) Bone Plate Distance (BPD) = 2mm.

Figure 6.5 shows interfragmentary strain experienced by normal and osteoporotic bone for different magnitude of applied loading. Perren (1979) have suggested that IFS under 2% would lead to intramembranous ossification while IFS between 2 – 10% would be favourable for endochondral ossification. Due to asymmetric IFM generated by LCP, Figure 6.5a shows that only far cortex of normal and osteoporotic bones would follow endochondral ossification healing pathway under healing of 100N. When loading

amplitude was increased to 200N, both near and far cortex of normal bone would go through endochondral ossification pathway. The osteoporotic bone experienced lower strain in near cortex for same loading amplitude, and therefore predicted to undergo intramembranous ossification pathway. This shows that healing mechanism designed through fixation stiffness and flexibility for normal bones may not be appropriate for osteoporotic bones, and the healing pathway desired may not be achieved.

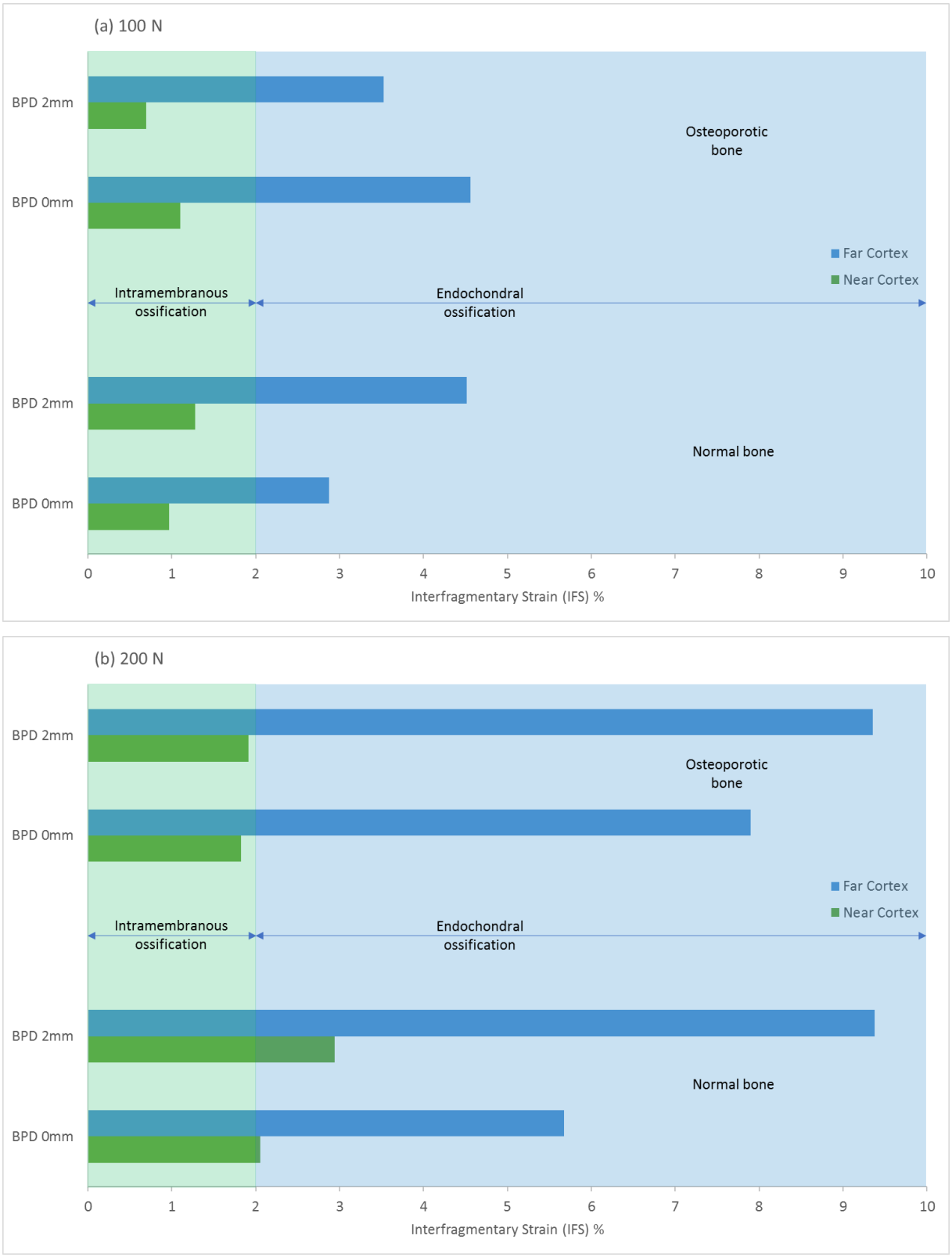

Figure 6.5 Interfragmentary Strain (IFS) defined as IFM / Fracture gap for normal and osteoporotic bones in near and far cortex for fixation configuration of BPD = 0mm and BPD = 2mm for (a) 100N and, (b) 200N loading conditions. IFS < 2 indicates

intramembranous ossification while 2< IFS <10 indicates endochondral ossification(Perren, 1979).

In case of normal bone, IFS strain increased with increase in applied load (from 100N to 200N) and higher flexibility of the fixation system (from BPD 0mm to BPD 2mm). For example, for an increase in applied load from 100N to 200N, the interfragmentary strain almost doubled in both near and far cortex (Figure 6.5a and b) in both BPD 0mm and BPD 2mm. By comparison, similar results were observed in osteoporotic bone in BPD 2mm when applied loading increased from 100N to 200N. The osteoporotic bone in BPD 0mm also experienced a larger IFM when loading was increased, however the increment was smaller comparative to other experimental groups.

6.6. Discussion

Previous studies have indicated the cortical thickness of osteoporotic bone is significantly reduced, as a result the mono cortical screws alone cannot provide sufficient bone-screw purchase (grip) and result in instability (Gautier and Sommer, 2003). Therefore, bicortical screws were used in this experimental study in osteoporotic bones. Similar screws were used in control to maintain consistency in fixation configuration.

The experimental results in this study showed that for the same magnitude of loading applied, osteoporotic bones experience more uneven IFM in near and far cortex compared to normal bone. This results in unequal callus stimulation and spatially dependent bone healing across fracture callus. This non-uniformity in IFM seems to worsen with more flexible fixation, in both normal and osteoporotic bone.

In addition, the ex-vivo biomechanical testing results suggested that there is no significant difference in IFM between normal and osteoporotic bone. Similar to our experiments study, a previous study in rat femurs identified no significant difference between normal and osteoporotic bone at various healing stages statistically in ovariectomised rat femur fractures (Wheeler, 2000). In another experiment, Kubo et al. (Kubo et al., 1999) observed significant decrease in the bone mineral density only during the later stages of healing which could be associated with impaired bone remodelling in osteoporotic conditions.

Nevertheless, it should be noted that, the inability to find significant difference between IFM of normal and osteoporotic bone in this study could be due to the Type II statistical error, i.e. failure to reject null hypothesis (i.e. no difference) when it's false as the sample size was very small in this experiment due to limited resources (n=8). The IFM of one of the normal sheep tibiae was very high compared to the other two in the group. As a result, the standard errors presented in the graph showed larger variation in normal bone. This not only resulted in large SD for this group, but also resulted in statistical insignificance between normal and osteoporotic group. This has highlighted that just one sample can have huge influence in the results when the sample size is very small. Therefore, further experimental dataset is required to verify the results of this pilot study.

As different IFM would lead to different cellular processes and healing outcomes, our results suggest that a different fracture healing treatment (fixation configuration and loading protocol) may need to be adopted for optimum healing outcomes of osteoporotic bones fractures.

This study has some limitations. Being a pilot experimental study, the sample size is very small. Therefore, larger dataset is necessary to validate the results. Nonetheless, this experiment has led to an understanding of how interfragmentary movement (IFM) in fracture gap would differ under different LCP configurations for osteoporotic bone and healthy bone.

6.7. Conclusions

The main findings of this study are summarised as follows:

1. Osteoporotic bone fractures experienced a relatively larger IFM compared to normal bone fracture, but the difference was not statistically significant.
2. Osteoporotic bones resulted in more asymmetric healing across near and far cortex compared to healthy bones in both BPD 0mm and BPD 2mm fixation configuration ($p=0.004$).
3. Increasing flexibility of fixation results in less uniform IFM in both healthy and osteoporotic bones.

4. Different rate of increase in induced IFM was observed in osteoporotic and normal bone, for similar increase in external stimulation.

Chapter 7.

Investigation of bone fracture healing under intramembranous and endochondral ossification

7.1. Abstract

After trauma, fractured bone starts healing directly through bone union or indirectly through callus formation process. Intramembranous and endochondral ossification are two commonly known mechanisms of indirect healing. The present study investigated the bone fracture healing under intramembranous and endochondral ossification by developing theoretical models in conjunction with performing a series of animal experiments. Using experimentally determined mean bone densities in sheep tibia stabilized by the Locking Compression Plate (LCP) fixation system, the research outcomes showed that intramembranous and endochondral ossification can be described by Hill Function with two unique sets of function parameters in mechanical stimuli mediated fracture healing. Two different thresholds exist within the range of

mechanical simulation index which could trigger significant intramembranous and endochondral ossification, with a relatively higher bone formation rate of endochondral ossification than that of intramembranous ossification. Furthermore, the increase of flexibility of the LCP system and the use of titanium LCP could potentially promote uniform bone formation across the fracture gap, ultimately better healing outcomes.

7.2. **Introduction**

Bone fractures can occur under traumatic (*e.g.* sport injuries or traffic accidents) or non-traumatic condition (*e.g.* osteoporosis and bone cancer) (Moroni et al., 2005, Rodan and Martin). Primary bone healing is a direct bone union process, which takes place on a very small fracture gap (order of 10-100μm) with strain under 2%, and often requires a rigid fixation like a conventional compression plate in place to maintain absolute stability of the fracture site for much longer time, even years (McKibbin, 1978a). In contrast, secondary healing (also known as indirect healing) is more common and occurs in fracture gaps with larger micro motions and can be achieved with flexible fixation system like locking plates (Perren, 2002a, Woo et al., 1983). Indirect healing consists of two main processes: intramembranous and endochondral ossification. During endochondral ossification cartilage is formed, calcified and finally replaced by bone; whereas in intramembranous ossification, bone tissue is directly synthesized by osteoblasts formed through mesenchymal stem cell differentiation (MSC)(Doblaré et al., 2004). Although direct and indirect healing have been qualitatively studied (Augat et al., 1998, Perren, 1979, Vetter et al., 2010), the fundamental mechano-regulation principles governing different bone formation rates under the healing processes of intramembranous and endochondral ossification are not presently understood. This is largely due to the large number of complex processes occurring simultaneously during bone repair (Marsell and Einhorn, 2011). It has also been shown that the mechano-regulation in various stages of healing may differ from species to species (Checa et al., 2011).

Over the last decades, several mechano-regulation theories have been developed to quantify complex mechanical stimuli mediating the healing processes (Pauwels, 1960, Perren, 1979, Prendergast et al., 1997, Carter et al., 1998b, Claes and Heigele, 1999). According to these theories, magnitude of stimuli determines the bone formation pathway under intramembranous ossification or endochondral ossification. In

particular, the mechano-regulation model proposed by Prendergast et al. (1997) has been widely accepted (Isaksson et al., 2006) and further extended to predict cell differentiation/ tissue formation during bone healing (Lacroix et al., 2002a, Checa and Prendergast, 2009, Khayyeri et al., 2009, Isaksson et al., 2008b, González-Torres et al., 2010b, Reina-Romo et al., 2011, Miramini et al., 2017b, Zhang et al., 2017a, Shanshan et al., 2019, Ganadhiepan et al., 2019c, Ganadhiepan et al., 2019a, Miramini and Yang, 2019). By treating callus as a poroelastic mixture in a computer model in conjunction with an *in vivo* experimental study, the authors have suggested that octahedral shear strain of the solid phase and interstitial fluid velocity relative to the solid phase are two important biophysical stimuli for mechano-regulatory pathway (Prendergast et al., 1997). Under low stimulus magnitude, the multi-potent mesenchymal stem cells (MSCs) differentiate directly into osteoblasts through the process of intramembranous ossification, while under moderate magnitude of stimulus, MSCs differentiate into chondrocytes through an endochondral ossification process. The current mechano-regulation models have limited capability of predicting the different bone formation rates under intramembranous and endochondral ossification processes.

The stiffness of bone fracture fixation is another important factor which can affect bone fracture healing processes. By adjusting the stiffness of a Locking Compression Plate (DePuy Synthes, Switzerland) through changing bone plate distance (BPD, defined as the distance between bone and fixation plate) and working length (WL, defined as the distance between two innermost screws), the study of Miramini et al. (2016) (Miramini et al., 2016b) demonstrated that the tissue differentiation behaviour in fracture callus could be significantly affected. It has also been shown that a relatively flexible fixation can potentially encourage bone healing (Augat et al., 1998).

Through developing numerical models in conjunction with animal experiments, the purpose of this study is to investigate the bone formation rate under intramembranous and endochondral ossification conditions. The models consider the spatial and time dependent changes in material properties of fractured bone as a result of the change of new bone content as healing progresses. In addition, the model has the capability of quantifying the healing outcomes under different fixation configurations and loading conditions.

7.3. Methods

7.3.1. Computational modelling

As shown in Figure. 7.1a, the proposed framework consists of a callus mechanics model and a mechano-regulation model. Detailed steps for developing the mechano-regulation model proposed in this study are shown in Figure. 7.1b. The total 8-week healing period is divided into several time-steps. Based on the configuration of fixation (LCP) system, axial force applied, and experimental bone density values determined each week, the callus mechanics model (refer to section 2.1) is used to estimate the mechanical stimuli (fluid flow and deformation resulting from the interfragmentary movement) in callus for the corresponding week. Using this data for each healing week, bone formation rate and other parameters in the mechano-regulation model (refer to Section 2.2) are determined using a parameter optimization tool (refer to Figure. 7.1b).

For the numerical simulation (Refer to Figure. 7.1a), the callus mechanics model and mechano-regulation model are fully coupled, i.e. new mechanical properties of healing bone defined by the mechano-regulation model along with the applied load and fixation determines new mechanical stimuli for the callus mechanics model, and ultimately, new bone formation at the next time step, and forming a feedback loop. Further, the calibrated mechano-regulation model is then employed to improve the understanding of stiffness requirements of fixation systems used for fracture management (i.e. titanium LCP over stainless-steel LCP) and fracture union progression.

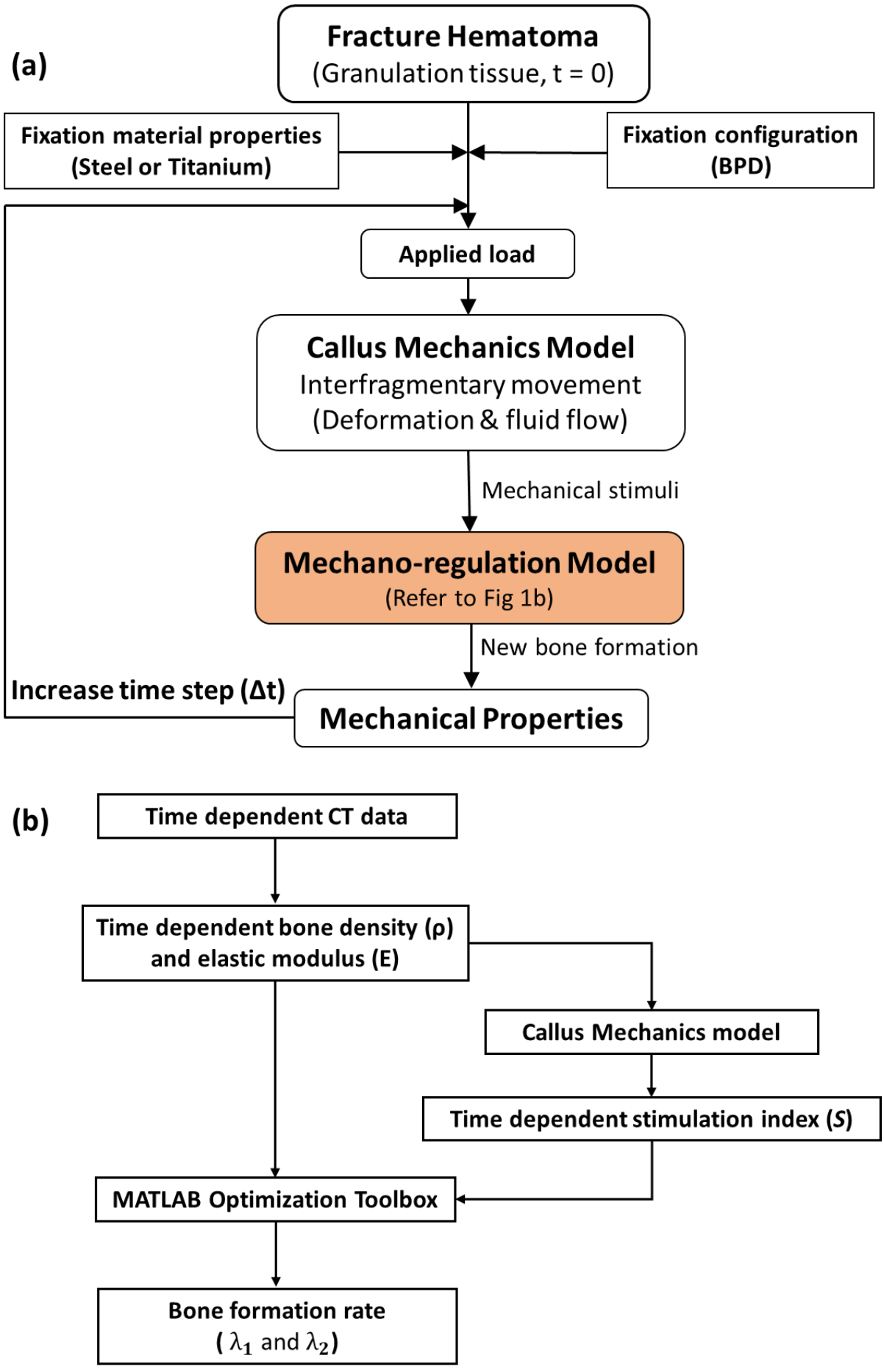
(a)
Fracture Hematoma
(Granulation tissue, t = 0)
Fixation material properties
(Steel or Titanium)
Fixation configuration
(BPD)
Applied load
Callus Mechanics Model
Interfragmentary movement
(Deformation & fluid flow)
Mechanical stimuli
Mechano-regulation Model
(Refer to Fig 1b)
New bone formation
Increase time step (Δt)
Mechanical Properties
(b)
Time dependent CT data
Time dependent bone density (ρ)
and elastic modulus (E)
Callus Mechanics model
Time dependent stimulation index (S)
MATLAB Optimization Toolbox
Bone formation rate
(λ1 and λ2)

Figure. 7.1 (a) A schematic diagram for predicting mechanical stimuli mediated healing under different fixation conditions; and (b) *Details of the mechano-regulation model proposed in this study.*

Callus Mechanics Model

The mechanical behaviour of fracture callus in Figure. 7.2 can be modelled by using a consolidation approach (Zhang et al., 2015a, Zhang et al., 2008b, Miramini et al., 2017a, Ghimire et al., 2018), which treats the callus as a porous media comprising an intrinsically solid phase (*i.e.* extracellular matrix) and an incompressible fluid phase. As at first estimate, the callus can be treated as an homogeneous material with a constant size and geometry (Garcia-Aznar et al., 2007, Gardnera et al., 2000). The relationship between the solid phase and fluid phase can be described as,

$$\nabla \bullet \left(\mathbf{v}^{s} - \kappa \nabla p \right) = 0 \tag{7.1}$$

$$-\nabla p + \nabla \bullet \sigma^{e} = 0 \tag{7.2}$$

where $\mathbf{v}^{s}$ is the solid phase velocity, p is the interstitial fluid pressure, σ^{e} is the elastic effective stress of solid matrix, and κ is the hydraulic permeability tensor.

As healing progresses, the elasticity and stiffness of callus increases (Moorcroft et al., 2001) with the increase in bone formation shown in experimentally determined bone density values in the callus (Refer to Table 7.1 and Table 7.2). Therefore, it is reasonable to assume that the callus can be modelled based on the mechanical properties of the tissue formed during bone healing. While fracture callus is a heterogeneous mixture of granulation tissue, fibrocartilage tissue and bone tissue, bony tissue has the highest stiffness among these components (Leong and Morgan, 2008). The mechanical properties of newly formed bone can be correlated to the average bone density (ρ) (kg/m3) across callus as follows:

$$E = 0.06\rho^{1.51} \tag{7.3}$$

where E is the elastic modulus (MPa) of fracture callus (Rho et al., 1995).

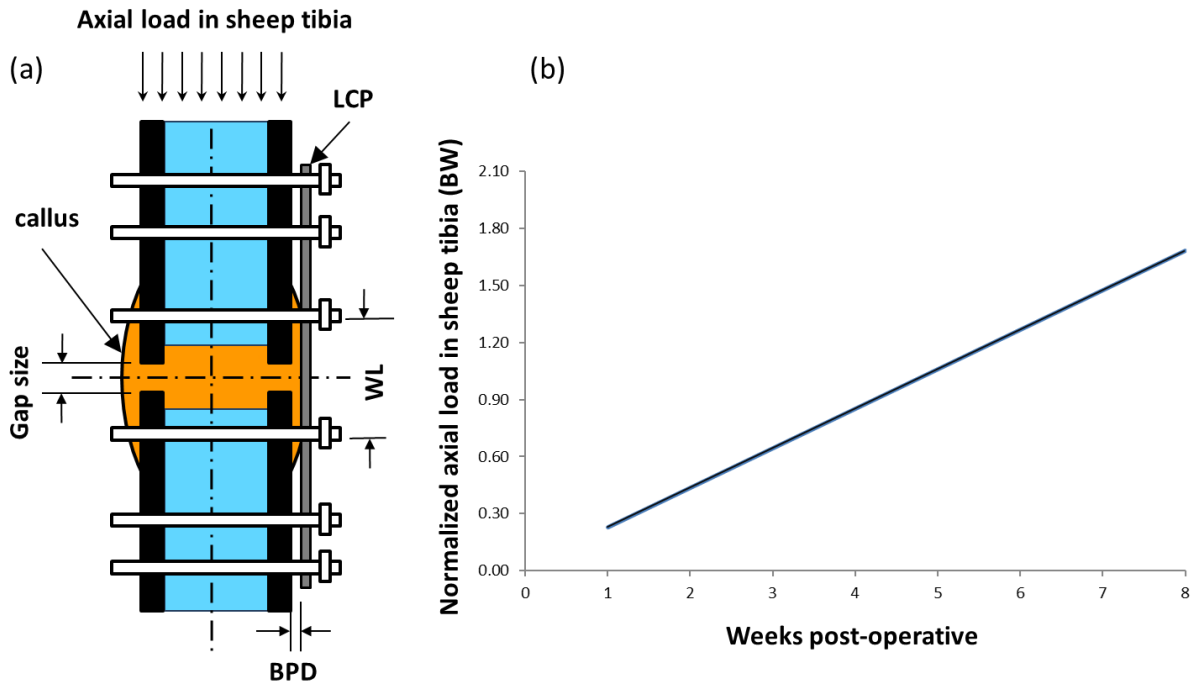

Figure. 7.2(a) A schematic diagram of the Locking compression plate (LCP) system used in this study. The mechanical stiffness can be regulated by adjusting bone plate distance (BPD = 0mm or 2mm and defined as the distance between bone and fixation plate) and working length (WL = 35mm and defined as the distance between two innermost screws); and (b) loading protocol where axial load in sheep tibia is normalized to its Body Weight (BW) and is assumed to increase linearly as healing progresses (Grasa et al., 2010, Döbele et al., 2010).

Table 7.1 Mean bone density values in HUs measured in near cortex (NC) and far cortex (FC) (BPD=0mm).

Sheep ID	Region	Week 1	Week 4	Week 6	Week 8	Remarks
#130	NC	277.4	675.1	688.5	723.5	sacrificed 8 wks post-op
	FC	451.3	1020.7	1325.7	1504.6	
#111	NC	254.3	604.6	949.2		

	FC	1066.6	1139.2	1182.7		sacrificed 6 wks post-op
#136	NC	326	604.3	610.8		sacrificed 6 wks post-op
	FC	1398.8	1800.7	1859.2		
#010	NC	533.1	850			sacrificed 4 wks post-op
	FC	1098.3	1253.9			
#007	NC	521.4				sacrificed 2wks post-op
	FC	1503.3				
Mean	NC	382.4	683.5	749.5	723.5	BPD = 0mm
	FC	1103.7	1303.6	1455.9	1504.6	
SD	NC	134.8	115.9	177.3	NA	
	FC	410.4	344.8	356.5	NA	

Table 7.2 Mean bone density values in HUs measured in (NC) and far cortex (FC) (BPD=2mm).

Sheep ID	Region	Week 1	Week 4	Week 6	Week 8	Remarks
#135	NC	256.9	401.2	604.8	1011.7	Sacrificed 8-weeks post-op
	FC	1053.4	1277.3	1696.2	1782.9	
#125	NC	398.4	435.9	515.7	787.3	Sacrificed 8-weeks post-op
	FC	378.5	1183.2	1226	1772.1	
#113	NC	287.5	537.9	857.6		Sacrificed 6-weeks post-op

	FC	907.2	1263.4	1400.7		
#035	NC	178.9	487.9			Sacrificed 4-weeks post-op
	FC	802.9	1063.9			
#037	NC	316.8				Sacrificed 2-weeks post-op
	FC	185.6				
Mean	NC	287.7	465.7	659.4	899.5	BPD = 2mm
	FC	665.5	1196.9	1440.9	1777.5	
SD	NC	80.5	59.9	177.4	158.7	
	FC	367.6	97.9	237.7	7.7	

Mechano-regulation Model

In the present study, it is assumed that the rate of bone formation during fracture healing can be expressed by "Hill Functions", which are commonly employed in biological systems (Alon, 2006). The total bone formation rate (B_p) is assumed to be composed of the basal bone formation rates (*i.e.* B_{p10} and B_{p20} in intramembranous and endochondral ossification, respectively) and mechanical stimuli induced bone formation rate, and is also limited by the maximum allowable bone density (ρ_m):

$$B_p = \begin{cases} \left(B_{p10} + \dfrac{\lambda_1 S^{n_1}}{K_1^{n_1} + S^{n_1}}\right)\left(1 - \dfrac{\rho}{\rho_m}\right) & 0 < S \le 1 \quad (7.4a) \quad \text{Intramembranous ossification} \\ \left(B_{p20} + \dfrac{\lambda_2 S^{n_2}}{K_2^{n_2} + S^{n_2}}\right)\left(1 - \dfrac{\rho}{\rho_m}\right) & 1 < S \le 3 \quad (7.4b) \quad \text{Endochondral ossification} \\ 0 & S > 3 \quad (7.4c) \quad \text{No bone formation} \end{cases}$$

where mechanical stimulation index (S) is dependent on the octahedral shear strain of the solid phase (τ^s) and the interstitial fluid velocity (v^f, $\mu m/s$) obtained by governing equations (1) and (2). That is,

$$S = \frac{\tau^s}{a} + \frac{v^f}{b} \qquad (7.5)$$

where a = 0.0375 and b = 3$\mu m/s$ are empirical constants (Prendergast et al., 1997). A relatively low magnitude of S at the early stage, *i.e.* $0 < S \le 1$ (Eq. 4a) leads to intramembranous ossification, whereas a medium magnitude of S at the early stage, *i.e.* $1 < S \le 3$ (Eq. 4b) results in endochondral ossification. In addition, an excessive simulation at the early stage of healing (*i.e.* $S > 3$) inhibits the healing (Eq. 4c).

The parameters λ_1 and λ_2 are mechanical stimuli mediated bone formation rates in intramembranous and endochondral ossification, respectively. The "activation coefficients" K_1 and K_2 define the threshold of S which could lead to a significant increase in bone formation in intramembranous and endochondral ossification, respectively. The parameters n_1 and n_2 are the steepness of the Hill function (ranging from 1-6) in intramembranous and endochondral ossification, respectively.

7.4. **Experimental study**

Ten healthy skeletally mature cross-bred male sheep of 39-49 kg body-weight were obtained from the Charles Sturt University sheep farms. The animal study was conducted

at the Veterinary Research Laboratory, Charles Sturt University, Australia. Sheep have been shown to be an ideal animal model for the study of fracture healing due to the comparable bone size and magnitude of applied loading to that of humans(Pearce et al., 2007, Rehman et al., 1995). This research was approved and conducted in accordance with, the Charles Sturt University (CSU) Animal Care and Ethics Committee (ACEC Approval Reference No. 14/031 and No. 15/099).

Study groups

The sheep with their sheep ID tag are presented in Table 7.1 and Table 7.2. All animals underwent an acclimatisation period of at least 6 days and a clinical examination prior to admission to the study. The examination information including appetite, weight, body condition and appearance, cardiovascular and respiratory system, mobility, skin, teeth and mouth, ears, eyes and nose were recorded in the animal health report form and found to be normal.

Surgical technique and fracture stabilisation

A standard tibial transverse osteotomy with a 3-mm gap width was created using oscillating bone saw in mid diaphyseal tibia of healthy, under anaesthetic sheep. The SYNTHES Veterinary 3.5mm broad stainless-steel LCP (VP4041.10-3.5 mm LCP Plate 10-hole, 131 mm) with 3.5mm locking screws was used to stabilize the osteotomised tibia, maintaining 3mm fracture gap. The sheep were divided into two groups, and each group of sheep were stabilized by either an LCP with a rigid configuration (i.e. BPD = 0), or with a relatively flexible configuration (i.e. BPD = 2mm). Previous experimental study has illustrated that an increased BPD with a SYNTHES LCP increases inter-fragmentary movement in the fracture gap (Miramini et al., 2016b). For both animal groups, six locking screws placed on either side of plate holes 2, 4 and 5 from the plate centre on a plate working length of 35mm. The sheep were then recovered in sternal recumbency and observed continuously until standing. In addition, to ensure the accuracy of the perspective of therapeutic effect, sheep were allowed to walk freely in a restricted area.

Post-operative care and follow-up examinations

For the first 7 days post-surgery, clinical observations were performed three times daily and analgesia was maintained throughout this period. The sheep were then

anaesthetized every second week, beginning two weeks post-surgery. Since anaesthesia is known to induce hypotension that can cause blood flow temporarily (Reich et al., 2005), the sheep were examined daily and no excessive hypotension was detected. The sheep underwent imaging examination and as per the predetermined post-surgical sacrifice the sheep were euthanized without recovery from the anaesthetic directly after their terminal CT scan.

Computed tomography (CT)

At 1-, 4-, 6- and 8-weeks post operation, bone mineral content in callus of right tibia was quantitatively determined by Densiscan 1000 scanner (Scanco Medical, Bassersdorf, Switzerland) which provides bone mineral density measurements in Hounsfield unit (HU) (Rho et al., 1995) That is,

$$\rho = 114 + 0.916HU \tag{7.6}$$

$$HU = 1000\frac{CT - CT_w}{CT_w - CT_a} \tag{7.7}$$

where ρ is bone density in kg/m^{3}and CT, CT_w and CT_a are the raw CT values of bone, saline and air, respectively. The CT machine was calibrated with a water phantom during each start-up cycle to ensure accurate image acquisition and images were taken directly prior to sacrifice. The relative degree of calcification is determined from the experimentally measured mean bone density value in HU normalized by that of intact sheep tibia in normal condition.

7.5. **Numerical simulation**

The tibia fracture model used in the computational simulation was created using our previous works (Miramini et al., 2016a). The fixation of screws to the bone is considered to have perfect bond in the model. Initially, the callus is filled with granulation tissue, and the material properties of bone components and the LCP are shown in Table 7.3 and Table 7.4, respectively. Since cartilage and fibrous tissue in fracture callus are transient tissues which will ultimately be replaced by bone, their material properties were not explicitly included in Table 3. However, cartilage and fibrous tissue were indirectly modelled during the endochondral ossification process since experimentally determined

bone density incorporates bone formation occurring through the cartilage calcification. The fractured limb is unable to bear total limb load at early stage of healing and as healing progresses, a graded increase in fracture load has been noted previously. Therefore, it is safe to assume that the applied axial force increases linearly from around 20% to around 160% of its body weight in normal condition, which is consistent with other studies (Döbele et al., 2010, Grasa et al., 2010) (Refer to Figure. 2b). To compare inter-fragmentary movement and degree of calcification between different configurations, same axial force is applied in both fixation configurations even though stiffness of fixator influences the application of external load. The numerical results were obtained by solving the governing equations using the commercial finite element software COMSOL MULTIPHYSICS v5.2 (COMSOL). The cortical bone, marrow, fracture callus and locking plate fixation were meshed with 13603, 6535, 14335 and 15683 second-order tetrahedral elements respectively, and the relative tolerance of 10 Pa for pressure and 10-4 m for displacement were employed for all calculations. The total Lagrangian formulation with material coordinate system was used to account for large deformation at early stage of healing when the callus is very soft (Levenston et al., 1998).

Table 7.3 Material properties of bone and callus components used in this study.

	Porosity	Poisson's Ratio	Permeability (m^4 /Ns)	Young's modulus (MPa)
Granulation Tissue	0.8(Lacroix and Prendergast, 2002)	0.167(Lacroix and Prendergast, 2002)	10^{-14}(Lacroix and Prendergast, 2002)	0.05(McCartney et al., 2005)
Marrow	0.8(Lacroix and Prendergast, 2002)	0.167(Lacroix and Prendergast, 2002)	10^{-14}(Lacroix and Prendergast, 2002)	2(Lacroix and Prendergast, 2002)
Cortical bone	0.04(Lacroix and	0.3(Lacroix and	10^{-17}(Lacroix and	2 x 10^4(Lacroix and

	Prendergast, 2002)	Prendergast, 2002)	Prendergast, 2002)	Prendergast, 2002)

(Lacroix and Prendergast, 2002) Lacroix & Prendergast, 2002

(McCartney et al., 2005) McCartney et al., 2005

Table 7.4 Material properties of the LCP used in this study **(Stoffel et al., 2003b)**.

	Young's modulus (GPa)	Poisson's Ratio
Stainless steel	220	0.34
Titanium	115	0.34

7.6. **Parameter estimation for rate of bone formation**

Our current experimental study provided two sets of time-dependent radio densitometry measurements of bone density in near and far cortex zones under different fixation conditions (*i.e.* BPD = 0mm and BPD = 2mm). The half cortex adjacent to fixation is referred to as near cortex and the opposite half-cortex as far cortex. First, the experimentally measured mean bone density (HU) in near and far cortex for each week (Section 2.2) and estimated mechanical stimulation index (S) from callus mechanics model (Section 2.1.1) for the corresponding week was used in the optimization process to determine parameters of bone formation rate (B_p) in Equation 4. Then, a non-linear least squares and curve-fitting feature of MATLAB's optimization toolbox (MATLAB, 2015) was used and the values of parameters in Equations 4a and 4b were determined, i.e. new bone formation rates (λ_1 and λ_2), the activation coefficients (K_1 and K_2), and the steepness of the Hill function (n_1 and n_2), as well as the basal bone formation rates of new bone (B_{p10} and B_{p20}).

7.7. Statistics

The statistical analysis was performed on the experimental data using an analysis of variance (ANOVA) test and following variables were compared for significant differences (< 0.05 level of confidence): near vs far cortex, changes over time, BPD = 0mm vs BPD = 2mm.

7.8. Results

7.8.1. Experimental results: Bone density values at near cortex and far cortex

As shown in Figure. 7.3, bone contents in near cortex and far cortex zones were quantitatively measured using CT. The experimentally measured mean bone density in HUs at 1-, 4-, 6- and 8-weeks post-operation are shown in Table 7.1 and Table 7.2, and presented in the experimental part of Figure. 4. Furthermore, Figure. 5 shows histological evaluations of new bone development using Masson's trichome staining at 8-weeks after animal scarification and removal of the fixation.

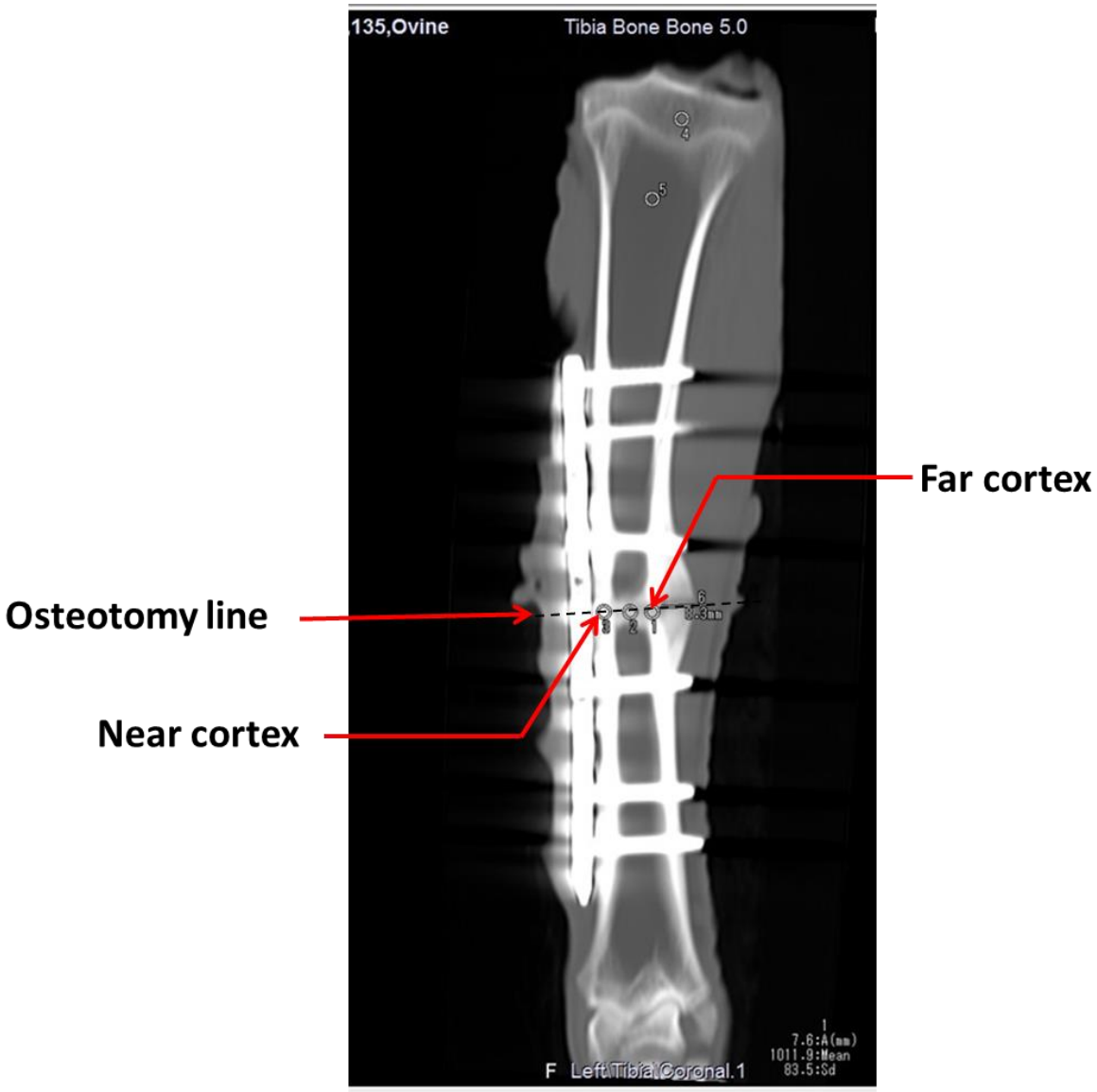

Figure. 7.3 CT imaging of fractured bone. Mean bone density was evaluated in the area located in near cortex and far cortex by using Hounsfield unit (HU)

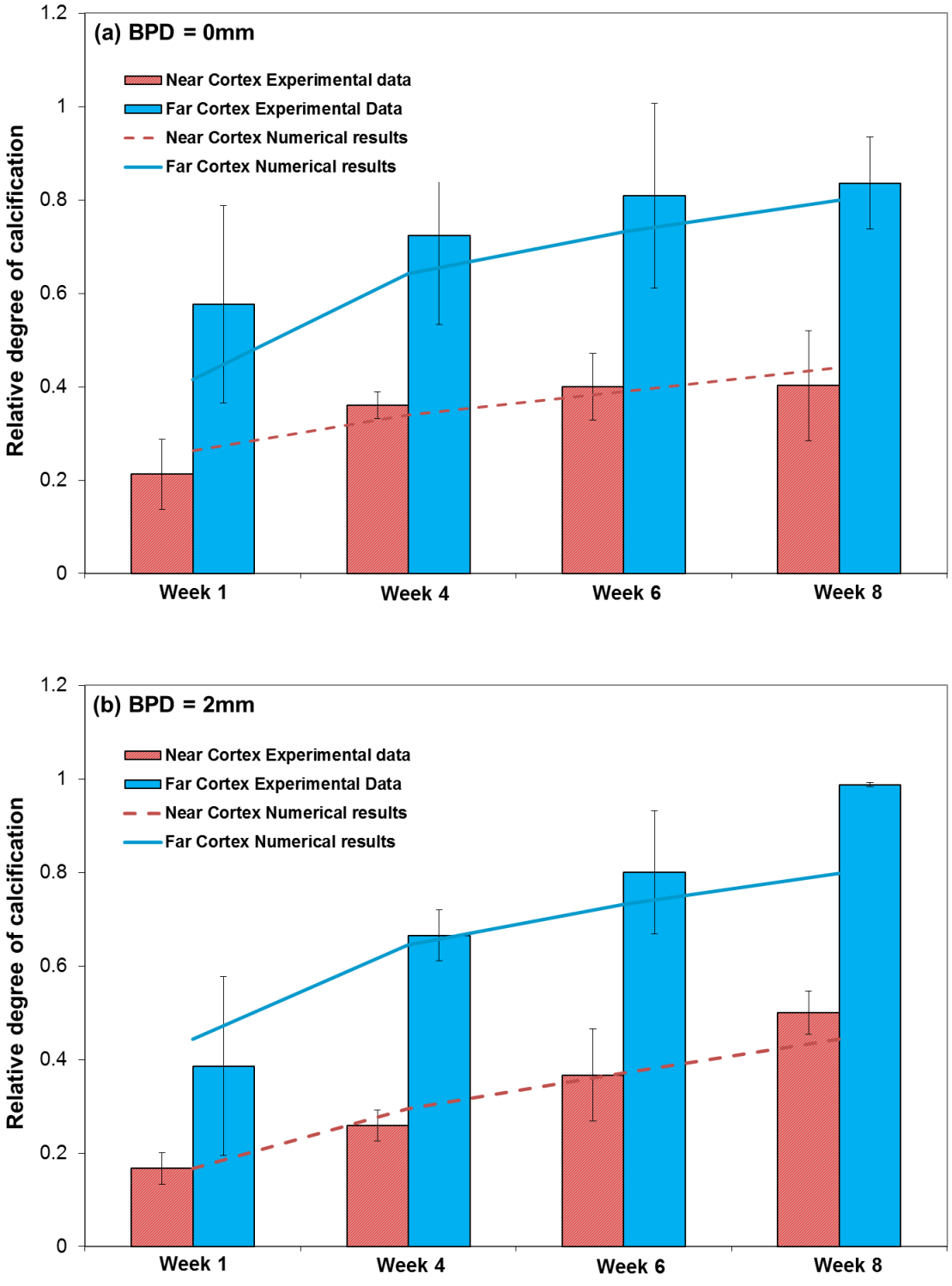

Figure. 7.4 Comparison of the numerical predictions to the animal experimental data. It can be seen that the experimental results are described remarkably well by numerical results using optimized model parameters.

Statistical analysis

A significant difference was present between the mean bone density at near and far cortex ($p<0.05$), which is consistent with the results of our previous study (Miramini et al., 2016b). Similarly, there was a significant difference between the change in mean bone densities over subsequent weeks. It showed that there is no significant difference in mean bone density between BPD = 0 mm and BPD = 2mm. It should be mentioned that the statistical analysis between change in degree of calcification over subsequent weeks, and between BPD = 0mm and BPD = 2mm could only be performed at week 1, 4 and 6 due to small sample size during later stage of healing, i.e. at week 8.

7.8.2. Calibration of model parameters

Using experimental data, the values of model parameters were calibrated using an optimization process and the calibrated model parameters are shown in

Figure. 7.6 shows the rate of relative degree of calcification induced by mechanical stimuli in intramembranous and endochondral ossification. The two sets of parameters were determined for intramembranous and endochondral ossification, i.e., (a) Intramembranous ossification: B_{p10}=8.96mg/ml/day, λ_1=69.26mg/ml/day, K_1=0.6, n_1 =4.92; (b) Endochondral ossification: B_{p20}=7.77mg/ml/day, λ_2=142.9mg/ml/day, K_2 =1.0, n_2=2. The parameters K_1=0.6 (intramembranous ossification) and K_2=1.0 (endochondral ossification) indicate the thresholds of *S* which could trigger significant development in intramembranous and endochondral ossification, respectively. For example, K_1 is the "activation coefficient" which describes that the significant change in the rate of relative degree of calcification is triggered when the mechanical stimuli index (S) reaches to certain value (i.e. S=0.6).

Table 7.5. The numerical model can reproduce experimentally observed change in bone content as shown in Figure. 7.4.

Figure. 7.6 shows the rate of relative degree of calcification induced by mechanical stimuli in intramembranous and endochondral ossification. The two sets of parameters were determined for intramembranous and endochondral ossification, i.e., (a) Intramembranous ossification: B_{p10}=8.96mg/ml/day, λ_1=69.26mg/ml/day, K_1=0.6, n_1 =4.92; (b) Endochondral ossification: B_{p20}=7.77mg/ml/day, λ_2=142.9mg/ml/day, K_2 =1.0, n_2=2. The parameters K_1=0.6 (intramembranous ossification) and K_2=1.0 (endochondral ossification) indicate the thresholds of *S* which could trigger significant development in intramembranous and endochondral ossification, respectively. For example, K_1 is the "activation coefficient" which describes that the significant change in the rate of relative degree of calcification is triggered when the mechanical stimuli index (S) reaches to certain value (i.e. S=0.6).

Table 7.5 Values of parameters obtained by calibrating the experimental data; suffix 1 and 2 in parameters refer to intramembranous and endochondral ossification respectively.

Parameter	Value	Remarks
B_{p10} (basal bone formation rate)	8.96 mg/ml/day	Intramembranous ossification
B_{p20} (basal bone formation rate)	7.77 mg/ml/day	Endochondral ossification
λ_1 (new bone formation rate)	69.26 mg/ml/day	Intramembranous ossification
λ_2 (new bone formation rate)	142.9 mg/ml/day	Endochondral ossification
K_1 (activation coefficient)	0.6	Intramembranous ossification
K_2 (activation coefficient)	1.0	Endochondral ossification
n_1 (steepness of Hill function)	4.92	Intramembranous ossification
n_2 (steepness of Hill function)	2.0	Endochondral ossification

7.8.3. Effects of fixation stiffness on healing

It can be seen from Figure. 7.4 that that the degree of calcification at far cortex is almost two-fold than that at near cortex under BPD = 0mm and BPD = 2mm. Therefore, bone formation was compared in near and far cortex for different fixation material using numerical simulation and the result is presented in Figure. 7. Under BPD = 0mm, a titanium could increase the degree of calcification at near cortex more than 100% in the first two weeks in comparison to a stainless-steel LCP, and this enhancement gradually

decreases with the increase of time (around 35 – 40 % at 8-weeks post operation). However, titanium LCP showed little influence in final bone formation at far cortex.

7.9. **Discussion**

The non-uniform inter-fragmentary movement resulting from the LCP configuration (i.e. the inter-fragmentary movement at near cortex is much less than that at far cortex) could lead to spatially dependent mechanical stimuli across fracture site (Miramini et al., 2015, Ghimire et al., 2019, Bottlang et al., 2010b, Miramini et al., 2014b, Zhang et al., 2013). Due to this spatially dependent mechanical stimuli across fracture site, the relative degree of calcification in near cortex is different to that of far cortex zone (refer to Figure. 7.4), which is consistent with the clinical study that measured asymmetrical callus formation in distal femur fractures stabilized with locking plates (Lujan et al., 2010).

In this study, a higher mean bone density for BPD = 0mm was observed at near and far cortex at week 1, 4 and 6 (refer to Table 1 and 2) compared to BPD = 2mm. However, this difference was not statistically significant, i.e. the change in bone plate distance from 0mm to 2mm had no significant difference on the mean bone density during fracture healing, even though lower bone plate distance has been regarded to provide better mechanical environment for healing(Ahmad et al., 2007, Stoffel et al., 2003a). Further, a higher mean bone density at week 8 was noted for BPD=2mm compared to BPD = 0 mm, which may indicate that a relatively flexible fixation improves healing process ultimately. However, statistical analysis couldn't be performed at week 8 due to small sample size and therefore, this result requires further investigation. Previous studies(Perren, 2002a, Henderson et al., 2008, Lujan et al., 2010, Claes, 2011, Ganadhiepan et al., 2019b, Ganadhiepan et al., 2019a, Smith et al., 2018) have also indicated that flexible fixation can lead to better healing outcomes.

Previous experimental studies (Augat et al., 1996, Einhorn, 1998, Marsell and Einhorn, 2011) show that endochondral ossification occurs between fractured bone and external to periosteal callus (under relatively large strain), while intramembranous ossification occurs simultaneously in callus away from fracture site directly adjacent to distal and periosteal end of cortex (under relatively low strain). Under LCP fixation, the micro-motion in far cortex zone of callus is relatively larger than that in near cortex zone

(Bottlang et al., 2010b, Lujan et al., 2010, Miramini et al., 2015). Based on the interfragmentary strain profile from near cortex to far cortex for a similar LCP configuration (BPD = 2mm & WL = 35.4mm) by Miramini et al. (2013)(Miramini et al., 2013b), endochondral ossification (2% to 10%) is most likely the dominated bone formation process in far cortex zone of callus, while intramembranous ossification (under 2%) is the dominated bone formation process in near cortex zone. This is also demonstrated in Figure. 4 and Figure. 5 which show a much higher time-dependent relative degree of calcification in far cortex zone than that in near cortex zone.

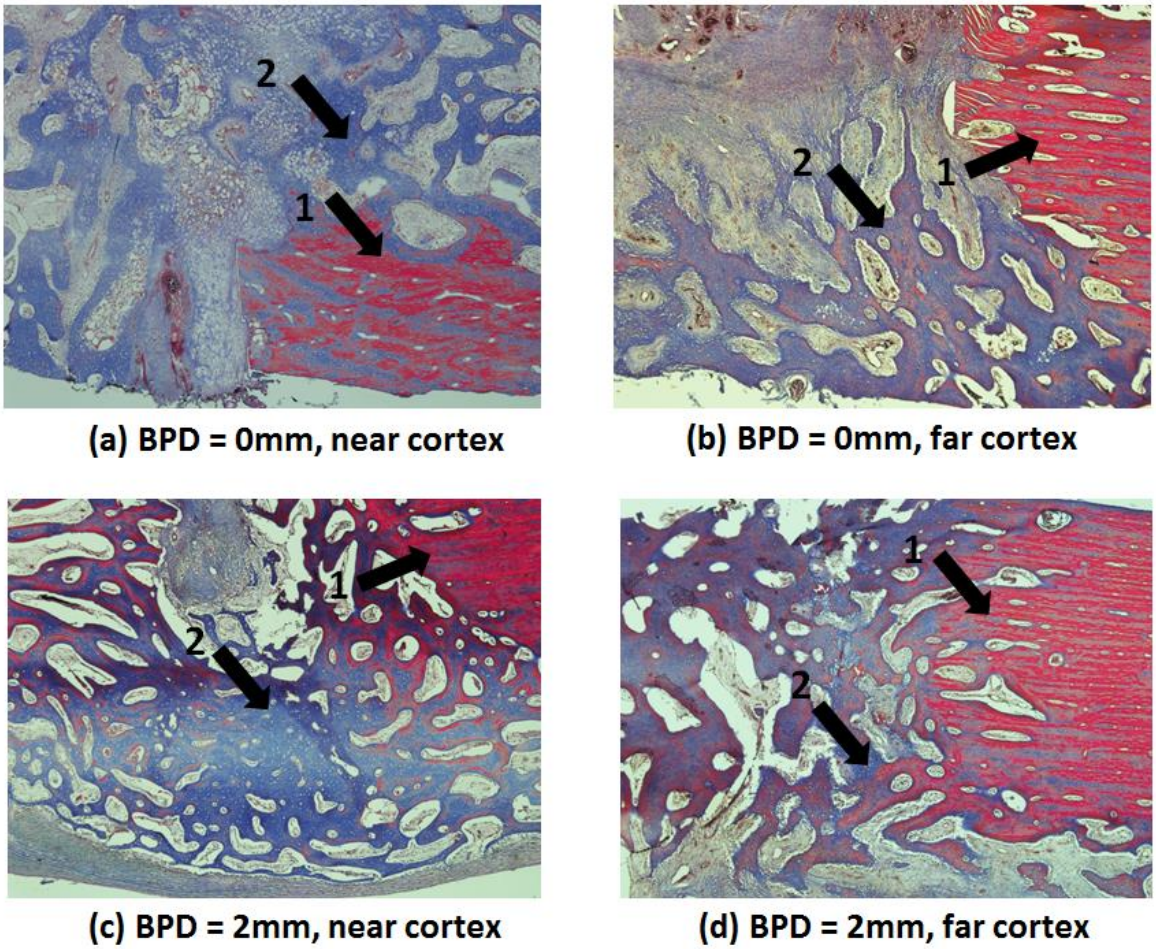

Figure. 7.5 Histological evaluations of new bone development using Masson's trichrome staining at 8-weeks after animal scarification and removal of the fixation. Arrow 1: new bone; Arrow 2: collagen.

Figure. **7.6** shows that the bone formation under intramembranous and endochondral ossification has different thresholds (0.6 and 1 respectively) within the widely accepted

magnitude range of mechanical stimuli index (S) by Prendergast et al. According to this theory, intramembranous ossification occurs within the stimuli index range of 0 to 1, and our study has further shown that there is a threshold (0.6) which triggers the significant bone formation under intramembranous ossification. Furthermore, a sensitivity analysis (Refer to **Figure. 7.7**) showed that the total bone formation rate is most sensitive to S, i.e. 10% increase in S resulted in 28% increase in the total bone formation rate *(B_p).* Therefore, this study demonstrates that, once a significant increase in bone formation is triggered, the bone formation rate in endochondral ossification (since it occurs between $1 < S < 3$) is generally higher than that in intramembranous ossification. This is consistent with other relevant experimental studies (A et al., 1980, Woo et al., 1983, McKibbin, 1978b), which suggested that endochondral ossification often results in faster bone union in comparison to intramembranous ossification.

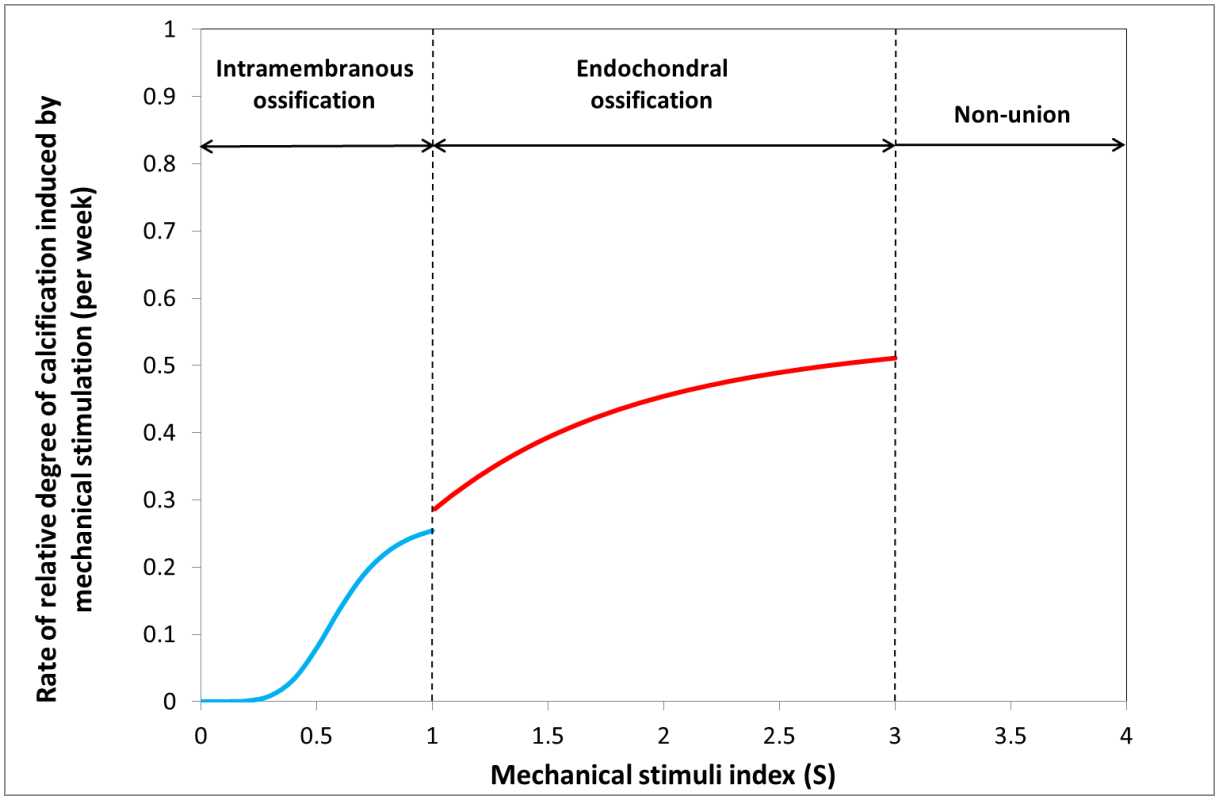

Figure. 7.6 Rate of relative degree of calcification (per week) induced by mechanical stimulation in intramembranous ossification ($0 < S \leq 1$) and endochondral ossification ($1 < S \leq 3$). It is assumed that the excessive S ($S > 3$) will lead to non-union.

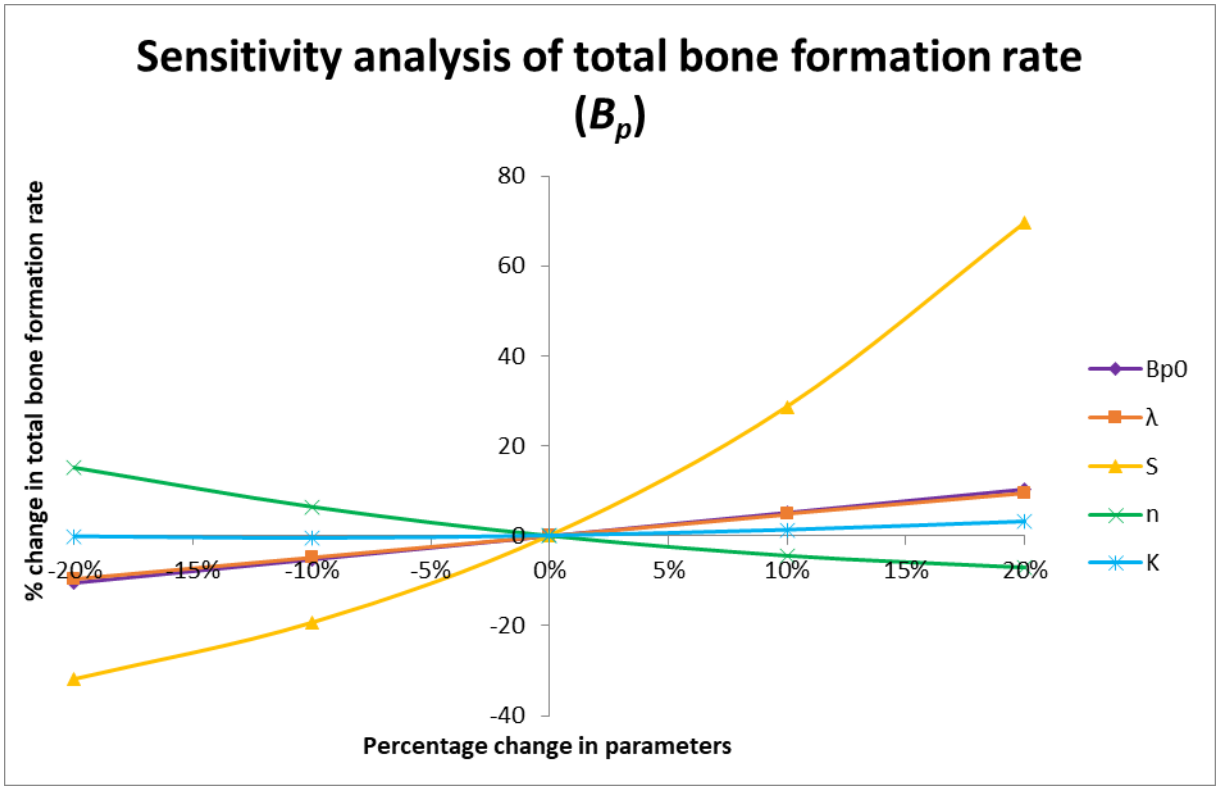

Figure. 7.7 Sensitivity analysis of the total bone formation rate (B_p) on depending parameters: basal bone formation rate (B_{p0}), new bone formation rate (λ), steepness of Hill's function (n), mechanical stimuli index (S) and activation coefficients (K).

Figure. 7.8 shows that the flexibility of the overall fixation system can be adjusted by not just changing the BPD and WL, but also by using less rigid materials (e.g. titanium) (Miramini et al., 2015). Further, with higher enhancement in near cortex compared to far cortex, titanium could lead to more uniform bone formation spatially. Thus, for the same fixation configuration, material properties of the fixation system could also significantly alter the healing outcomes.

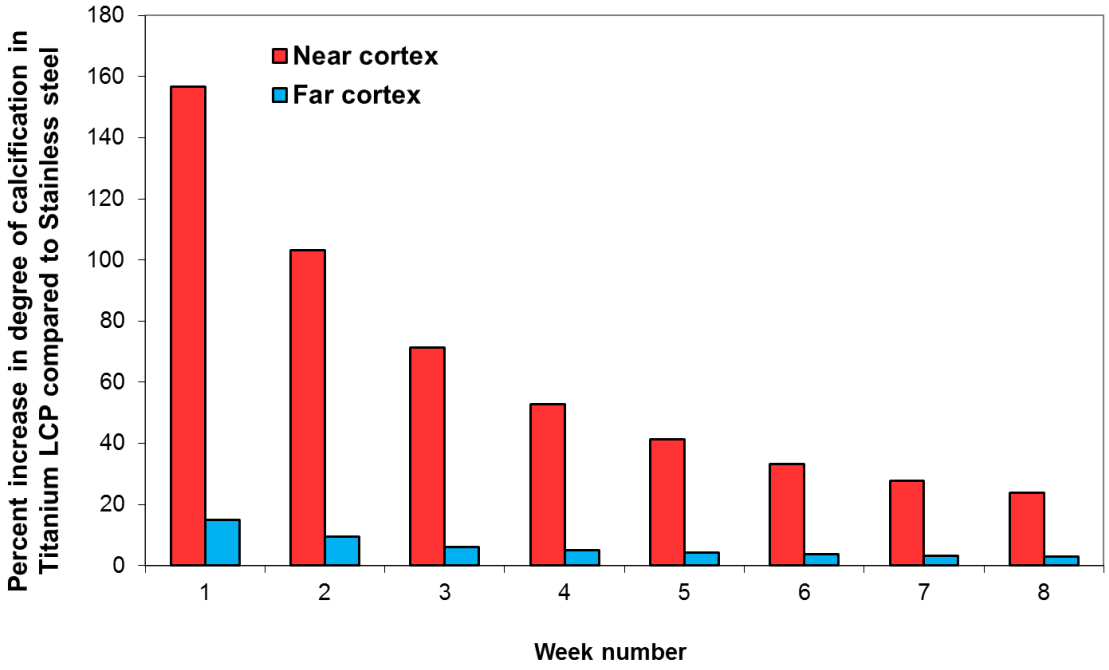

Figure. 7.8 Percent increase in degree of calcification as a function of time post-operation (weeks) by using titanium LCP relative to the control (i.e. Stainless steel LCP).

An ANOVA test was performed for comparing bone density values between fixation configuration of BPD = 0mm and BPD = 2mm, and a significant difference ($p<0.05$ ANOVA) couldn't be established in the relative degree of calcification between these two fixation configuration in week 1, 4 or 6. In the later stage of healing (i.e. by week 8), the statistical assessment to determine the accuracy of the data wasn't viable due to the small sample size. Therefore, more experimental data is required to perform statistical analysis on the mean density values for different fixation configuration.

Current pilot study shows that at week #1, sheep #125 and #037 show an opposite trend of bone density (higher in the near cortex). This observation contrasts with the previous clinical and experimental studies who have reported smaller callus formation and interfragmentary movement at near cortex compared to far cortex in locking compression constructs (Bottlang et al., 2010a, Richter et al., 2015, Bottlang et al., 2010b). The observed irregularities in the experimental data should be further verified by large-scale experimental works.

7.9.1. Limitation

Since sheep were anaesthetized every two weeks, this might have affected fracture healing of sheep over time in a cumulative manner. The influence of anaesthesia is an uncontrolled variable in this experiment, which should be investigated in further experimental works by having one control group of sheep scanned only once after 8 weeks and then compared to the group that underwent anaesthesia and scanning throughout the healing. Owing to the large variations in the data, more experimental data is required to further validate these results. The developed model needs to be further validated against large experimental datasets to fundamentally understand the synergistic effects of chemical and mechanical stimuli on fracture healing. In addition, it should be mentioned that the rate of bone formation during the healing process could be affected in diseased conditions (i.e. osteoporosis) (Zhang et al., 2017c, Zhang et al., 2012b) and therefore further investigation is required.

7.10. Conclusions

The purpose of this study was to investigate different bone formation rate under intramembranous and endochondral ossification processes during bone fracture healing by performing animal experiments in conjunction with theoretical modelling. The following were major findings:

- The mechanical stimuli mediated fracture healing showed that there are two unique sets of parameters of Hill Function which could describe the intramembranous and endochondral ossification.
- There are two different thresholds for intramembranous and endochondral ossification, which could trigger significant bone formation (i.e. Hill Function K_1 =0.6 and K_2=1 obtained through optimization process*)*.
- Once reaching thresholds that trigger significant bone formation, the rate of bone formation in endochondral ossification is generally higher than that in intramembranous ossification.
- There is a significant difference between relative degree of calcification under both fixation configuration (*i.e.* BPD = 0mm and BPD = 2mm) can be seen throughout the healing process (p<0.05 ANOVA).

- An increase of the LCP flexibility by adjusting WL or BPD or using titanium LCP could potentially promote uniform bone formation across the fracture gap, ultimately better healing outcomes.

Chapter 8.

Conclusions and recommendations

8.1. Conclusions

In this research, we developed an experimentally validated computational model to evaluate the influence of dynamic loading on the early stage of bone healing. At first, the research (chapter 3) investigated the cellular activities including proliferation, migration, differentiation and tissue formation mediated by both biochemical stimuli (i.e. growth factors) and mechanical stimuli (i.e. strain and fluid velocity) during early stage of bone fracture healing. The results demonstrated that dynamic loading enhances MSC transport in a spatially dependent manner. For example, in comparison to free diffusion, a dynamic loading could significantly increase MSC content in endosteal zone of callus but has little influence in periosteal and cortical zones. In addition, the dynamic loading is seen to significantly increase the uptake of chondrogenic growth factors in both cortical and periosteal zones of cartilage but has little effect on the osteogenic growth factor uptake in callus. Major findings are as follows.

- During the first week after the fracture, the major component of callus is fibrous tissue and other tissues such as bone are distributed spatially.
- A physiologically relevant dynamic loading could enhance the transport of MSCs further into the endosteal callus (around 20% during the first hour of loading) however it has limited influence in MSC uptake in periosteal and cortical callus.
- Dynamic loading enhances the uptake of chondrogenic growth factor uptake by around 100% and 60% in cortical and periosteal callus, respectively, but has little effect on the transport of osteogenic growth factor.
- An optimal dynamic loading regime (i.e. 10% strain @ 1Hz) produces the best healing outcomes through encouraging endochondral ossification by enhancing cartilage tissue formation and suppressing fibrous tissue content.

The finite element results presented in chapter 4 show that dynamic loading enhanced transport of bone cells and growth factors in the fracture callus is much dependent on the flexibility of LCP. In comparison to free diffusion, a relatively flexible LCP together with dynamic loading could significantly enhance solute transport in callus. For example, a flexible LCP achieved by increasing WL (Working Length) and BPD (Bone Plate Distance) (*e.g.* WL=100mm and BPD=2mm) together with a 5-hour 150N@1Hz dynamic loading could increase the uptake of chondrocytes by around 280% compared to free diffusion, osteoblasts by around 180%, osteogenic growth factors by around 120% and chondrogenic growth factors by around 220%. In addition, dynamic loading enhanced transport of cells and growth factors under LCP is spatially dependent with a relatively higher enhancement in far cortex zone than that in near cortex zone. Major findings are summarised below.

- In comparison to free diffusion, a relatively flexible LCP together with dynamic loading could significantly enhance transport of cells and growth factors in callus.
- Dynamic loading enhanced transport of cells and growth factors under LCP is spatially dependent with a relatively higher enhancement in the cortical zone away from plate than that in cortical zone adjacent to the plate fixation.
- Compared to free diffusion, dynamic loading enhances transport of cells (i.e. MSCs, fibroblasts, chondrocytes and osteoblasts) and growth factors (i.e. osteogenic and chondrogenic growth factor) under various LCP configurations and gaps sizes.

The research presented in chapter 5 aimed to quantify the relationship between different angles of obliquity and maximum permissible load that allow angiogenesis during early stages of healing under different LCP configurations. The results showed that fracture callus can undertake extremely low weightbearing (around 3 – 10% BW) during initial granulation stage. As granulation tissue is replaced by soft cartilaginous tissue during soft callus stage, the callus gets stiffer and can potentially withstand higher loading. The model predicted that, an allowable level of partial weightbearing of up to 60% BW could be applied to the fracture callus during early soft callus stage without exerting any damage to the regenerating blood vessels as healing progresses. Further, the model results indicated that oblique fractures are able to withstand much lower weightbearing compared to transverse fractures during early stages of healing.

A different IFM would lead to different cellular processes and healing outcomes, therefore an ex-vivo experimental study was conducted and presented in chapter 6 to compare the fracture IFM between normal and osteoporotic bones. The findings demonstrated that osteoporotic bones experienced more asymmetric healing across near and far cortex compared to healthy bones. For a loading of 200N, near cortex of normal bone underwent endochondral ossification while that of osteoporotic bone underwent intramembranous ossification. Therefore, our results suggest that a different fracture healing treatment (fixation configuration and loading protocol) may need to be adopted for optimum healing outcomes of osteoporotic bones fractures to achieve similar healing pathway to healthy bones. Major findings of this chapter are as follows.

- Osteoporotic bones resulted in more asymmetric healing across near and far cortex compared to healthy bones in both BPD 0mm and BPD 2mm fixation configuration
- Increasing flexibility of fixation resulted in less uniform IFM in both healthy and osteoporotic bones.
- Different rate of increase in IFM was observed in osteoporotic and normal bone, for similar increase in external loading.

Finally, the investigation of bone fracture healing under intramembranous and endochondral ossification, in chapter 7, indicated that intramembranous and

endochondral ossification can be described by Hill Function with two unique sets of function parameters in mechanical stimuli mediated fracture healing. Two different thresholds exist within the range of mechanical simulation index which could trigger significant intramembranous and endochondral ossification, with a relatively higher bone formation rate of endochondral ossification than that of intramembranous ossification. Furthermore, the increase of flexibility of the LCP system and the use of titanium LCP could potentially promote uniform bone formation across the fracture gap, ultimately better healing outcomes.

The major findings are:

- The mechanical stimuli mediated fracture healing showed that there are two unique sets of parameters of Hill Function which could describe the intramembranous and endochondral ossification.
- There are two different thresholds for intramembranous and endochondral ossification, which could trigger significant bone formation (i.e. Hill Function K_1 =0.6 and K_2=1 obtained through optimization process*)*. Once reaching thresholds that trigger significant bone formation, the rate of bone formation in endochondral ossification is generally higher than that in intramembranous ossification.
- There is a significant difference between relative degree of calcification under both fixation configuration (*i.e.* BPD = 0mm and BPD = 2mm) can be seen throughout the healing process (p<0.05 ANOVA).
- An increase of the LCP flexibility by adjusting WL or BPD or using titanium LCP could potentially promote uniform bone formation across the fracture gap, ultimately better healing outcomes.

In conclusion, this research has further extended the current understanding of impact of biomechanical micro-environment on cell differentiation and tissue development during fracture healing processes. The outcomes from present research could potentially assist orthopaedic surgeons to determine LCP configurations and optimal loading regimes with consideration of patient specific parameters including fracture geometry and osteoporosis condition.

8.2. Recommendation on future works

Following recommendations can be made for further works.

- This research is mainly focused on the early stage of bone healing when both biochemical and mechanical factors are of critical importance for the entire healing process. As healing progresses, mechanical properties of fracture callus changes with the development of angiogenesis. Therefore, further research should incorporate time dependent angiogenesis which plays crucial role in bone fracture healing.
- The developed model needs to be further validated against large experimental datasets to fundamentally understand the synergistic effects of chemical and mechanical stimuli on fracture healing. In particular, the experiment on osteoporotic bones had very small sample size. Therefore, experiment on large scale is necessary to validate the results.
- This research has investigated bone healing stabilized by locking compression plate (LCP) fixation configurations. Research on fractures stabilized by other fixations could lead to different healing outcomes, therefore further research could compare the healing outcomes on fracture stabilized under different fixations.
- The comparison study of the fracture IFM between normal and osteoporotic bones has been conducted only by an ex-vivo experiment. Further works could be done to conduct theoretical modelling and simulation.

Only axial loading has been considered in this research. Throughout the life-span, bone is subjected to various types of physiologically relevant loads, such as axial compression, bending, shear and torsion from muscle, ligament or joint movement. Therefore, further research could incorporate different loading regimes to investigate the effects of dynamic loading on bone fracture healing.

Bibliography

A, A. S., MULLIS, D. L., LATTA, L. L., TARR, R. R. & ALVAREZ, R. 1980. A quantitative comparative analysis of fracture healing under the influence of compression plating vs. closed weight-bearing treatment. Clinical Orthopaedics & Related Research, 149, 232-239.

AGUILA, AGUILA, A. Z., MANOS, J. M., ORLANSKY, A. S., TODHUNTER, R. J., TROTTER, E. J. & VAN DER MEULEN, M. C. H. 2005. In vitro biomechanical comparison of limited contact dynamic compression plate and locking compression plate. Veterinary and comparative orthopaedics and traumatology, 18, 220-226.

AHMAD, M., NANDA, R., BAJWA, A., CANDAL-COUTO, J., GREEN, S. & HUI, A. 2007. Biomechanical testing of the locking compression plate: when does the distance between bone and implant significantly reduce construct stability? Injury, 38, 358-364.

ALIERTA, J., PÉREZ, M., SERAL, B. & GARCÍA-AZNAR, J. 2016. Biomechanical assessment and clinical analysis of different intramedullary nailing systems for oblique fractures. Computer methods in BiomeChaniCs and BiomediCal engineering, 19, 1266-1277.

ALON, U. 2006. An introduction to systems biology. Chapman & Hall/CRC, Taylor & Francis Group.

AMBARD, D. & SWIDER, P. 2006. A predictive mechano-biological model of the bone-implant healing. European Journal of Mechanics-A/Solids, 25, 927-937.

AMOR, N., GERIS, L., VANDER SLOTEN, J. & VAN OOSTERWYCK, H. 2009. Modelling the early phases of bone regeneration around an endosseous oral implant. Computer methods in biomechanics and biomedical engineering, 12, 459-468.

AMOR, N., GERIS, L., VANDER SLOTEN, J. & VAN OOSTERWYCK, H. 2011. Computational modelling of biomaterial surface interactions with blood platelets and osteoblastic cells for the prediction of contact osteogenesis. Acta biomaterialia, 7, 779-790.

ANAKWE, R., AITKEN, S. & KHAN, L. 2008. Osteoporotic periprosthetic fractures of the femur in elderly patients: outcome after fixation with the LISS plate. Injury, 39, 1191-1197.

ANDREYKIV, A., VAN KEULEN, F. & PRENDERGAST, P. J. 2008. Simulation of fracture healing incorporating mechanoregulation of tissue differentiation and dispersal/proliferation of cells. Biomech Model Mechanobiol, 7, 443-61.

ARMSTRONG, C. & MOW, V. 1982. Variations in the intrinsic mechanical properties of human articular cartilage with age, degeneration, and water content. The Journal of bone and joint surgery. American volume, 64, 88-94.

ARO, H. T., KELLY, P. J., LEWALLEN, D. G. & CHAO, E. Y. 1990. The effects of physiologic dynamic compression on bone healing under external fixation. Clinical Orthopaedics and Related Research®, 260-273.

ARO, H. T., WAHNER, H. T. & CHAO, E. Y. 1991. Healing patterns of transverse and oblique osteotomies in the canine tibia under external fixation. Journal of orthopaedic trauma, 5, 351-364.

AUGAT, P., BURGER, J., SCHORLEMMER, S., HENKE, T., PERAUS, M. & CLAES, L. 2003. Shear movement at the fracture site delays healing in a diaphyseal fracture model. Journal of orthopaedic research, 21, 1011-1017.

AUGAT, P., MARGEVICIUS, K., SIMON, J., WOLF, S., SUGER, G. & CLAES, L. 1998. Local tissue properties in bone healing: Influence of size and stability of the osteotomy gap. Journal of Orthopaedic Research, 16, 475-481.

AUGAT, P., MERK, J., GENANT, H. K. & CLAES, L. 1997. Quantitative Assessment of Experimental Fracture Repair by Peripheral Computed Tomography. Calcified Tissue International, 60, 194-199.

AUGAT, P., MERK, J., IGNATIUS, A., MARGEVICIUS, K., BAUER, G., ROSENBAUM, D. & CLAES, L. 1996. Early, full weightbearing with flexible fixation delays fracture healing. Clinical orthopaedics and related research, 328, 194-202.

AUGAT, P., MERK, J., WOLF, S. & CLAES, L. 2001. Mechanical stimulation by external application of cyclic tensile strains does not effectively enhance bone healing. Journal of orthopaedic trauma, 15, 54-60.

AUGAT, P., PENZKOFER, R., NOLTE, A., MAIER, M., PANZER, S., V OLDENBURG, G., PUESCHL, K., SIMON, U. & BÜHREN, V. 2008. Interfragmentary movement in diaphyseal tibia fractures fixed with locked intramedullary nails. Journal of orthopaedic trauma, 22, 30-36.

AUGAT, P., SIMON, U., LIEDERT, A. & CLAES, L. 2005. Mechanics and mechano-biology of fracture healing in normal and osteoporotic bone. Osteoporos Int, 16 Suppl 2, S36-43.

BAI, Z., GAO, S., HU, Z. & LIANG, A. 2018. Comparison of Clinical Efficacy of Lateral and Lateral and Medial Double-plating Fixation of Distal Femoral Fractures. Scientific reports, 8, 4863.

BAILON-PLAZA, A. & VAN DER MEULEN, M. C. 2001. A mathematical framework to study the effects of growth factor influences on fracture healing. J Theor Biol, 212, 191-209.

BAILÓN-PLAZA, A. & VAN DER MEULEN, M. C. H. 2003. Beneficial effects of moderate, early loading and adverse effects of delayed or excessive loading on bone healing. Journal of Biomechanics, 36, 1069-1077.

BAKSH, D., SONG, L. & TUAN, R. S. 2004. Adult mesenchymal stem cells: characterization, differentiation, and application in cell and gene therapy. Journal of Cellular and Molecular Medicine, 8, 301-316.

BARKER, M. K. & SEEDHOM, B. B. 2001. The relationship of the compressive modulus of articular cartilage with its deformation response to cyclic loading: does cartilage optimize its modulus so as to minimize the strains arising in it due to the prevalent loading regime? Rheumatology (Oxford), 40, 274-84.

BARNES, G. L., KOSTENUIK, P. J., GERSTENFELD, L. C. & EINHORN, T. A. 1999. Growth Factor Regulation of Fracture Repair. Journal of bone and mineral research, 14, 1805-1815.

BARRIOS, C., BROSTRÖM, L., STARK, A. & WALHEIM, G. 1993. Healing complications after internal fixation of trochanteric hip fractures: the prognostic value of osteoporosis. Journal of orthopaedic trauma, 7, 438-442.

BISHOP, N., VAN RHIJN, M., TAMI, I., CORVELEIJN, R., SCHNEIDER, E. & ITO, K. 2006. Shear does not necessarily inhibit bone healing. Clinical orthopaedics and related research, 443, 307-314.

BOARDMAN, K. & SWARTZ, M. 2003. Interstitial flow as a guide for lymphangiogenesis. Circulation research, 92, 801-808.

BONASSAR, L. J., GRODZINSKY, A. J., FRANK, E. H., DAVILA, S. G., BHAKTAV, N. R. & TRIPPEL, S. B. 2001. The effect of dynamic compression on the response of articular cartilage to insulin-like growth factor-I. Journal of Orthopaedic Research, 19, 11-17.

BOTTLANG, M., DOORNINK, J., LUJAN, T. J., FITZPATRICK, D. C., MARSH, J. L., AUGAT, P., VON RECHENBERG, B., LESSER, M. & MADEY, S. M. 2010a. Effects of Construct Stiffness on Healing of Fractures Stabilized with Locking Plates. JBJS, 92, 12-22.

BOTTLANG, M., LESSER, M., KOERBER, J., DOORNINK, J., RECHENBERG, B. V., AUGAT, P., FITZPATRICK, D. C., MADEY, S. M. & MARSH, J. L. 2010b. Far cortical locking can improve healing of fractures stabilized with locking plates The Journal of Bone & Joint Surgery, 92, 1652-1660.

BOTTLANG, M., TSAI, S., BLIVEN, E. K., VON RECHENBERG, B., KINDT, P., AUGAT, P., HENSCHEL, J., FITZPATRICK, D. C. & MADEY, S. M. 2017. Dynamic stabilization of simple fractures with active plates delivers stronger healing than conventional compression plating. Journal of orthopaedic trauma, 31, 71.

BRANDI, M. L. & PISCITELLI, P. 2013. Epidemiology of Osteoporosis and Fragility Fractures. Osteoporosis and Bone Densitometry Measurements. Springer.

BRIGHTON, C. T. & HUNT, R. M. 1991. Early histological and ultrastructural changes in medullary fracture callus. JBJS, 73, 832-847.

BRINKER, M. R. & BAILEY, D. E. 1997. Fracture healing in tibia fractures with an associated vascular injury. Journal of Trauma and Acute Care Surgery, 42, 11-19.

BURKE, D. P. & KELLY, D. J. 2012. Substrate stiffness and oxygen as regulators of stem cell differentiation during skeletal tissue regeneration: a mechanobiological model. PloS one, 7, e40737.

CALORI, G., MAZZA, E., COLOMBO, M., RIPAMONTI, C. & TAGLIABUE, L. 2011. Treatment of long bone non-unions with polytherapy: indications and clinical results. Injury, 42, 587-590.

CAPLAN, A. I. & DENNIS, J. E. 2006. Mesenchymal stem cells as trophic mediators. Journal of cellular biochemistry, 98, 1076-1084.

CARLIER, A., GERIS, L., VAN GASTEL, N., CARMELIET, G. & VAN OOSTERWYCK, H. 2015. Oxygen as a critical determinant of bone fracture healing—a multiscale model. Journal of theoretical biology, 365, 247-264.

CARTER, D., BLENMAN, P. & BEAUPRE, G. 1988. Correlations between mechanical stress history and tissue differentiation in initial fracture healing. Journal of Orthopaedic Research, 6, 736-748.

CARTER, D. R., BEAUPRE, G. S., GIORI, N. J. & HELMS, J. A. 1998a. Mechanobiology of skeletal regeneration. Clin Orthop Relat Res, S41-55.

CARTER, D. R., BEAUPRÉ, G. S., GIORI, N. J. & HELMS, J. A. 1998b. Mechanobiology of skeletal regeneration. Clinical orthopaedics and related research, 355, S41-S55.

CHAO, E. Y., INOUE, N., ELIAS, J. J. & ARO, H. 1998. Enhancement of fracture healing by mechanical and surgical intervention. Clinical orthopaedics and related research, 355, S163-S178.

CHECA, S. & PRENDERGAST, P. J. 2009. A mechanobiological model for tissue differentiation that includes angiogenesis: a lattice-based modeling approach. Annals of biomedical engineering, 37, 129-145.

CHECA, S., PRENDERGAST, P. J. & DUDA, G. N. 2011. Inter-species investigation of the mechano-regulation of bone healing: Comparison of secondary bone healing in sheep and rat. Journal of Biomechanics, 44, 1237-1245.

CHENG, H., JIANG, W., PHILLIPS, F. M., HAYDON, R. C., PENG, Y., ZHOU, L., LUU, H. H., AN, N., BREYER, B., VANICHAKARN, P., SZATKOWSKI, J. P., PARK, J. Y. & HE, T. C. 2004. Osteogenic activity of the fourteen types of human bone morphogenetic proteins (BMPs). Urologic Oncology: Seminars and Original Investigations, 22, 79-80.

CHIDGEY, L., CHAKKALAKAL, D., BLOTCKY, A. & CONNOLLY, J. 1986. Vascular reorganization and return of rigidity in fracture healing. Journal of orthopaedic research, 4, 173-179.

CHO, T. J., GERSTENFELD, L. C. & EINHORN, T. A. 2002. Differential temporal expression of members of the transforming growth factor β superfamily during murine fracture healing. Journal of Bone and Mineral Research, 17, 513-520.

CLAES, CLAES, L. E., WILKE, H. J., AUGAT, P., RÜBENACKER, S. & MARGEVICIUS, K. J. 1995a. Effect of dynamization on gap healing of diaphyseal fractures under external fixation. Clinical biomechanics (Bristol), 10, 227-234.

CLAES, L. 2011. Biomechanical principles and mechanobiologic aspects of flexible and locked plating. Journal of orthopaedic trauma, 25, S4-S7.

CLAES, L., AUGAT, P., SUGER, G. & WILKE, H. J. 1997. Influence of size and stability of the osteotomy gap on the success of fracture healing. Journal of orthopaedic research, 15, 577-584.

CLAES, L., ECKERT-HÜBNER, K. & AUGAT, P. 2002. The effect of mechanical stability on local vascularization and tissue differentiation in callus healing. Journal of Orthopaedic Research, 20, 1099-1105.

CLAES, L., ECKERT-HÜBNER, K. & AUGAT, P. 2003. The fracture gap size influences the local vascularization and tissue differentiation in callus healing. Langenbeck's Archives of Surgery, 388, 316-322.

CLAES, L., RECKNAGEL, S. & IGNATIUS, A. 2012. Fracture healing under healthy and inflammatory conditions. Nature Reviews Rheumatology, 8, 133.

CLAES, L. E. & HEIGELE, C. A. 1999. Magnitudes of local stress and strain along bony surfaces predict the course and type of fracture healing. Journal of Biomechanics, 32, 255-266.

CLAES, L. E., HEIGELE, C. A., NEIDLINGER-WILKE, C., KASPAR, D., SEIDL, W., MARGEVICIUS, K. J. & AUGAT, P. 1998. Effects of mechanical factors on the fracture healing process. Clin Orthop Relat Res, 355, S132-47.

CLAES, L. E., WILKE, H. J., AUGAT, P., RUBENACKER, S. & MARGEVICIUS, K. J. 1995b. Effect of dynamization on gap healing of diaphyseal fractures under external fixation. Clin Biomech (Bristol, Avon), 10, 227-234.

COMISKEY, D., MACDONALD, B., MCCARTNEY, W., SYNNOTT, K. & O'BYRNE, J. 2013. Predicting the external formation of callus tissues in oblique bone fractures: idealised and clinical case studies. Biomechanics and modeling in mechanobiology, 12, 1277-1282.

COMSOL Multiphysics® v. 5.2. COMSOL AB, Stockholm, Sweden.

COWIN, S. C. 1999. Bone poroelasticity. Journal of biomechanics, 32, 217-238.

CUSSLER, E. C., GOING, S. B., HOUTKOOPER, L. B., STANFORD, V. A., BLEW, R. M., FLINT-WAGNER, H. G., METCALFE, L. L., CHOI, J.-E. & LOHMAN, T. G. 2005. Exercise frequency and calcium intake predict 4-year bone changes in postmenopausal women. Osteoporosis International, 16, 2129-2141.

DECARIS, M. L., BINDER, B. Y., SOICHER, M. A., BHAT, A. & LEACH, J. K. 2012. Cell-derived matrix coatings for polymeric scaffolds. Tissue engineering Part A, 18, 2148-2157.

DEVESCOVI, V., LEONARDI, E., CIAPETTI, G. & CENNI, E. 2008. Growth factors in bone repair. La Chirurgia degli organi di movimento, 92, 161-168.

DIMITRIOU, R., TSIRIDIS, E. & GIANNOUDIS, P. V. 2005. Current concepts of molecular aspects of bone healing. Injury, 36, 1392-1404.

DÖBELE, S., HORN, C., EICHHORN, S., BUCHHOLTZ, A., LENICH, A., BURGKART, R., NÜSSLER, A. K., LUCKE, M., ANDERMATT, D., KOCH, R. & STÖCKLE, U. 2010. The dynamic locking screw (DLS) can increase interfragmentary motion on the near cortex of locked plating constructs by reducing the axial stiffness. Langenbeck's Archives of Surgery, 395, 421-428.

DOBLARÉ, M., GARCıA, J. & GÓMEZ, M. 2004. Modelling bone tissue fracture and healing: a review. Engineering Fracture Mechanics, 71, 1809-1840.

DUDA, G. N., ECKERT-HÜBNER, K., SOKIRANSKI, R., KREUTNER, A., MILLER, R. & CLAES, L. 1997a. Analysis of inter-fragmentary movement as a function of musculoskeletal loading conditions in sheep. Journal of biomechanics, 31, 201-210.

DUDA, G. N., MANDRUZZATO, F., HELLER, M., KASSI, J.-P., KHODADADYAN, C. & HAAS, N. P. 2002. Mechanical conditions in the internal stabilization of proximal tibial defects. Clinical Biomechanics, 17, 64-72.

DUDA, G. N., SCHNEIDER, E. & CHAO, E. Y. 1997b. Internal forces and moments in the femur during walking. Journal of biomechanics, 30, 933-941.

ECONOMICS, A. 2006. Breaking point: the economic cost of not adhering to bisphosphonate treatment for osteoporosis. Access Economics, Canberra.

EGERMANN, M., GOLDHAHN, J. & SCHNEIDER, E. 2005. Animal models for fracture treatment in osteoporosis. Osteoporosis International, 16, S129-S138.

EINHORN, T. A. 1998. The cell and molecular biology of fracture healing. Clinical orthopaedics and related research, 355, S7-S21.

EPARI, D. R., DUDA, G. N. & THOMPSON, M. S. 2010. Mechanobiology of bone healing and regeneration: in vivo models. Proceedings of the Institution of Mechanical Engineers, Part H: Journal of Engineering in Medicine, 224, 1543-1553.

EPARI, D. R., SCHELL, H., DUDA, G. N. & KASSI, J.-P. 2007. Timely fracture-healing requires optimization of axial fixation stability. JBJS, 89, 1575-1585.

EPARI, D. R., TAYLOR, W. R., HELLER, M. O. & DUDA, G. N. 2006. Mechanical conditions in the initial phase of bone healing. Clinical Biomechanics, 21, 646-655.

EVANS, R. & QUINN, T. 2006. Solute convection in dynamically compressed cartilage. Journal of Biomechanics, 39, 1048-1055.

FAYAZ, H. C., GIANNOUDIS, P. V., VRAHAS, M. S., SMITH, R. M., MORAN, C., PAPE, H. C., KRETTEK, C. & JUPITER, J. B. 2011. The role of stem cells in fracture healing and nonunion. International orthopaedics, 35, 1587.

FILIPOWICZ, D., LANZ, O., MCLAUGHLIN, R., ELDER, S. & WERRE, S. 2009. A biomechanical comparison of 3.5 locking compression plate fixation to 3.5 limited contact dynamic compression plate fixation in a canine cadaveric distal humeral metaphyseal gap model. Veterinary and Comparative Orthopaedics and Traumatology, 22, 1-8.

FLEGG, J. A., MENON, S. N., MAINI, P. K. & MCELWAIN, D. 2015. On the mathematical modeling of wound healing angiogenesis in skin as a reaction-transport process. Frontiers in physiology, 6, 262.

FLORIN, M., ARZDORF, M., LINKE, B. & AUER, J. A. 2005. Assessment of stiffness and strength of 4 different implants available for equine fracture treatment: a study on a 20° oblique long-bone fracture model using a bone substitute. Veterinary surgery, 34, 231-238.

FOUAD, H. 2010. Effects of the bone-plate material and the presence of a gap between the fractured bone and plate on the predicted stresses at the fractured bone. Medical Engineering & Physics, 32, 783-789.

GANADHIEPAN, G., MIRAMINI, S., MENDIS, P., PATEL, M. & ZHANG, L. 2019a. Bone fracture healing under Ilizarov fixator: influence of fixator configuration, fracture geometry and loading. International Journal for Numerical Methods in Biomedical Engineering (in press).

GANADHIEPAN, G., ZHANG, L., MIRAMINI, S., MENDIS, P., PATEL, M., EBELING, P. & WANG, Y. 2019b. The effects of dynamic loading on bone fracture healing under Ilizarov Circular Fixators. Journal of Biomechanical Engineering (ASME), 141, 051005-1-12.

GANADHIEPAN, G., ZHANG, L., MIRAMINI, S., MENDIS, P., PATEL, M., EBELING, P. & WANG, Y. 2019c. The Effects of Dynamic Loading on Bone Fracture Healing Under Ilizarov Circular Fixators. Journal of biomechanical engineering, 141, 051005.

GARCIA-AZNAR, J. M., KUIPER, J. H., GOMEZ-BENITO, M. J., DOBLARE, M. & RICHARDSON, J. B. 2007. Computational simulation of fracture healing: influence of interfragmentary movement on the callus growth. J Biomech, 40, 1467-76.

GARDINER, B., SMITH, D., PIVONKA, P., GRODZINSKY, A., FRANK, E. & ZHANG, L. 2007. Solute transport in cartilage undergoing cyclic deformation. Computer methods in biomechanics and biomedical engineering, 10, 265-278.

GARDNER, M. J., VAN DER MEULEN, M. C., DEMETRAKOPOULOS, D., WRIGHT, T. M., MYERS, E. R. & BOSTROM, M. P. 2006. In vivo cyclic axial compression affects bone healing in the mouse tibia. Journal of Orthopaedic Research, 24, 1679-1686.

GARDNER, T. & MISHRA, S. 2003. The biomechanical environment of a bone fracture and its influence upon the morphology of healing. Medical engineering & physics, 25, 455-464.

GARDNERA, T. N., STOLL, T., MARKS, L., MISHRA, S. & KNOTHE TATE, M. 2000. The influence of mechanical stimulus on the pattern of tissue differentiation in a long bone fracture — an FEM study. Journal of Biomechanics, 33, 415-425.

GARNAVOS, GARNAVOS, C., KANAKARIS, N., LASANIANOS, N., TZORTZI, P. & WEST, R. M. 2012. New Classification System for Long-bone Fractures Supplementing the AO/OTA Classification. Orthopedics, 35, e709-e719.

GAUTIER, E. & SOMMER, C. 2003. Guidelines for the clinical application of the LCP. Injury, 34, B63-76.

GERIS, L., ANDREYKIV, A., VAN OOSTERWYCK, H., VANDER SLOTEN, J., VAN KEULEN, F., DUYCK, J. & NAERT, I. 2004. Numerical simulation of tissue differentiation around loaded titanium implants in a bone chamber. Journal of biomechanics, 37, 763-769.

GERIS, L., GERISCH, A., MAES, C., CARMELIET, G., WEINER, R., VANDER SLOTEN, J. & VAN OOSTERWYCK, H. 2006. Mathematical modeling of fracture healing in mice: comparison between experimental data and numerical simulation results. Medical and Biological Engineering and Computing, 44, 280-289.

GERIS, L., GERISCH, A., SLOTEN, J. V., WEINER, R. & OOSTERWYCK, H. V. 2008. Angiogenesis in bone fracture healing: a bioregulatory model. Journal of Theoretical Biology, 251, 137-58.

GERIS, L., VAN OOSTERWYCK, H., VANDER SLOTEN, J., DUYCK, J. & NAERT, I. 2003. Assessment of mechanobiological models for the numerical simulation of tissue differentiation around immediately loaded implants. Computer methods in biomechanics and biomedical engineering, 6, 277-288.

GERIS, L., VANDER SLOTEN, J. & VAN OOSTERWYCK, H. 2010. Connecting biology and mechanics in fracture healing: an integrated mathematical modeling framework for the study of nonunions. Biomechanics and modeling in mechanobiology, 9, 713-724.

GERSTENFELD, L. C., CULLINANE, D. M., BARNES, G. L., GRAVES, D. T. & EINHORN, T. A. 2003. Fracture healing as a post-natal developmental process: molecular, spatial, and temporal aspects of its regulation. J Cell Biochem, 88, 873-84.

GHIMIRE, S., MIRAMINI, S., RICHARDSON, M., MENDIS, P. & ZHANG, L. 2018. Role of Dynamic Loading on Early Stage of Bone Fracture Healing. Annals of biomedical engineering, 1-17.

GHIMIRE, S., MIRAMINI, S., RICHARDSON, M., MENDISA, P. & ZHANG, L. 2019. Effects of dynamic loading on fracture healing under different locking compression plate configurations: A finite element study. Journal of the Mechanical Behavior of Biomedical Materials, 94, 74-85.

GOEL, A., SANGWAN, S., SIWACH, R. & ALI, A. M. 2005. Percutaneous bone marrow grafting for the treatment of tibial non-union. Injury, 36, 203-206.

GÓMEZ-BENITO, M. J., GONZÁLEZ-TORRES, L. A., REINA-ROMO, E., GRASA, J., SERAL, B. & GARCÍA-AZNAR, J. M. 2011. Influence of high-frequency cyclical stimulation on the bone fracture-healing process: mathematical and experimental models. Phil. Trans. R. Soc. A, 369, 4278-4294.

GOMEZ BENITO, M. J., GÓMEZ BENITO, M. J., GARCÍA AZNAR, J. M., KUIPER, J. H. & DOBLARÉ, M. 2005. Influence of fracture gap size on the pattern of long bone healing: a computational study. Journal of theoretical biology, 235, 105-119.

GONZÁLEZ-TORRES, L., GÓMEZ-BENITO, M., DOBLARÉ, M. & GARCÍA-AZNAR, J. 2010a. Influence of the frequency of the external mechanical stimulus on bone healing: a computational study. Medical engineering & physics, 32, 363-371.

GONZÁLEZ-TORRES, L. A., GÓMEZ-BENITO, M. J., DOBLARÉ, M. & GARCÍA-AZNAR, J. M. 2010b. Influence of the frequency of the external mechanical stimulus on bone healing: A computational study. Medical Engineering & Physics, 32, 363-371.

GOODSHIP, A. & KENWRIGHT, J. 1985. The influence of induced micromovement upon the healing of experimental tibial fractures. Bone & Joint Journal, 67, 650-655.

GOODSHIP, A. E., CUNNINGHAM, J. L. & KENWRIGHT, J. 1998. Strain rate and timing of stimulation in mechanical modulation of fracture healing. Clinical orthopaedics and related research, 355, S105-S115.

GRANT, C. A., SCHUETZ, M. & EPARI, D. 2015. Mechanical testing of internal fixation devices: A theoretical and practical examination of current methods. Journal of biomechanics, 48, 3989-3994.

GRASA, J., GÓMEZ-BENITO, M. J., GONZÁLEZ-TORRES, L. A., ASIAÍN, D., QUERO, F. & GARCÍA-AZNAR, J. M. 2010. Monitoring in vivo load transmission through an external fixator. Annals of Biomedical Engineering, 38, 605-612.

GRIFFITH, J. F. 2013. Bone marrow changes in osteoporosis. Osteoporosis and Bone Densitometry Measurements. Springer.

GUÉRIN, G., AMBARD, D. & SWIDER, P. 2009. Cells, growth factors and bioactive surface properties in a mechanobiological model of implant healing. Journal of Biomechanics, 42, 2555-2561.

GUILAK, F., COHEN, D. M., ESTES, B. T., GIMBLE, J. M., LIEDTKE, W. & CHEN, C. S. 2009. Control of stem cell fate by physical interactions with the extracellular matrix. Cell Stem Cell, 5, 17-26.

HAN, L., GRODZINSKY, A. J. & ORTIZ, C. 2011. Nanomechanics of the Cartilage Extracellular Matrix. Annu Rev Mater Res, 41, 133-168.

HARRISON, L. J., CUNNINGHAM, J. L., STRÖMBERG, L. & GOODSHIP, A. E. 2003. Controlled induction of a pseudoarthrosis_a study using a rodent model. Journal of orthopaedic trauma, 17, 11-21.

HECK, T., VAEYENS, M.-M. & VAN OOSTERWYCK, H. 2015. Computational models of sprouting angiogenesis and cell migration: towards multiscale mechanochemical models of angiogenesis. Mathematical Modelling of Natural Phenomena, 10, 108-141.

HELM, C.-L., FLEURY, M., ZISCH, A., BOSCHETTI, F. & SWARTZ, M. 2005. Synergy between interstitial flow and VEGF directs capillary morphogenesis in vitro through a gradient amplification mechanism. Proceedings of the National Academy of Sciences of the United States of America, 102, 15779-15784.

HENDERSON, C. E., BOTTLANG, M., MARSH, J. L., FITZPATRICK, D. C. & MADEY, S. M. 2008. Does locked plating of periprosthetic supracondylar femur fractures promote bone healing by callus formation? Two cases with opposite outcomes. The Iowa orthopaedic journal, 28, 73.

HENRICSON, A., HULTH, A. & JOHNELL, O. 1987. The cartilaginous fracture callus in rats. Acta orthopaedica Scandinavica, 58, 244-248.

HERNIGOU, P., POIGNARD, A., BEAUJEAN, F. & ROUARD, H. 2005. Percutaneous autologous bone-marrow grafting for nonunions: influence of the number and concentration of progenitor cells. JBJS, 87, 1430-1437.

HORN, C., DÖBELE, S., VESTER, H., SCHÄFFLER, A., LUCKE, M. & STÖCKLE, U. C. 2011. Combination of interfragmentary screws and locking plates in distal meta-diaphyseal fractures of the tibia: A retrospective, single-centre pilot study. Injury, 42, 1031-1037.

HOU, T., LI, Q., LUO, F., XU, J., XIE, Z., WU, X. & ZHU, C. 2009. Controlled dynamization to enhance reconstruction capacity of tissue-engineered bone in healing critically sized bone defects: an in vivo study in goats. Tissue Engineering Part A, 16, 201-212.

HUISKES, R., VAN DRIEL, W., PRENDERGAST, P. & SØBALLE, K. 1997. A biomechanical regulatory model for periprosthetic fibrous-tissue differentiation. Journal of materials science: Materials in medicine, 8, 785-788.

HUND, S. J. & ANTAKI, J. F. 2009. An extended convection diffusion model for red blood cell-enhanced transport of thrombocytes and leukocytes. Physics in medicine and biology, 54, 6415.

ISAKSSON, H. 2012. Recent advances in mechanobiological modeling of bone regeneration. Mechanics Research Communications, 42, 22-31.

ISAKSSON, H., COMAS, O., VAN DONKELAAR, C. C., MEDIAVILLA, J., WILSON, W., HUISKES, R. & ITO, K. 2007. Bone regeneration during distraction osteogenesis: mechano-regulation by shear strain and fluid velocity. Journal of biomechanics, 40, 2002-2011.

ISAKSSON, H., VAN DONKELAAR, C. C., HUISKES, R. & ITO, K. 2008a. A mechano-regulatory bone-healing model incorporating cell-phenotype specific activity. J Theor Biol, 252, 230-46.

ISAKSSON, H., VAN DONKELAAR, C. C., HUISKES, R. & ITO, K. 2008b. A mechano-regulatory bone-healing model incorporating cell-phenotype specific activity. Journal of theoretical biology, 252, 230-246.

ISAKSSON, H., WILSON, W., VAN DONKELAAR, C. C., HUISKES, R. & ITO, K. 2006. Comparison of biophysical stimuli for mechano-regulation of tissue differentiation during fracture healing. Journal of biomechanics, 39, 1507-1516.

ITO, H. 2011. Chemokines in mesenchymal stem cell therapy for bone repair: a novel concept of recruiting mesenchymal stem cells and the possible cell sources. Modern rheumatology, 21, 113-121.

IVKOVIC, A., MARIJANOVIC, I., HUDETZ, D., PORTER, R. M., PECINA, M. & EVANS, C. H. 2011. Regenerative medicine and tissue engineering in orthopaedic surgery. Front Biosci (Elite Ed), 3, 923-944.

JOHNSON, M., CHAKKALAKAL, D., HARPER, R., KATZ, J. & ROUHANA, S. 1982. Fluid flow in bone in vitro. Journal of Biomechanics, 15, 881-885.

JOYCE, M., TEREK, R., JINGUSHI, S. & BOLANDER, M. 1990a. Role of Transforming Growth Factor-β in Fracture Repair. Annals of the New York Academy of Sciences, 593, 107-123.

JOYCE, M. E., ROBERTS, A. B., SPORN, M. B. & BOLANDER, M. E. 1990b. Transforming growth factor-beta and the initiation of chondrogenesis and osteogenesis in the rat femur. The Journal of cell biology, 110, 2195-2207.

KANIS, J., BURLET, N., COOPER, C., DELMAS, P., REGINSTER, J.-Y., BORGSTROM, F. & RIZZOLI, R. 2008. European guidance for the diagnosis and management of osteoporosis in postmenopausal women. Osteoporosis international, 19, 399-428.

KASPER, G., DANKERT, N., TUISCHER, J., HOEFT, M., GABER, T., GLAESER, J., ZANDER, D., TSCHIRSCHMANN, M., THOMPSON, M., MATZIOLIS, G. & DUDA, G. 2007. Mesenchymal

Stem Cells Regulate Angiogenesis According to Their Mechanical Environment. Stem cells, 25, 903-910.

KELLY, D. J. & JACOBS, C. R. 2010. The role of mechanical signals in regulating chondrogenesis and osteogenesis of mesenchymal stem cells. Birth Defects Research Part C: Embryo Today: Reviews, 90, 75-85.

KEMMLER, W., LAUBER, D., WEINECK, J., HENSEN, J., KALENDER, W. & ENGELKE, K. 2004. Benefits of 2 years of intense exercise on bone density, physical fitness, and blood lipids in early postmenopausal osteopenic women: results of the Erlangen Fitness Osteoporosis Prevention Study (EFOPS). Archives of Internal Medicine, 164, 1084-1091.

KENWRIGHT, J. & GOODSHIP, A. E. 1989. Controlled mechanical stimulation in the treatment of tibial fractures. Clinical orthopaedics and related research, 241, 36-47.

KENWRIGHT, J., RICHARDSON, J., CUNNINGHAM, J., WHITE, S., GOODSHIP, A., ADAMS, M., MAGNUSSEN, P. & NEWMAN, J. 1991. Axial movement and tibial fractures. A controlled randomised trial of treatment. Bone & Joint Journal, 73, 654-659.

KHAYYERI, H., CHECA, S., TÄGIL, M. & PRENDERGAST, P. J. 2009. Corroboration of mechanobiological simulations of tissue differentiation in an in vivo bone chamber using a lattice-modeling approach. Journal of Orthopaedic Research, 27, 1659-1666.

KLEIN, P., SCHELL, H., STREITPARTH, F., HELLER, M., KASSI, J. P., KANDZIORA, F., BRAGULLA, H., HAAS, N. P. & DUDA, G. N. 2003. The initial phase of fracture healing is specifically sensitive to mechanical conditions. Journal of orthopaedic research, 21, 662-669.

KUBIAK, E. N., BEEBE, M. J., NORTH, K., HITCHCOCK, R. & POTTER, M. Q. 2013. Early weight bearing after lower extremity fractures in adults. JAAOS-Journal of the American Academy of Orthopaedic Surgeons, 21, 727-738.

KUBO, KUBO, T., SHIGA, T., HASHIMOTO, J., YOSHIOKA, M., HONJO, H., URABE, M., KITAJIMA, I., SEMBA, I. & HIRASAWA, Y. 1999. Osteoporosis influences the late period of fracture healing in a rat model prepared by ovariectomy and low calcium diet. Journal of steroid biochemistry and molecular biology, 68, 197-202.

LACROIX, D. & PRENDERGAST, P. 2002. A mechano-regulation model for tissue differentiation during fracture healing: analysis of gap size and loading. Journal of biomechanics, 35, 1163-1171.

LACROIX, D., PRENDERGAST, P. J., LI, G. & MARSH, D. 2002a. Biomechanical model to simulate tissue differentiation and bone regeneration: Application to fracture healing. Medical and Biological Engineering and Computing, 40, 14-21.

LACROIX, D., PRENDERGAST, P. J., LI, G. & MARSH, D. 2002b. Biomechanical model to simulate tissue differentiation and bone regeneration: application to fracture healing. Med Biol Eng Comput, 40, 14-21.

LE, A., MICLAU, T., HU, D. & HELMS, J. 2001. Molecular aspects of healing in stabilized and non-stabilized fractures. Journal of Orthopaedic Research, 19, 78-84.

LEONG, P. & MORGAN, E. 2008. Measurement of fracture callus material properties via nanoindentation. Acta biomaterialia, 4, 1569-1575.

LEVENSTON, M., FRANK, E. & GRODZINSKY, A. 1998. Variationally derived 3-field finite element formulations for quasistatic poroelastic analysis of hydrated biological tissues. Computer methods in applied mechanics and engineering, 156, 231-246.

LEWIS, G. S., CAROOM, C. T., WEE, H., JURGENSMEIER, D., ROTHERMEL, S. D., BRAMER, M. A. & REID, J. S. 2015. Tangential bicortical locked fixation improves stability in Vancouver B1 periprosthetic femur fractures: a biomechanical study. Journal of orthopaedic trauma, 29, e364.

LIENAU, J., SCHELL, H., DUDA, G. N., SEEBECK, P., MUCHOW, S. & BAIL, H. J. 2005. Initial vascularization and tissue differentiation are influenced by fixation stability. Journal of Orthopaedic Research, 23, 639-645.

LOBOA, E. G., BEAUPRE, G. S. & CARTER, D. R. 2001. Mechanobiology of initial pseudarthrosis formation with oblique fractures. J Orthop Res, 19, 1067-72.

LOWENBERG, D. W., NORK, S. & ABRUZZO, F. M. 2008. Correlation of shear to compression for progressive fracture obliquity. Clinical orthopaedics and related research, 466, 2947-2954.

LU, C., MICLAU, T., HU, D. & MARCUCIO, R. S. 2007. Ischemia leads to delayed union during fracture healing: a mouse model. Journal of orthopaedic research, 25, 51-61.

LUJAN, T. J., HENDERSON, C. E., MADEY, S. M., FITZPATRICK, D. C., MARSH, J. L. & BOTTLANG, M. 2010. Locked plating of distal femur fractures leads to inconsistent and asymmetric callus formation. Journal of orthopaedic trauma, 24, 156-162.

MALIZOS, K. N. & PAPATHEODOROU, L. K. 2005. The healing potential of the periosteum: molecular aspects. Injury, 36, S13-S19.

MARKEL, M. D., WIKENHEISER, M. A. & CHAO, E. 1990. A study of fracture callus material properties: relationship to the torsional strength of bone. Journal of orthopaedic research, 8, 843-850.

MARSELL, R. & EINHORN, T. A. 2009. The role of endogenous bone morphogenetic proteins in normal skeletal repair. Injury, 40, S4-S7.

MARSELL, R. & EINHORN, T. A. 2011. The biology of fracture healing. Injury, 42, 551-555.

MATLAB 2015. MATLAB. The MathWorks, Inc.

MAUCK, R. L., HUNG, C. T. & ATESHIAN, G. A. 2003. Modeling of Neutral Solute Transport in a Dynamically Loaded Porous Permeable Gel: Implications for Articular Cartilage Biosynthesis and Tissue Engineering. Journal of Biomechanical Engineering, 125, 602-614.

MCCARTNEY, W., DONALD, B. J. M. & HASHMI, M. S. J. 2005. Comparative performance of a flexible fixation implant to a rigid implant in static and repetitive incremental loading. Journal of materials processing technology, 169, 476-484.

MCKIBBIN, B. 1978a. The biology of fracture healing in long bones. J Bone Joint Surg Br 60-B, 150-162.

MCKIBBIN, B. 1978b. The biology of fracture healing in long bones. The Journal of bone and joint surgery. British volume, 60, 150.

MEYER JR, R. A., TSAHAKIS, P. J., MARTIN, D. F., BANKS, D. M., HARROW, M. E. & KIEBZAK, G. M. 2001. Age and ovariectomy impair both the normalization of mechanical properties and the accretion of mineral by the fracture callus in rats. Journal of Orthopaedic Research, 19, 428-435.

MICLAU, T., THOMPSON, Z., COLNOT, C., HUANG, S., WERB, Z. & HELMS, J. The effect of early stability on fracture repair. TRANSACTIONS OF THE ANNUAL MEETING-ORTHOPAEDIC RESEARCH SOCIETY, 2002. 709-709.

MILLER, M. A., IVKOVIC, A., PORTER, R., HARRIS, M. B., ESTOK, D. M., SMITH, R. M., EVANS, C. H. & VRAHAS, M. S. 2011. Autologous bone grafting on steroids: preliminary clinical results. A novel treatment for nonunions and segmental bone defects. International orthopaedics, 35, 599-605.

MIRAMINI, S., MENDIS, P., ZHANG, L. & RICHARDSON, M. 2013a. From Materials to Structures: Advancement through Innovation.

MIRAMINI, S., SMITH, D. W., ZHANG, L. & GARDINER, B. S. 2017a. The spatio-temporal mechanical environment of healthy and injured human cartilage during sustained activity and its role in cartilage damage. Journal of the Mechanical Behavior of Biomedical Materials.

MIRAMINI, S. & YANG, Y. 2019. A probabilistic-based approach for computational simulation of bone fracture healing. Computer Methods and Programs in Biomedicine, 105011.

MIRAMINI, S., ZHANG, L., RICHARDSON, M. & MENDIS, P. 2014a. Computational Simulation of Mechanical Microenvironment of Early Stage of Bone Healing under Locking Compression Plate with Dynamic Locking Screws. Applied Mechanics and Materials, 553, 281-286.

MIRAMINI, S., ZHANG, L., RICHARDSON, M. & MENDIS, P. 2017b. The Role of Locking Plate Stiffness in Bone Fracture Healing Stabilized by Far Cortical Locking Technique. International Journal of Computational Methods, 1850024.

MIRAMINI, S., ZHANG, L., RICHARDSON, M. & MENDIS, P. 2018. The Role of Locking Plate Stiffness in Bone Fracture Healing Stabilized by Far Cortical Locking Technique. International Journal of Computational Methods, 15, 1850024.

MIRAMINI, S., ZHANG, L., RICHARDSON, M., MENDIS, P. & EBELING, P. 2016a. Influence of fracture geometry on bone healing under locking plate fixations: A comparison between oblique and transverse tibial fractures. Medical engineering & physics, 38, 1100-1108.

MIRAMINI, S., ZHANG, L., RICHARDSON, M., MENDIS, P., OLOYEDE, A. & EBELING, P. 2016b. The relationship between interfragmentary movement and cell differentiation in early fracture healing under locking plate fixation. Australas Phys Eng Sci Med.

MIRAMINI, S., ZHANG, L., RICHARDSON, M., PIRPIRIS, M., MENDIS, P., OLOYEDE, K. & EDWARDS, G. 2013b. Computational simulation of the early stage of bone healing under different configurations of locking compression plates. Comput Methods Biomech Biomed Engin, 18, 900-13.

MIRAMINI, S., ZHANG, L., RICHARDSON, M., PIRPIRIS, M., MENDIS, P., OLOYEDE, K. & EDWARDS, G. 2015. Computational simulation of the early stage of bone healing under different Locking Compression Plate configurations. Computer Methods in Biomechanics and Biomedical Engineering, 18, 900-913.

MIRAMINI, S., ZHANG, L. H., RICHARDSON, M. & MENDIS, P. Computational simulation of mechanical microenvironment of early stage of bone healing under locking compression plate with dynamic locking screws. Applied Mechanics and Materials, 2014b. Trans Tech Publ, 281-286.

MOALLI, M., CALDWELL, N., PATIL, P. & GOLDSTEIN, S. 2000. An In Vivo Model for Investigations of Mechanical Signal Transduction in Trabecular Bone. Journal of bone and mineral research, 15, 1346-1353.

MOORCROFT, C. I., OGRODNIK, P. J., THOMAS, P. B. & WADE, R. H. 2001. Mechanical properties of callus in human tibial fractures: a preliminary investigation. Clinical Biomechanics, 16, 776-782.

MORONI, A., HOANG-KIM, A., LIO, V. & GIANNINI, S. 2005. Current augmentation fixation techniques for the osteoporotic patient. Sandinavian Journal of Surgery, 94, 103-109.

NASSIRI, M., MACDONALD, B. & O'BYRNE, J. 2013. Computational modelling of long bone fractures fixed with locking plates–How can the risk of implant failure be reduced? Journal of orthopaedics, 10, 29-37.

NEIDLINGER-WILKE, C., STALLA, I., CLAES, L., BRAND, R., HOELLEN, I., RÜBENACKER, S., ARAND, M. & KINZL, L. 1995. Human osteoblasts from younger normal and osteoporotic donors show differences in proliferation and TGFβ-release in response to cyclic strain. Journal of biomechanics, 28, 1411-1418.

NG, C. & SWARTZ, M. 2003. Fibroblast alignment under interstitial fluid flow using a novel 3-D tissue culture model. American journal of physiology. Heart and circulatory physiology, 284, H1771-H1777.

NUTTALL, M. E., PATTON, A. J., OLIVERA, D. L., NADEAU, D. P. & GOWEN, M. 1998. Human trabecular bone cells are able to express both osteoblastic and adipocytic phenotype: implications for osteopenic disorders. Journal of Bone and Mineral Research, 13, 371-382.

O'HARA, B., URBAN, J. & MAROUDAS, A. 1990. Influence of cyclic loading on the nutrition of articular cartilage. Annals of the rheumatic diseases, 49, 536-539.

O'REILLY, A. & KELLY, D. J. 2017. A computational model of osteochondral defect repair following implantation of stem cell-laden multiphase scaffolds. Tissue Engineering Part A, 23, 30-42.

OLSEN, L., SHERRATT, J. A. & MAINI, P. K. 1995. A mechanochemical model for adult dermal wound contraction: on the permanence of the contracted tissue displacement profile. Journal of theoretical biology, 177, 113-128.

PARK, S. H. 1998. The influence of active shear or compressive motion on fracture-healing. Journal of Bone & Joint Surgery - American Volume, 80, 868.

PAUWELS, F. 1960. [A new theory on the influence of mechanical stimuli on the differentiation of supporting tissue. The tenth contribution to the functional anatomy and causal morphology of the supporting structure]. Z Anat Entwicklungsgesch, 121, 478-515.

PEARCE, A., RICHARDS, R., MILZ, S., SCHNEIDER, E. & PEARCE, S. 2007. Animal models for implant biomaterial research in bone: a review. Eur Cell Mater, 13, 1-10.

PEĆINA, M. & VUKIČEVIĆ, S. 2007. Biological aspects of bone, cartilage and tendon regeneration. International orthopaedics, 31, 719-720.

PEIFFER, V., GERISCH, A., VANDEPITTE, D., OOSTERWYCK, H. V. & GERIS, L. 2011. A hybrid bioregulatory model of angiogenesis during bone fracture healing. Biomech Model Mechanobiol, 10, 383-395.

PERREN, S. M. 1979. Physical and biological aspects of fracture healing with special reference to internal fixation. Clinical Orthopaedics & Related Research, 138, 175-196.

PERREN, S. M. 2002a. Evolution of the internal fixation of long bone fractures. JOURNAL OF BONE AND JOINT SURGERY-BRITISH VOLUME-, 84, 1093-1110.

PERREN, S. M. 2002b. Evolution of the internal fixation of long bone fractures. The scientific basis of biological internal fixation: choosing a new balance between stability and biology. J Bone Joint Surg Br, 84, 1093-110.

PERREN, S. M. 2002c. Evolution of the internal fixation of long bone fractures: the scientific basis of biological internal fixation: choosing a new balance between stability and biology. The Journal of bone and joint surgery. British volume, 84, 1093-1110.

PERREN, S. M. 2008. Fracture healing. The evolution of our understanding. Acta chirurgiae orthopaedicae et traumatologiae Cechoslovaca, 75, 241.

PETERS, A., SCHELL, H., BAIL, H. J., HANNEMANN, M., SCHUMANN, T., DUDA, G. N. & LIENAU, J. 2010. Standard bone healing stages occur during delayed bone healing, albeit with a different temporal onset and spatial distribution of callus tissues. Histology and histopathology, Vol. 25, nº 9 (2010).

PIERCE, M. C., BERTOCCI, G., VOGELEY, E. & MORELAND, M. 2004. Evaluating long bone fractures in children: a biomechanical approach with illustrative cases. Child abuse & neglect, 28, 505-524.

PITTENGER, M. F., MACKAY, A. M., BECK, S. C., JAISWAL, R. K., DOUGLAS, R., MOSCA, J. D., MOORMAN, M. A., SIMONETTI, D. W., CRAIG, S. & MARSHAK, D. R. 1999. Multilineage potential of adult human mesenchymal stem cells. science, 284, 143-147.

PIVONKA, P. & DUNSTAN, C. R. 2012. Role of mathematical modeling in bone fracture healing. Bonekey Rep, 1, 221.

POKORNÁ, P., HEJCMANOVÁ, P., HEJCMAN, M. & PAVLU, V. 2013. Activity time budget patterns of sheep and goats co-grazing on semi-natural species-rich dry grassland. Czech Journal of Animal Science, 58, 208-16.

POLACHECK, W., CHAREST, J. & KAMM, R. 2011. Interstitial flow influences direction of tumor cell migration through competing mechanisms. Proceedings of the National Academy of Sciences of the United States of America, 108, 11115-11120.

POSTACCHINI, F., GUMINA, S., PERUGIA, D. & DE MARTINO, C. 1995. Early Fracture Callus in the Diaphysis of Human Long Bones: Histologic and Ultrastructural Study. Clinical orthopaedics and related research, 218-228.

PRENDERGAST, P. J., HUISKES, R. & SØBALLE, K. 1997. Biophysical stimuli on cells during tissue differentiation at implant interfaces. Journal of Biomechanics, 30, 539-548.

REHMAN, I., SMITH, R., HENCH, L. & BONFIELD, W. 1995. Structural evaluation of human and sheep bone and comparison with synthetic hydroxyapatite by FT-Raman spectroscopy. Journal of biomedical materials research, 29, 1287-1294.

REICH, D. L., HOSSAIN, S., KROL, M., BAEZ, B., PATEL, P., BERNSTEIN, A. & BODIAN, C. A. 2005. Predictors of hypotension after induction of general anesthesia. Anesthesia & Analgesia, 101, 622-628.

REINA-ROMO, E., GÓMEZ-BENITO, M. J., DOMÍNGUEZ, J., NIEMEYER, F., SIMON, T. W. & CLAES, L. E. 2011. Effect of the fixator stiffness on the young regenerate bone after bone transport: Computational approach. Journal of Biomechanics, 5, 917-923.

RHO, J. Y., HOBATHO, M. C. & ASHMAN, R. B. 1995. Relations of mechanical properties to density and CT numbers in human bone. Medical Engineering & Physics, 17, 347-355.

RICHTER, H., PLECKO, M., ANDERMATT, D., FRIGG, R., KRONEN, P., KLEIN, K., NUSS, K., FERGUSON, S., STÖCKLE, U. & VON RECHENBERG, B. 2015. Dynamization at the near cortex in locking plate osteosynthesis by means of dynamic locking screws: an experimental study of transverse tibial osteotomies in sheep. Journal of Bone & Joint Surgery - American Volume, 97, 208-215.

RIMINUCCI, M., REMOLI, C., ROBEY, P. G. & BIANCO, P. 2015. Stem cells and bone diseases: New tools, new perspective. Bone, 70, 55-61.

ROBERTS, T. T. & ROSENBAUM, A. J. 2012. Bone grafts, bone substitutes and orthobiologics: the bridge between basic science and clinical advancements in fracture healing. Organogenesis, 8, 114-124.

RODAN, G. A. & MARTIN, T. J. Therapeutic approaches to bone diseases. Science, 289, 1508-1514.

ROSSET, P., DESCHASEAUX, F. & LAYROLLE, P. 2014. Cell therapy for bone repair. Orthopaedics & Traumatology: Surgery & Research, 100, S107-S112.

ROUBELAKIS, M. G., PAPPA, K. I., BITSIKA, V., ZAGOURA, D., VLAHOU, A., PAPADAKI, H. A., ANTSAKLIS, A. & ANAGNOU, N. P. 2007. Molecular and proteomic characterization of human mesenchymal stem cells derived from amniotic fluid: comparison to bone marrow mesenchymal stem cells. Stem cells and development, 16, 931-952.

SAMBROOK, P. N., SEEMAN, E., PHILLIPS, S. R. & EBELING, P. R. 2002. Preventing osteoporosis: outcomes of the Australian fracture prevention summit. Medical Journal of Australia, 176, S1-S16.

SAMIEZADEH, SAMIEZADEH, S., TAVAKKOLI AVVAL, P., FAWAZ, Z. & BOUGHERARA, H. 2014. Biomechanical assessment of composite versus metallic intramedullary nailing system in femoral shaft fractures: A finite element study. Clinical biomechanics (Bristol), 29, 803-810.

SCHAFFLER, M. B. & BURR, D. B. 1988. Stiffness of compact bone: effects of porosity and density. Journal of biomechanics, 21, 13-16.

SCHELL, H., THOMPSON, M. S., BAIL, H. J., HOFFMANN, J.-E., SCHILL, A., DUDA, G. N. & LIENAU, J. 2008. Mechanical induction of critically delayed bone healing in sheep: radiological and biomechanical results. Journal of biomechanics, 41, 3066-3072.

SCHINDELER, A., MCDONALD, M. M., BOKKO, P. & LITTLE, D. G. 2008. Bone remodeling during fracture repair: The cellular picture. Semin Cell Dev Biol, 19, 459-66.

SCHMAL, H., STROHM, P. C., JAEGER, M. & SÜDKAMP, N. P. 2011. Flexible fixation and fracture healing: do locked plating 'internal fixators' resemble external fixators? Journal of orthopaedic trauma, 25, S15-S20.

SCHMIDT-BLEEK, K., SCHELL, H., SCHULZ, N., HOFF, P., PERKA, C., BUTTGEREIT, F., VOLK, H.-D., LIENAU, J. & DUDA, G. N. 2012. Inflammatory phase of bone healing initiates the regenerative healing cascade. Cell and tissue research, 347, 567-573.

SHANSHAN, G., WANG, Y., WANG, K., LONG, J., LV, X., HUANG, Z., YANG, Y., MIRAMINI, S. & ZHANG, L. 2019. Robot-assisted weight-bearing exercise for stroke patients with limited mobility. Journal of Low Frequency Noise, Vibration and Active Control, 38, 879-892.

SHIELDS, J., FLEURY, M., YONG, C., TOMEI, A., RANDOLPH, G. & SWARTZ, M. 2007. Autologous Chemotaxis as a Mechanism of Tumor Cell Homing to Lymphatics via Interstitial Flow and Autocrine CCR7 Signaling. Cancer cell, 11, 526-538.

SIMON, U., AUGAT, P., UTZ, M. & CLAES, L. 2011. A numerical model of the fracture healing process that describes tissue development and revascularisation. Computer methods in biomechanics and biomedical engineering, 14, 79-93.

SIWACH, R., SANGWAN, S., SINGH, R. & GOEL, A. 2001. Role of percutaneous bone marrow grafting in delayed unions, non-unions and poor regenerates. Indian journal of medical sciences, 55, 326-336.

SMIT, T. H., HUYGHE, J. M. & COWIN, S. C. 2002. Estimation of the poroelastic parameters of cortical bone. Journal of biomechanics, 35, 829-835.

SMITH, D. W., GARDINER, B. S., ZHANG, L. & GRODZINSKY, A. J. 2018. Articular Cartilage Dynamics, Springer.

SOLHEIM, E. 1998. Growth factors in bone. Int Orthop, 22, 410-6.

STEINER, M., CLAES, L., IGNATIUS, A., NIEMEYER, F., SIMON, U. & WEHNER, T. 2013. Prediction of fracture healing under axial loading, shear loading and bending is possible using distortional and dilatational strains as determining mechanical stimuli. Journal of the Royal Society Interface, 10, 20130389.

STEINER, M., CLAES, L., IGNATIUS, A., SIMON, U. & WEHNER, T. 2014. Disadvantages of interfragmentary shear on fracture healing—mechanical insights through numerical simulation. Journal of Orthopaedic Research, 32, 865-872.

STOFFEL, K., DIETER, U., STACHOWIAK, G., GÄCHTER, A. & KUSTER, M. S. 2003a. Biomechanical testing of the LCP--how can stability in locked internal fixators be controlled? Injury, 34, B11-9.

STOFFEL, K., DIETER, U., STACHOWIAK, G., GÄCHTER, A. & KUSTER, M. S. 2003b. Biomechanical testing of the LCP–how can stability in locked internal fixators be controlled? Injury, 34, 11-19.

SZYPRYT, P. & FORWARD, D. 2009. The use and abuse of locking plates. Orthopaedics and Trauma, 23, 281-290.

TALKOWSKI, J., LENZE, E., MUNIN, M., HARRISON, C. & BRACH, J. 2009. Patient Participation and Physical Activity During Rehabilitation and Future Functional Outcomes in Patients After Hip Fracture. Archives of physical medicine and rehabilitation, 90, 618-622.

TAN, S. E. & BALOGH, Z. J. 2009. Indications and limitations of locked plating. Injury, 40, 683-691.

TEIPNER, W. A. & MAST, J. 1980. Internal fixation of forearm diaphyseal fractures: double plating versus single compression (tension band) plating--a comparative study. The Orthopedic clinics of North America, 11, 381-391.

TEPIC, S., MACIROWSKI, T. & MANN, R. W. 1983. Mechanical properties of articular cartilage elucidated by osmotic loading and ultrasound. Proceedings of the National Academy of Sciences, 80, 3331-3333.

TEPIC, S., REMIGER, A. R., MORIKAWA, K., PREDIERI, M. & PERREN, S. M. 1997. Strength recovery in fractured sheep tibia treated with a plate or an internal fixator: an experimental study with a two-year follow-up. Journal of orthopaedic trauma, 11, 14-23.

THOMPSON, Z., MICLAU, T., HU, D. & HELMS, J. A. 2002. A model for intramembranous ossification during fracture healing. Journal of Orthopaedic Research, 20, 1091-1098.

TODD, J. & ROBINSON, R. 2003. Osteoporosis and exercise. Postgraduate medical journal, 79, 320-323.

TOLOMIO, S., ERMOLAO, A., LALLI, A. & ZACCARIA, M. 2010. The effect of a multicomponent dual-modality exercise program targeting osteoporosis on bone health status and physical function capacity of postmenopausal women. Journal of women & aging, 22, 241-254.

TORRES, L. A. G., E ALONSO, S. D. C. & MEIRELES, A. B. 2018. Low amplitude and high frequency mechanical stimulation does not affect directly cell differentiation during bone healing. Ciência e Natura, 40, 56.

TSIRIDIS, E., UPADHYAY, N. & GIANNOUDIS, P. 2007. Molecular aspects of fracture healing: which are the important molecules? Injury, 38, S11-S25.

TUFEKCI, P., TAVAKOLI, A., DLASKA, C., NEUMANN, M., SHANKER, M., SAIFZADEH, S., STECK, R., SCHUETZ, M. & EPARI, D. 2018. Early mechanical stimulation only permits timely bone healing in sheep. Journal of Orthopaedic Research®, 36, 1790-1796.

TZIOUPIS, C. & GIANNOUDIS, P. V. 2007. Prevalence of long-bone non-unions. Injury, 38, S3-S9.

VETTER, A., EPARI, D. R., SEIDEL, R., SCHELL, H., FRATZL, P., DUDA, G. N. & WEINKAMER, R. 2010. Temporal tissue patterns in bone healing of sheep. Journal of Orthopaedic Research, 28, 1440-1447.

WANG, M., YANG, N. & WANG, X. 2017. A review of computational models of bone fracture healing. Medical & biological engineering & computing, 55, 1895-1914.

WATERS, R. V., GAMRADT, S. C., ASNIS, P., VICKERY, B. H., AVNUR, Z., HILL, E. & BOSTROM, M. 2000. Systemic corticosteroids inhibit bone healing in a rabbit ulnar osteotomy model. Acta Orthopaedica Scandinavica, 71, 316-321.

WATTS, J. J., ABIMANYI-OCHOM, J. & SANDERS, K. M. 2013. Osteoporosis costing all Australian: a new burden of disease analysis-2012 to 2022.

WEHNER, T., GRUCHENBERG, K., BINDL, R., RECKNAGEL, S., STEINER, M., IGNATIUS, A. & CLAES, L. 2014. Temporal delimitation of the healing phases via monitoring of fracture callus stiffness in rats. Journal of Orthopaedic Research, 32, 1589-1595.

WEISS, S., BAUMGART, R., JOCHUM, M., STRASBURGER, C. & BIDLINGMAIER, M. 2002. Systemic regulation of distraction osteogenesis: a cascade of biochemical factors. Journal of Bone and Mineral Research, 17, 1280-1289.

WHEELER, D. L. 2000. Mechanical strength of fracture callus in osteopenic bone at different phases of healing. Journal of Orthopaedic Trauma, 14, 86.

WILSON, A. W., DAVIES, H. M., EDWARDS, G. A. & GRILLS, B. L. 1999. Can some physical therapy and manual techniques generate potentially osteogenic levels of strain within mammalian bone? Physical Therapy, 79, 931-938.

WILSON, C. J., SCHUETZ, M. A. & EPARI, D. R. 2015. Effects of strain artefacts arising from a pre-defined callus domain in models of bone healing mechanobiology. Biomechanics and modeling in mechanobiology, 14, 1129-1141.

WITT, F., DUDA, G. N., BERGMANN, C. & PETERSEN, A. 2014. Cyclic mechanical loading enables solute transport and oxygen supply in bone healing: an in vitro investigation. Tissue Engineering Part A, 20, 486-493.

WOLF, J., WHITE, A., PANJABI, M. & SOUTHWICK, W. 1981. Comparison of cyclic loading versus constant compression in the treatment of long-bone fractures in rabbits. J Bone Joint Surg Am, 63, 805-810.

WOLF, S., JANOUSEK, A., PFEIL, J., VEITH, W., HAAS, F., DUDA, G. & CLAES, L. 1998. The effects of external mechanical stimulation on the healing of diaphyseal osteotomies fixed by flexible external fixation. Clinical biomechanics, 13, 359-364.

WOO, S., LOTHRINGER, K., AKESON, W., COUTTS, R., WOO, Y., SIMON, B. & GOMEZ, M. 1983. Less rigid internal fixation plates: historical perspectives and new concepts. Journal of orthopaedic research, 1, 431-449.

YAMAGISHI, M. & YOSHIMURA, Y. 1955. The biomechanics of fracture healing. JBJS, 37, 1035-1068.

YAMAGUCHI, A. Regulation of differentiation pathway of skeletal mesenchymal cells in cell lines by transforming growth factor-β superfamily. Seminars in cell biology, 1995. Elsevier, 165-173.

ZHANG, L. 2011. Solute transport in cyclic deformed heterogeneous articular cartilage. International Journal of Applied Mechanics, 3, 507-524.

ZHANG, L., GARDINER, B. S., SMITH, D. W., PIVONKA, P. & GRODZINSKY, A. 2007. The effect of cyclic deformation and solute binding on solute transport in cartilage. Arch Biochem Biophys, 457, 47-56.

ZHANG, L., GARDINER, B. S., SMITH, D. W., PIVONKA, P. & GRODZINSKY, A. 2008a. A fully coupled poroelastic reactive-transport model of cartilage. Molecular and Cellular Biomechanics, 5, 133.

ZHANG, L., GARDINER, B. S., SMITH, D. W., PIVONKA, P. & GRODZINSKY, A. J. 2008b. A fully coupled poroelastic reactive-transport model of cartilage. Molecular & Cellular Biomechanics, 5, 133-153.

ZHANG, L., GARDINER, B. S., SMITH, D. W., PIVONKA, P. & GRODZINSKY, A. J. 2008c. IGF uptake with competitive binding in articular cartilage. Journal of Biological Systems, 16, 175-195.

ZHANG, L., GARDINER, B. S., SMITH, D. W., PIVONKA, P. & GRODZINSKY, A. J. 2009. Integrated model of IGF-I mediated biosynthesis in a deformed articular cartilage. Journal of Engineering Mechanics, 135, 439-449.

ZHANG, L., GARDINER, B. S., SMITH, D. W., PIVONKA, P. & GRODZINSKY, A. J. 2010a. On the role of diffusible binding partners in modulating the transport and concentration of proteins in tissues. Journal of theoretical biology, 263, 20-29.

ZHANG, L., MIRAMINI, S., GARDINER, B. S., SMITH, D. W. & GRODZINSKY, A. J. 2015a. Time evolution of deformation in a human cartilage under cyclic loading. Annals of Biomedical Engineering, 43, 1166-1177.

ZHANG, L., MIRAMINI, S., MENDIS, P., RICHARDSON, M., PIRPIRIS, M. & OLOYEDE, K. 2013. The effects of flexible fixation on early stage bone fracture healing. International Journal of Aerospace and Lightweight Structures, 3, 181-189.

ZHANG, L., MIRAMINI, S., RICHARDSON, M., EBELING, P., LITTLE, D., YANG, Y. & HUANG, Z. 2017a. Computational modelling of bone fracture healing under partial weight-bearing exercise. Medical engineering & physics, 42, 65-72.

ZHANG, L., MIRAMINI, S., RICHARDSON, M., MENDIS, P. & EBELING, P. 2017b. The role of impairment of mesenchymal stem cell function in osteoporotic bone fracture healing. Australasian physical & engineering sciences in medicine, 40, 603-610.

ZHANG, L., MIRAMINI, S., RICHARDSON, M., MENDIS, P. & EBELING, P. 2017c. The role of impairment of mesenchymal stem cell function in osteoporotic bone fracture healing. Medical Engineering and Physics, 40, 603-610.

ZHANG, L., MIRAMINI, S., SMITH, D. W., GARDINER, B. S. & GRODZINSKY, A. J. 2015b. Time evolution of deformation in a human cartilage under cyclic loading. Ann Biomed Eng, 43, 1166-77.

ZHANG, L., RICHARDSON, M. & MENDIS, P. 2012a. Role of chemical and mechanical stimuli in mediating bone fracture healing. Clinical and Experimental Pharmacology and Physiology, 39, 706-710.

ZHANG, L., RICHARDSON, M. & MENDIS, P. 2012b. Role of chemical and mechanical stimuli in mediating bone fracture healing. Clinical and Experimental Pharmacology and Physiology 39, 706-710.

ZHANG, L., SMITH, D., GARDINER, G., PIVONKA, P. & GRODZINSKY, A. J. 2010b. The transport of insulin-like growth factor through cartilage. Porous Media: Applications in Biological Systems and Biotechnology, 399-453.

ZURA, ZURA, R., XIONG, Z., EINHORN, T., WATSON, J. T., OSTRUM, R., PRAYSON, M., DELLA ROCCA, G., MEHTA, S., MCKINLEY, T., WANG, Z. & STEEN, R. G. 2016. Epidemiology of Fracture Nonunion in 18 Human Bones. JAMA Surgery, 151, e162775.